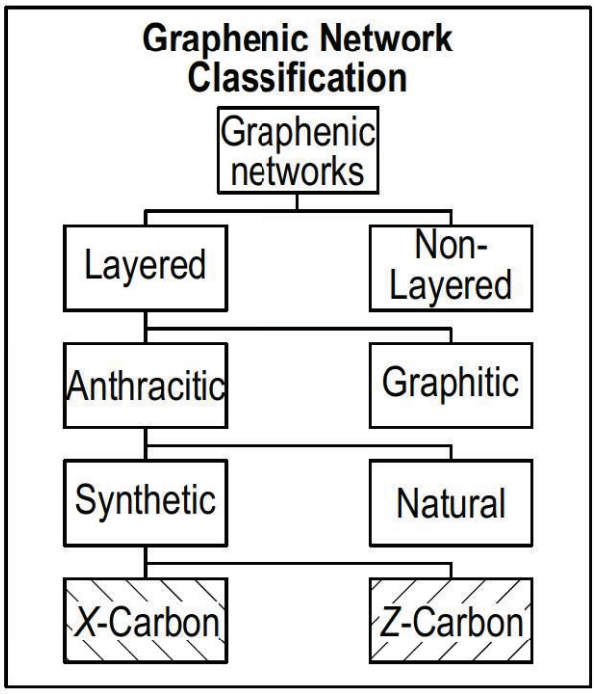
Graphenic Network Classification
Graphenic networks
Layered
Non-Layered
Anthracitic
Graphitic
Synthetic
Natural
X-Carbon
Z-Carbon

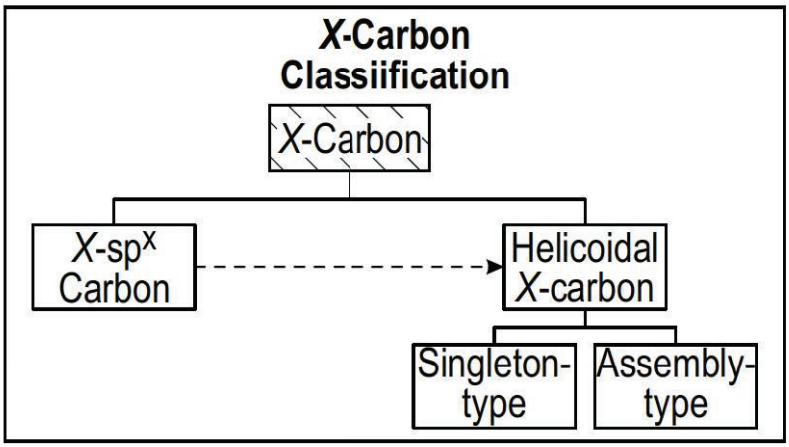
X-Carbon Classiification
X-Carbon
X-sp^x Carbon
Helicoidal X-carbon
Singleton-type
Assembly-type

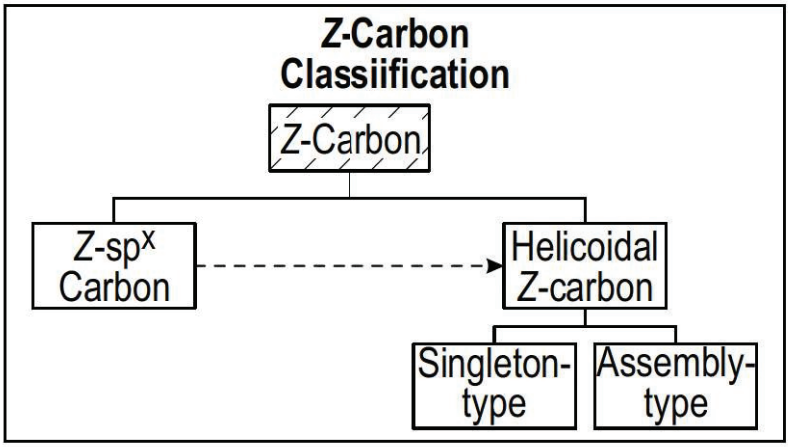
Z-Carbon Classiification
Z-Carbon
Z-sp^x Carbon
Helicoidal Z-carbon
Singleton-type
Assembly-type

FIG. 1

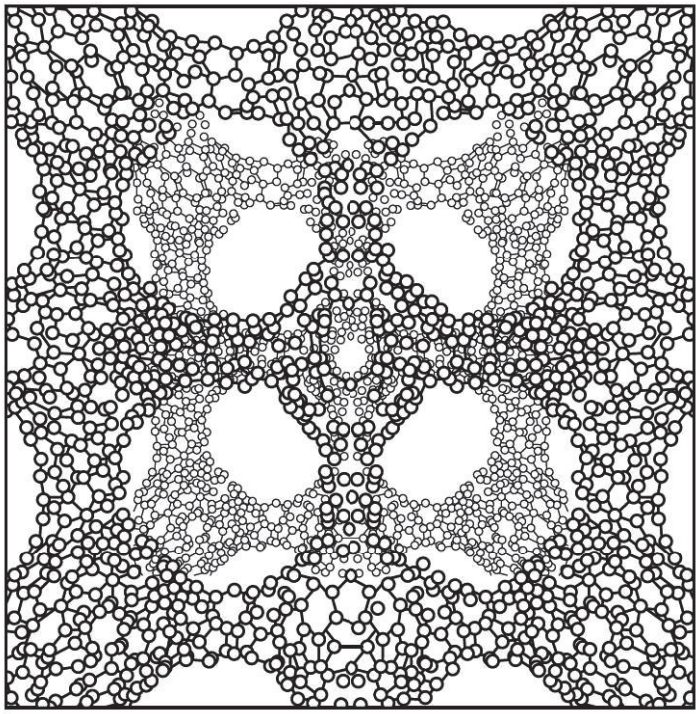

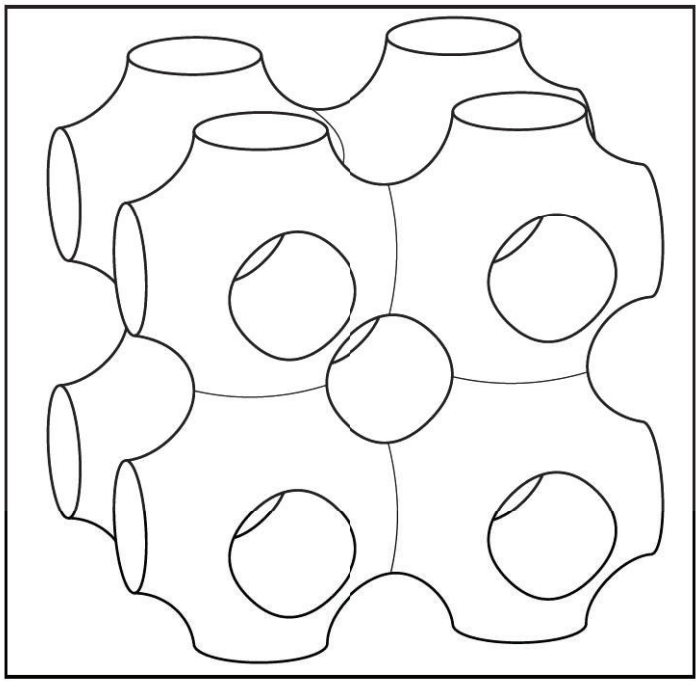

FIG. 2

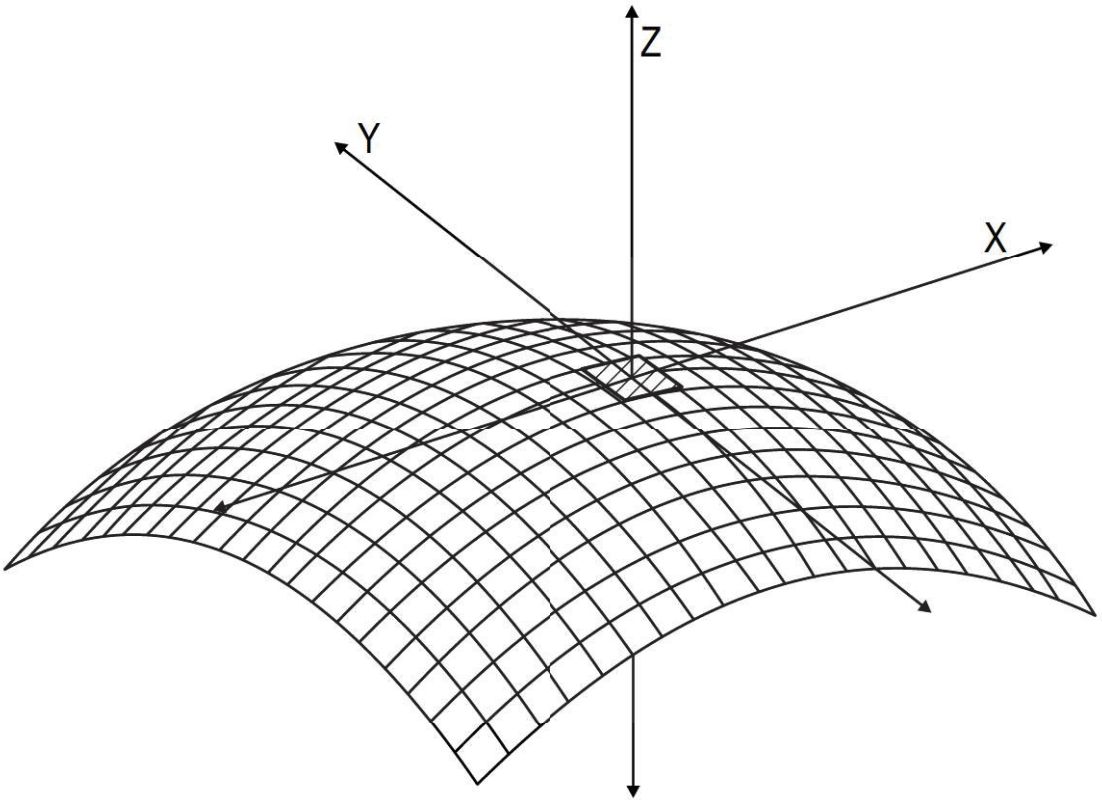

FIG. 3

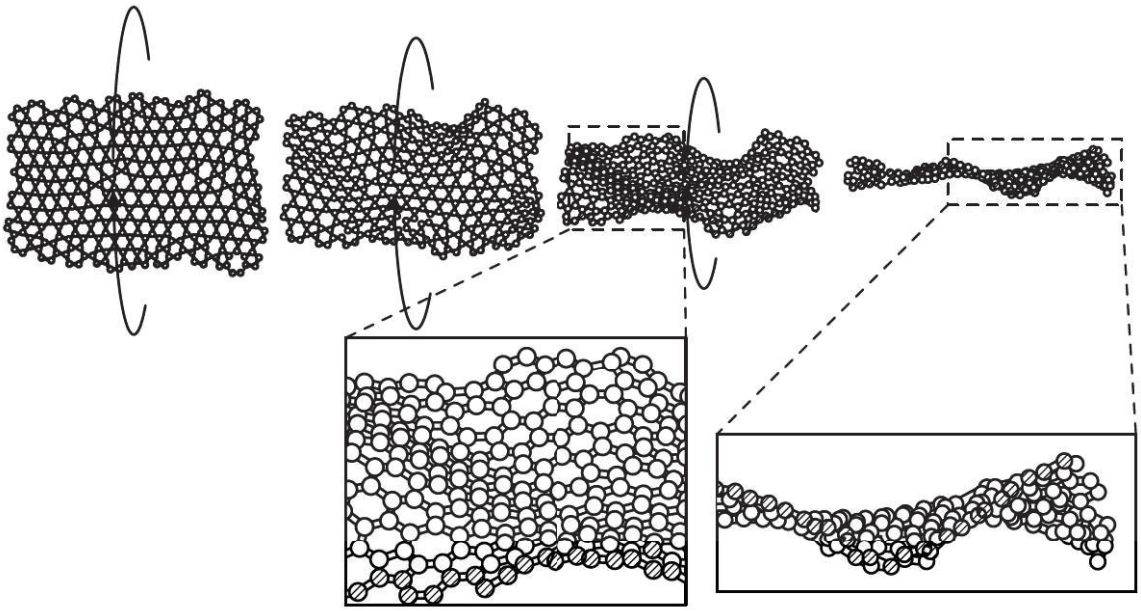

FIG. 4

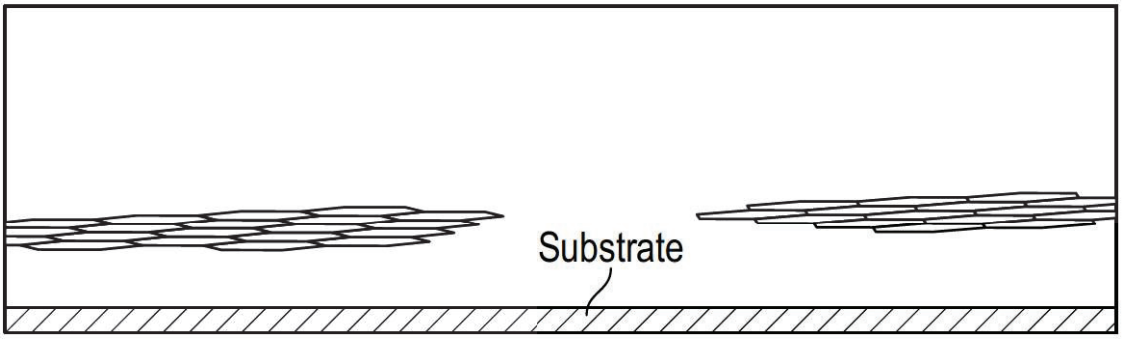

FIG. 5A

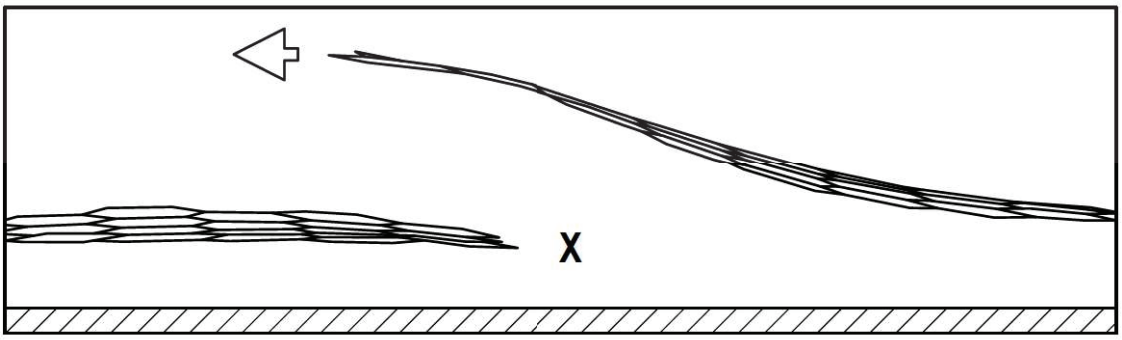

FIG. 5B

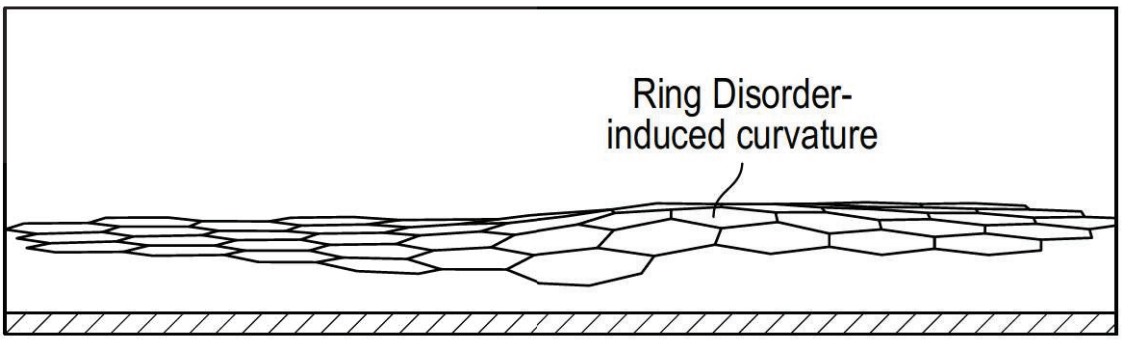

FIG. 5C

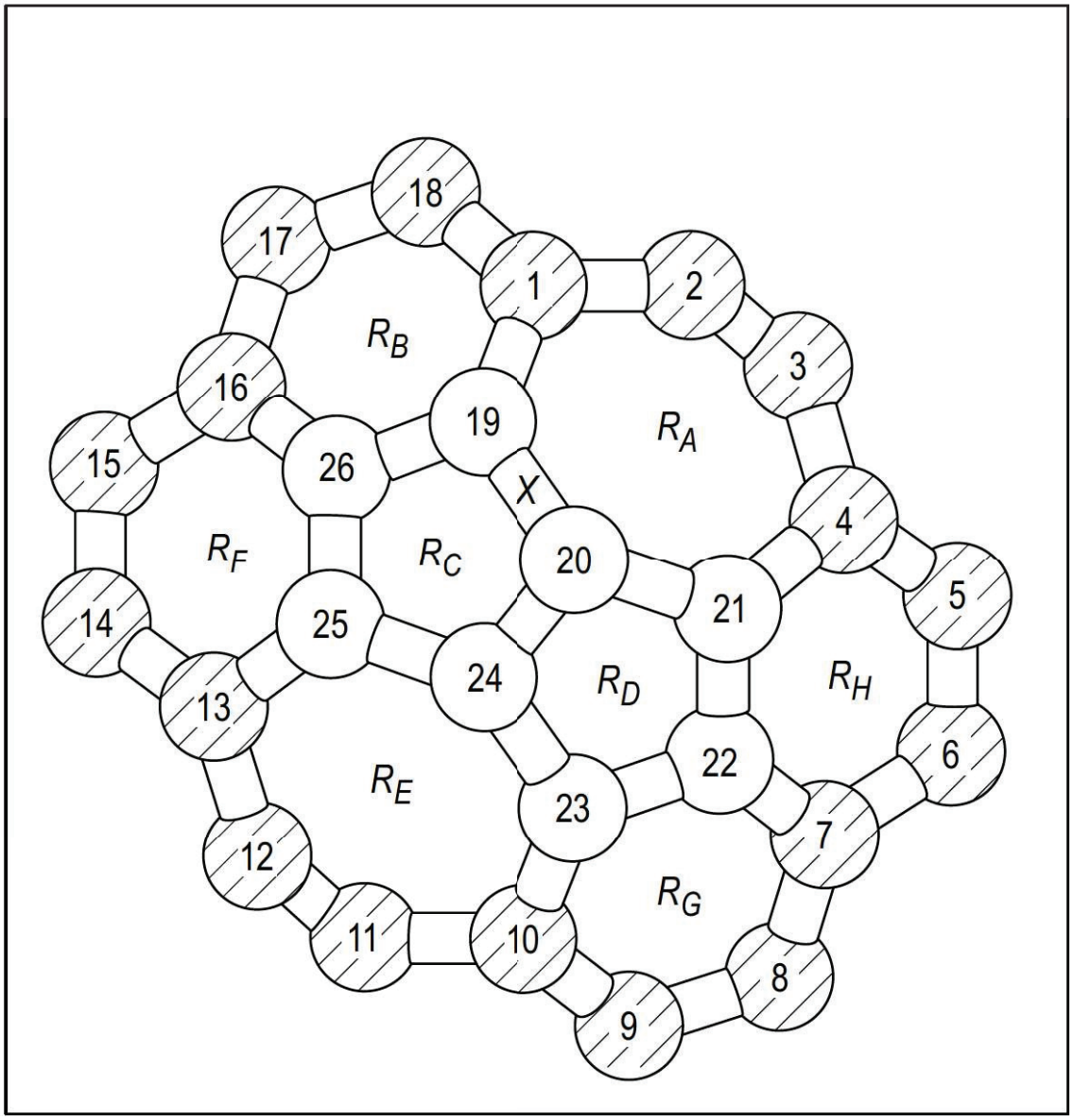
18
17
1
2
R_B
3
16
19
R_A
15
26
X
4
R_F
R_C
20
14
25
21
5
24
R_D
R_H
13
22
6
R_E
23
12
7
R_G
11
10
8
9

FIG. 6A

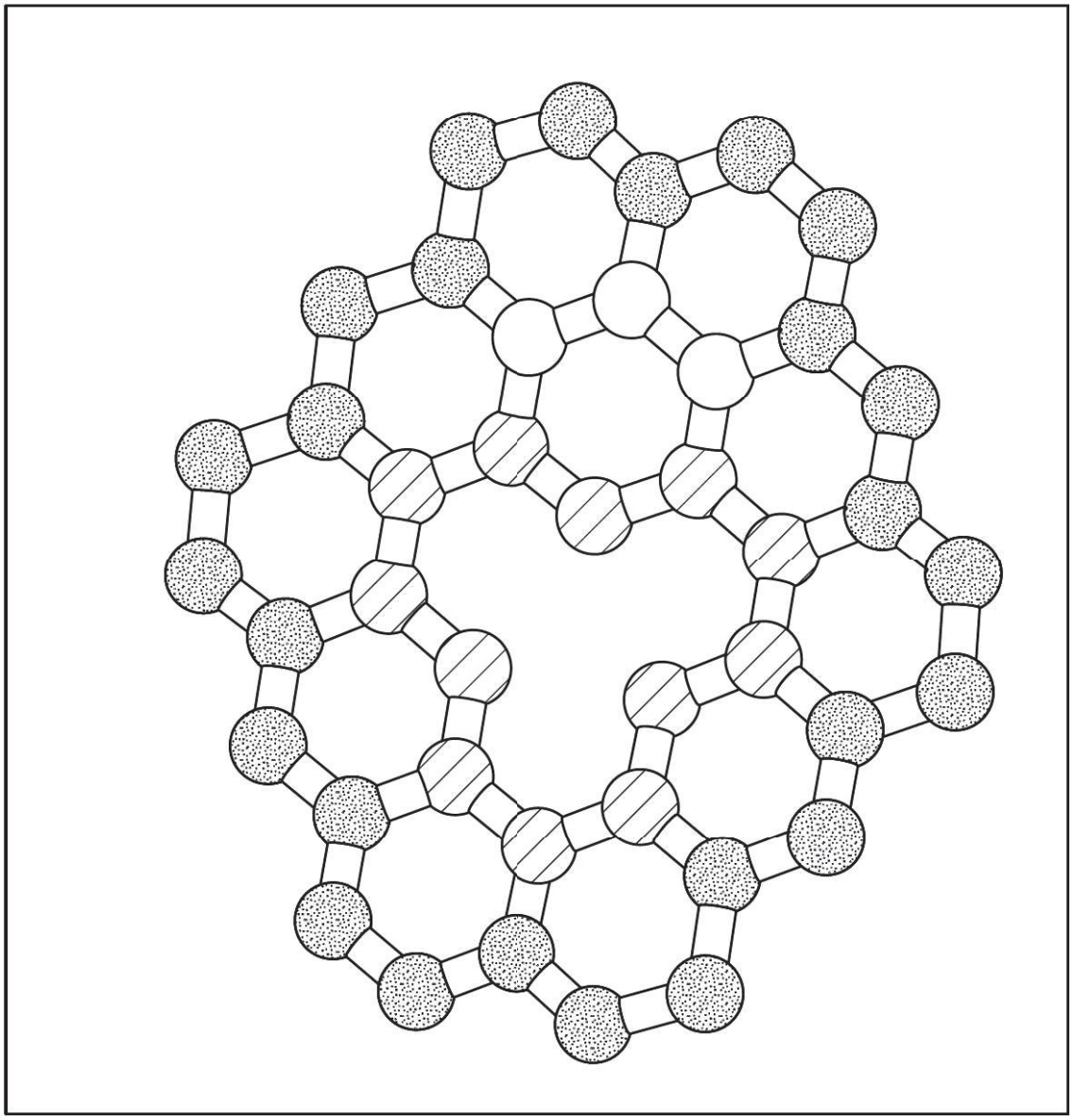

FIG. 6B

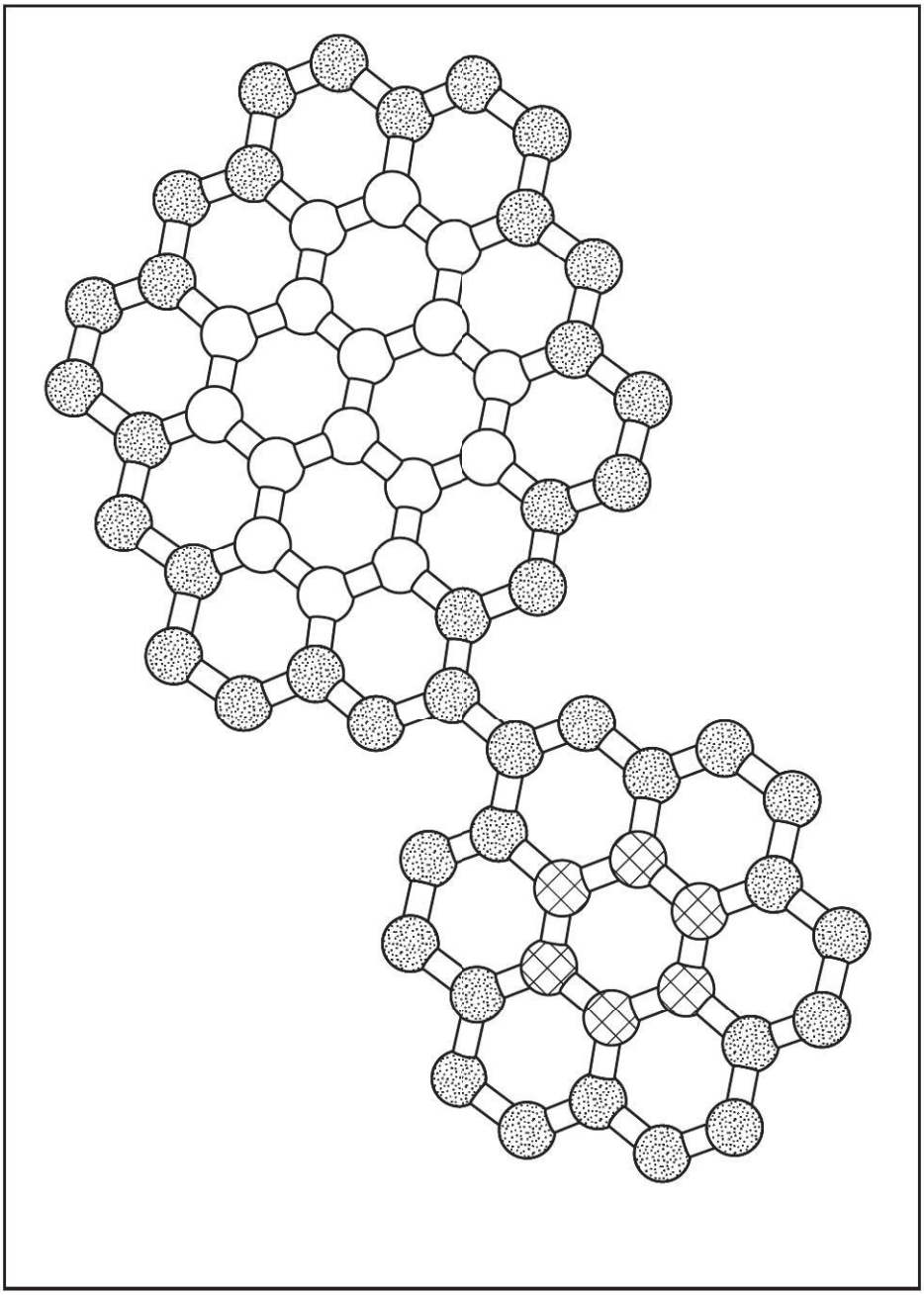

FIG. 6C

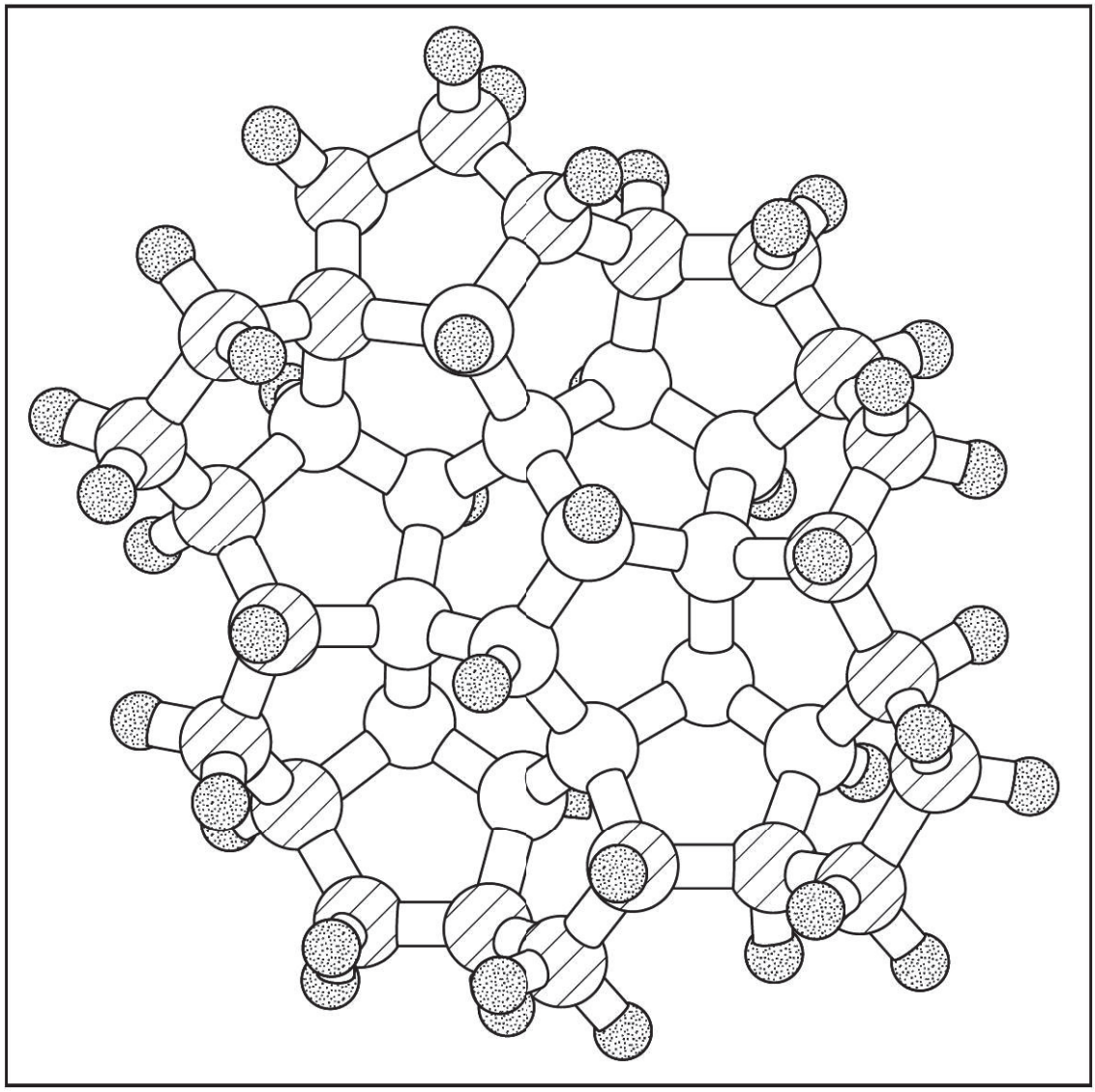

FIG. 6D

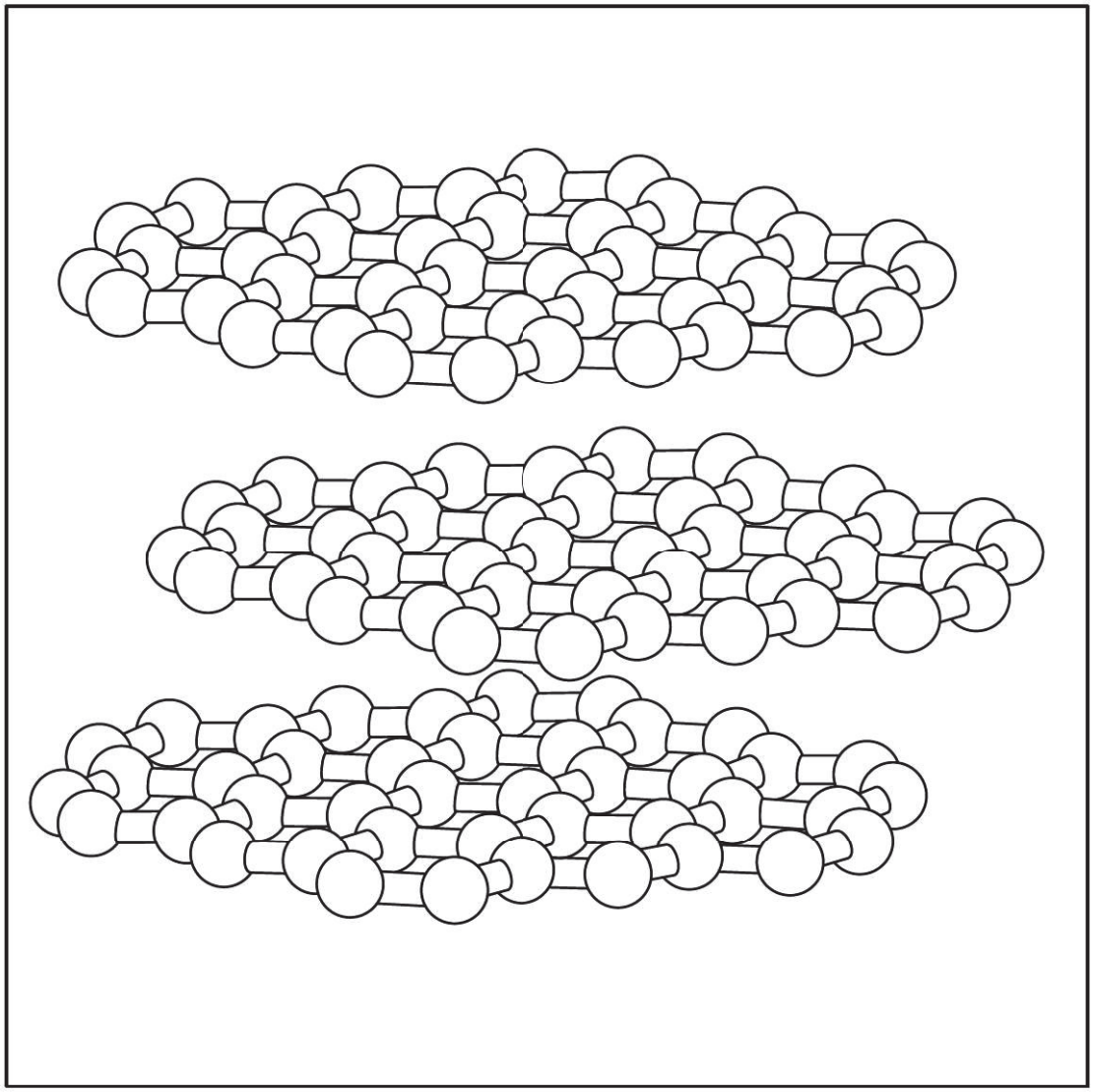

FIG. 6E

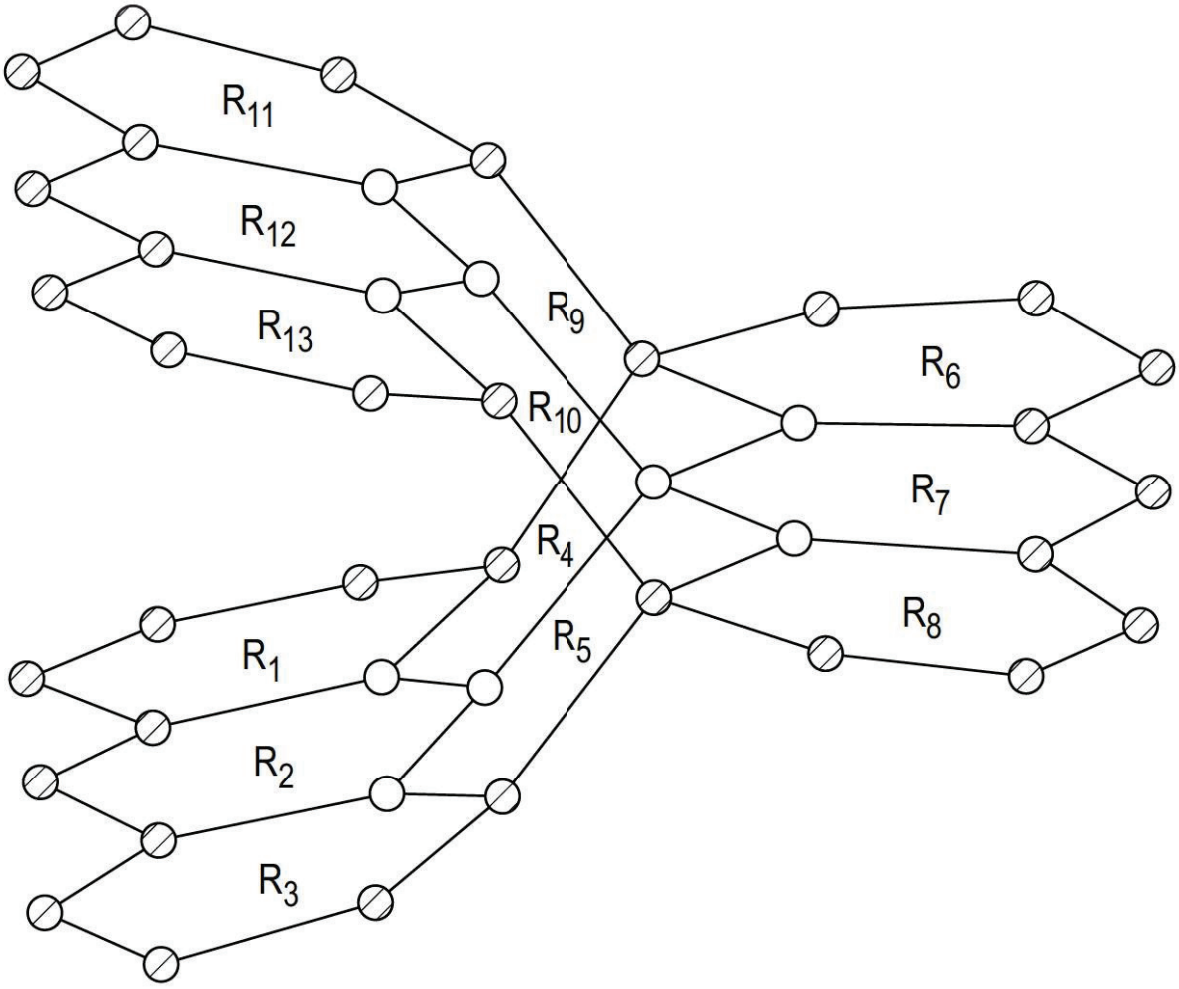

FIG. 7A

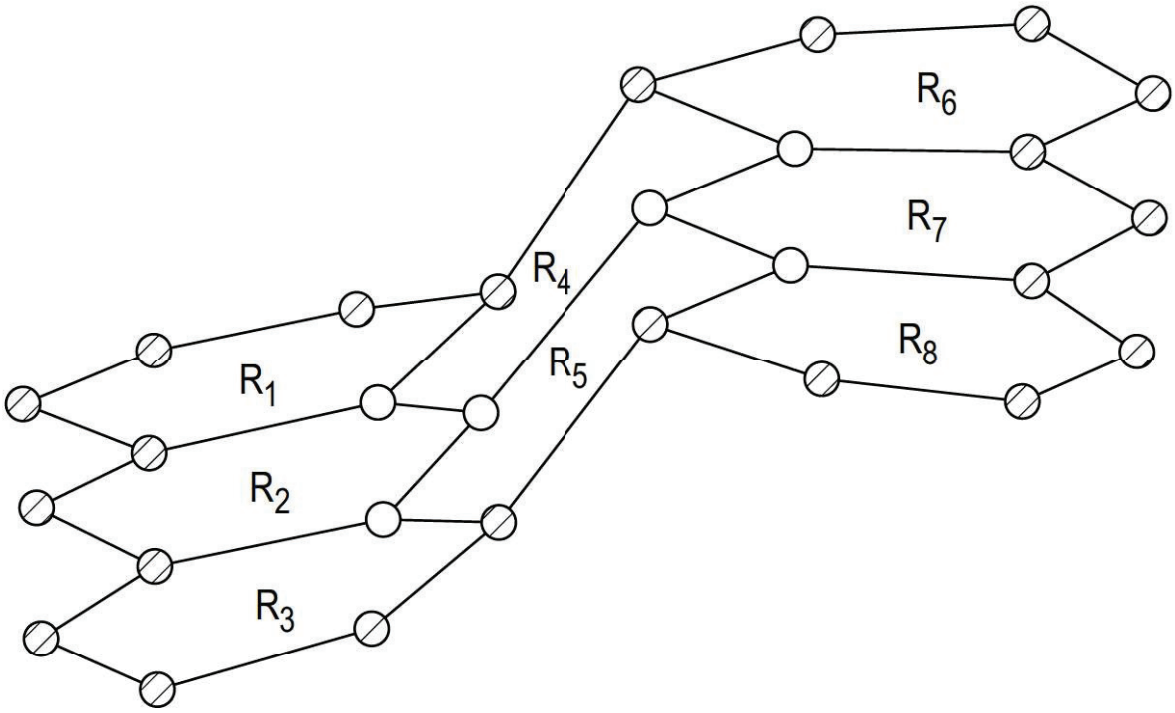

FIG. 7B

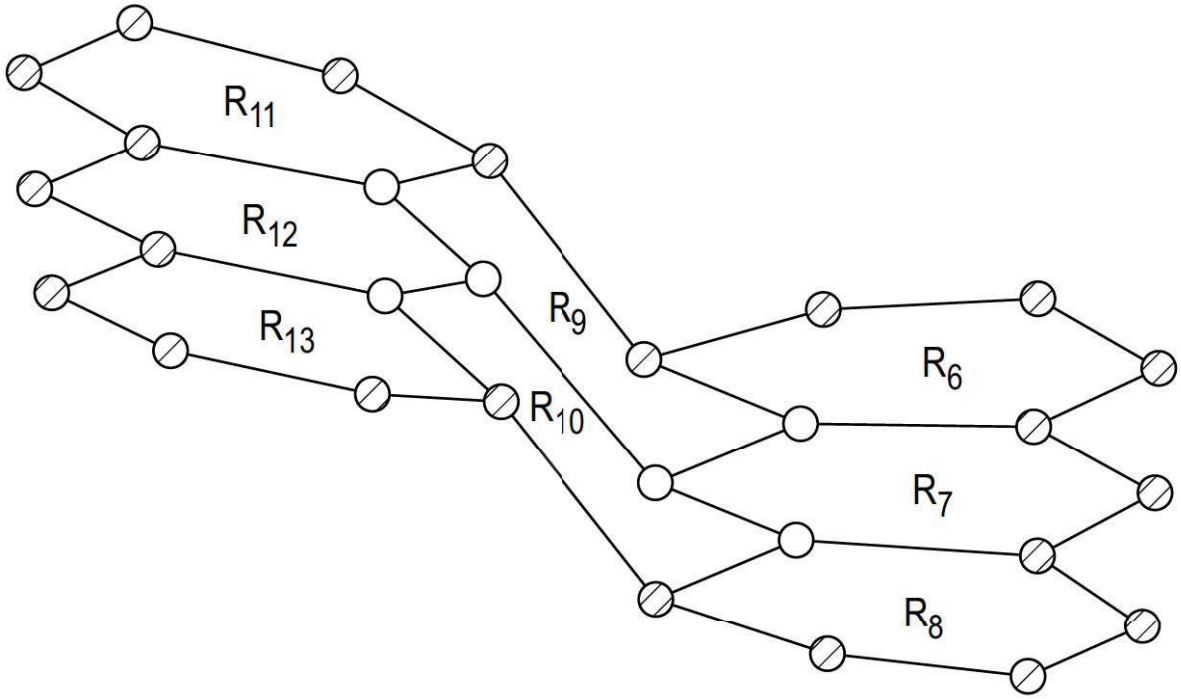

FIG. 7C

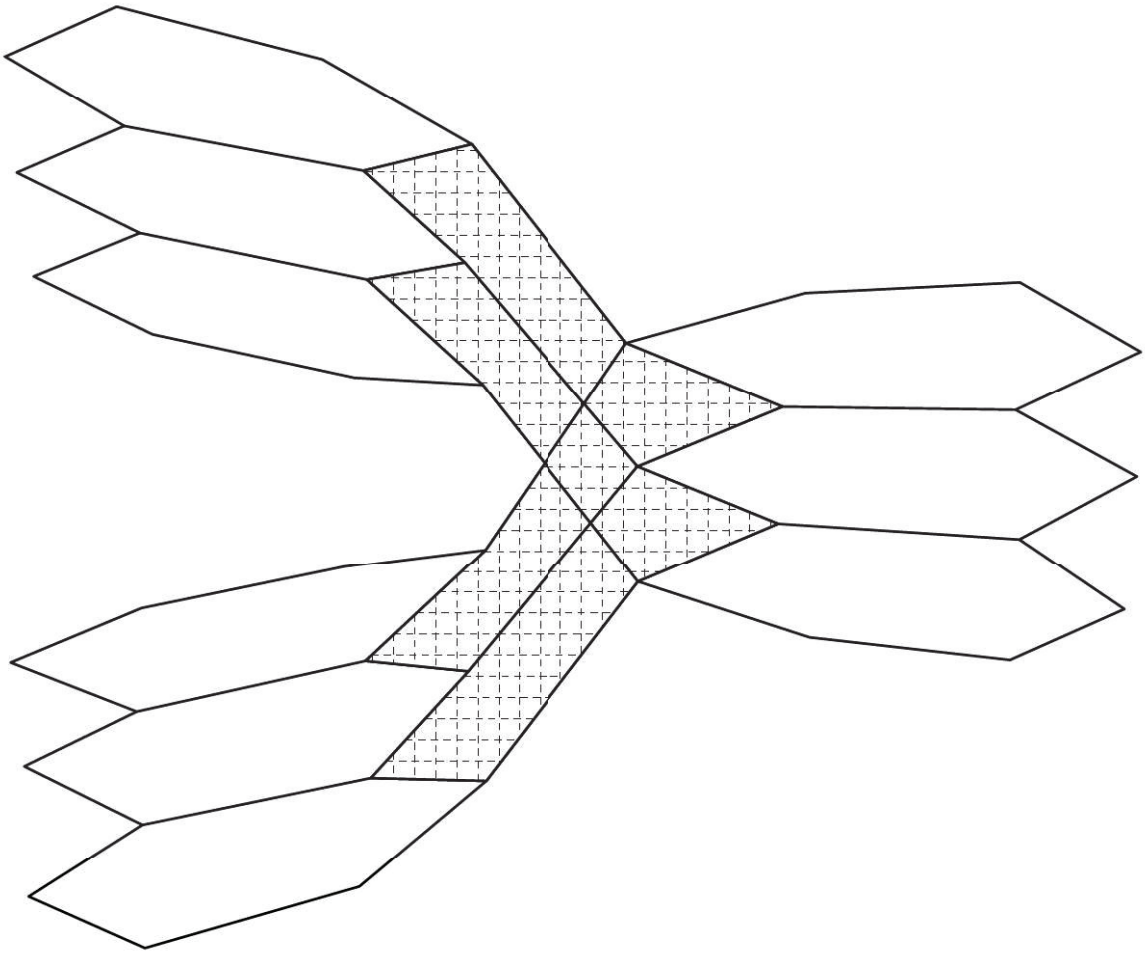

FIG. 7D

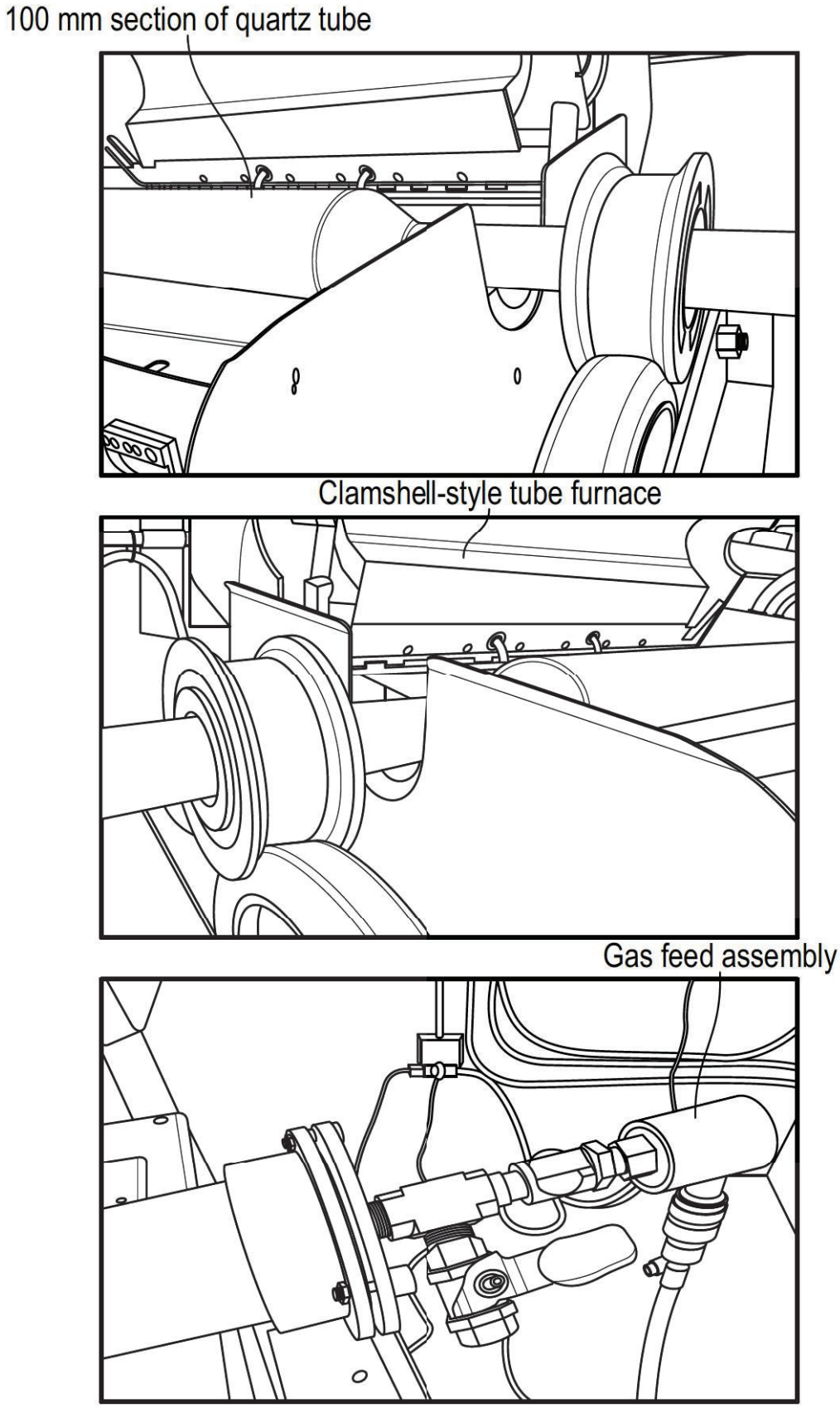
100 mm section of quartz tube
Clamshell-style tube furnace
Gas feed assembly

FIG. 8A

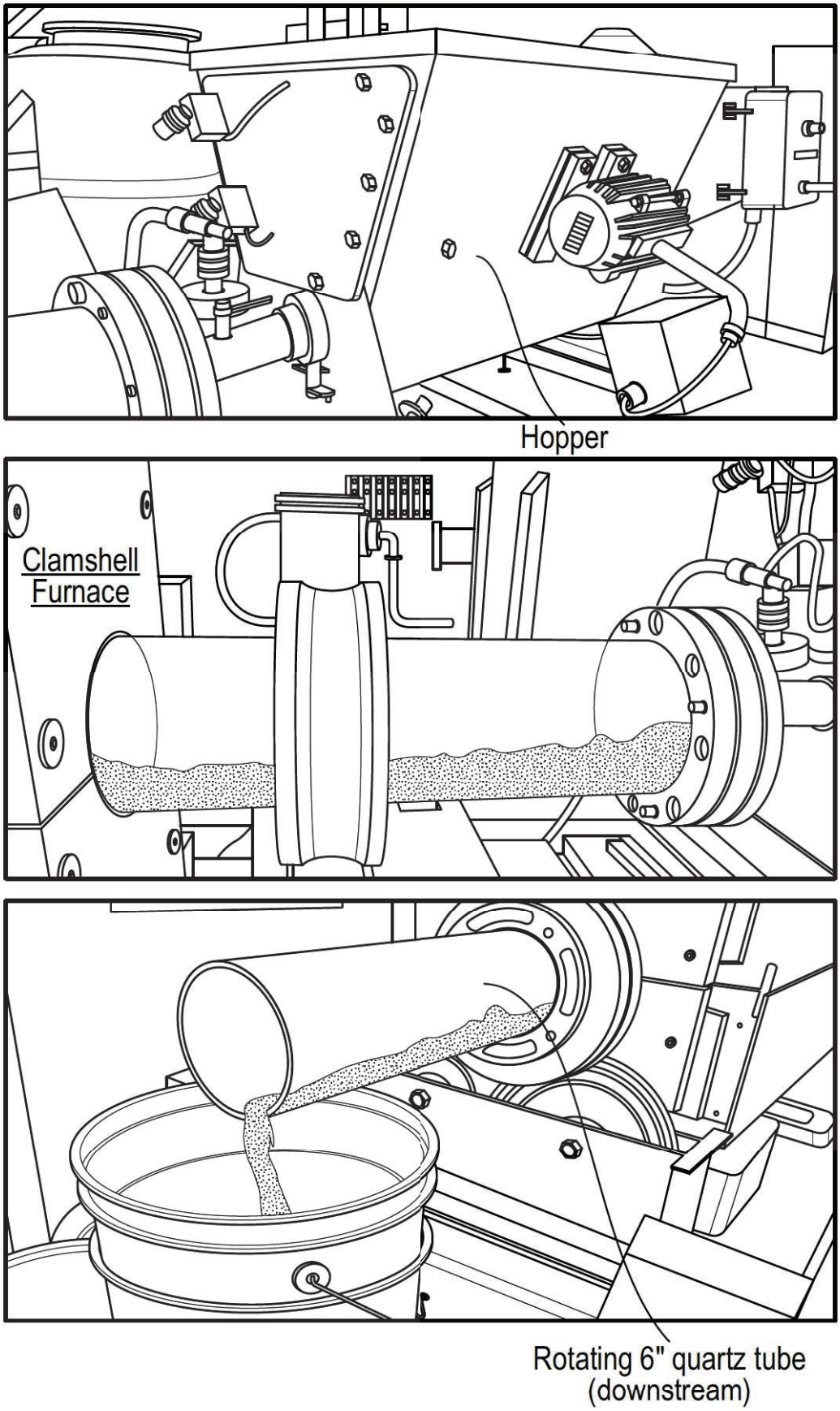
Hopper
Clamshell
Furnace
Rotating 6" quartz tube
(downstream)

FIG. 8B

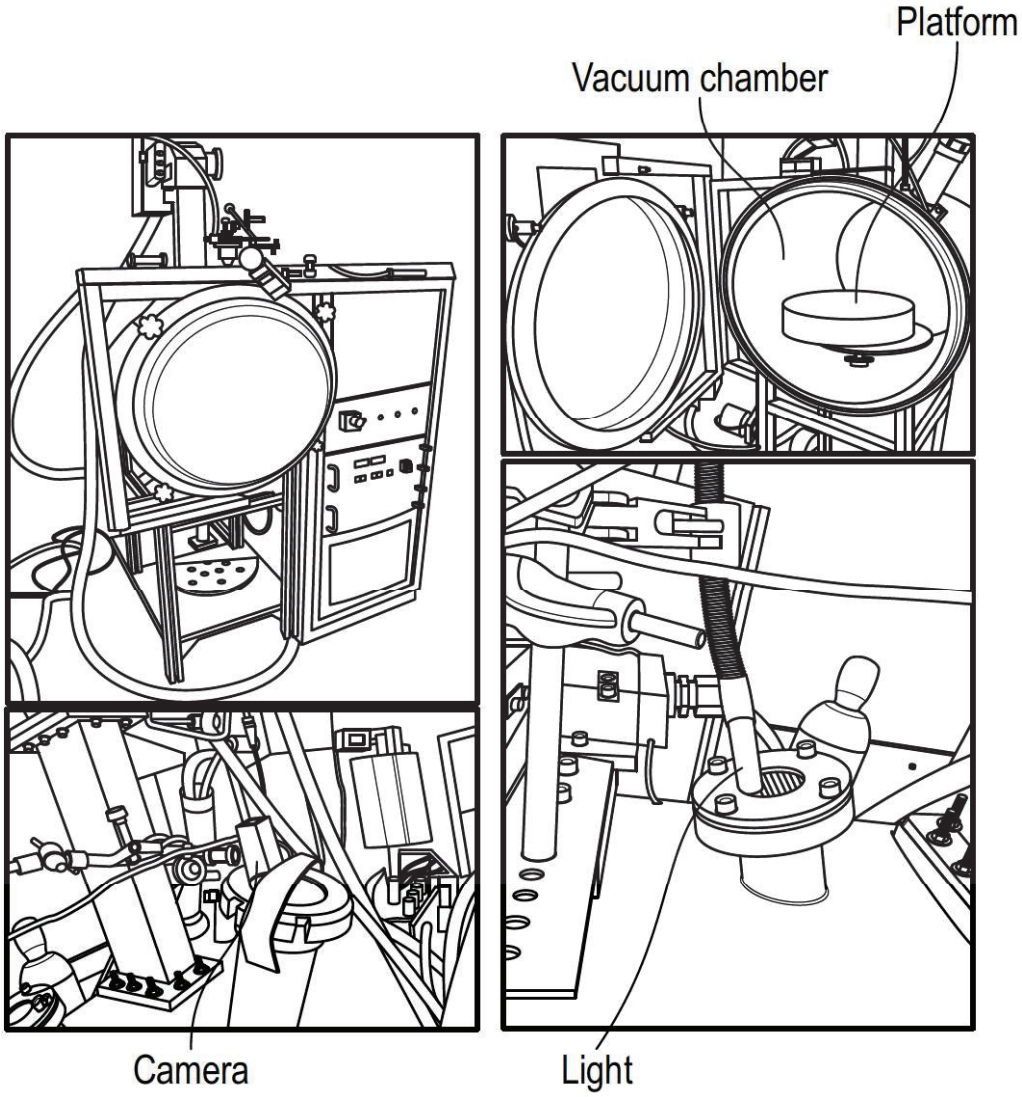

FIG. 8C

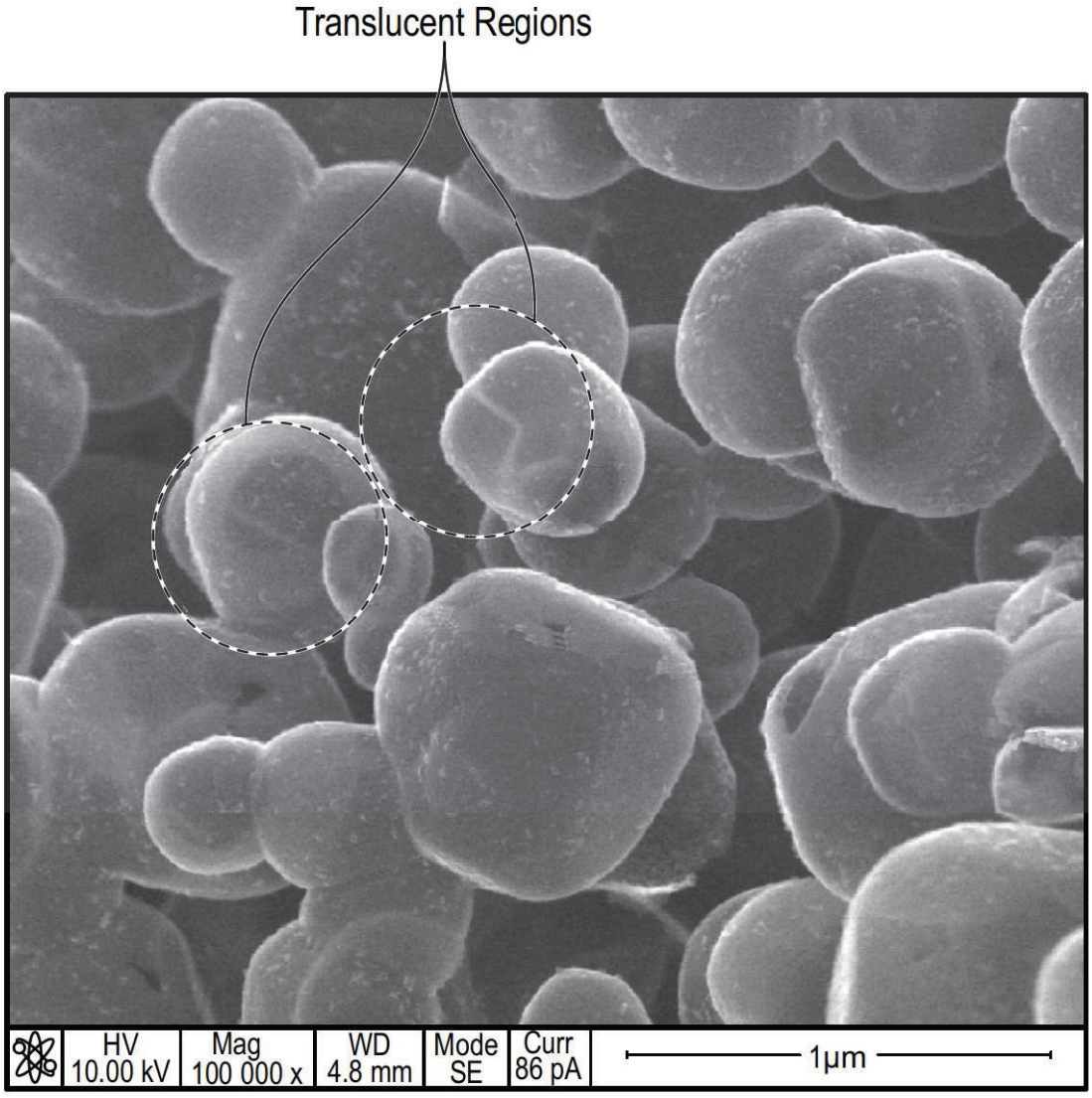
Translucent Regions
HV
10.00 kV
Mag
100 000 x
WD
4.8 mm
Mode
SE
Curr
86 pA
1µm

FIG. 9

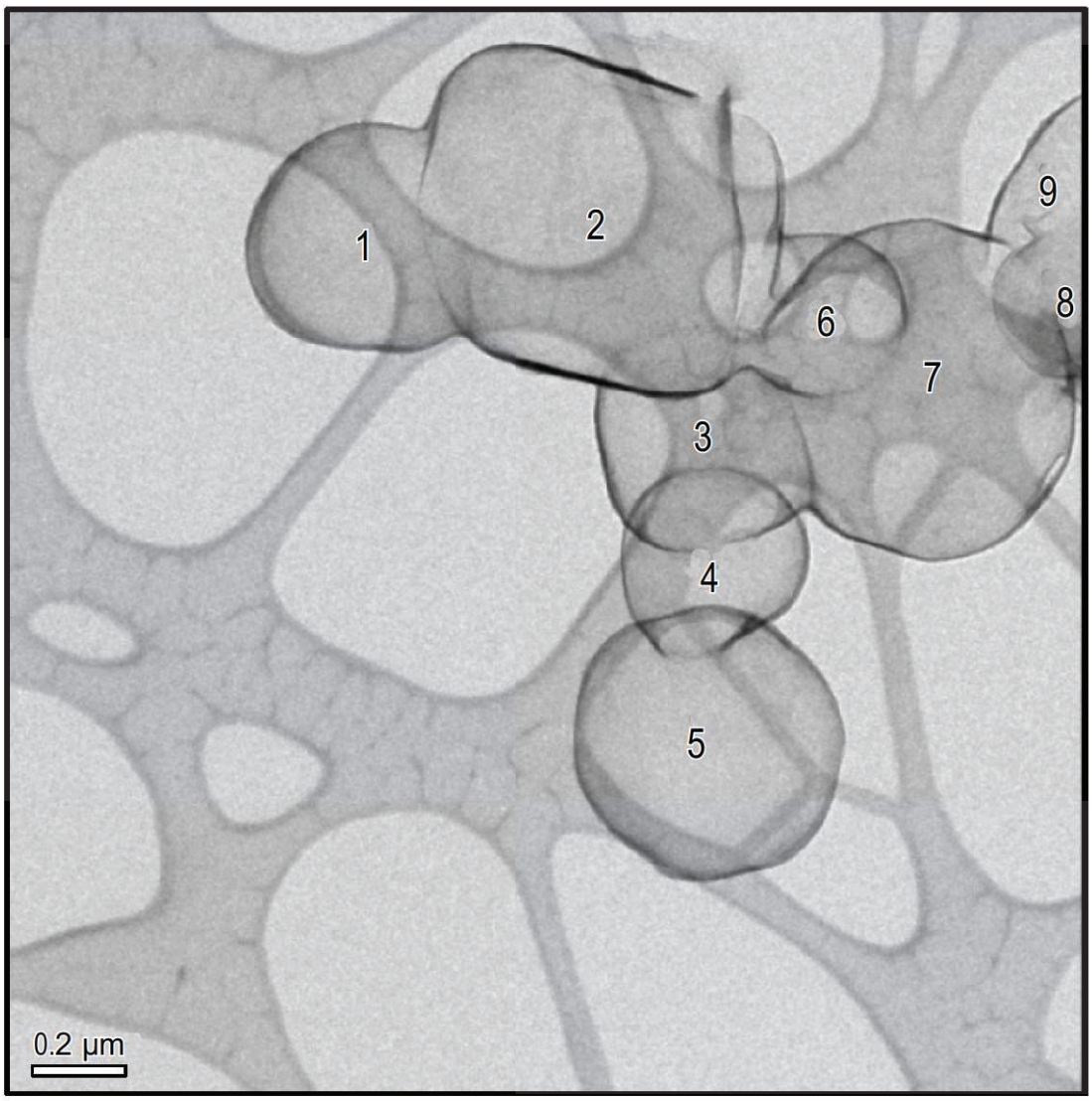

FIG. 10A

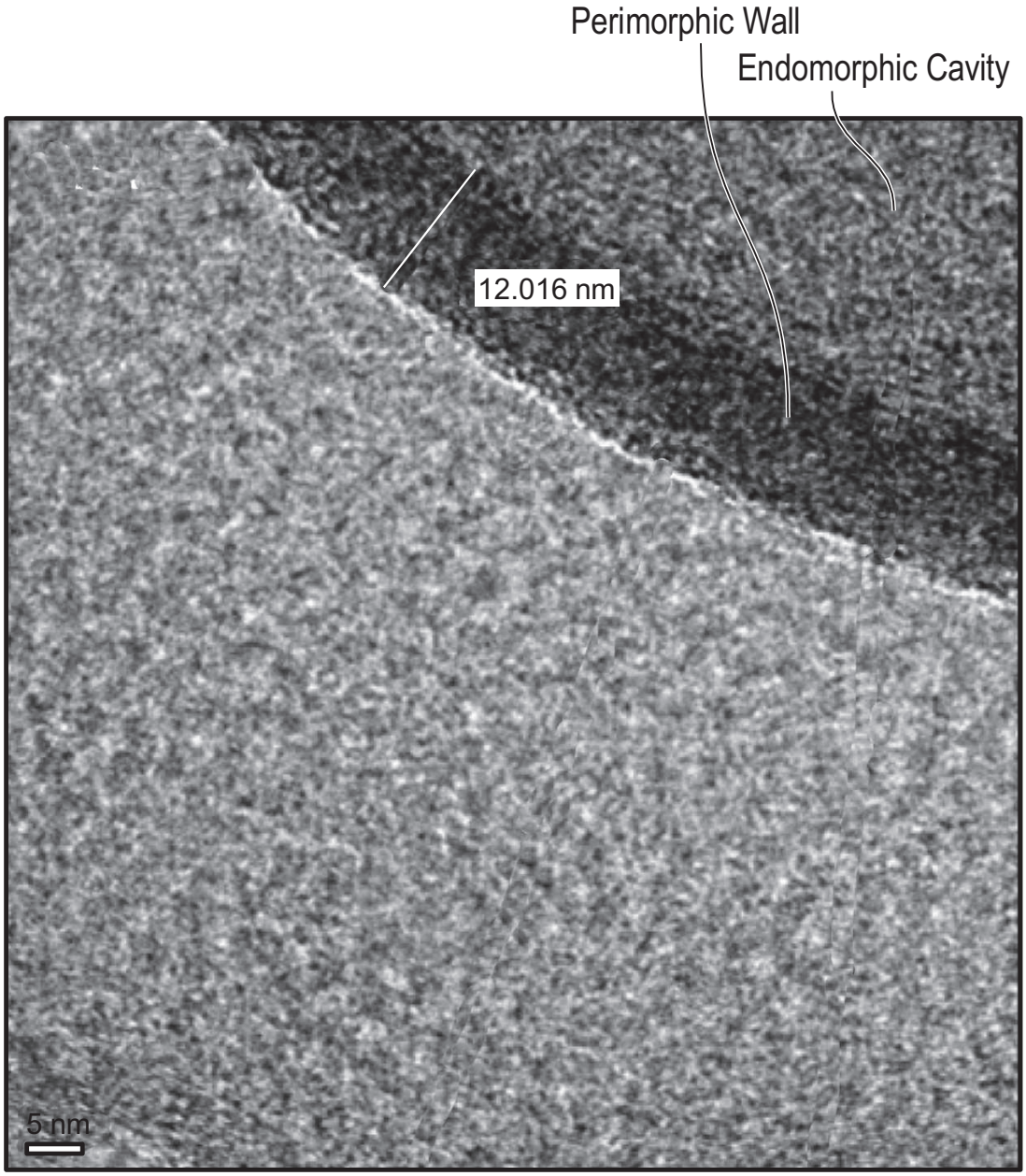

FIG. 10B

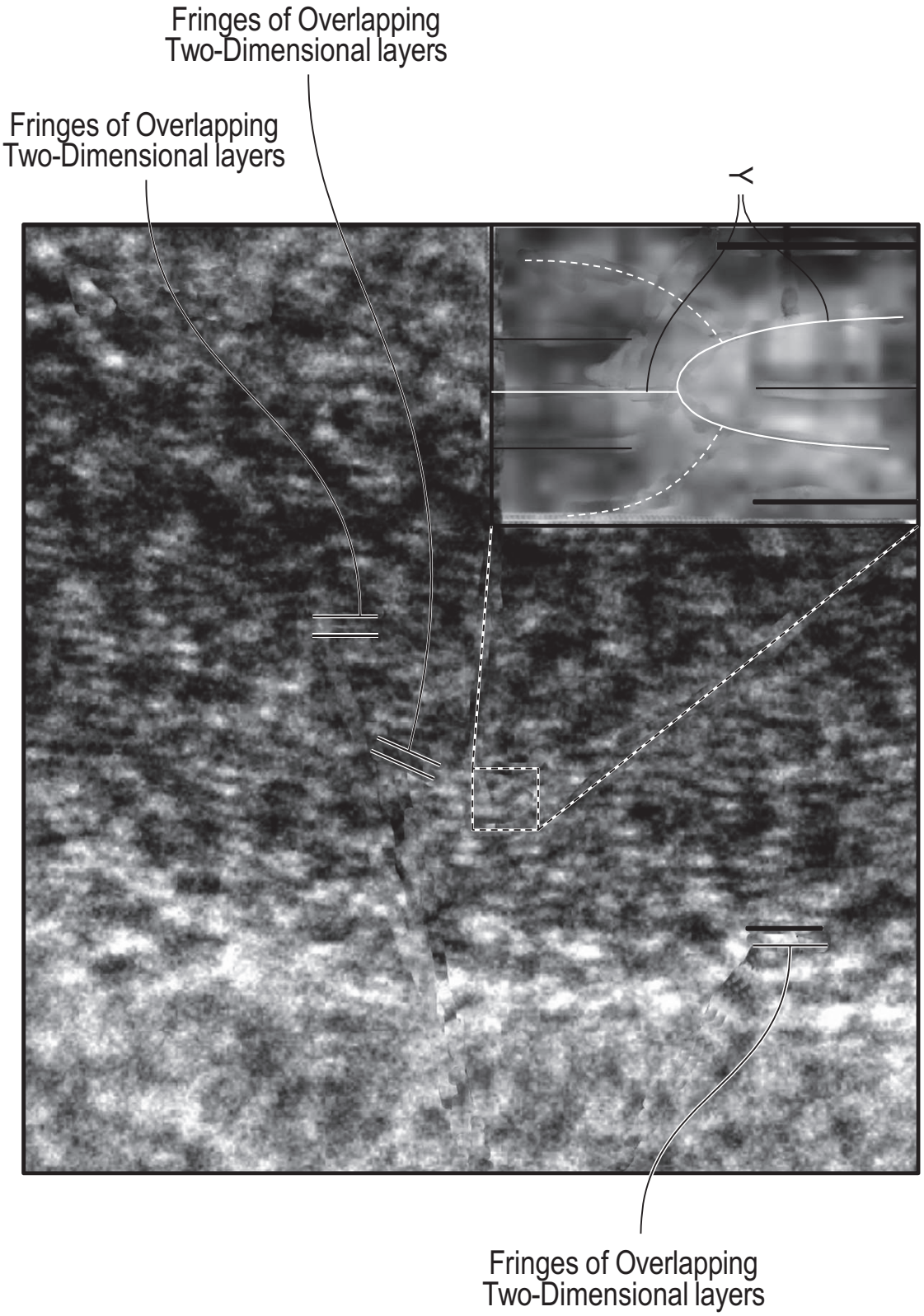
Fringes of Overlapping
Two-Dimensional layers
Fringes of Overlapping
Two-Dimensional layers
Fringes of Overlapping
Two-Dimensional layers

FIG. 10C

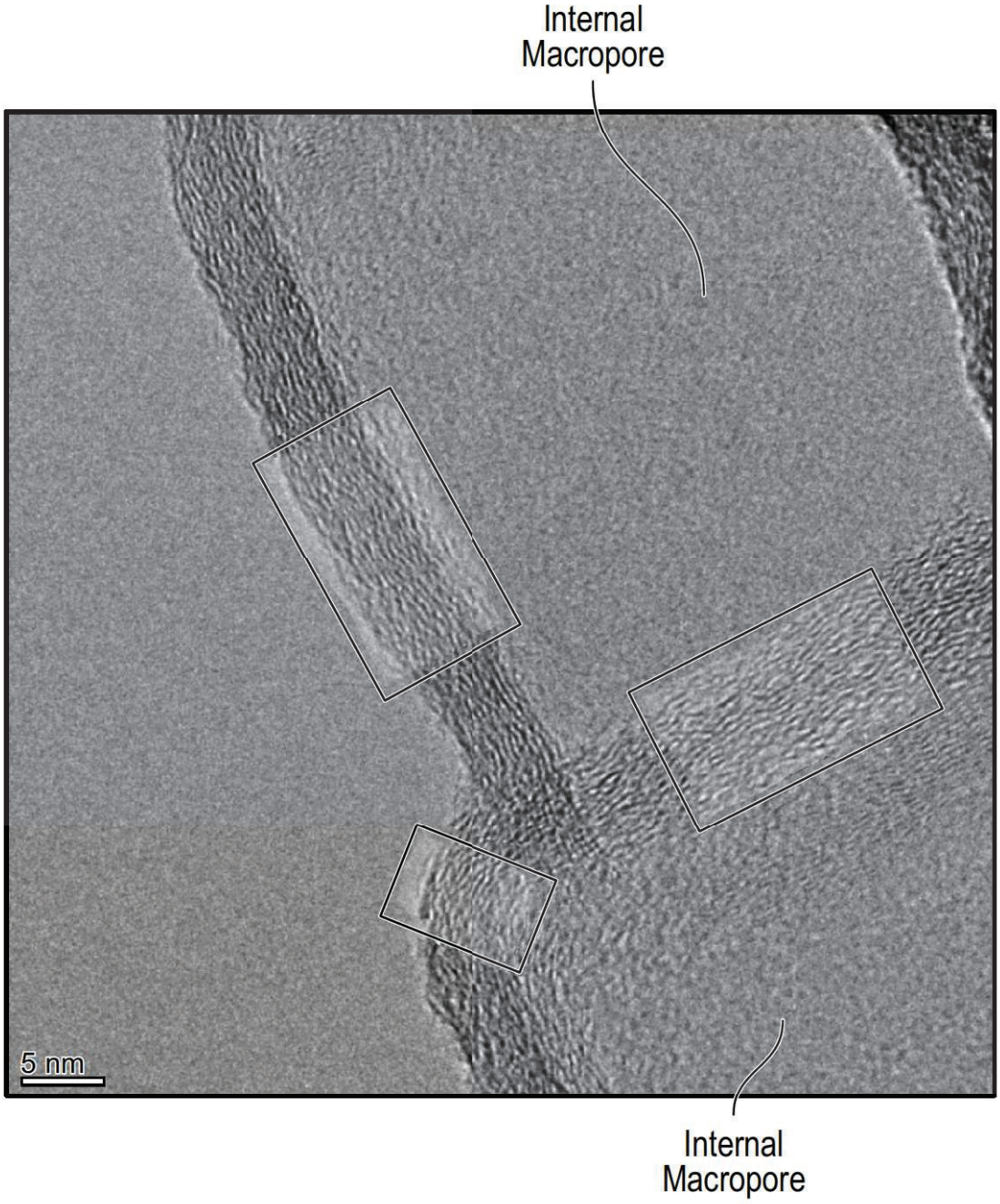

FIG. 11

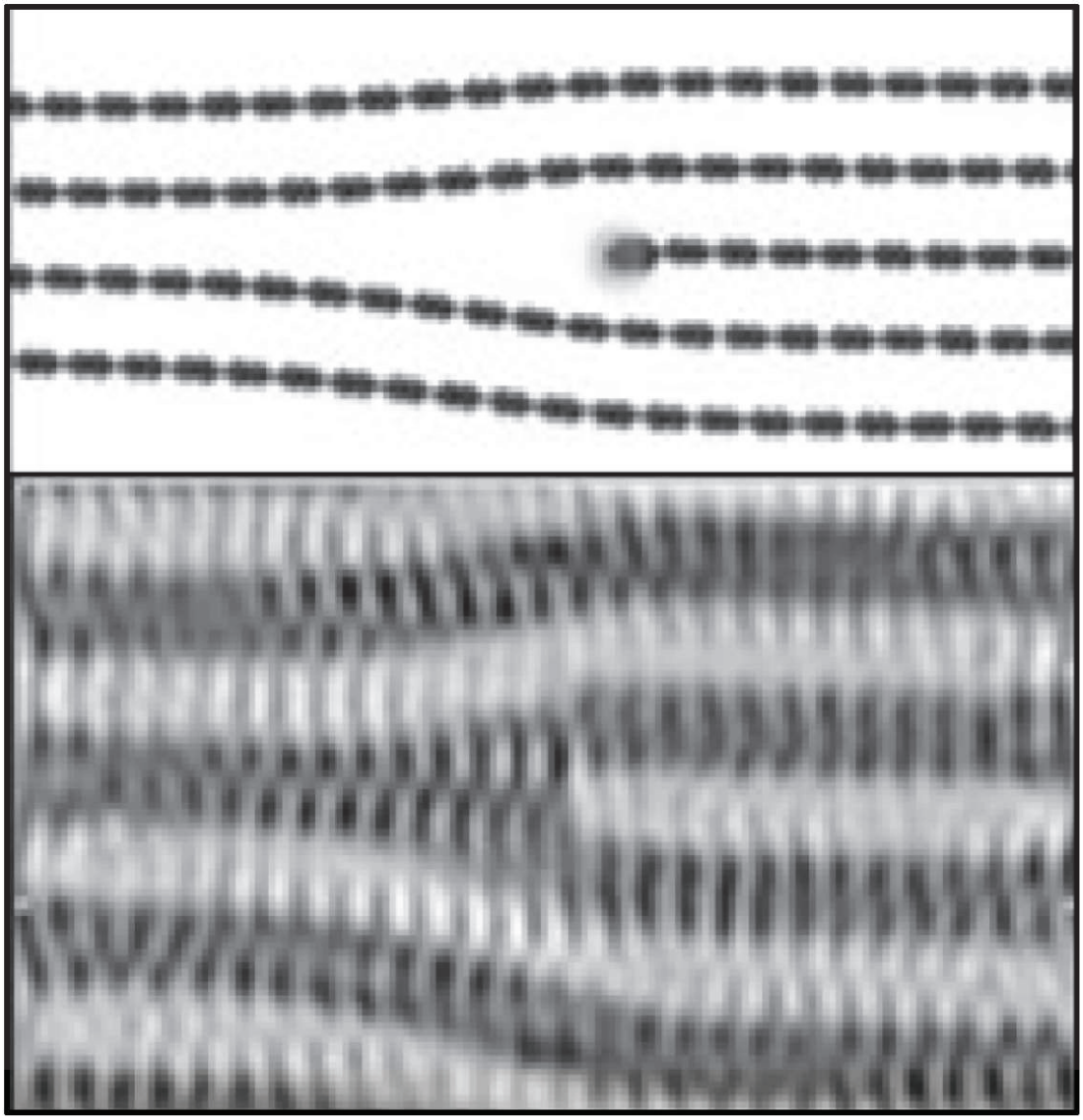

FIG. 12A

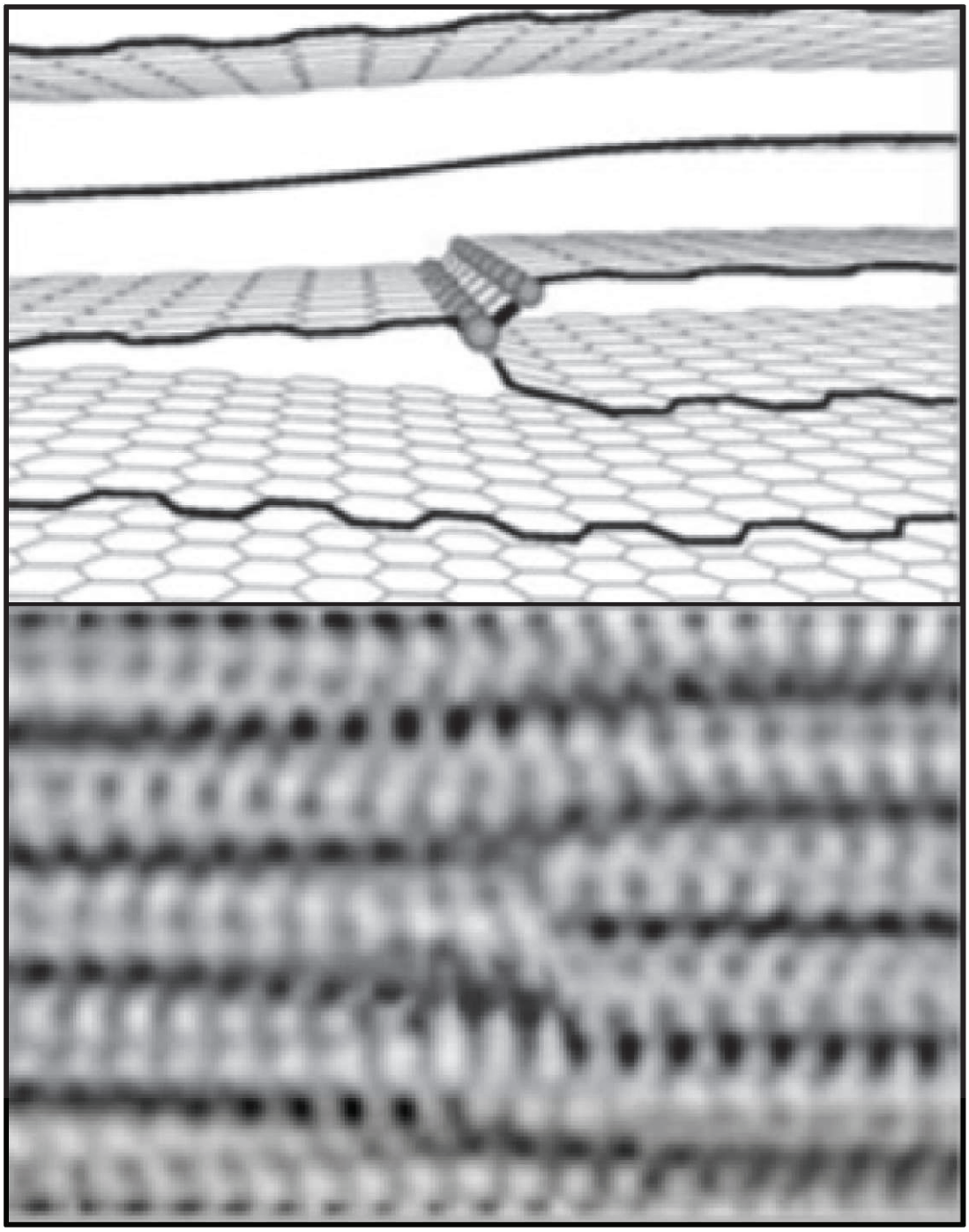

FIG. 12B

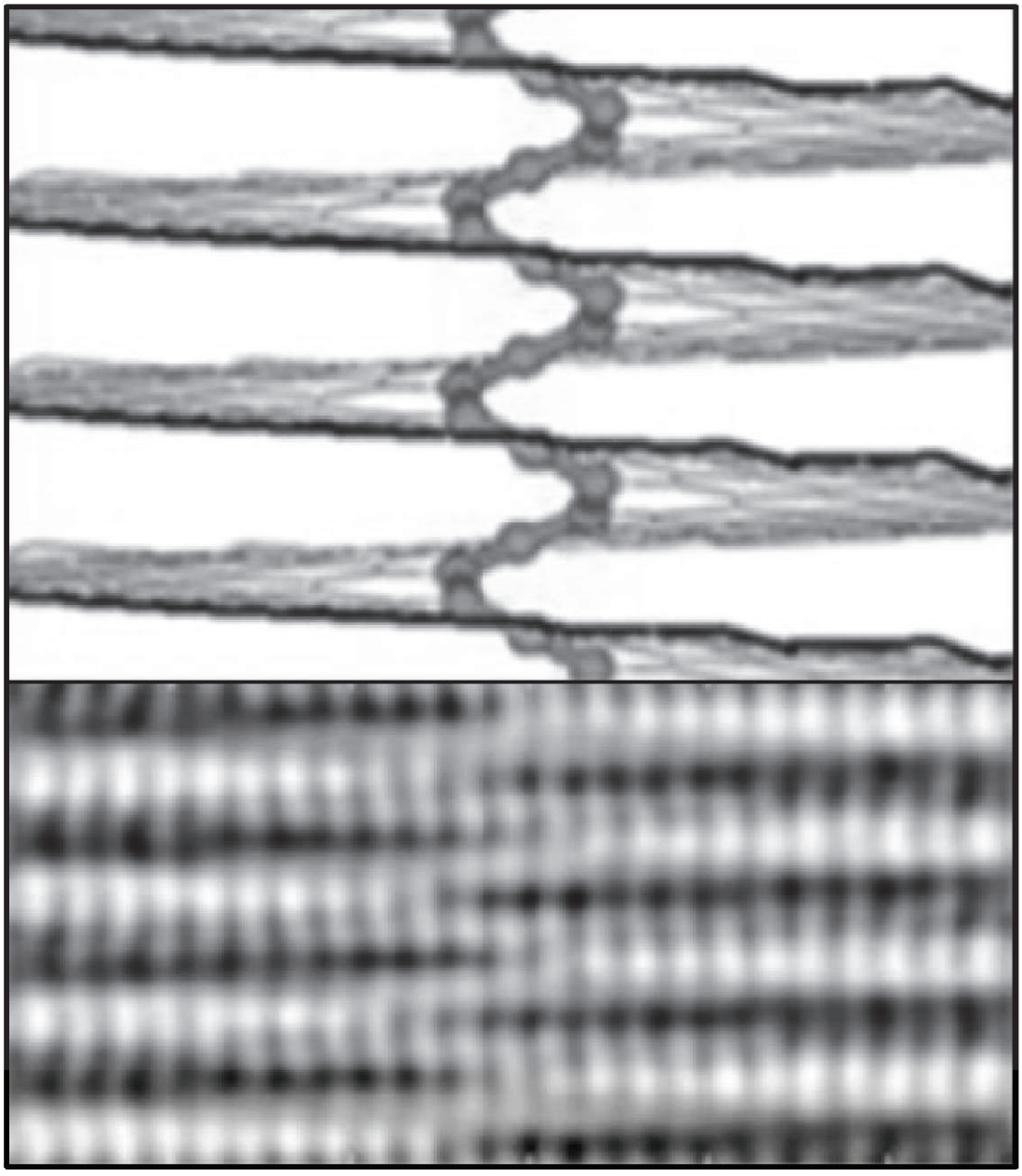

FIG. 12C

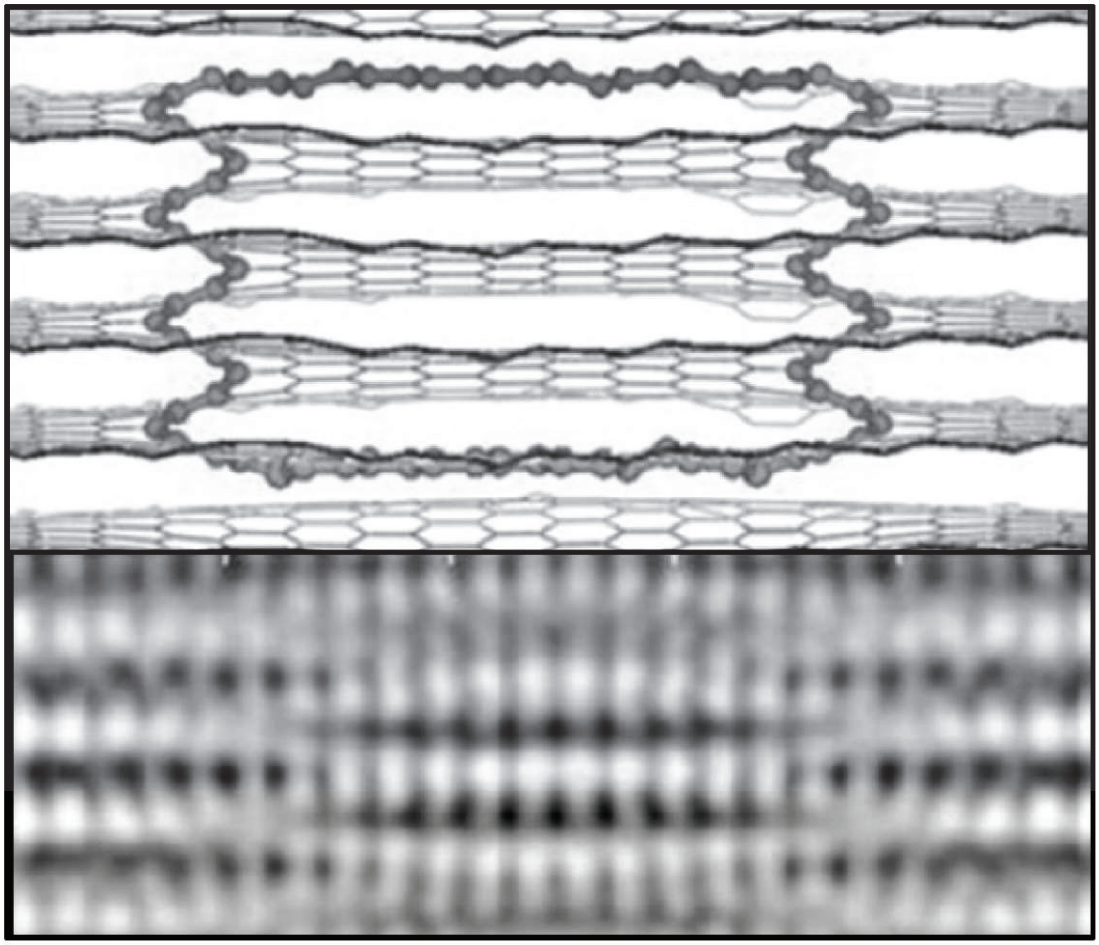

FIG. 12D

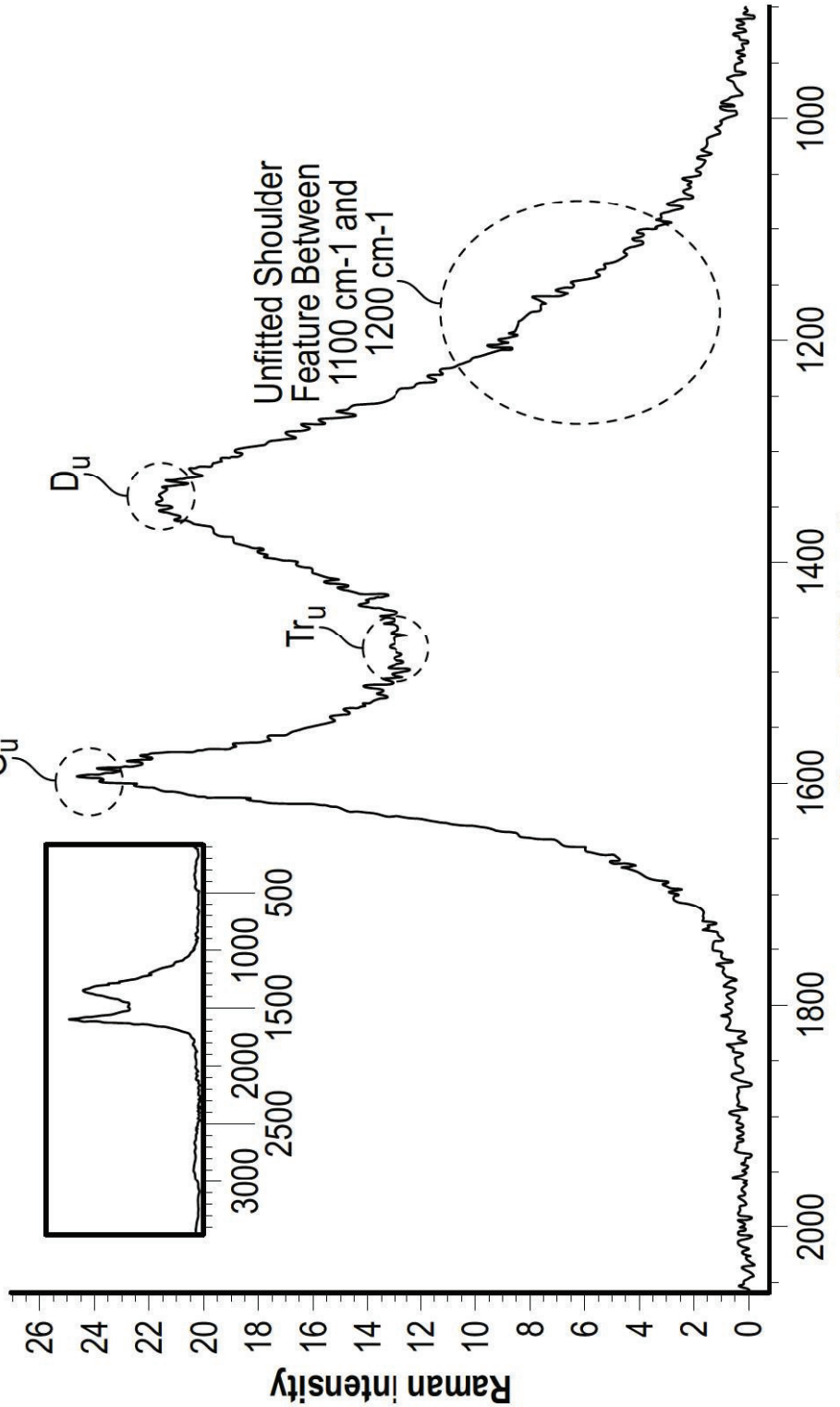
Raman intensity
0
2
4
6
8
10
12
14
16
18
20
22
24
26
2000
1800
1600
1400
1200
1000
Raman Shift (cm-1)
G_u
Tr_u
D_u
Unfitted Shoulder Feature Between 1100 cm-1 and 1200 cm-1
3000
2500
2000
1500
1000
500

FIG. 13

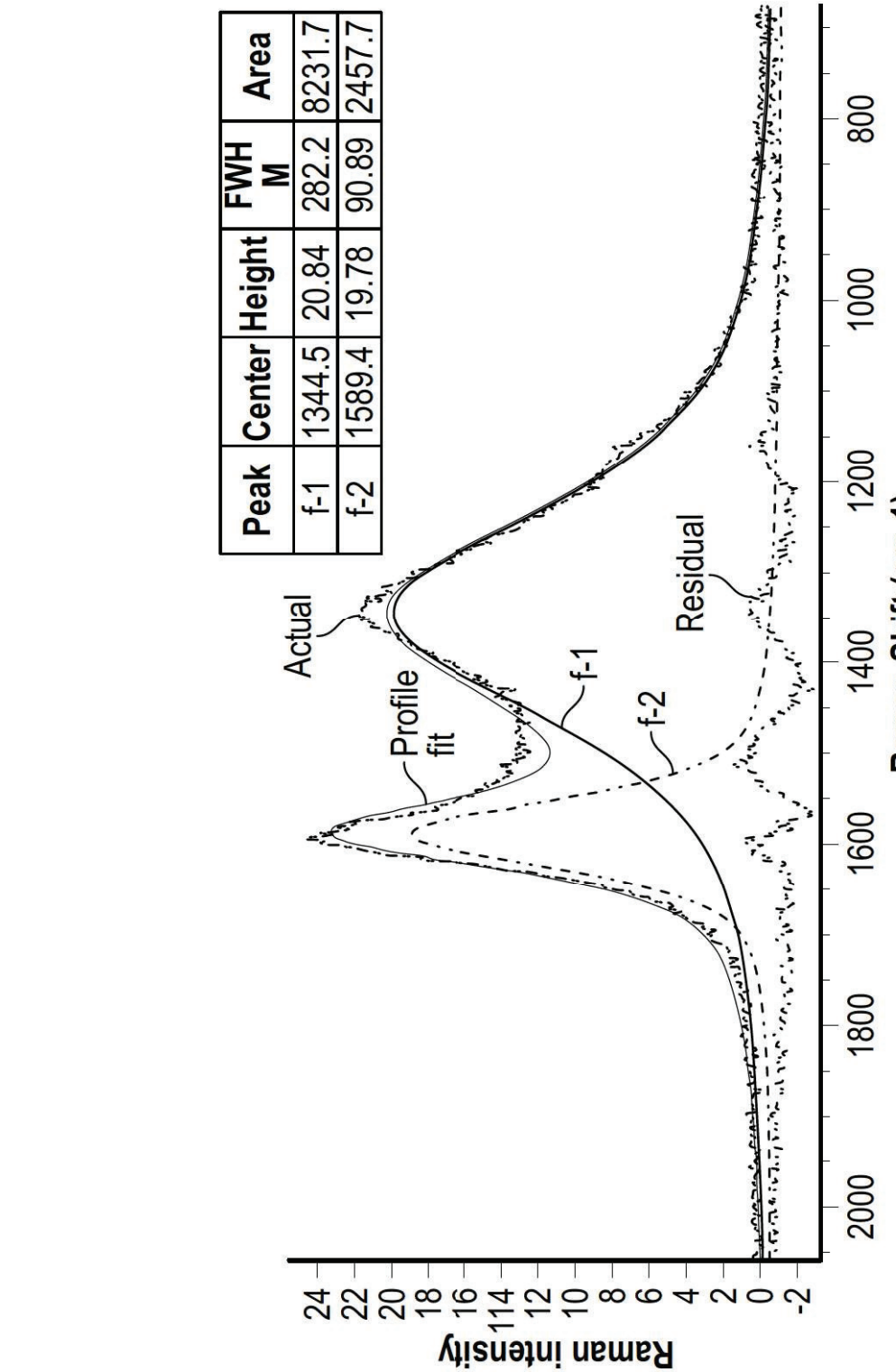
Peak | Center | Height | FWHM | Area
f-1 | 1344.5 | 20.84 | 282.2 | 8231.7
f-2 | 1589.4 | 19.78 | 90.89 | 2457.7
Actual
Profile fit
f-1
f-2
Residual
Raman intensity
Raman Shift (cm-1)
24
22
20
18
16
14
12
10
8
6
4
2
0
-2
2000
1800
1600
1400
1200
1000
800

FIG. 14

Peak #	Center	Height	FWHM	Area
f-1	1339.8	21.78	252..5	8397.8
f-2	1566.5	9.047	146.9	1415.1
f-3	1596.8	12.57	57.89	927.91

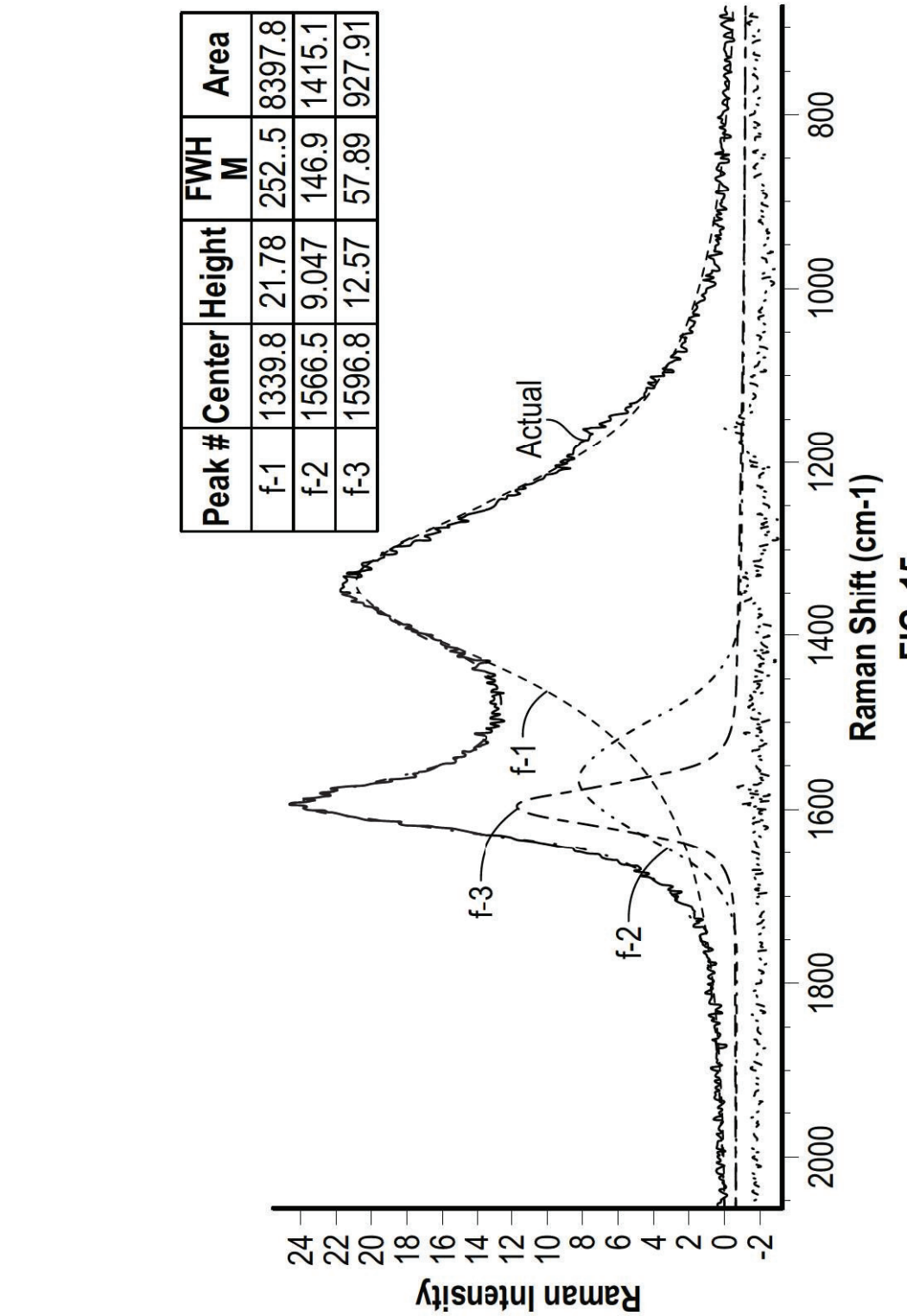

FIG. 15

Peak #	Center	Height	FWHM	Gauss	Area
f-1	1185	6.35	180.0	.720	1375
f-2	1343	19.33	167.2	.999	3440
f-3	1514	8.99	153.8	.889	1548
f-4	1596	19.51	77.1	.118	2266

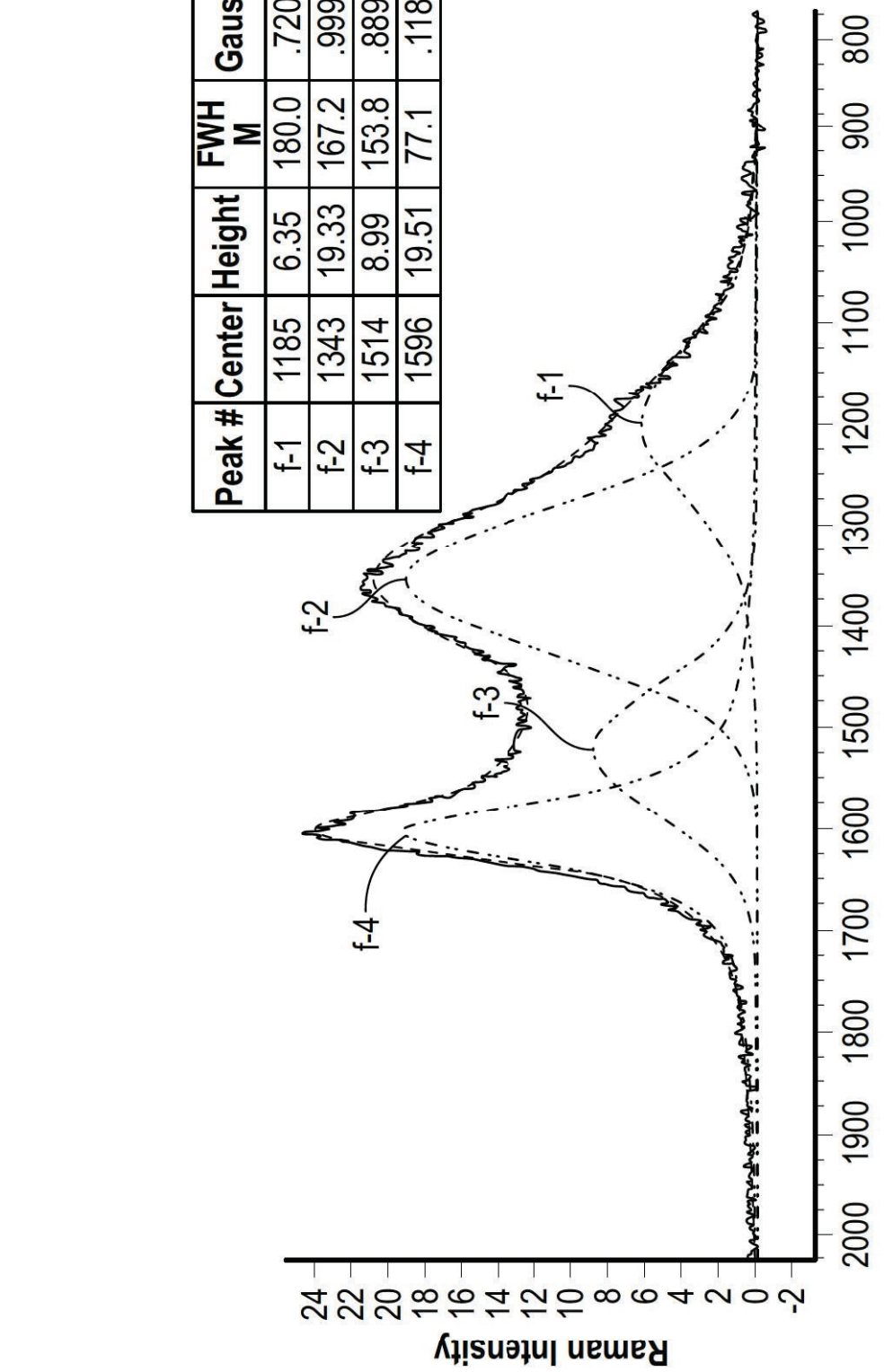

FIG. 16

Peak #	Center	Height	FWHM	Gauss	Area
f-1	1180	1.29	167.1	.606	272
f-2	1349	4.76	154.3	.639	914
f-3	1482	2.41	153.4	.552	477
f-4	1596	5.29	99.5	.409	717

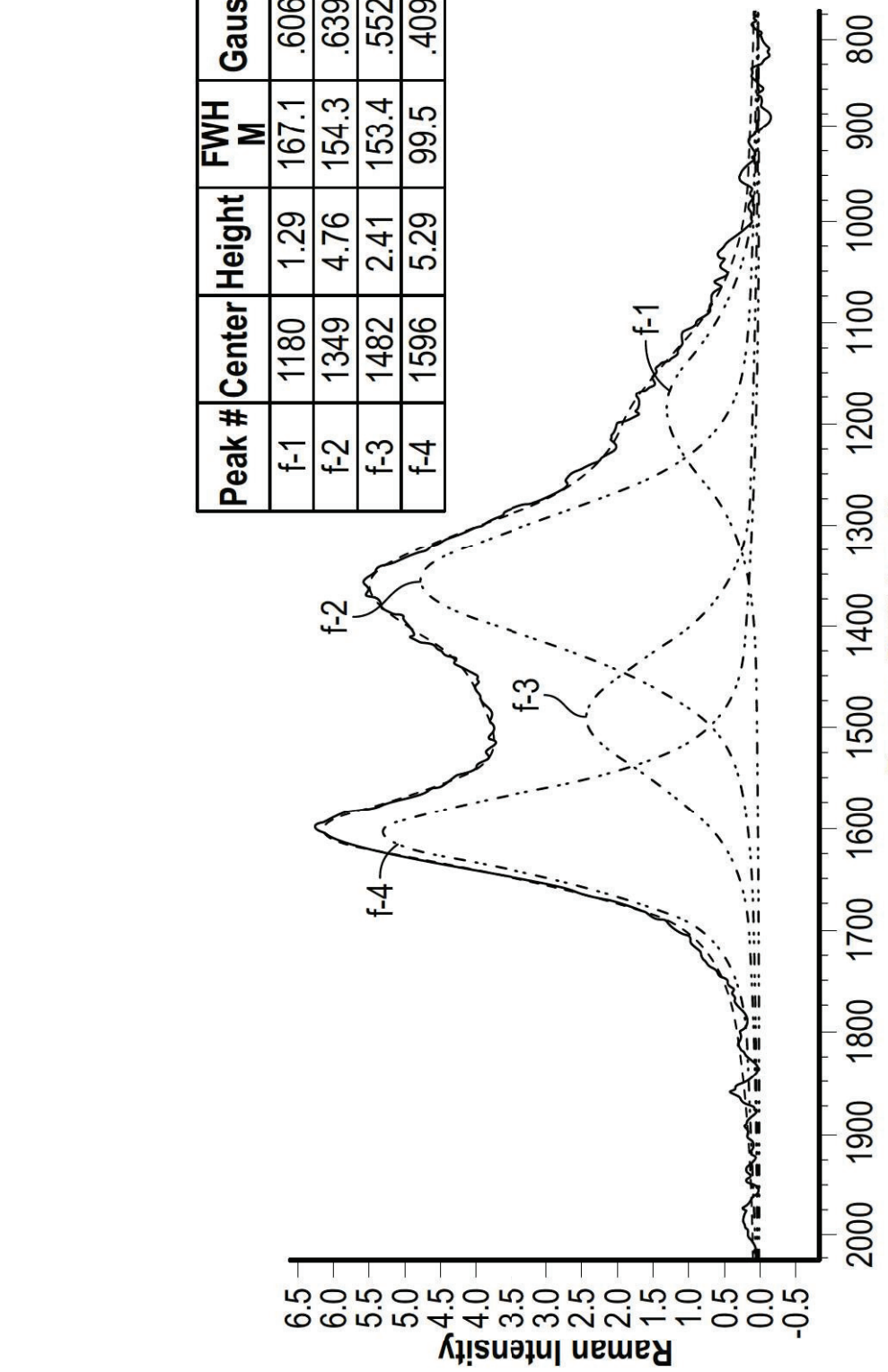

FIG. 17

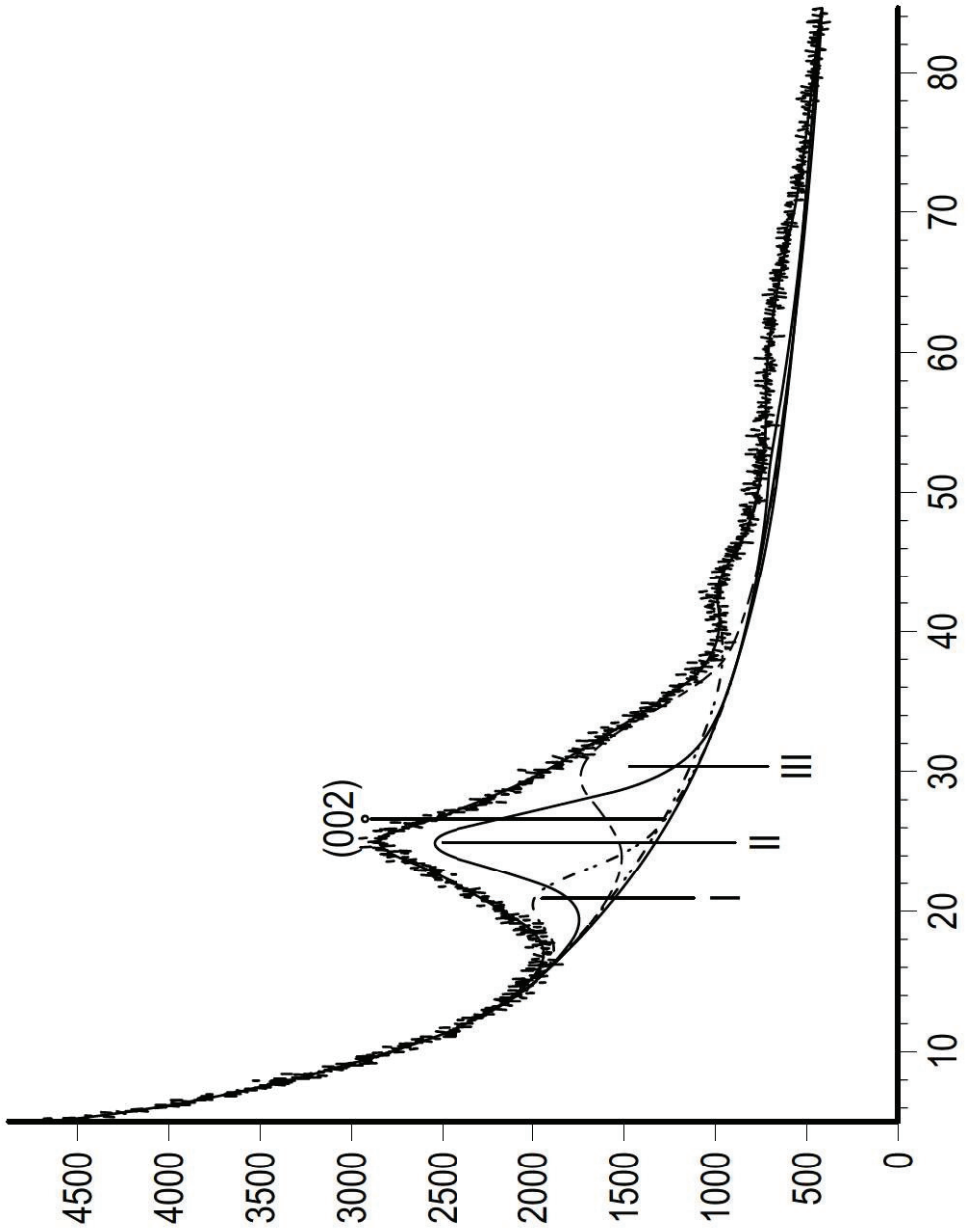
4500
4000
3500
3000
2500
2000
1500
1000
500
0
10
20
30
40
50
60
70
80
(002)
I
II
III

FIG. 18

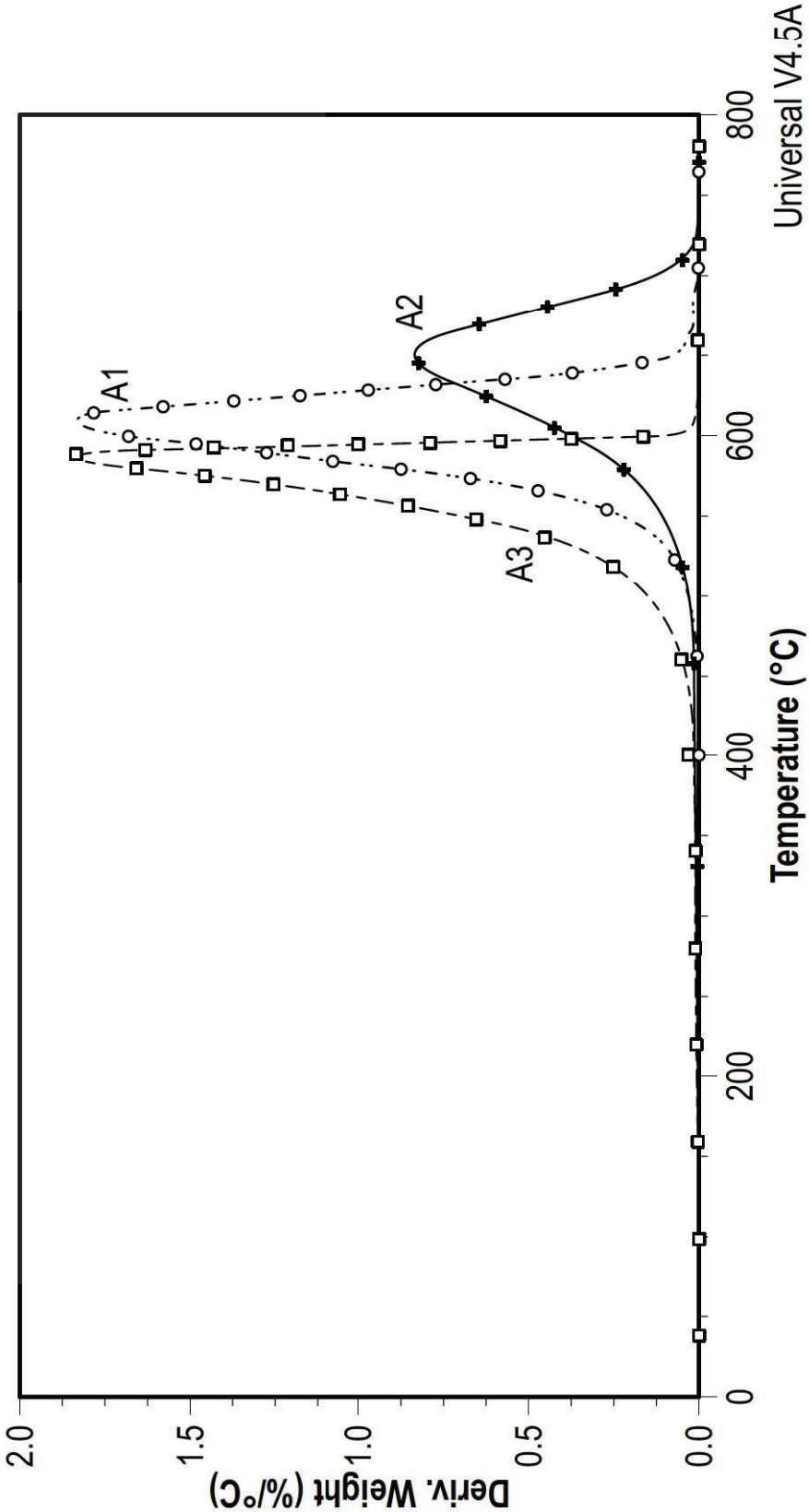
Deriv. Weight (%/°C)
2.0
1.5
1.0
0.5
0.0
0
200
400
600
800
Temperature (°C)
Universal V4.5A
A1
A2
A3

FIG. 19

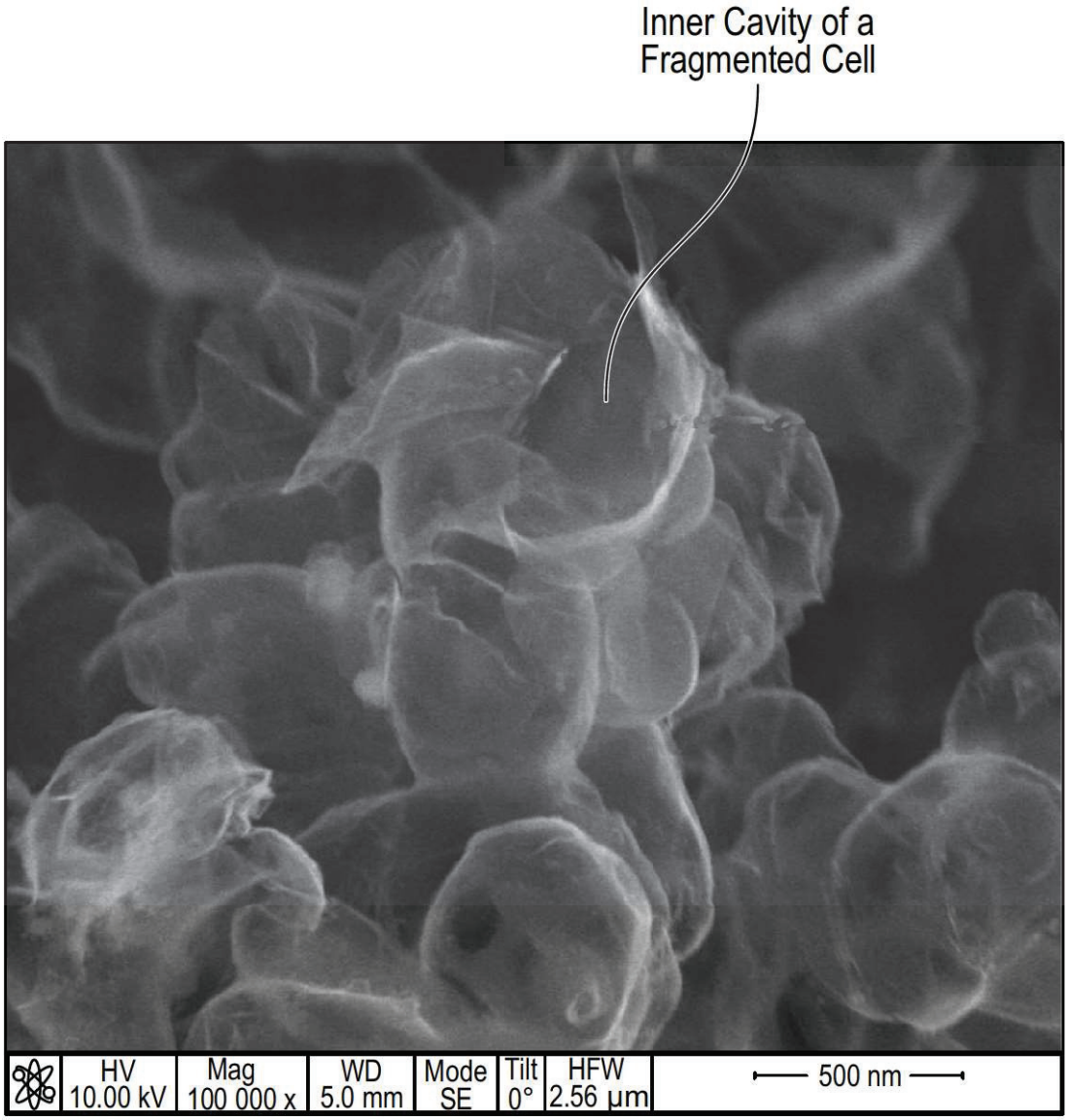
Inner Cavity of a
Fragmented Cell
HV
10.00 kV
Mag
100 000 x
WD
5.0 mm
Mode
SE
Tilt
0°
HFW
2.56 µm
500 nm

FIG. 20

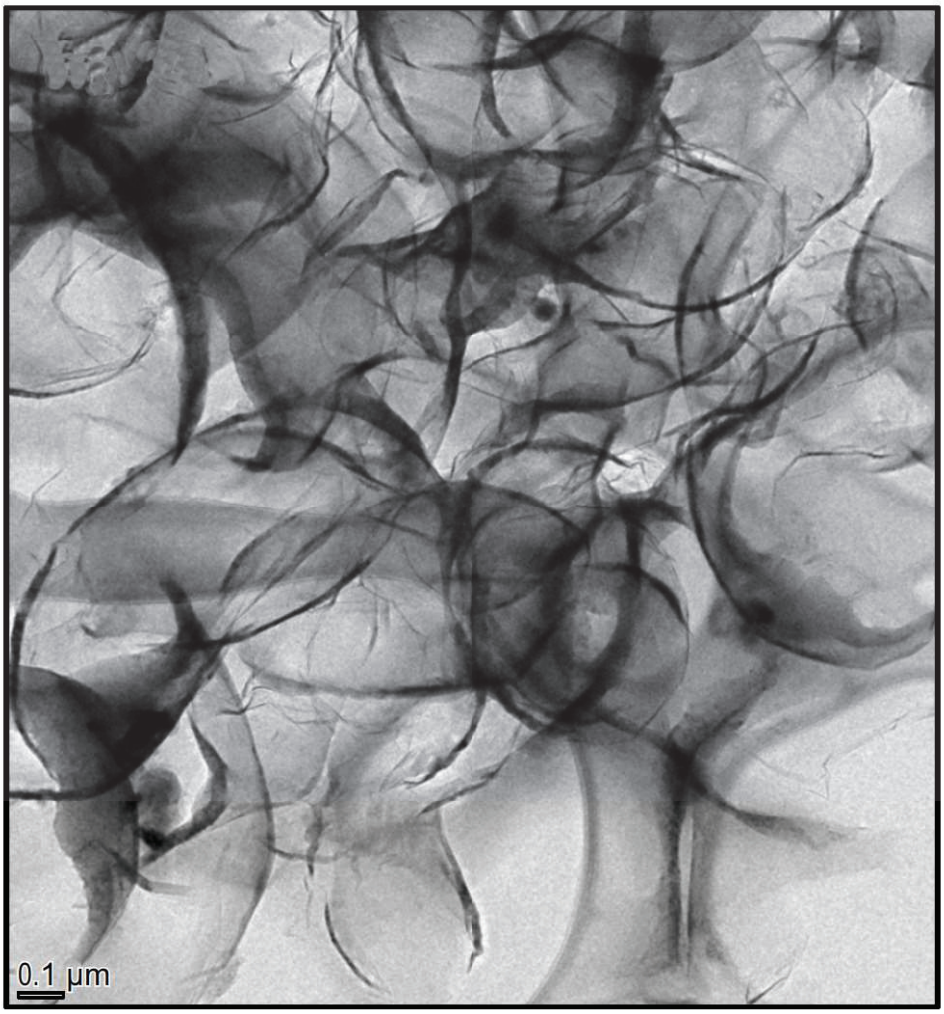

FIG. 21A



FIG. 21B

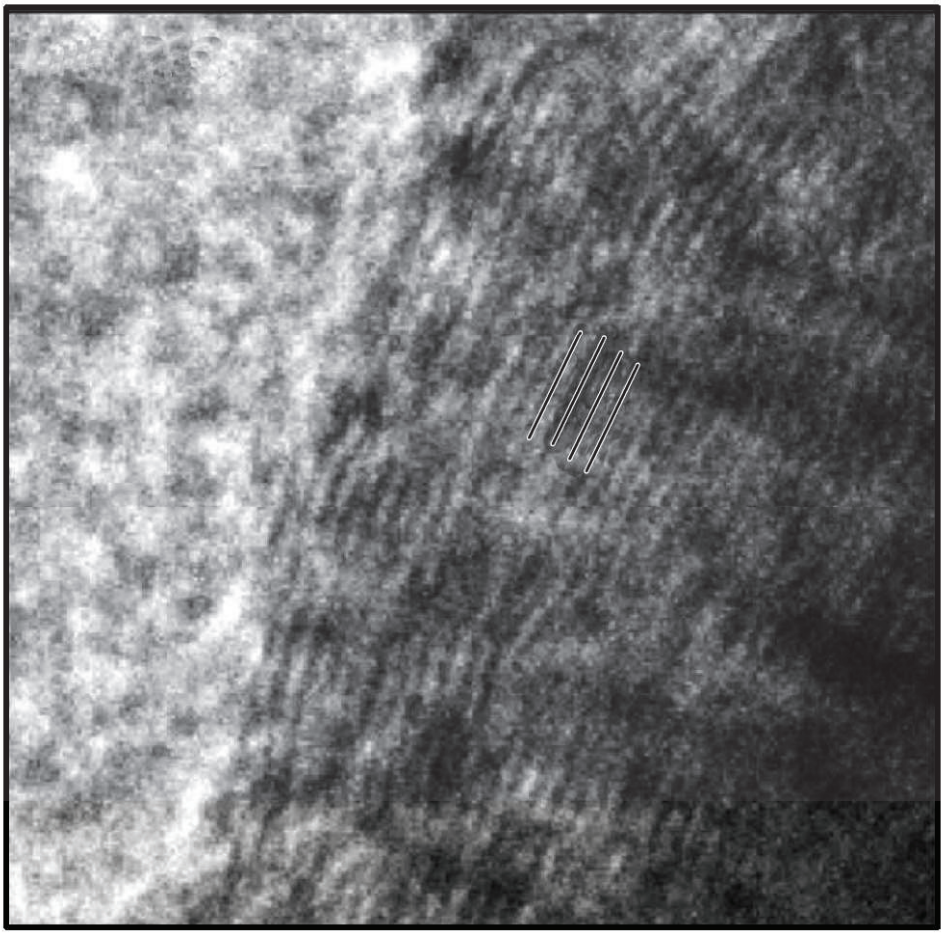

FIG. 21C

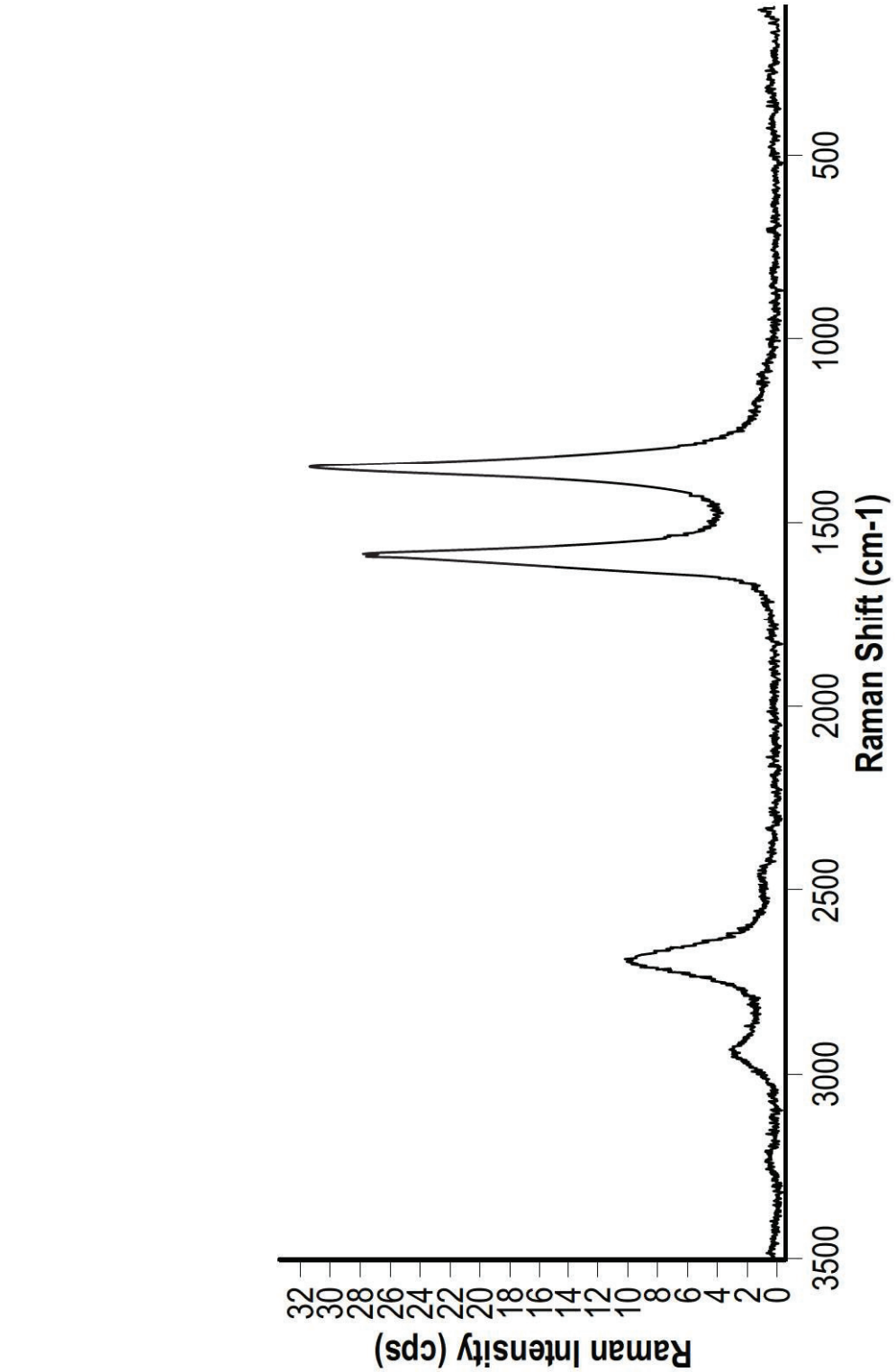
Raman Intensity (cps)
32
30
28
26
24
22
20
18
16
14
12
10
8
6
4
2
0
3500
3000
2500
2000
1500
1000
500
Raman Shift (cm-1)

FIG. 22

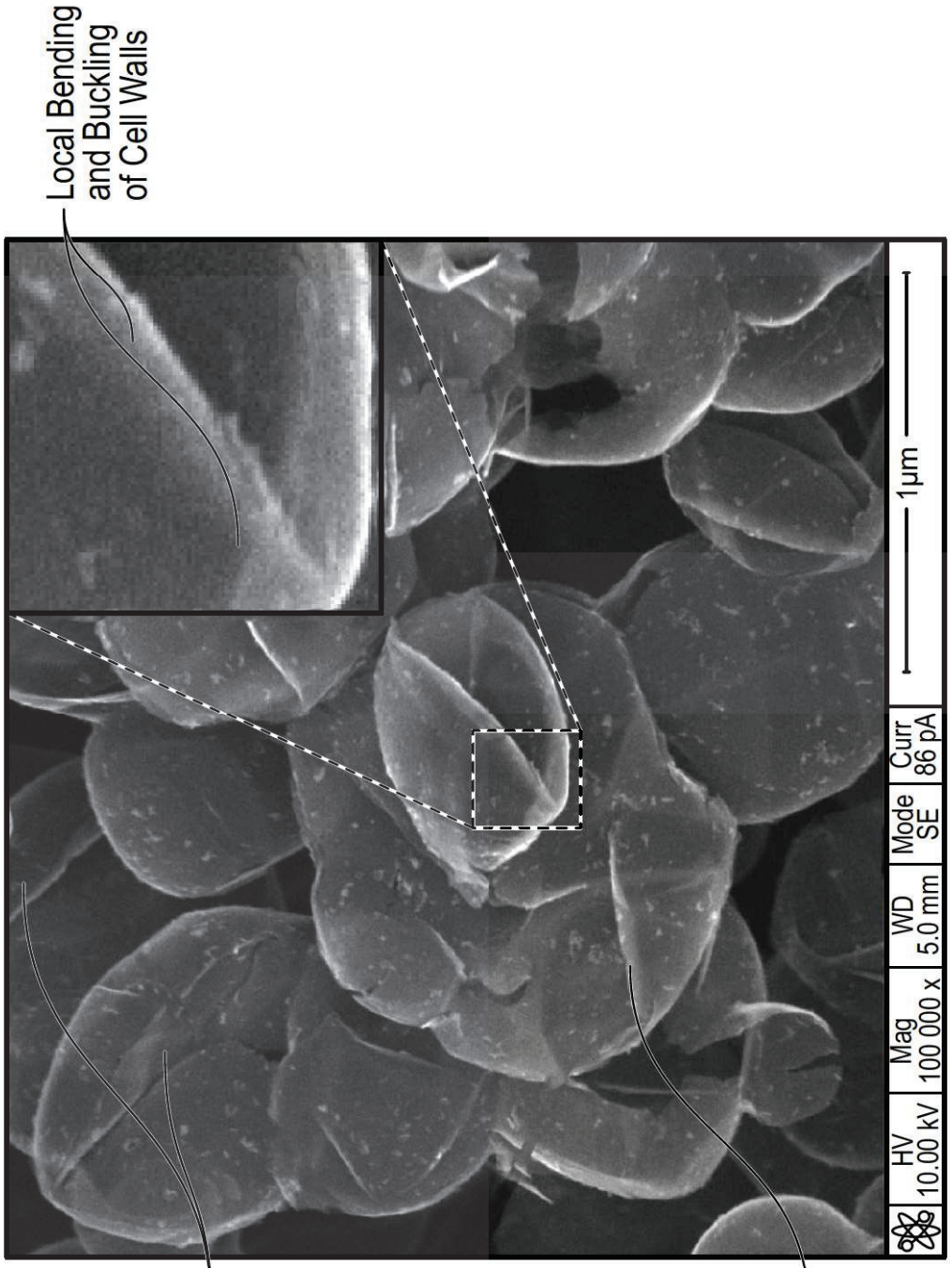
Local Bending and Buckling of Cell Walls
Recurring Linear Features Observed Post-Compression
Recurring Linear Features Observed Post-Compression
HV 10.00 kV
Mag 100 000 x
WD 5.0 mm
Mode SE
Curr 86 pA
1µm

FIG. 23

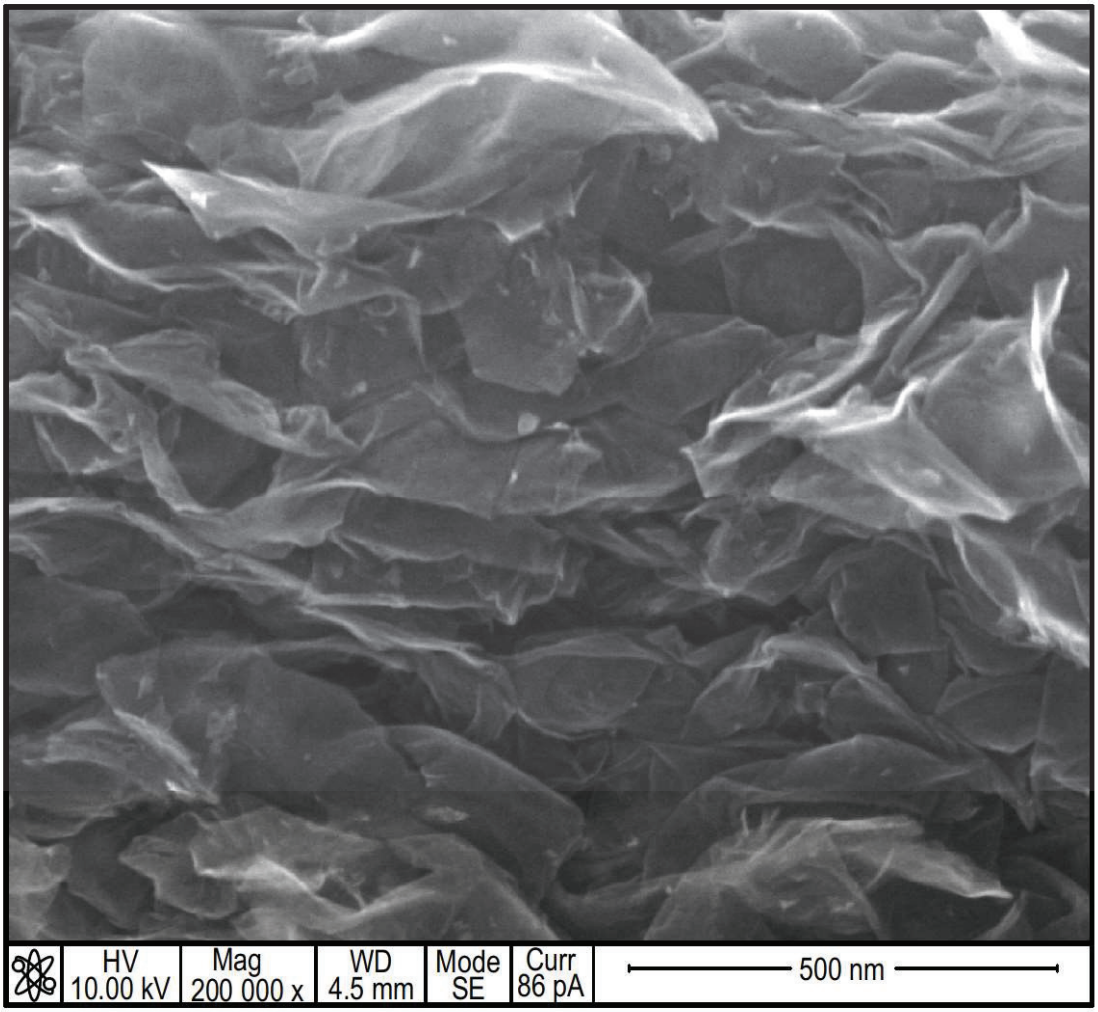

FIG. 24

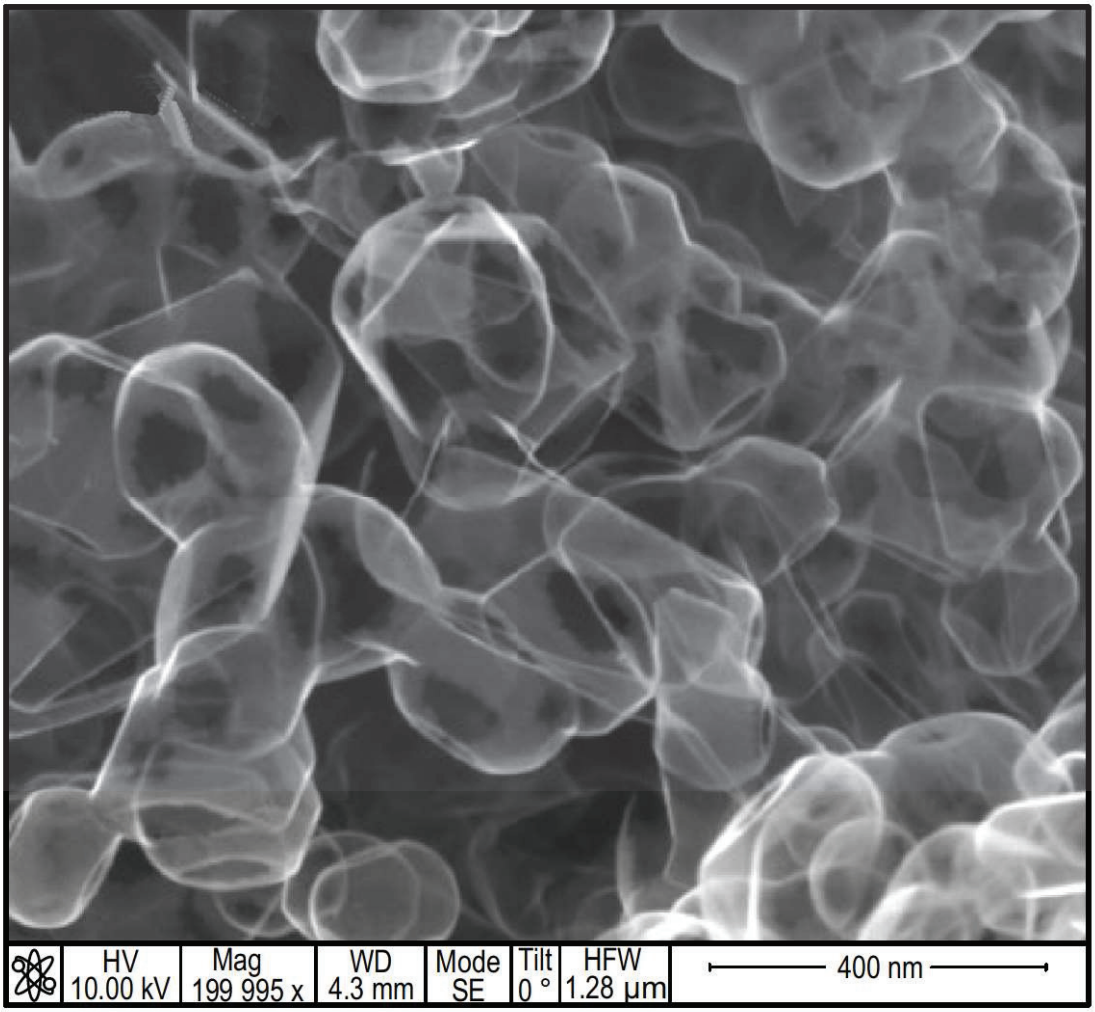

FIG. 25A

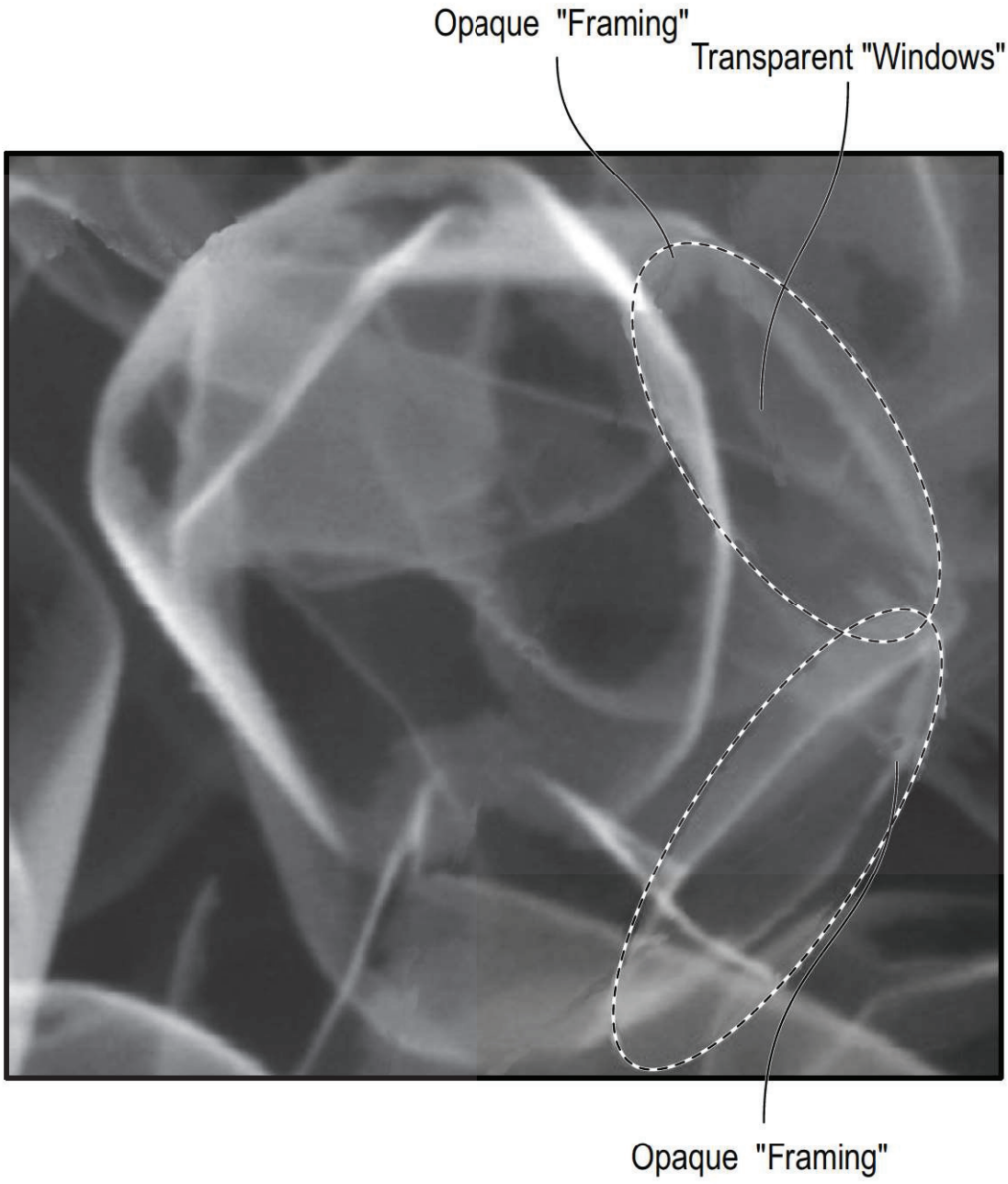

FIG. 25B

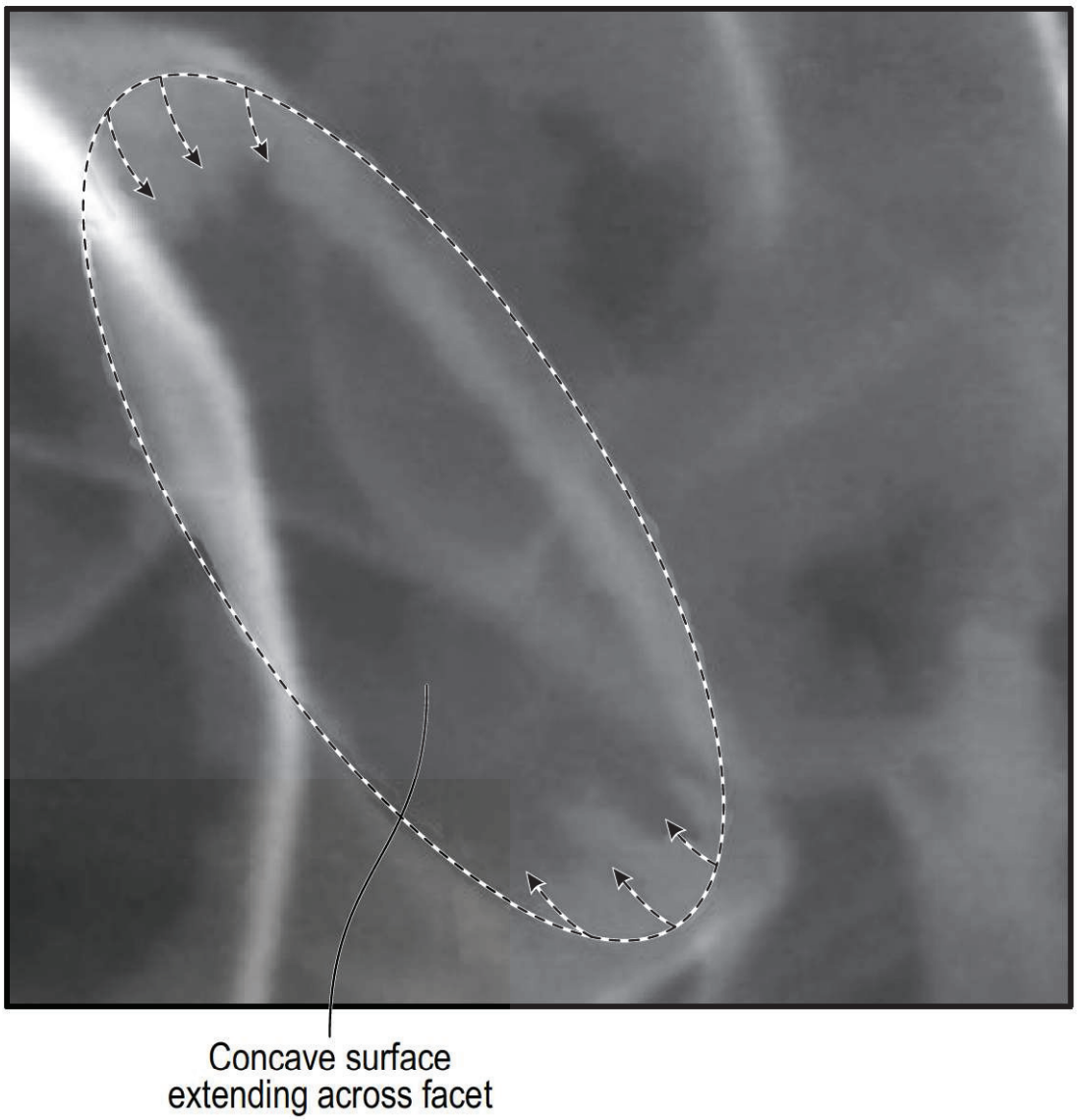

FIG. 25C

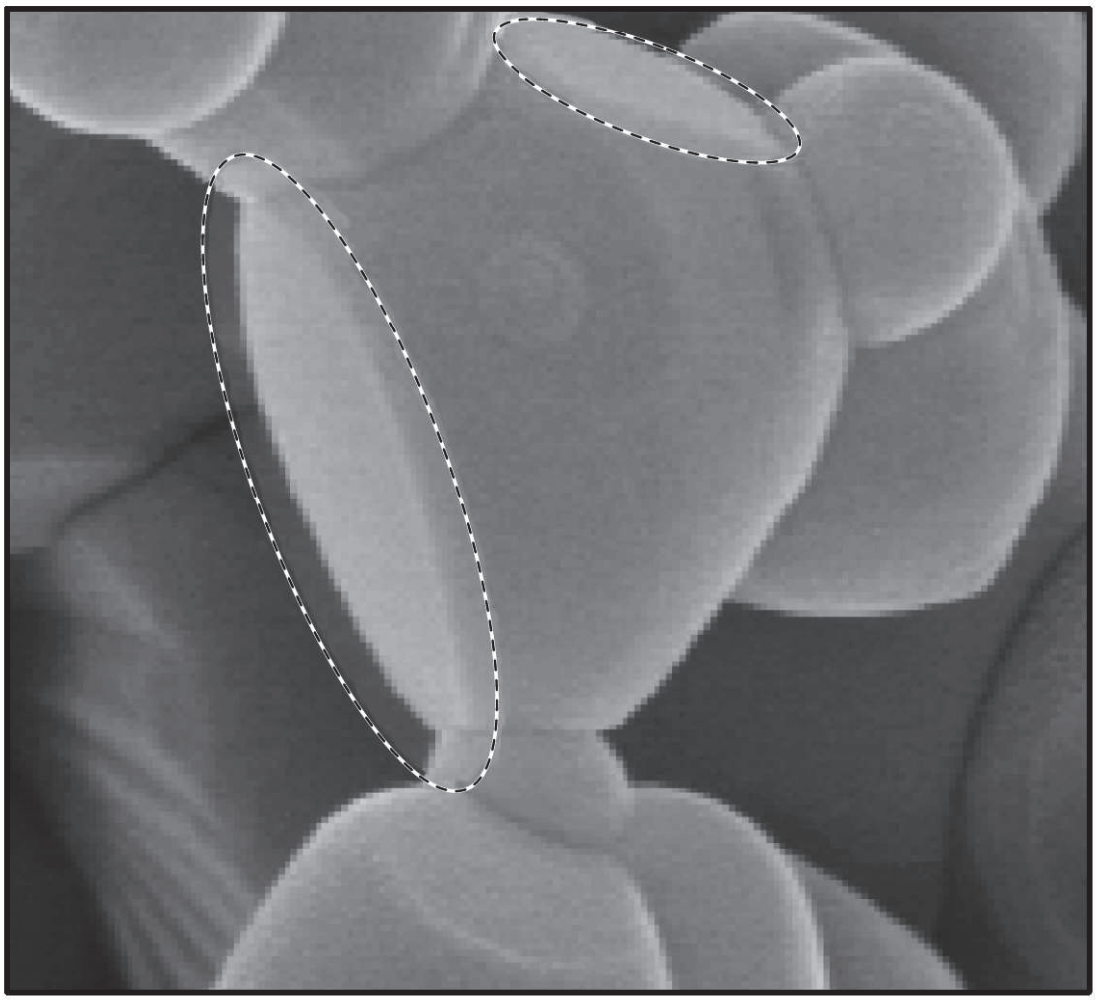

FIG. 26

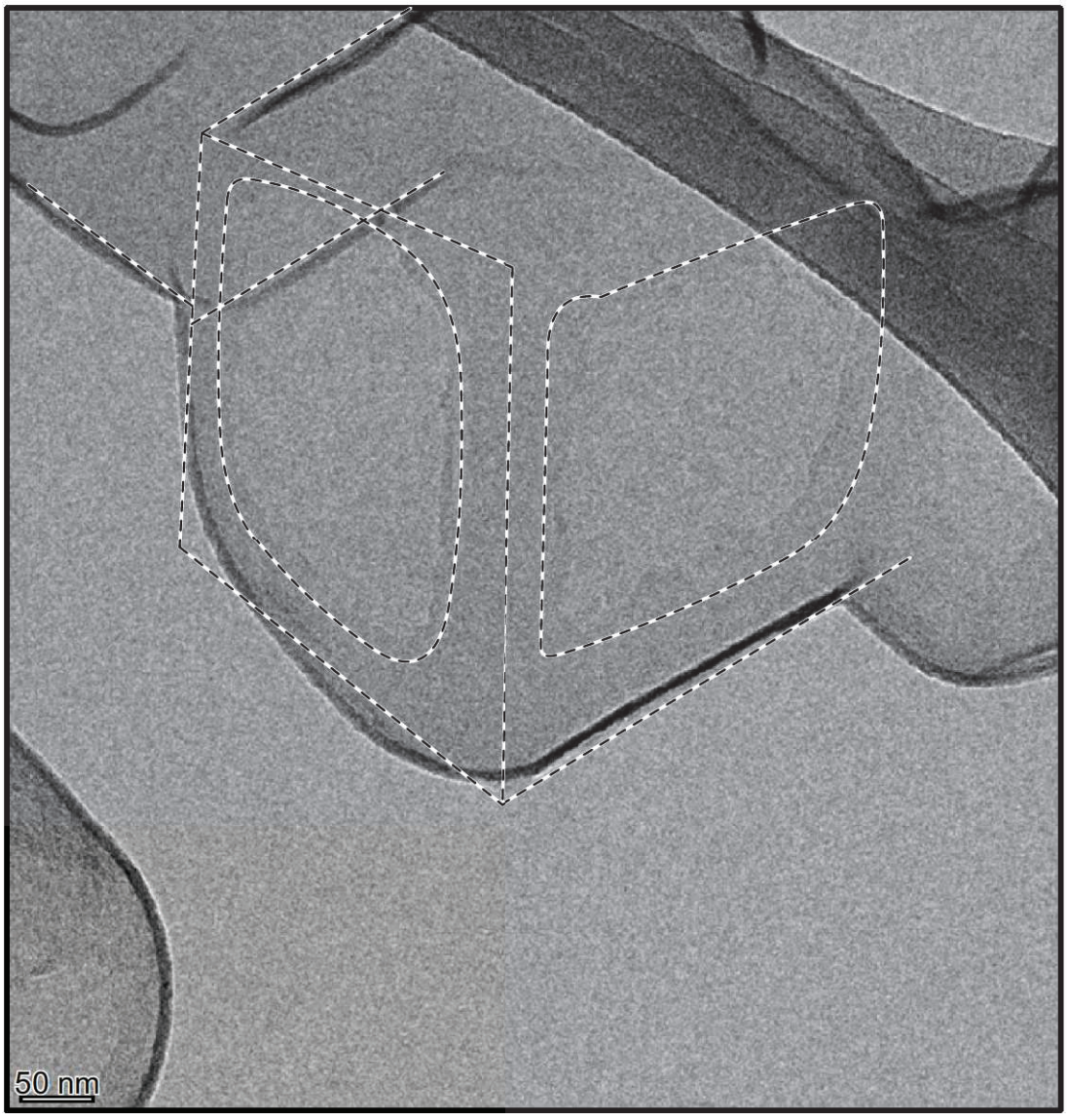

FIG. 27A

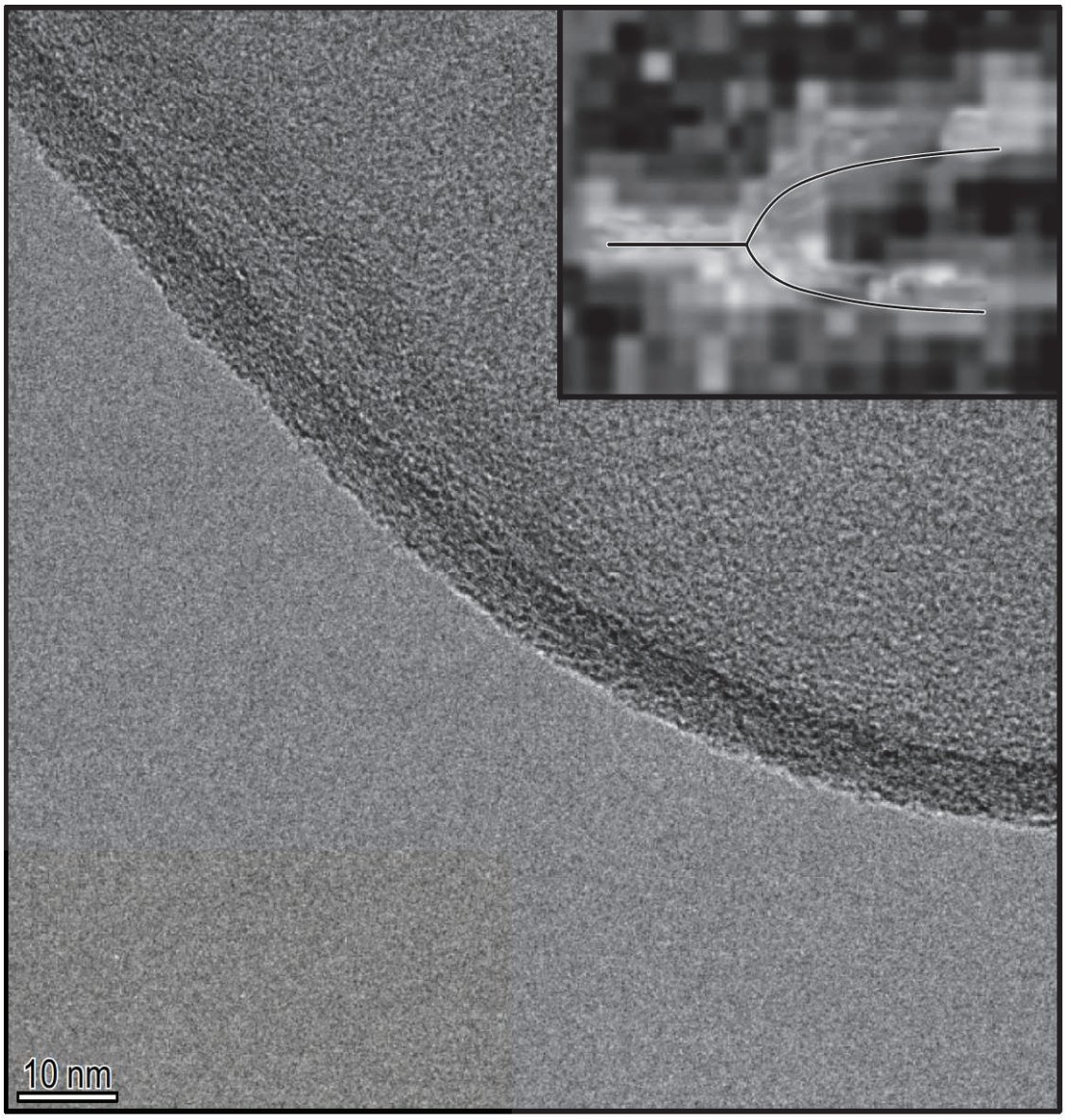

FIG. 27B

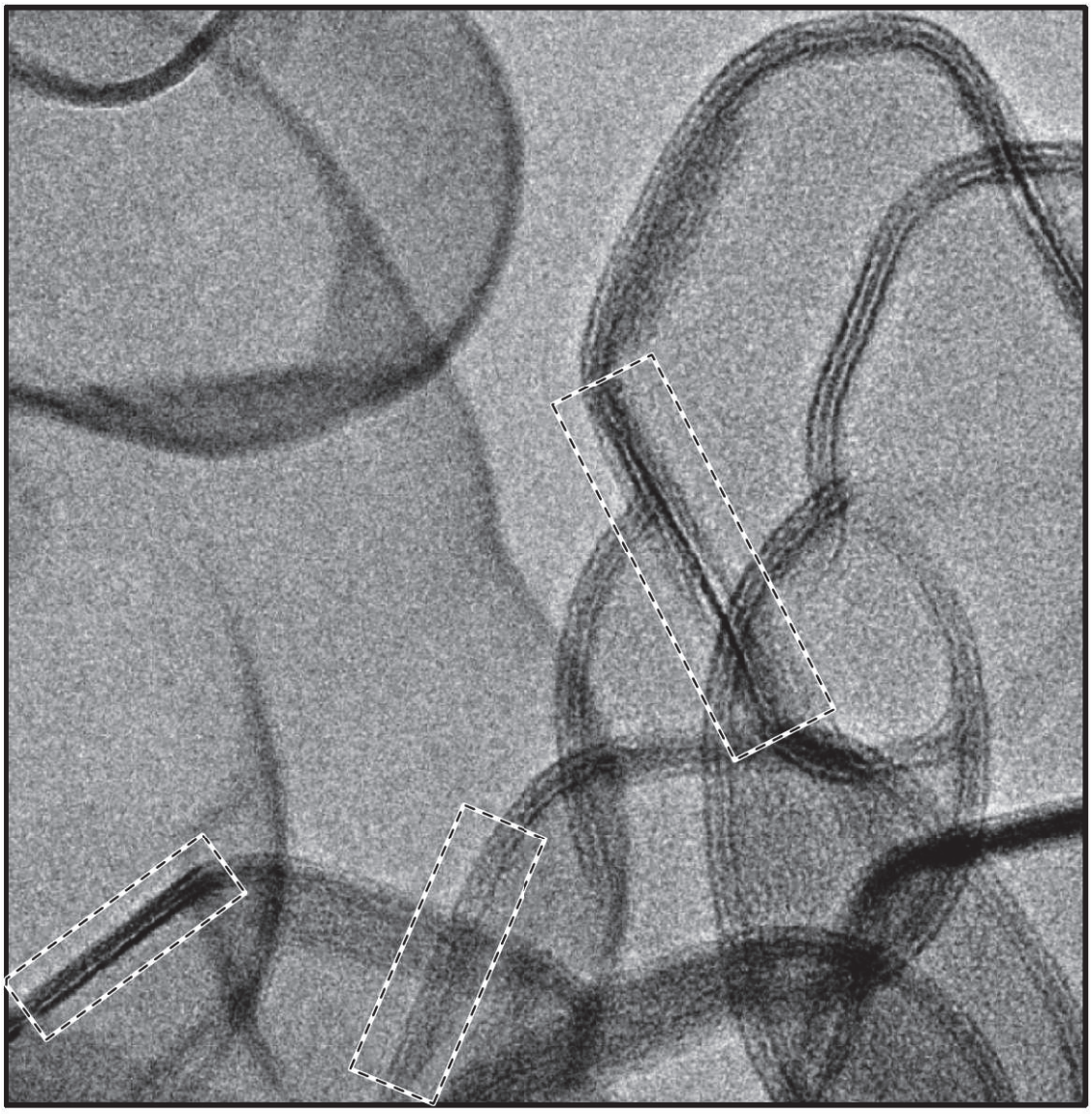

FIG. 27C

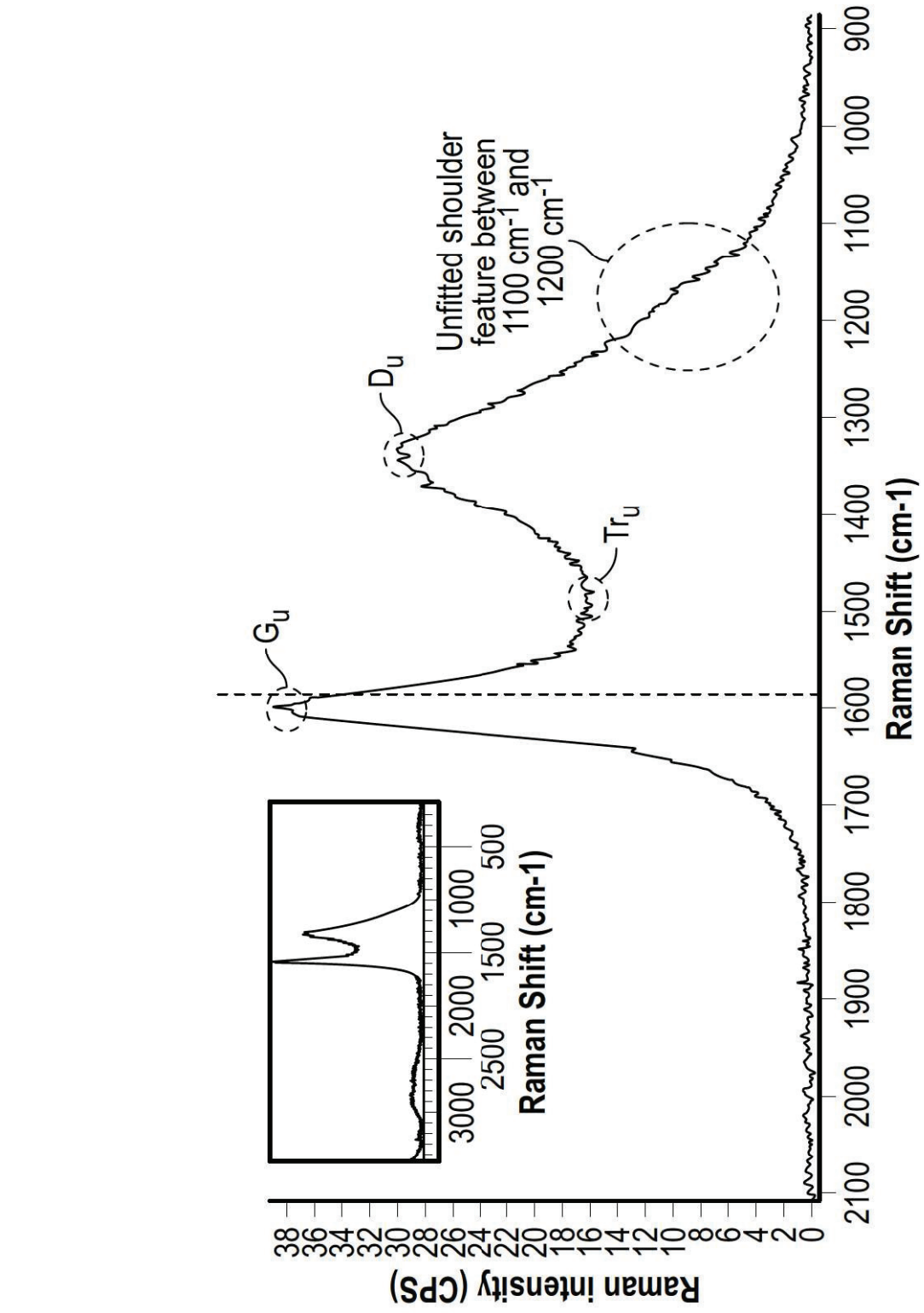
Raman intensity (CPS)
0
2
4
6
8
10
12
14
16
18
20
22
24
26
28
30
32
34
36
38
2100
2000
1900
1800
1700
1600
1500
1400
1300
1200
1100
1000
900
Raman Shift (cm-1)
G_u
D_u
Tr_u
Unfitted shoulder feature between 1100 cm-1 and 1200 cm-1
3000
2500
2000
1500
1000
500
Raman Shift (cm-1)

FIG. 28

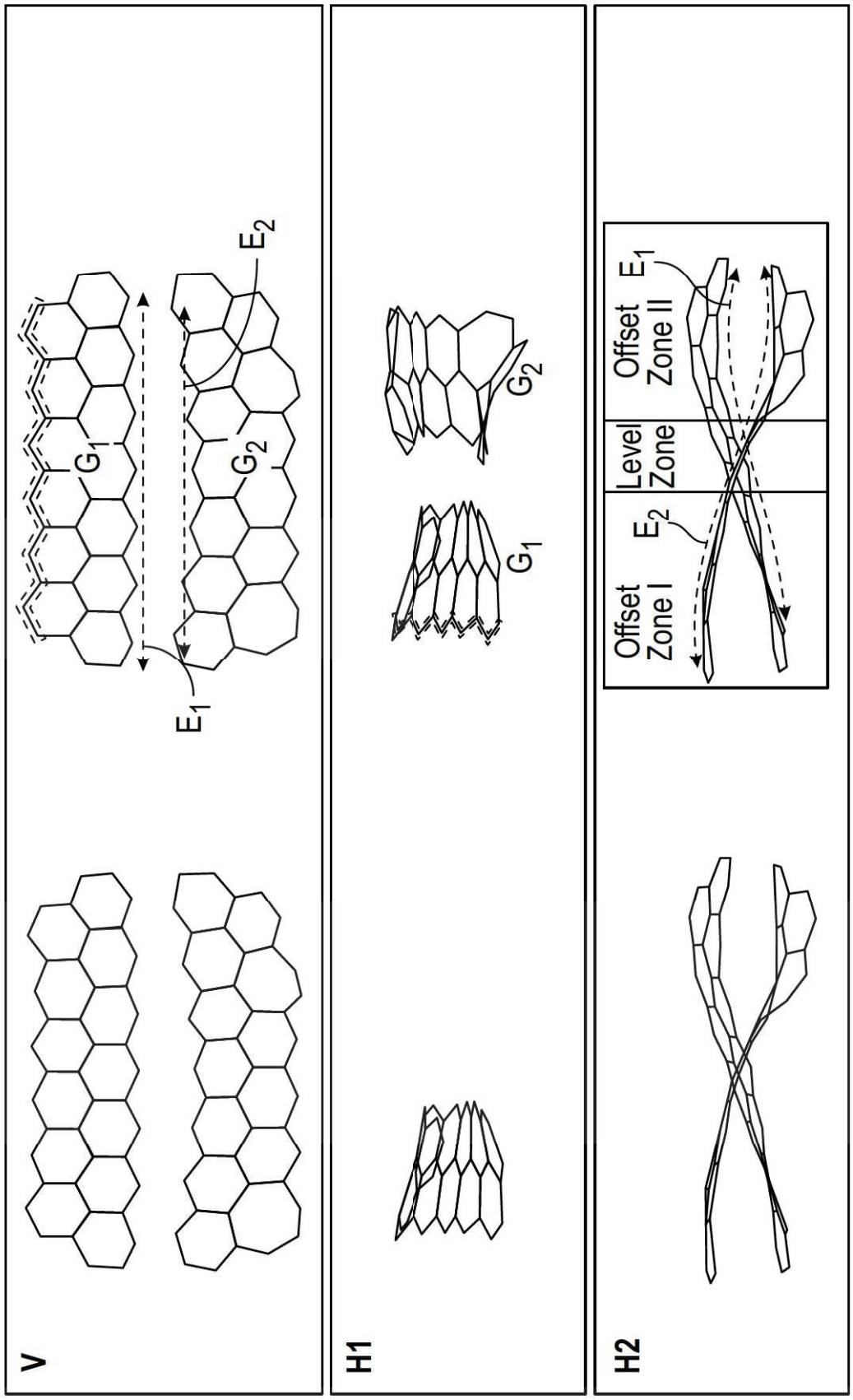

FIG. 29

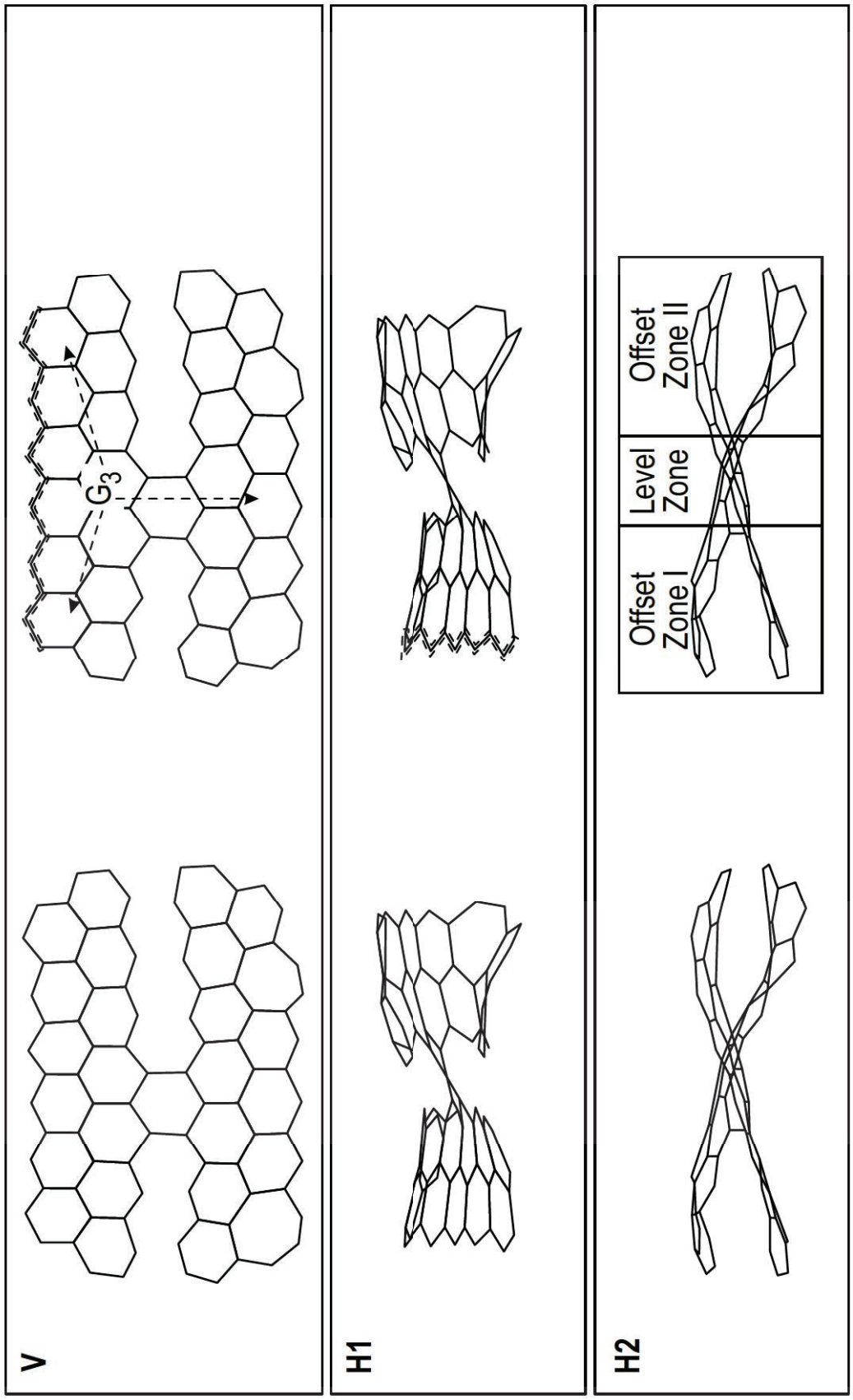

FIG. 30

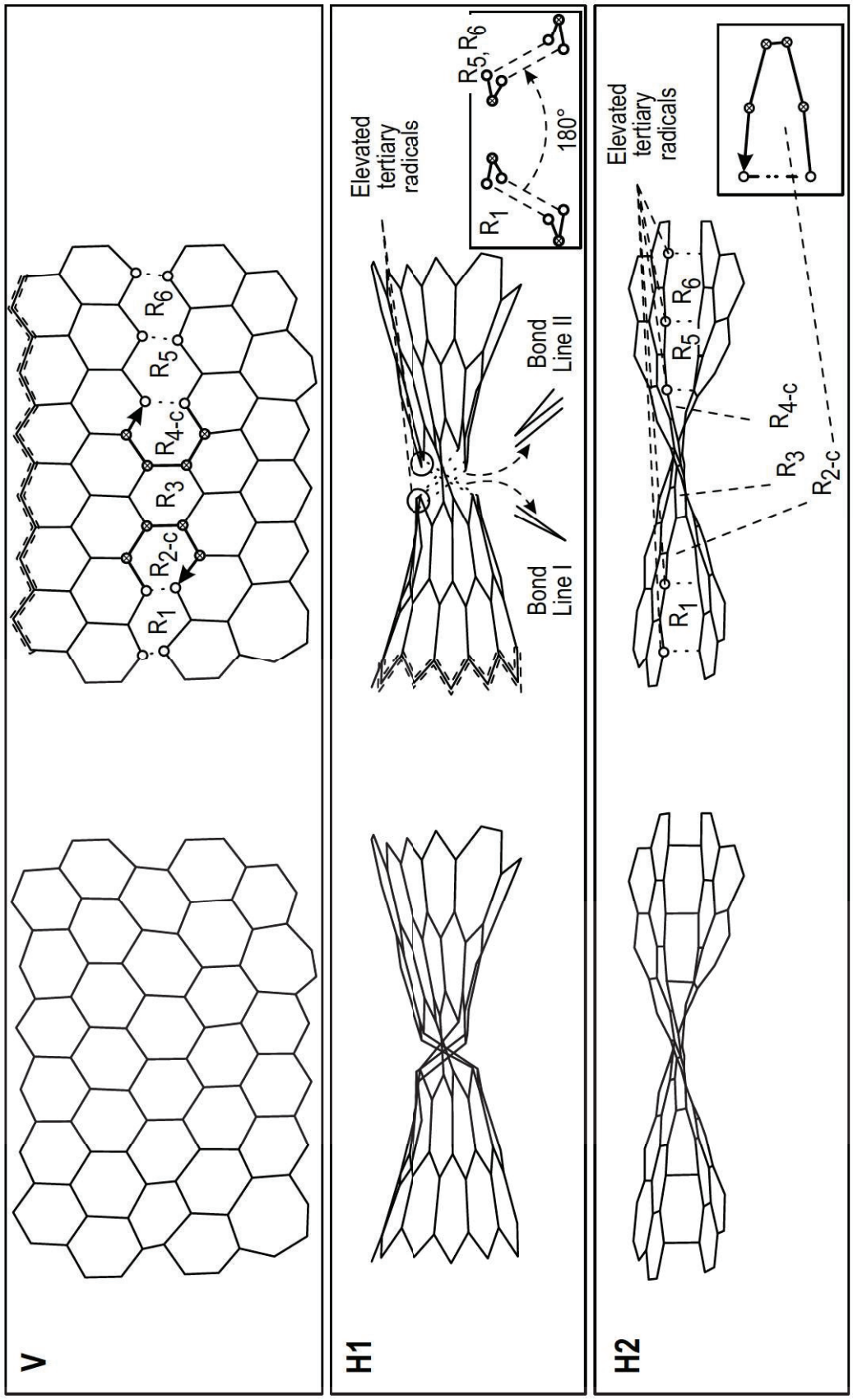
V
H1
H2
R1
R2-c
R3
R4-c
R5
R6
Elevated tertiary radicals
Bond Line I
Bond Line II
180°

FIG. 31

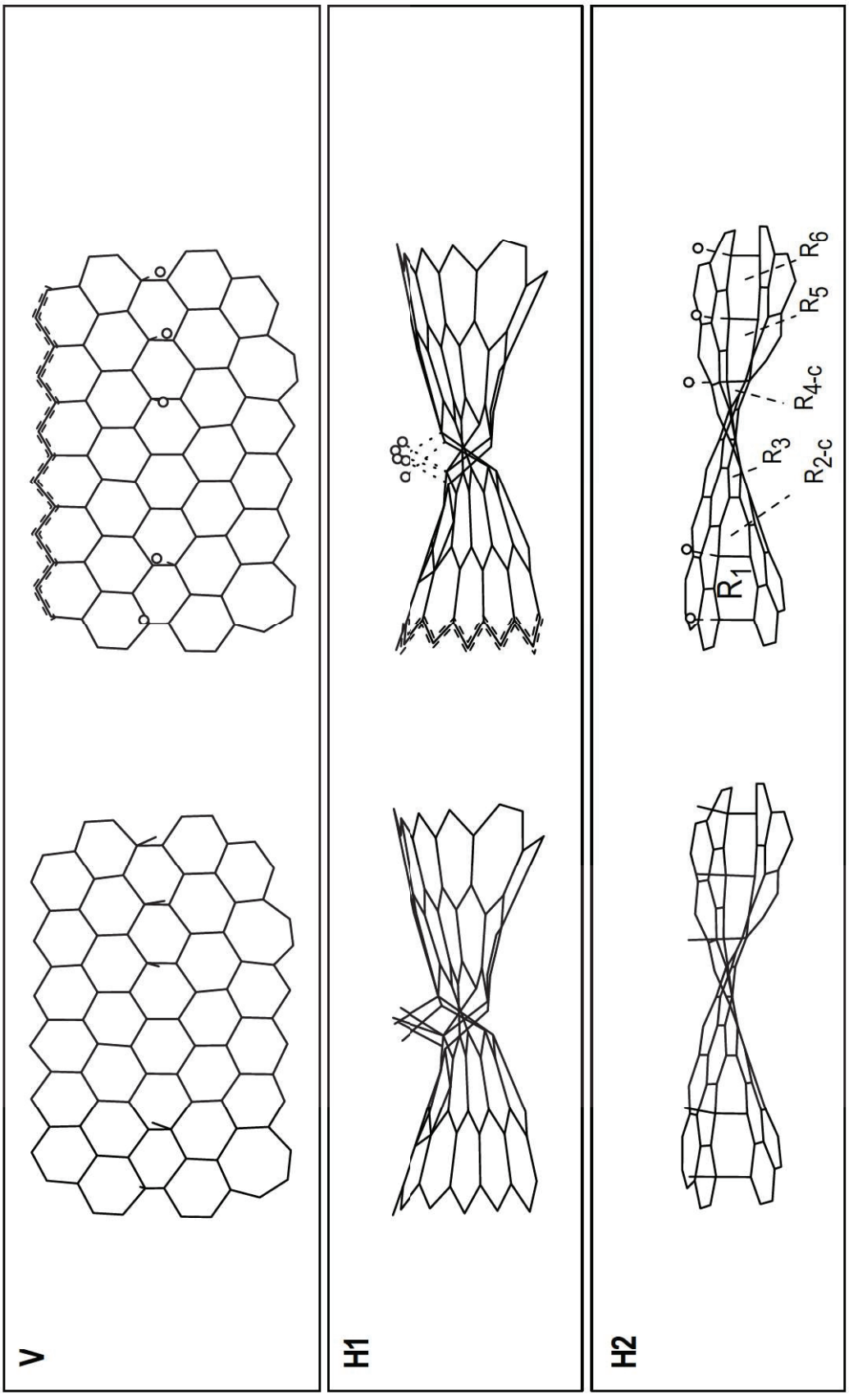

FIG. 32

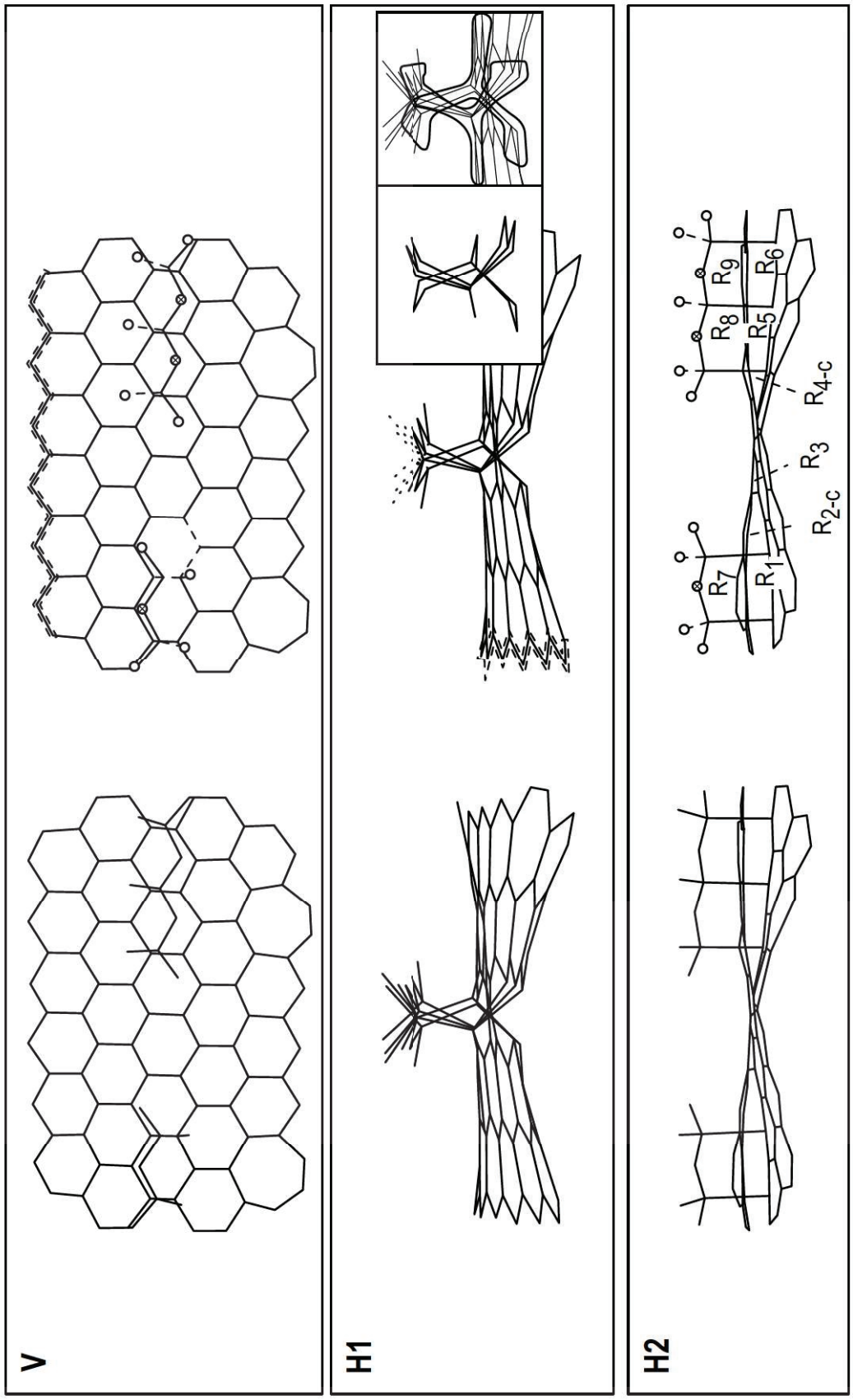

FIG. 33

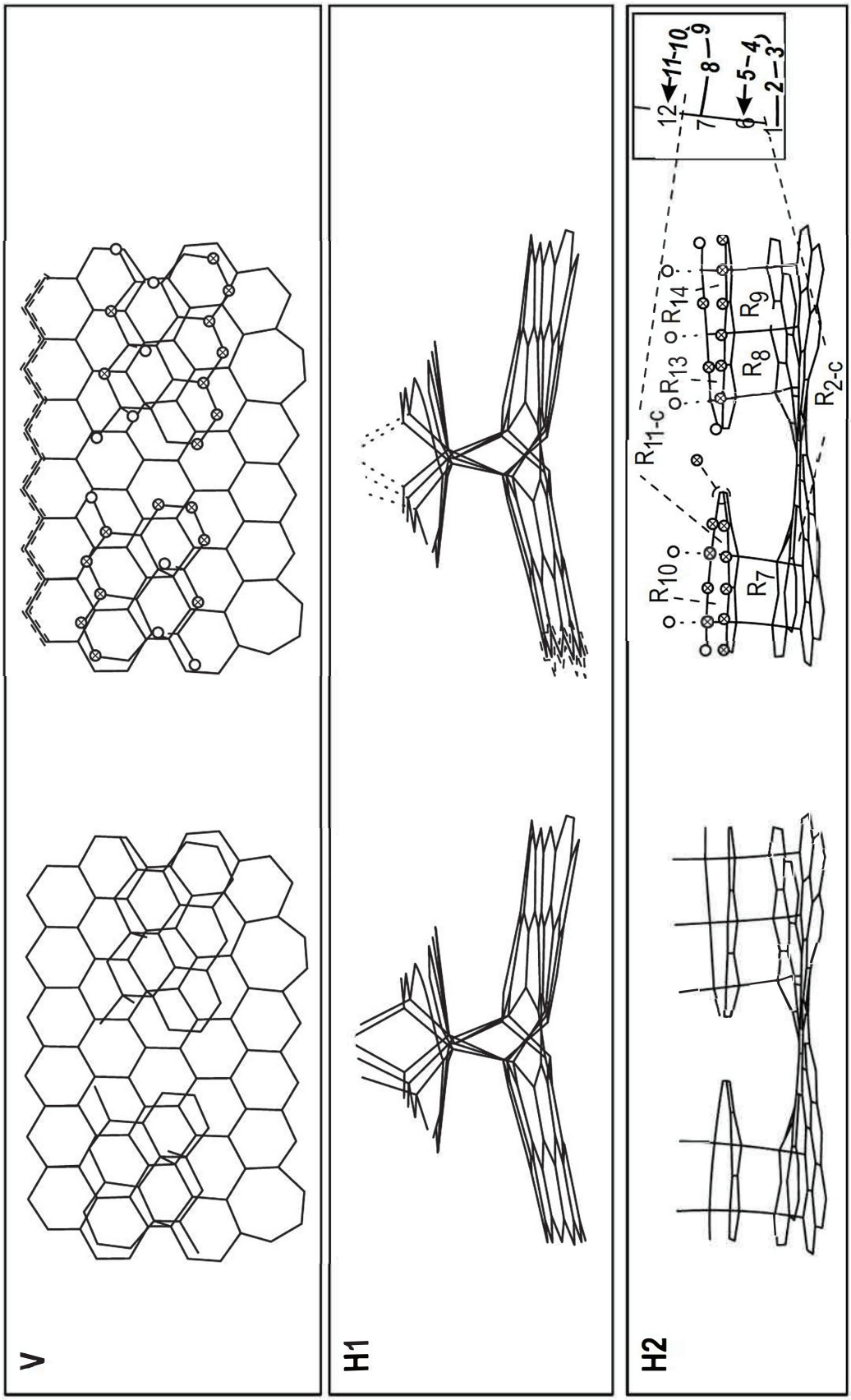

FIG. 34

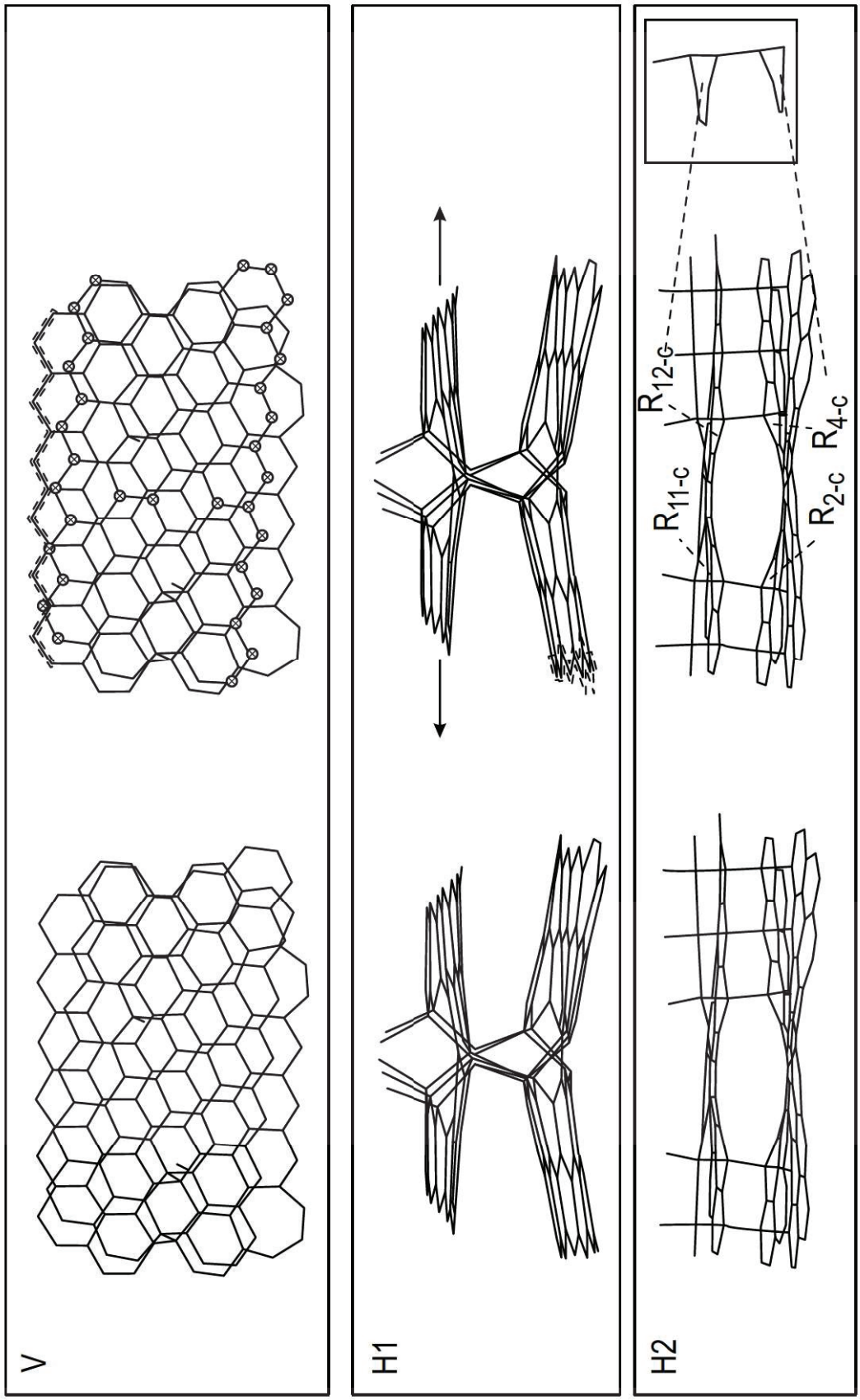

FIG. 35

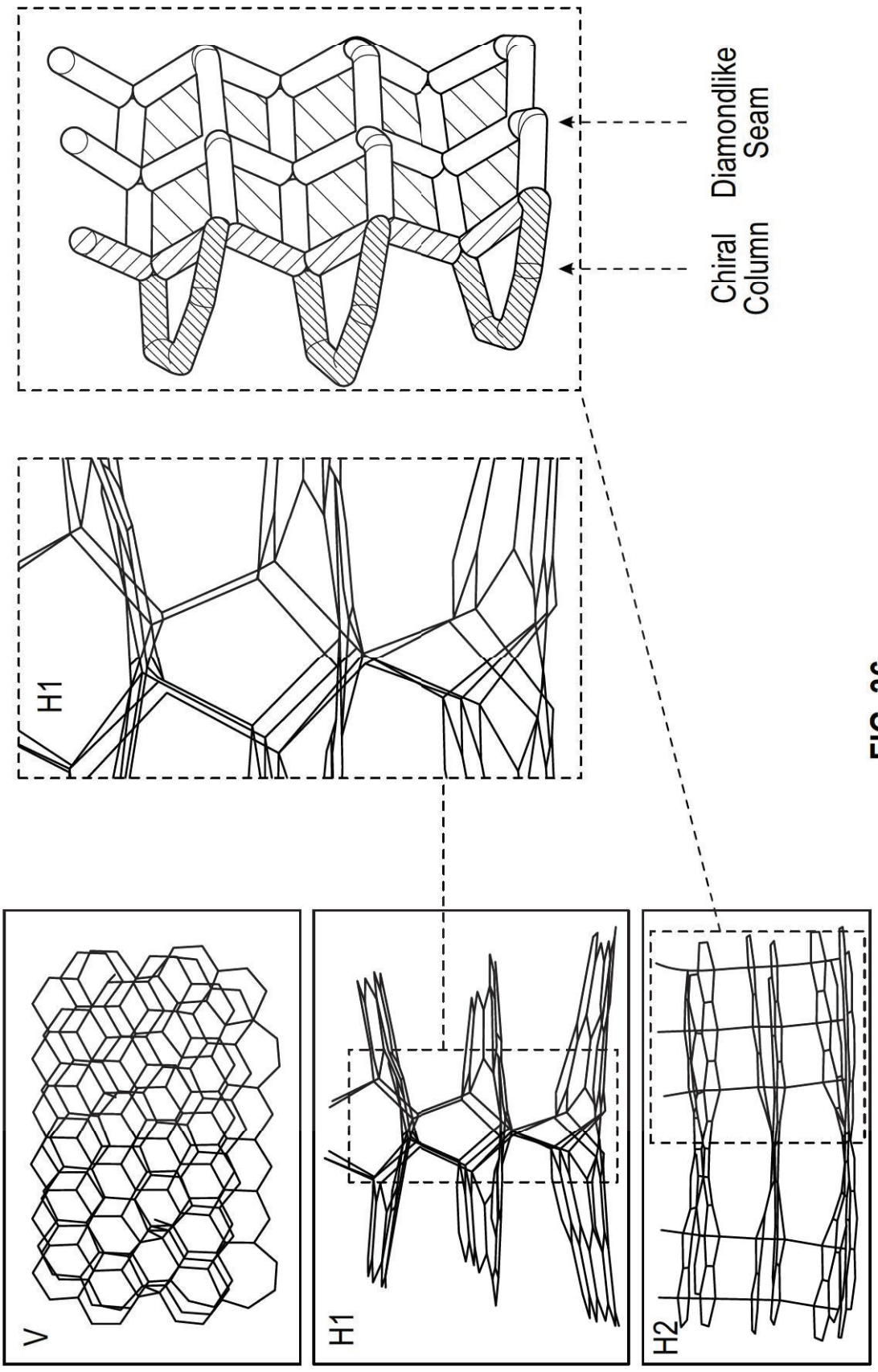

FIG. 36

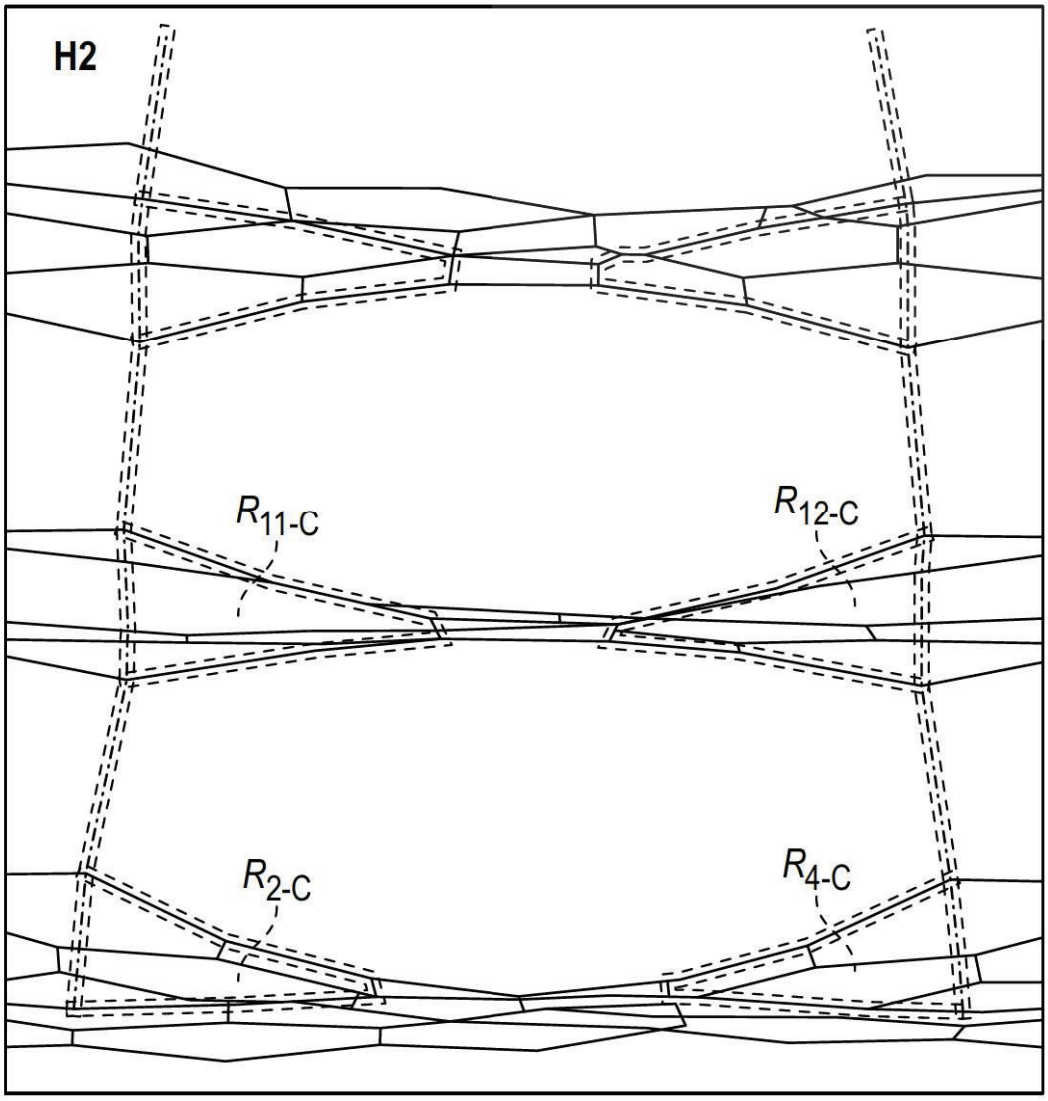

FIG. 37A

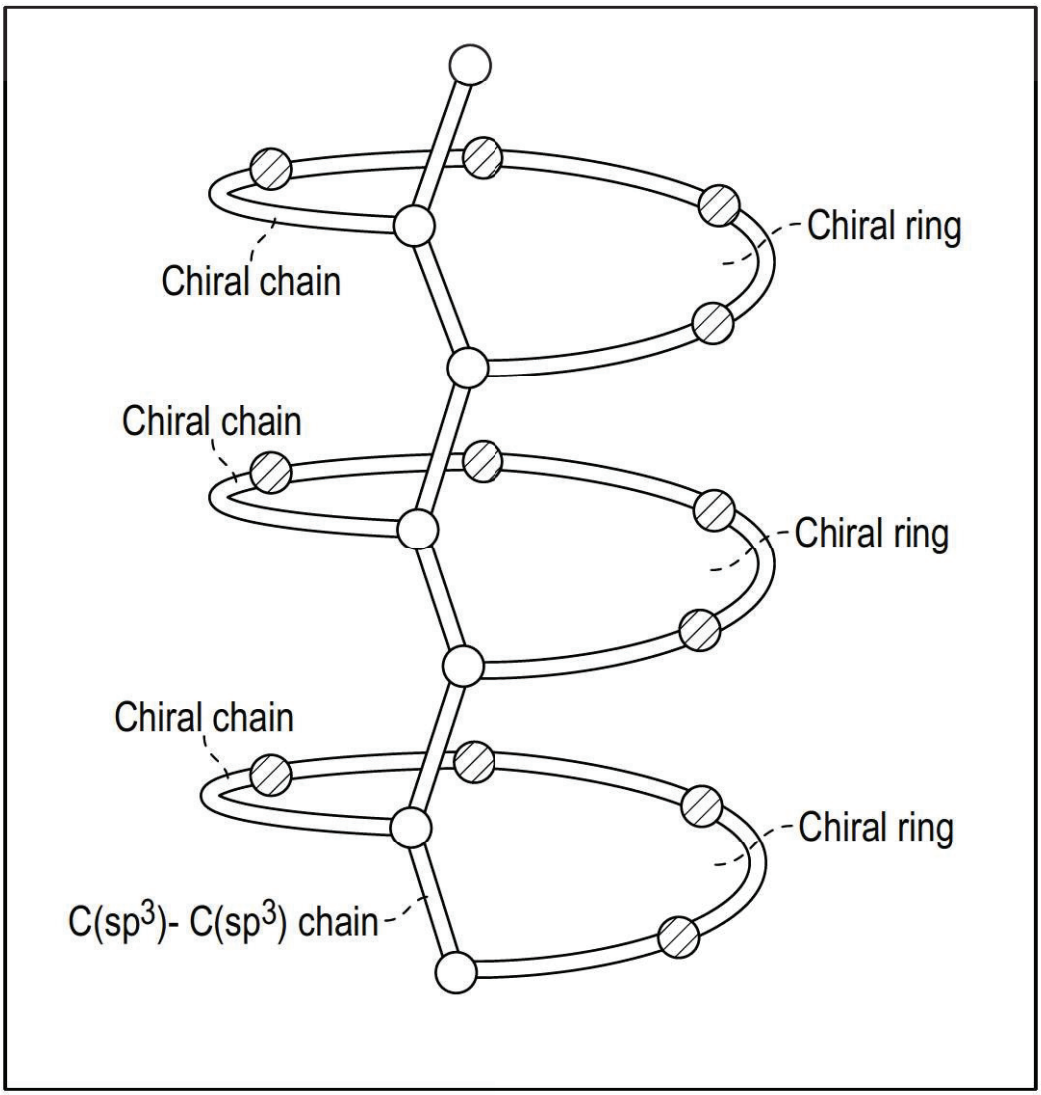
Chiral chain
Chiral ring
Chiral chain
Chiral ring
Chiral chain
Chiral ring
C(sp3)- C(sp3) chain

FIG. 37B

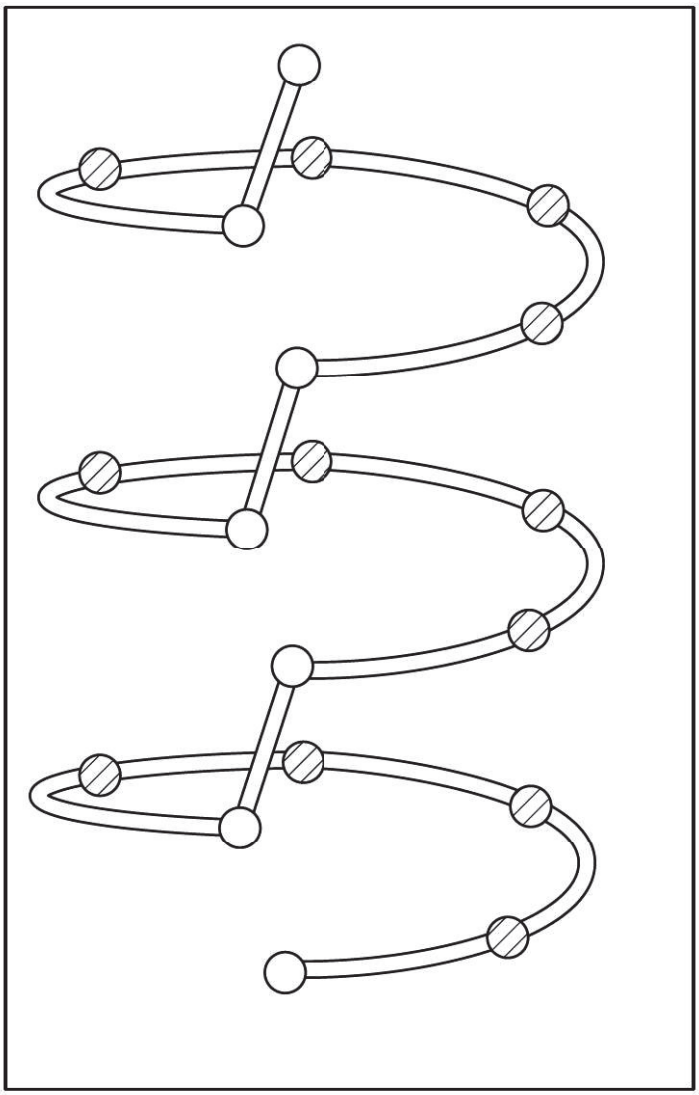

FIG. 37C

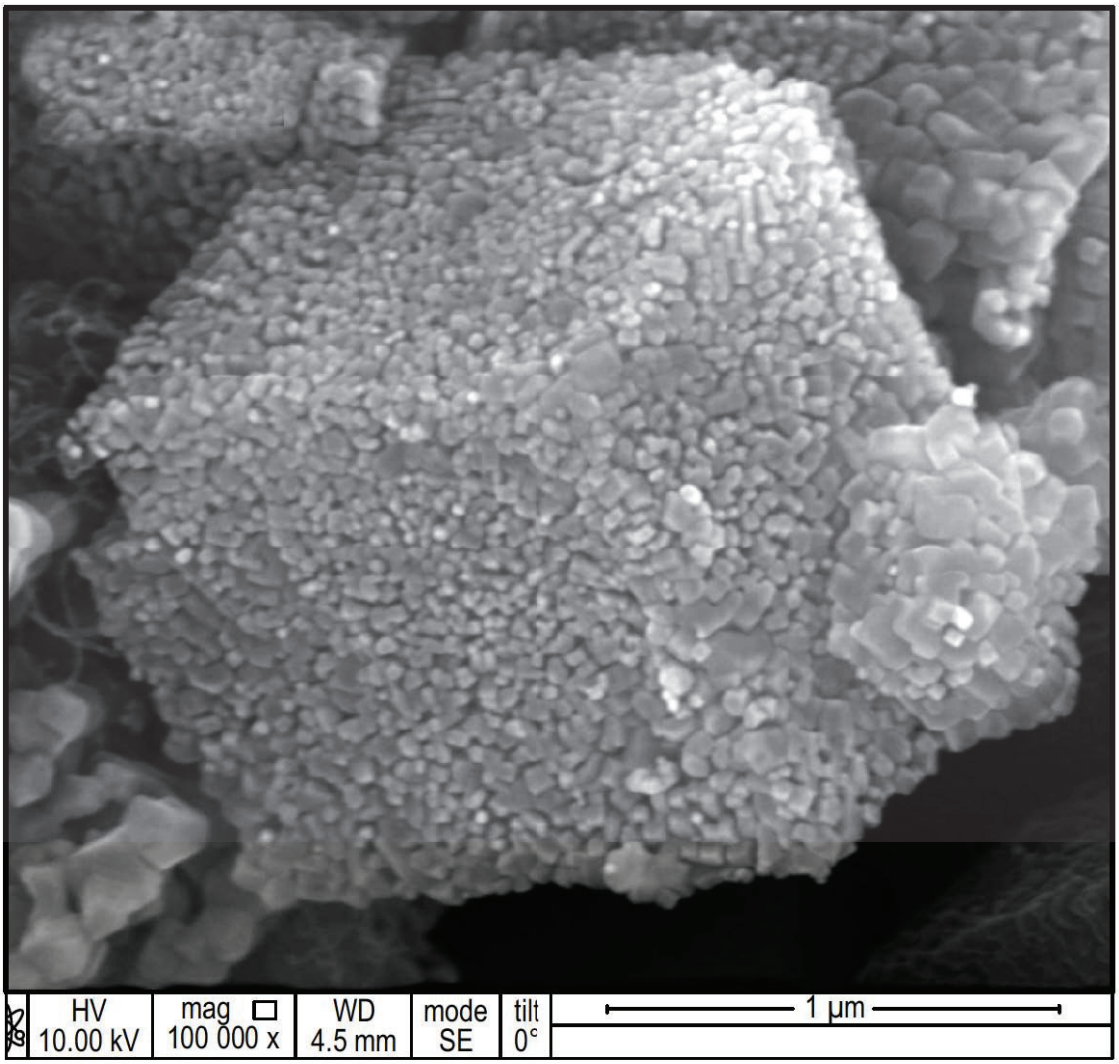

FIG. 38A

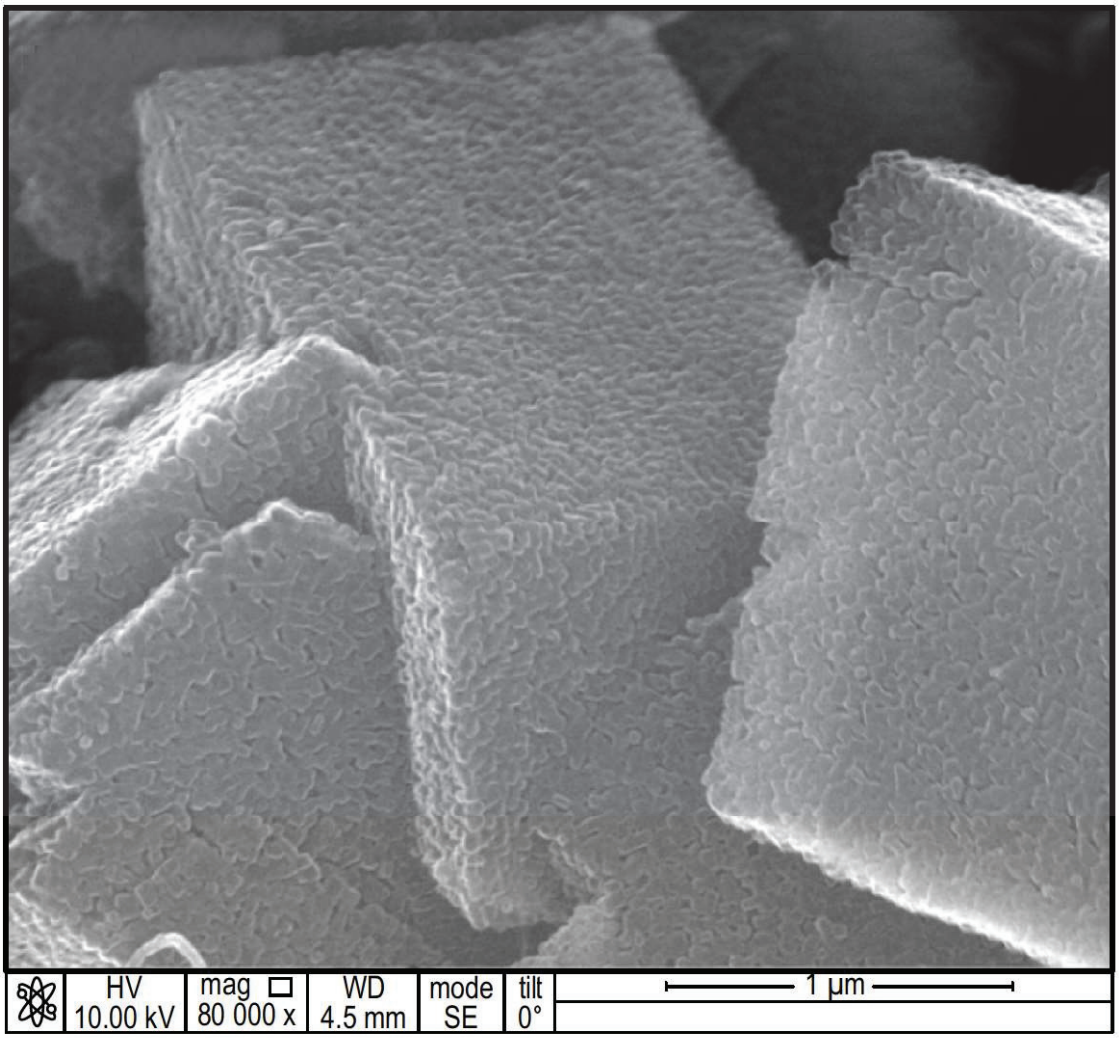

FIG. 38B

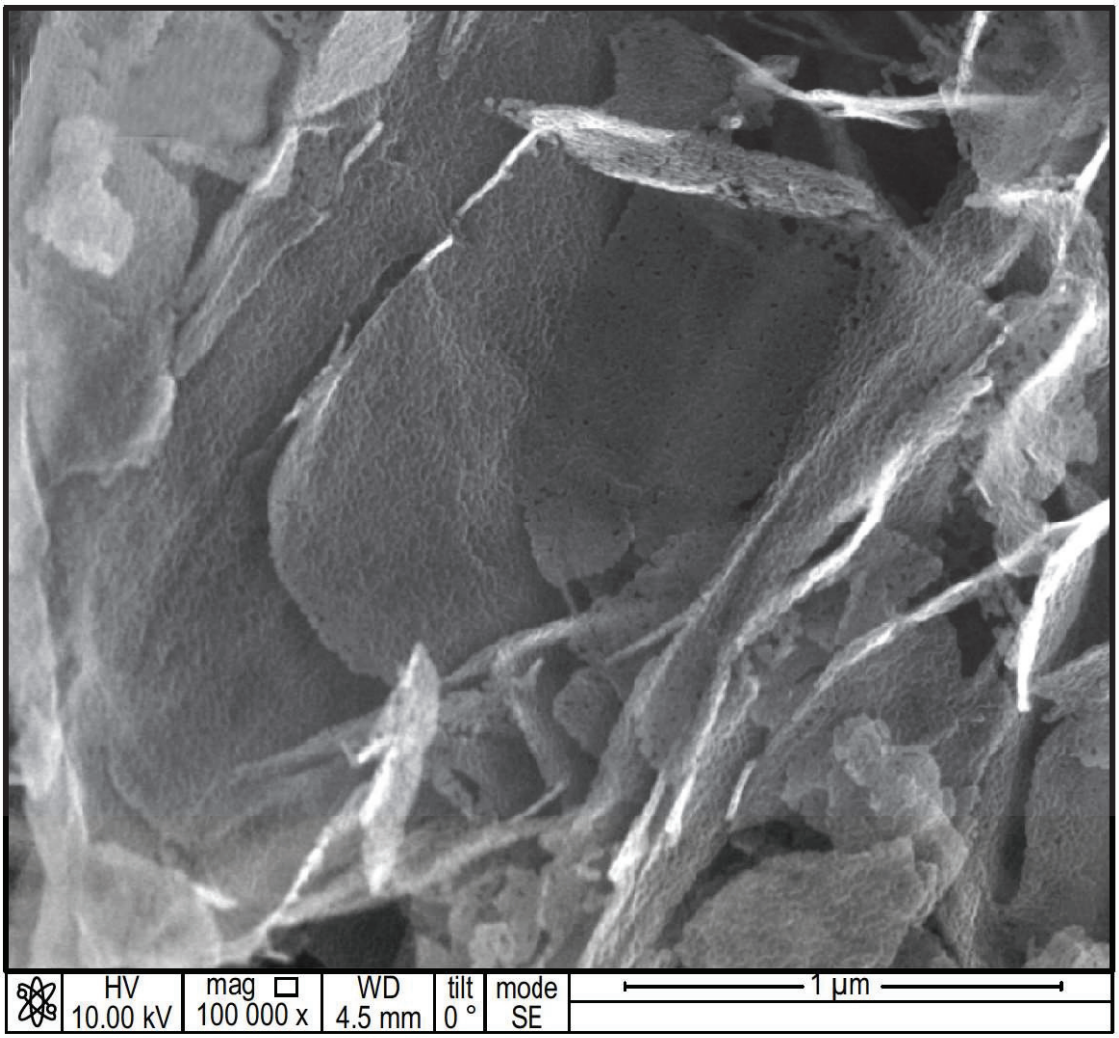

FIG. 38C

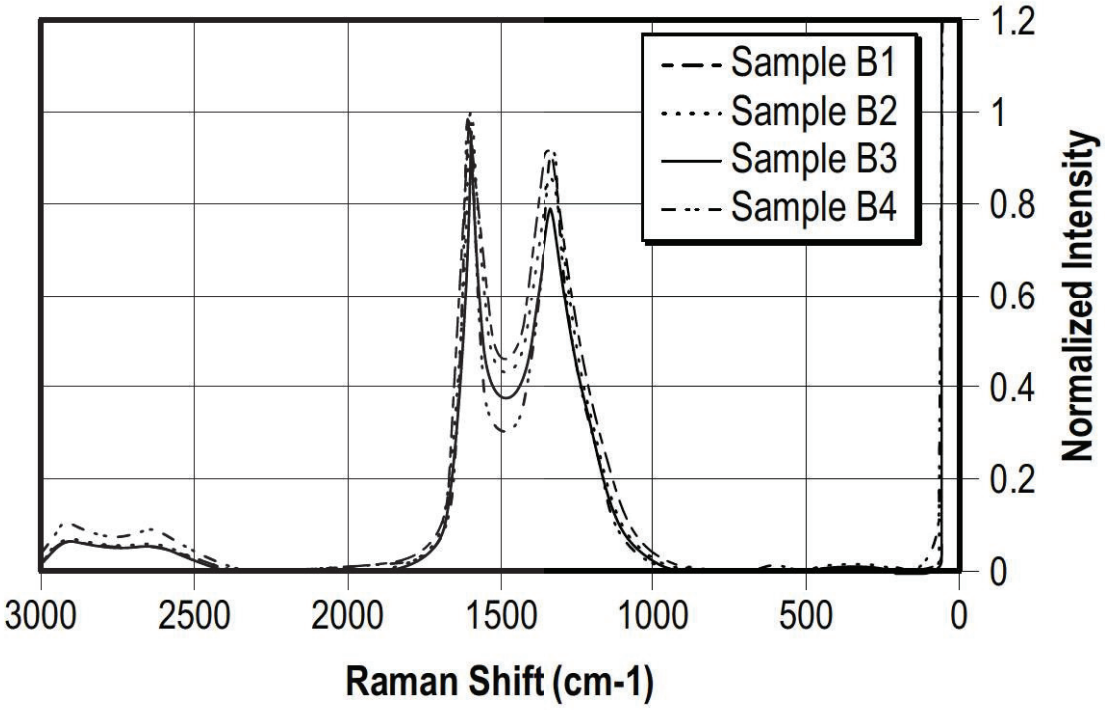
Sample B1
Sample B2
Sample B3
Sample B4
1.2
1
0.8
0.6
0.4
0.2
0
Normalized Intensity
3000
2500
2000
1500
1000
500
0
Raman Shift (cm-1)

FIG. 39A

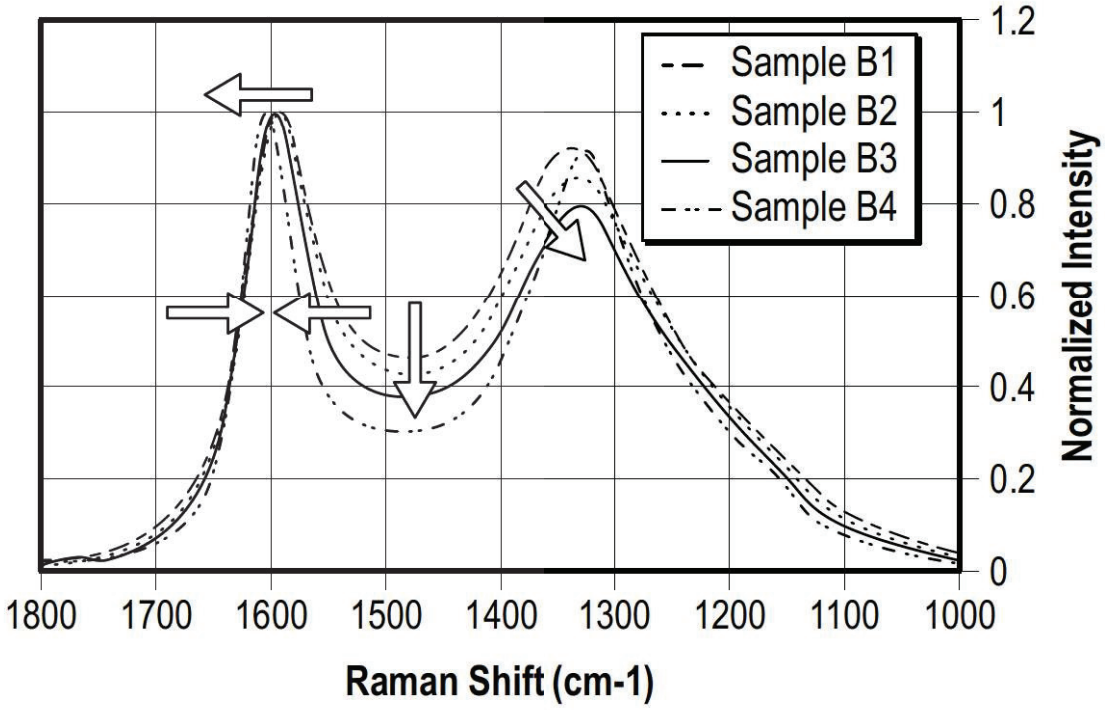
Sample B1
Sample B2
Sample B3
Sample B4
1.2
1
0.8
0.6
0.4
0.2
0
Normalized Intensity
1800
1700
1600
1500
1400
1300
1200
1100
1000
Raman Shift (cm-1)

FIG. 39B

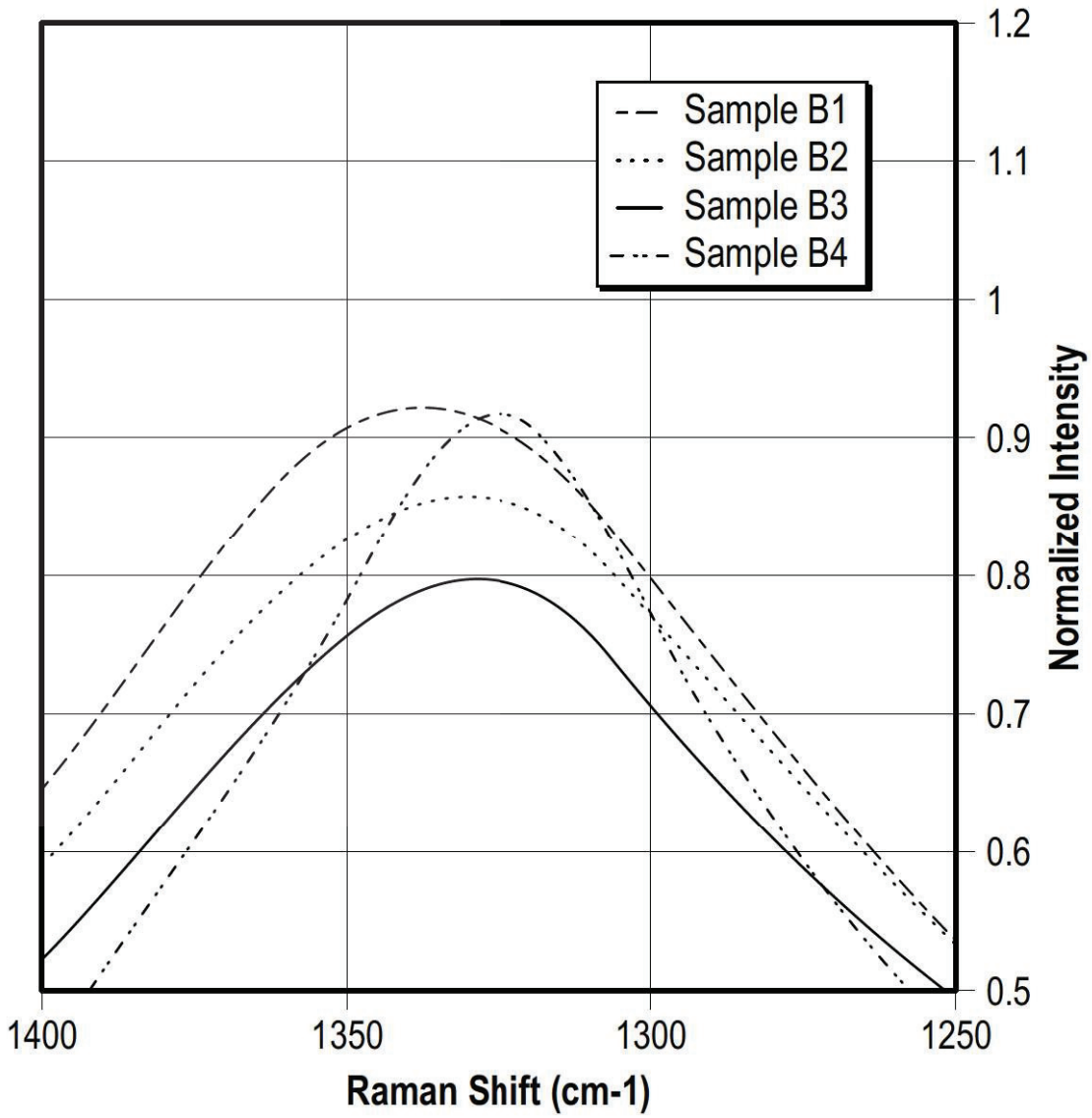
Sample B1
Sample B2
Sample B3
Sample B4
1.2
1.1
1
0.9
0.8
0.7
0.6
0.5
Normalized Intensity
1400
1350
1300
1250
Raman Shift (cm-1)

FIG. 39C

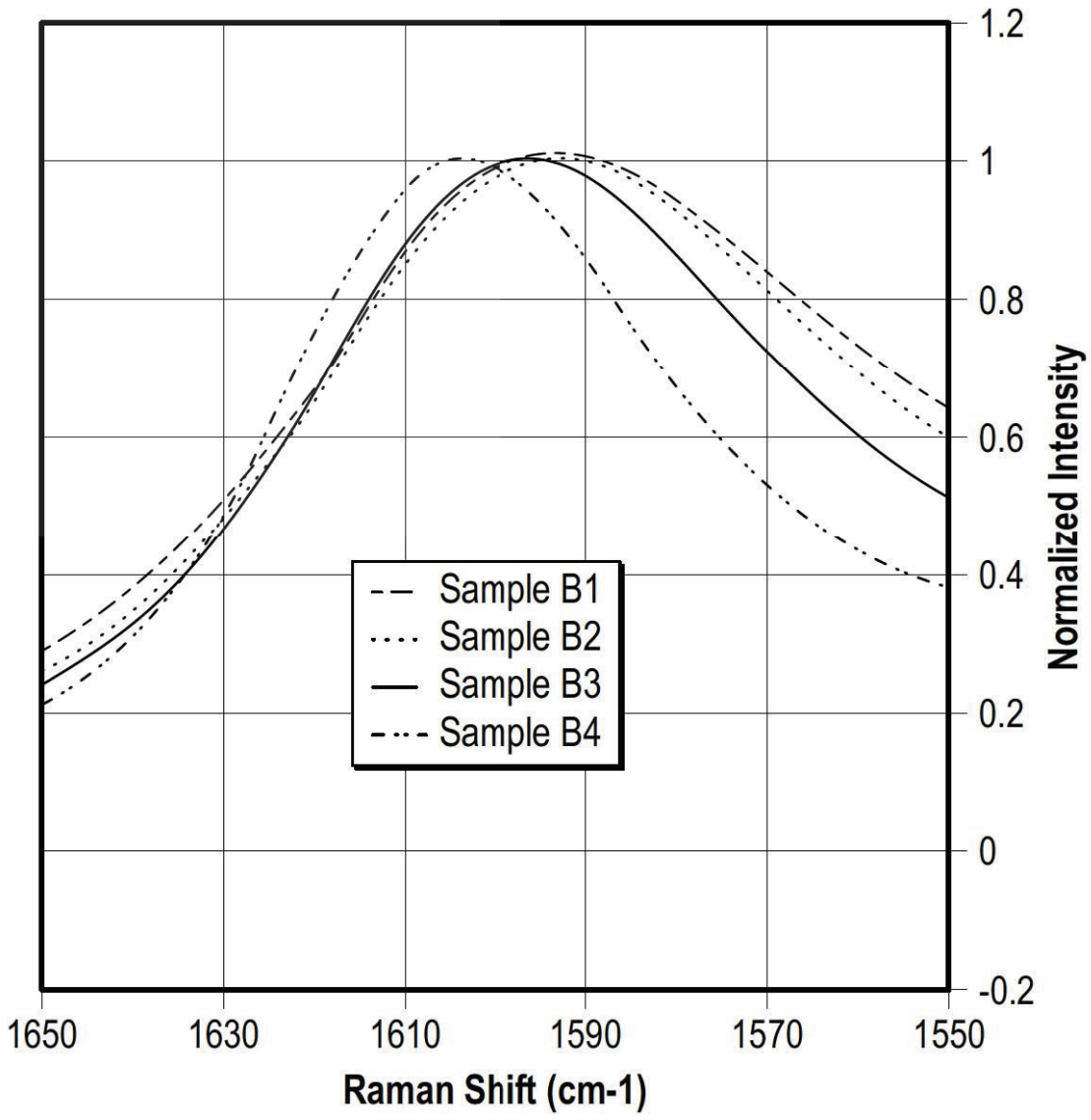
1.2
1
0.8
0.6
0.4
0.2
0
-0.2
Normalized Intensity
Sample B1
Sample B2
Sample B3
Sample B4
1650
1630
1610
1590
1570
1550
Raman Shift (cm-1)

FIG. 39D

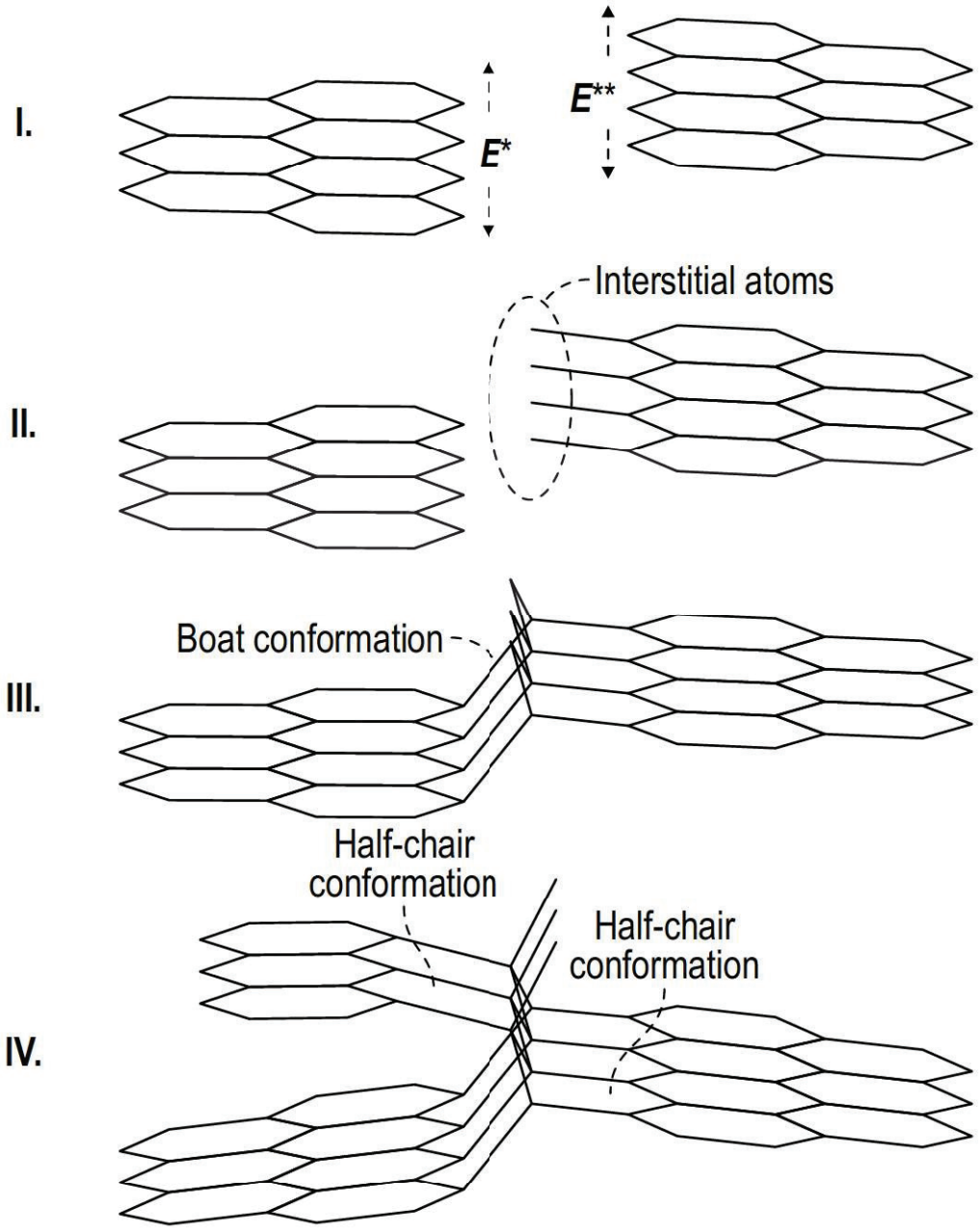
I.
E*
E**
II.
Interstitial atoms
III.
Boat conformation
IV.
Half-chair conformation
Half-chair conformation

FIG. 40

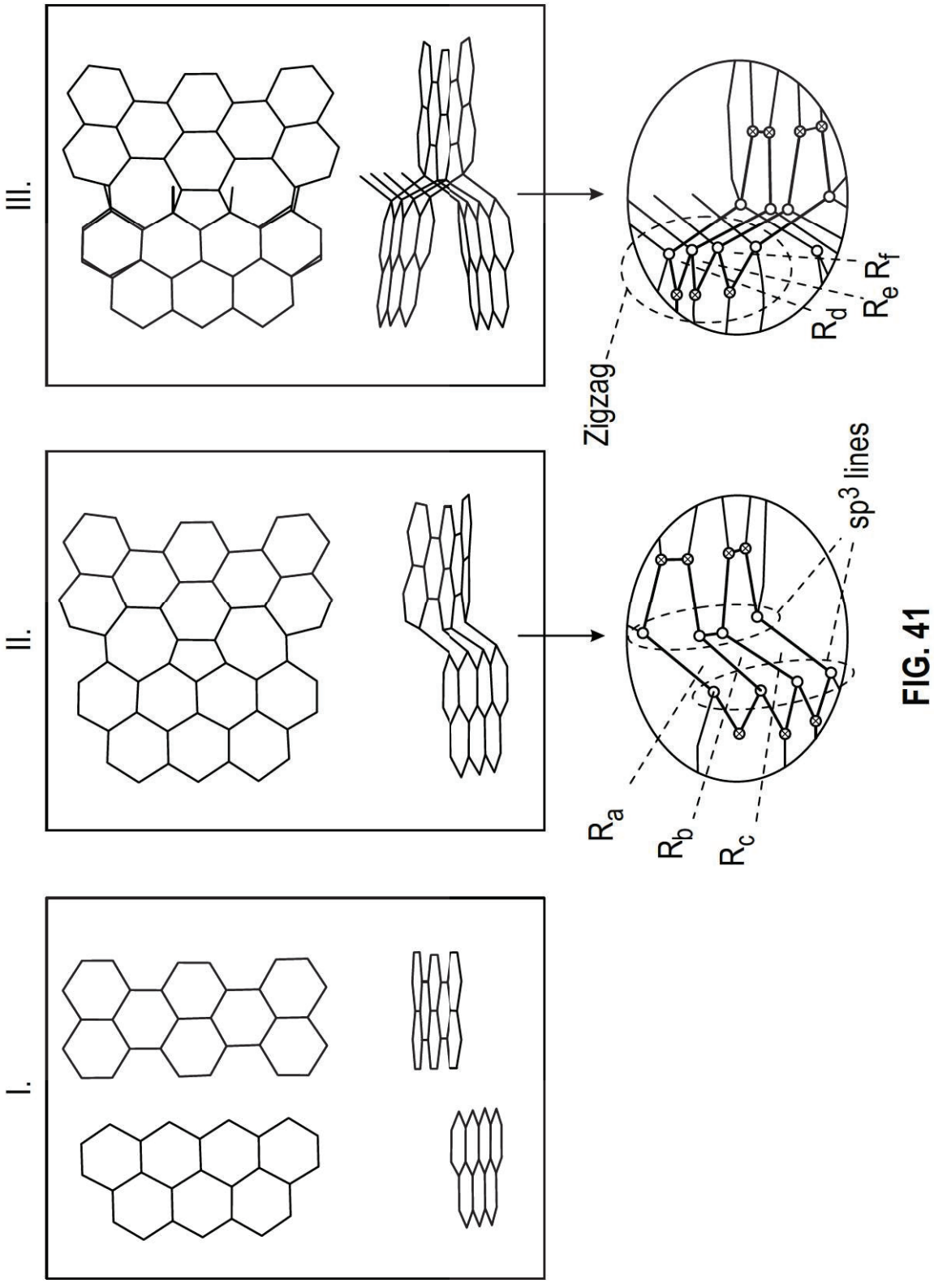

FIG. 41

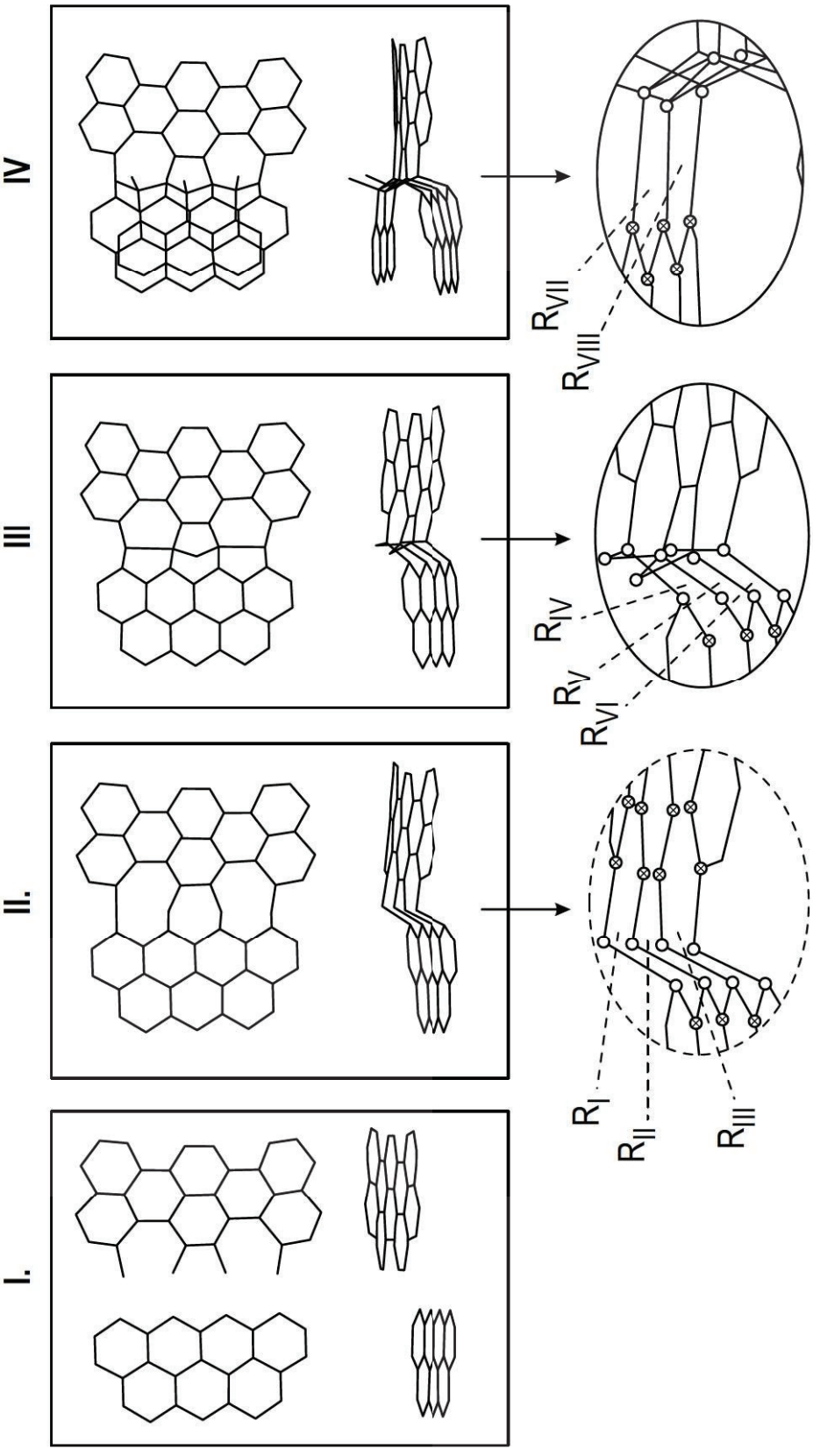

FIG. 42

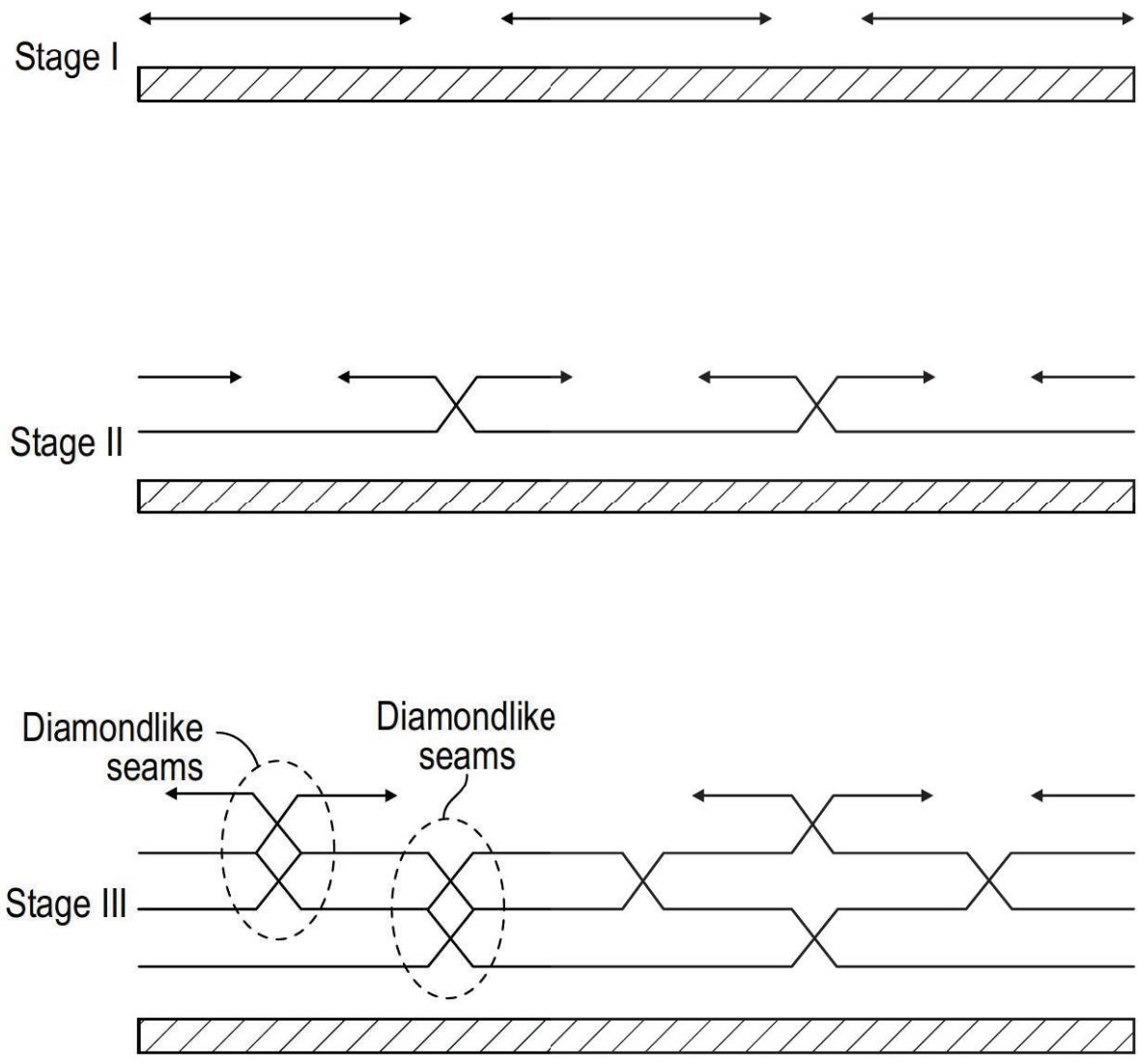
Stage I
Stage II
Diamondlike seams
Diamondlike seams
Stage III

FIG. 43

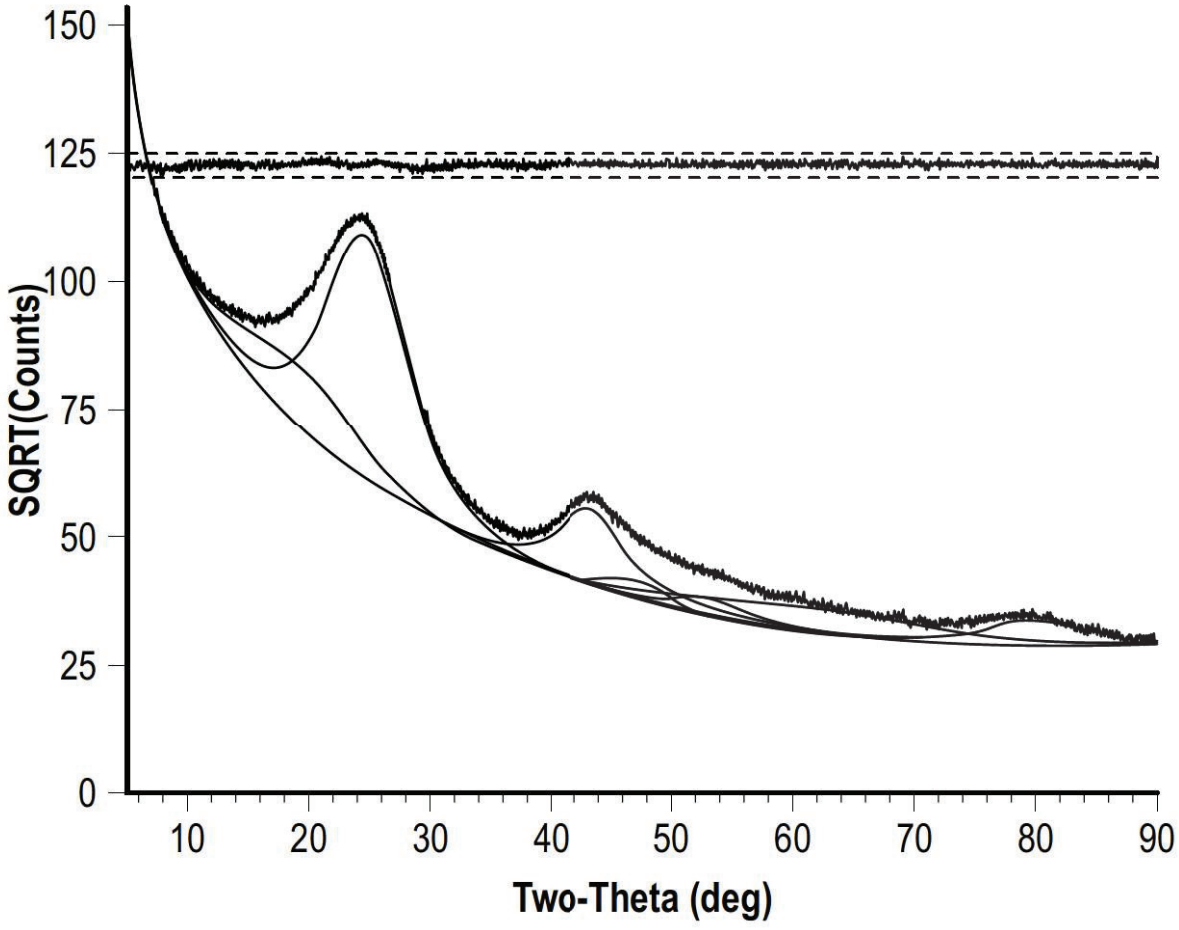
150
125
100
75
50
25
0
SQRT(Counts)
10
20
30
40
50
60
70
80
90
Two-Theta (deg)

FIG. 44



460°C 400°C

FIG. 45

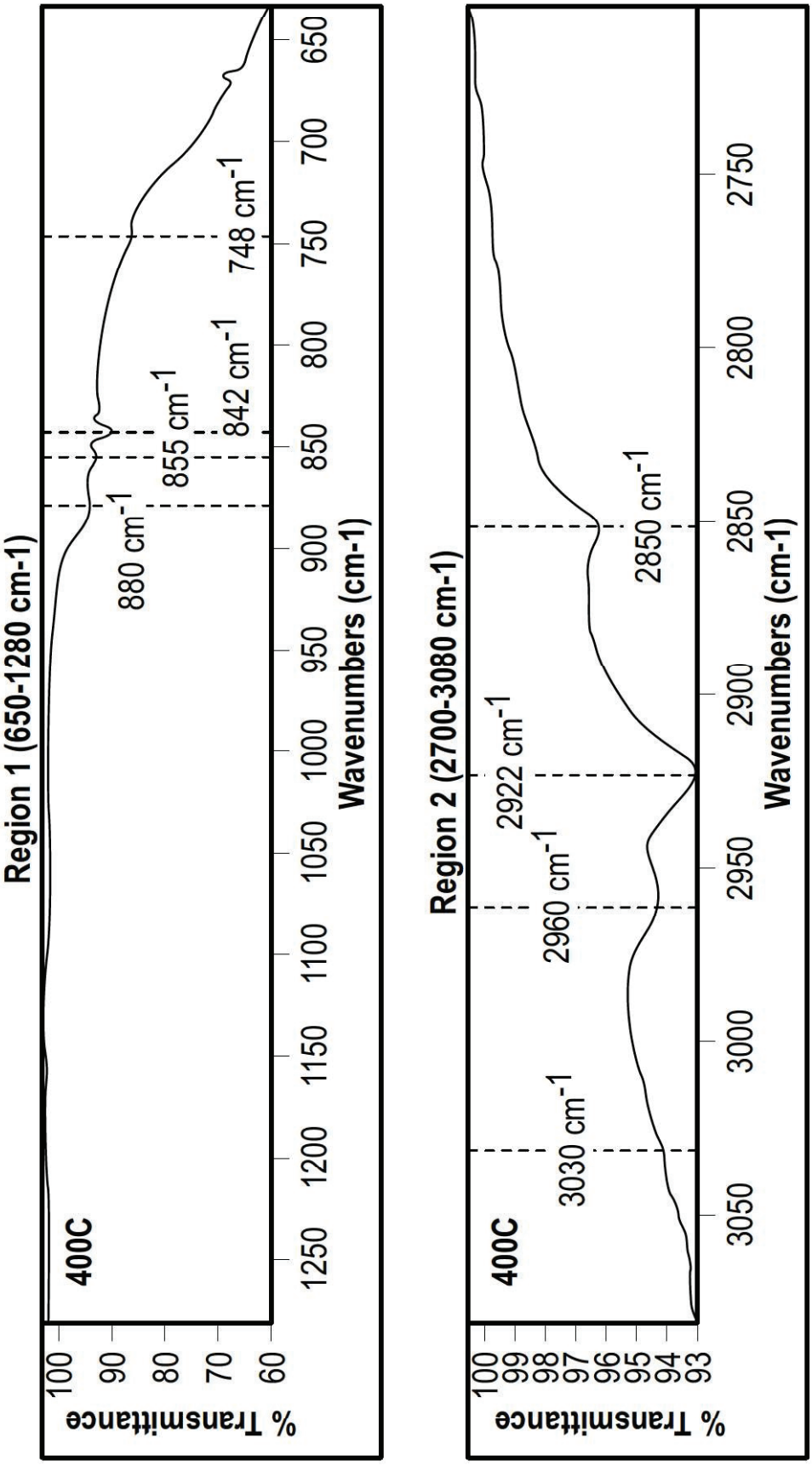
Region 1 (650-1280 cm-1)
400C
% Transmittance
100
90
80
70
60
1250
1200
1150
1100
1050
1000
950
900
850
800
750
700
650
Wavenumbers (cm-1)
880 cm-1
855 cm-1
842 cm-1
748 cm-1
Region 2 (2700-3080 cm-1)
400C
% Transmittance
100
99
98
97
96
95
94
93
3050
3000
2950
2900
2850
2800
2750
Wavenumbers (cm-1)
3030 cm-1
2960 cm-1
2922 cm-1
2850 cm-1

FIG. 46A

	Region 1				Region 2			
Peak pos. (cm^{-1})	880	855	842	748	3030	2960	2922	2850
	X	X	X	X	X	X	X	X
Peak Assignment	geminal disub alkene			mono/orthodi -sub aromatic	sp2 C-H stretch	sp3 C-H stretch		
	sp2 CH bend for aromatics							
	sp2 CH bend for alkenes							

FIG. 46B

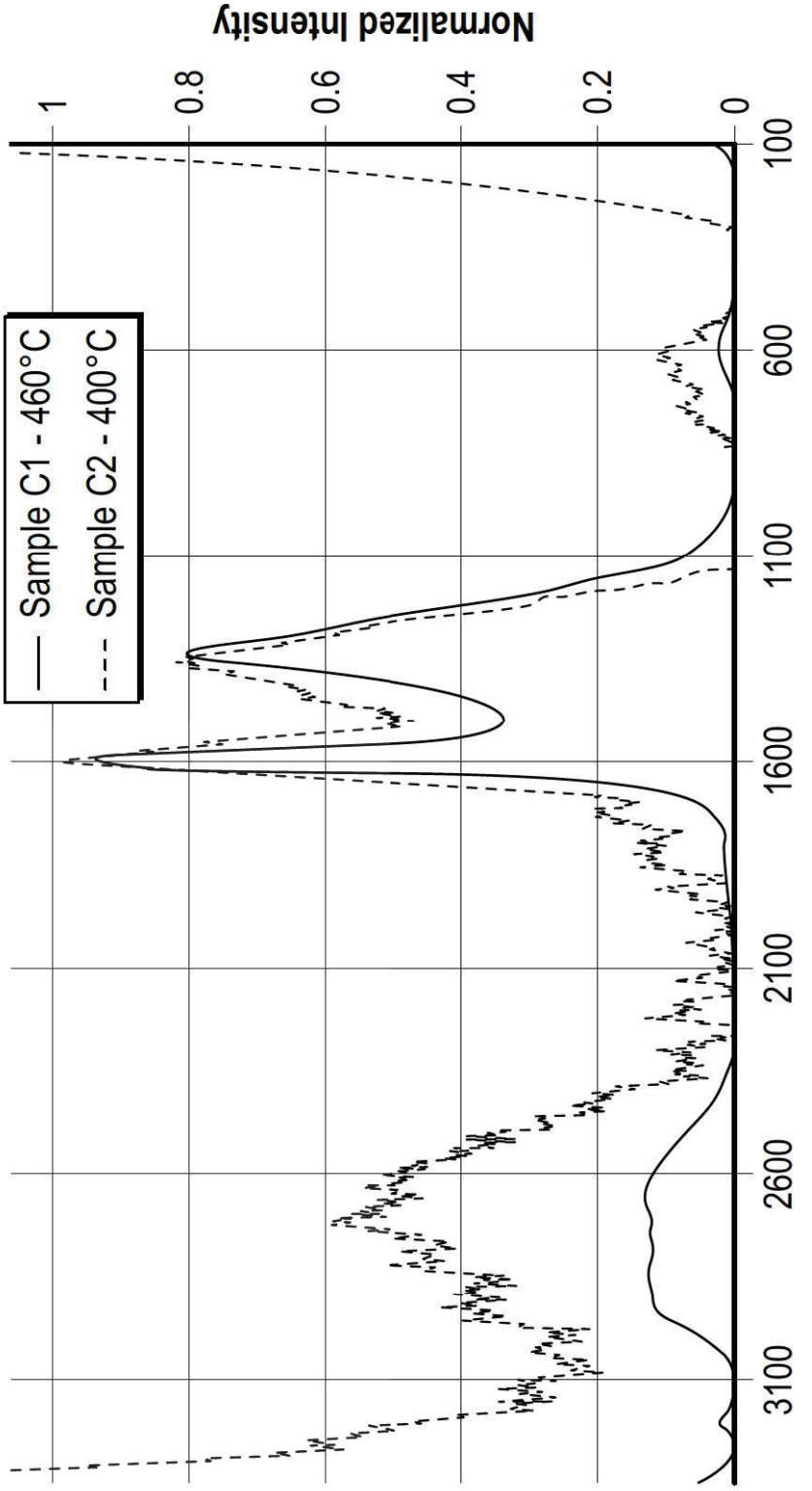
Normalized Intensity
1
0.8
0.6
0.4
0.2
0
Sample C1 - 460°C
Sample C2 - 400°C
100
600
1100
1600
2100
2600
3100
Raman Shift (cm-1)

FIG. 47

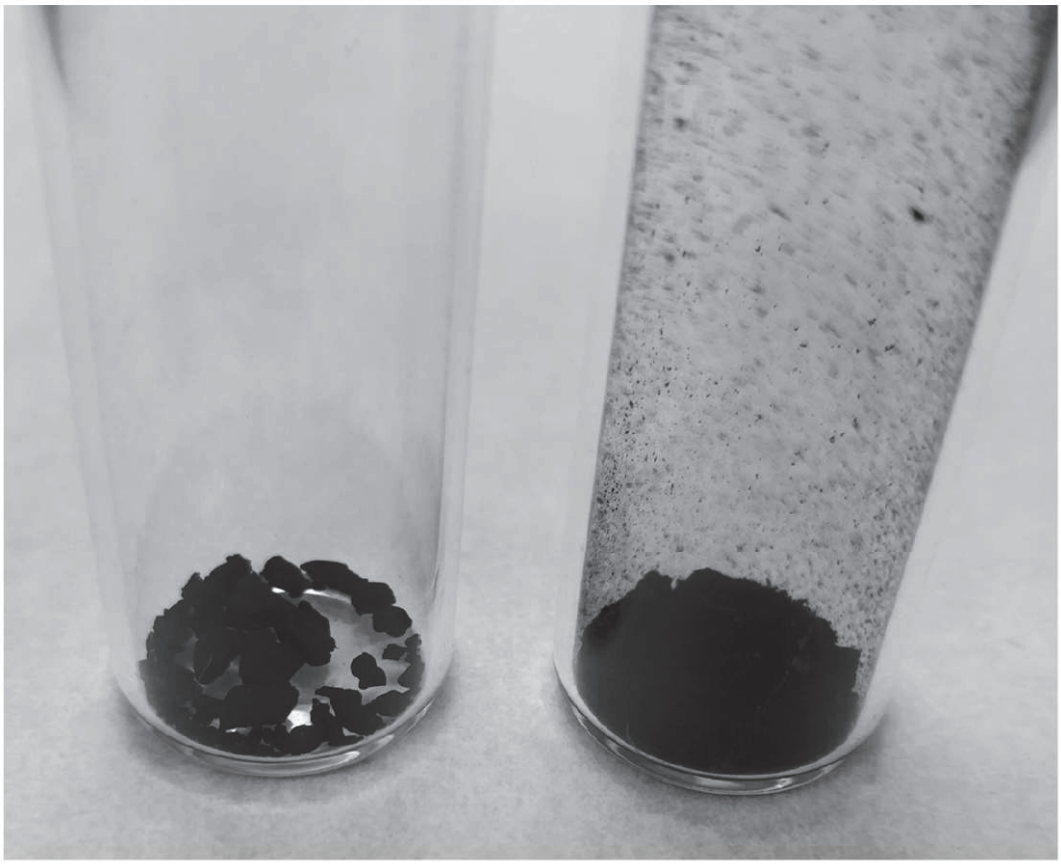

FIG. 48

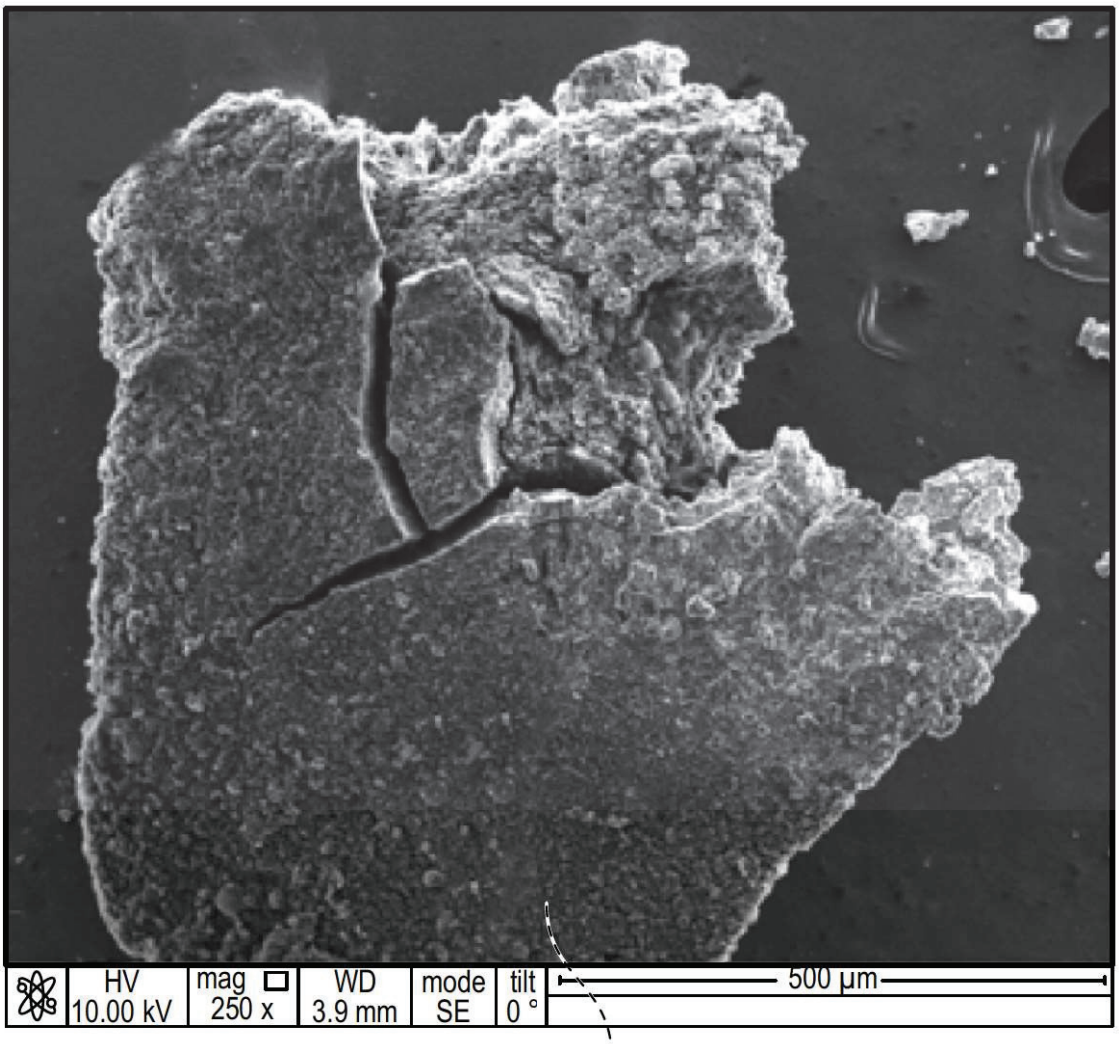
HV
10.00 kV
mag
250 x
WD
3.9 mm
mode
SE
tilt
0 °
500 µm
Dense, macroscopic granules

FIG. 49A

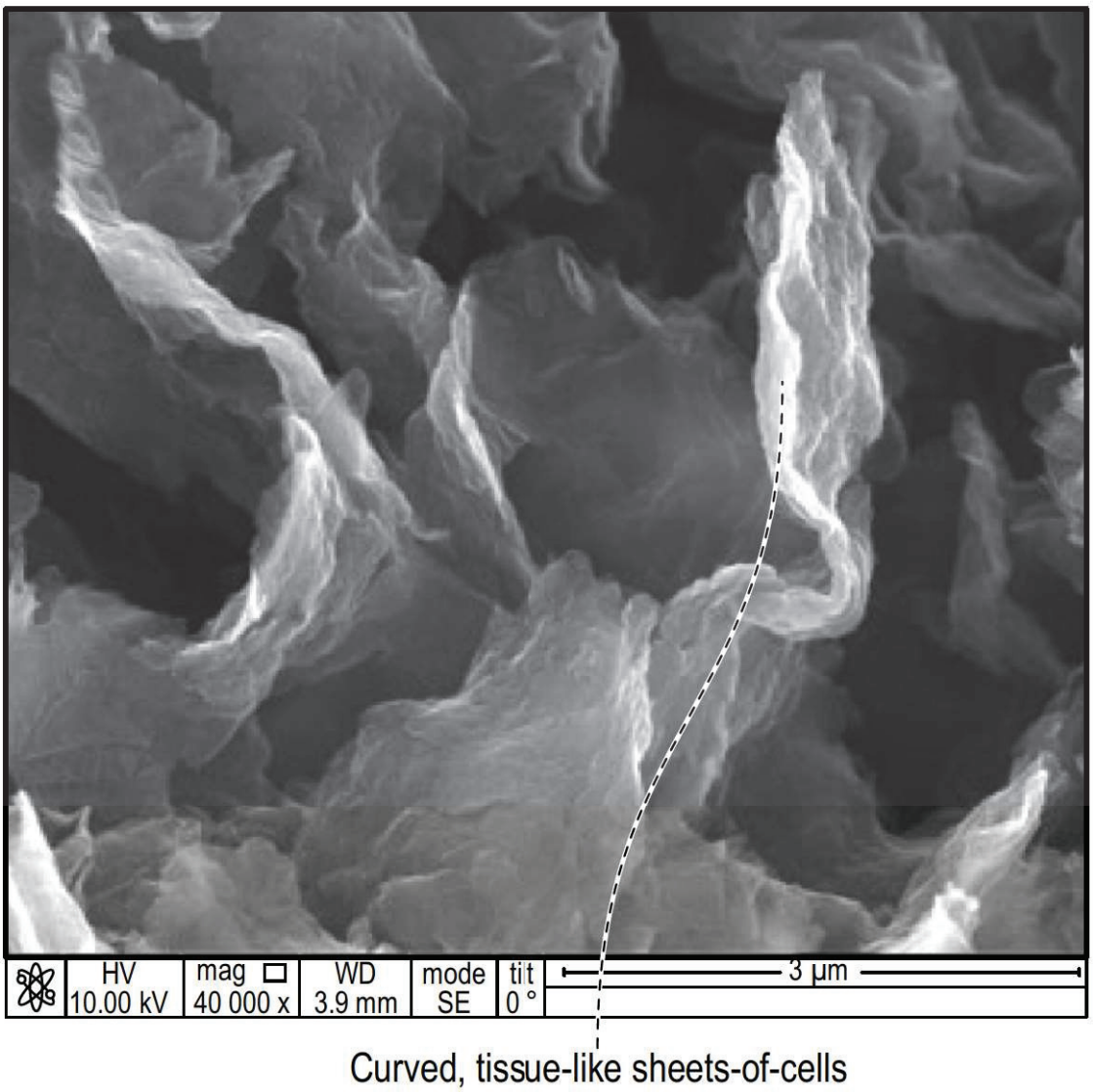
HV
10.00 kV
mag
40 000 x
WD
3.9 mm
mode
SE
tilt
0 °
3 µm
Curved, tissue-like sheets-of-cells

FIG. 49B

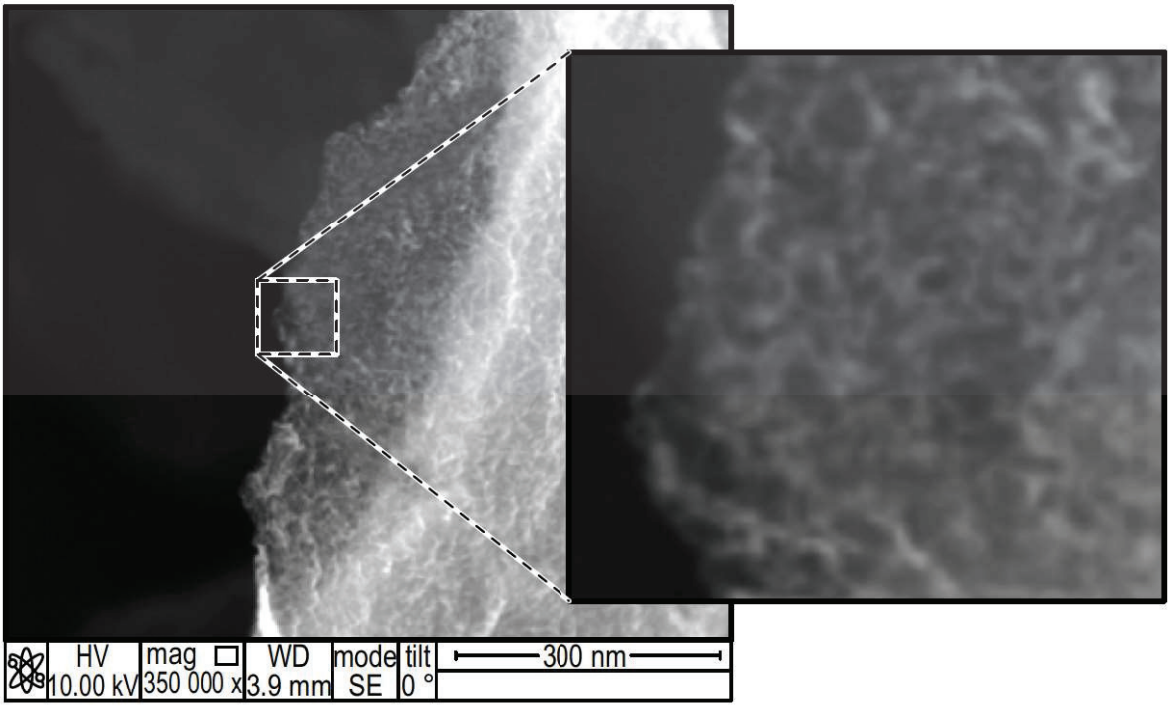

FIG. 49C

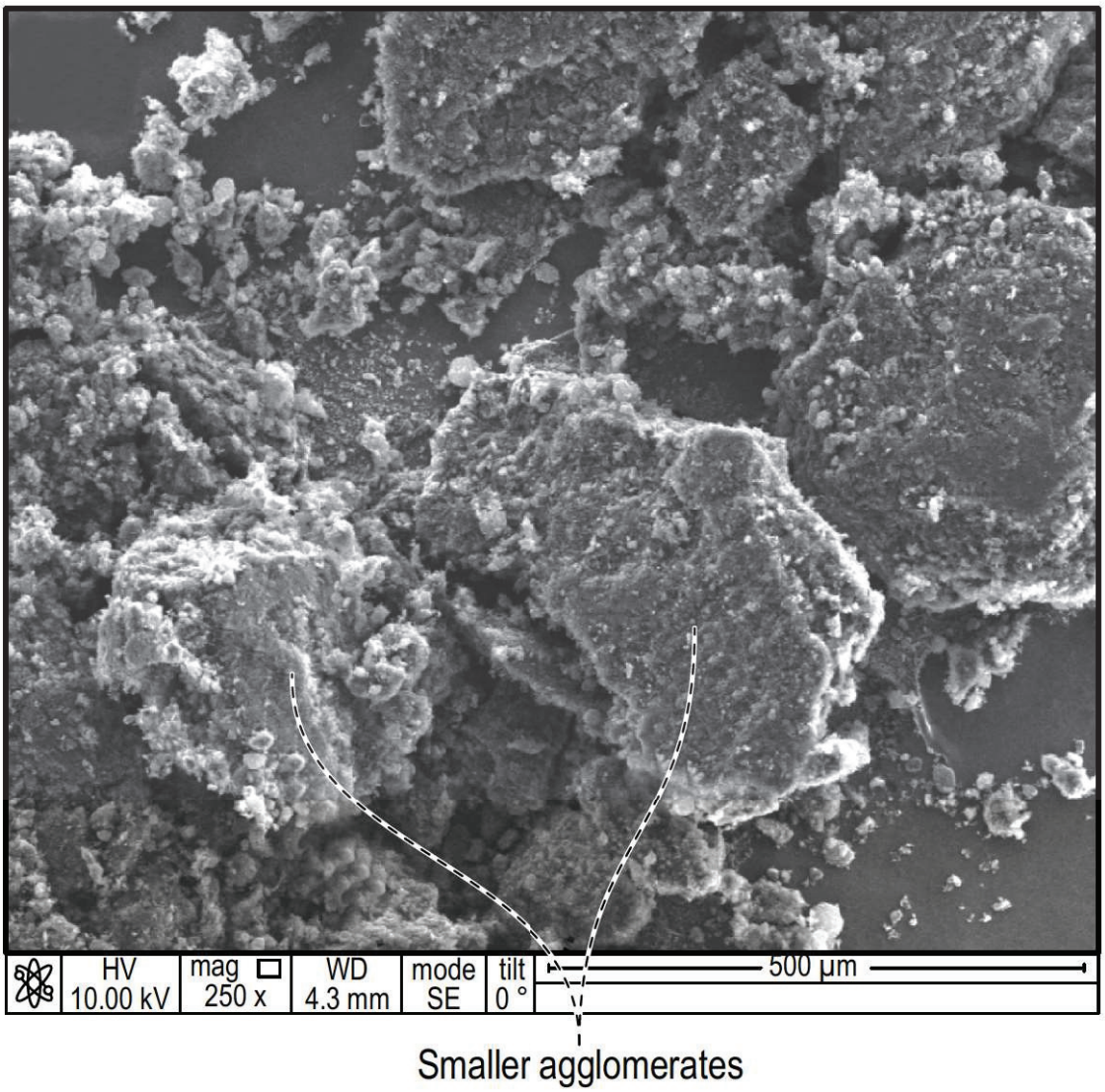
HV
10.00 kV
mag
250 x
WD
4.3 mm
mode
SE
tilt
0 °
500 µm
Smaller agglomerates

FIG. 49D

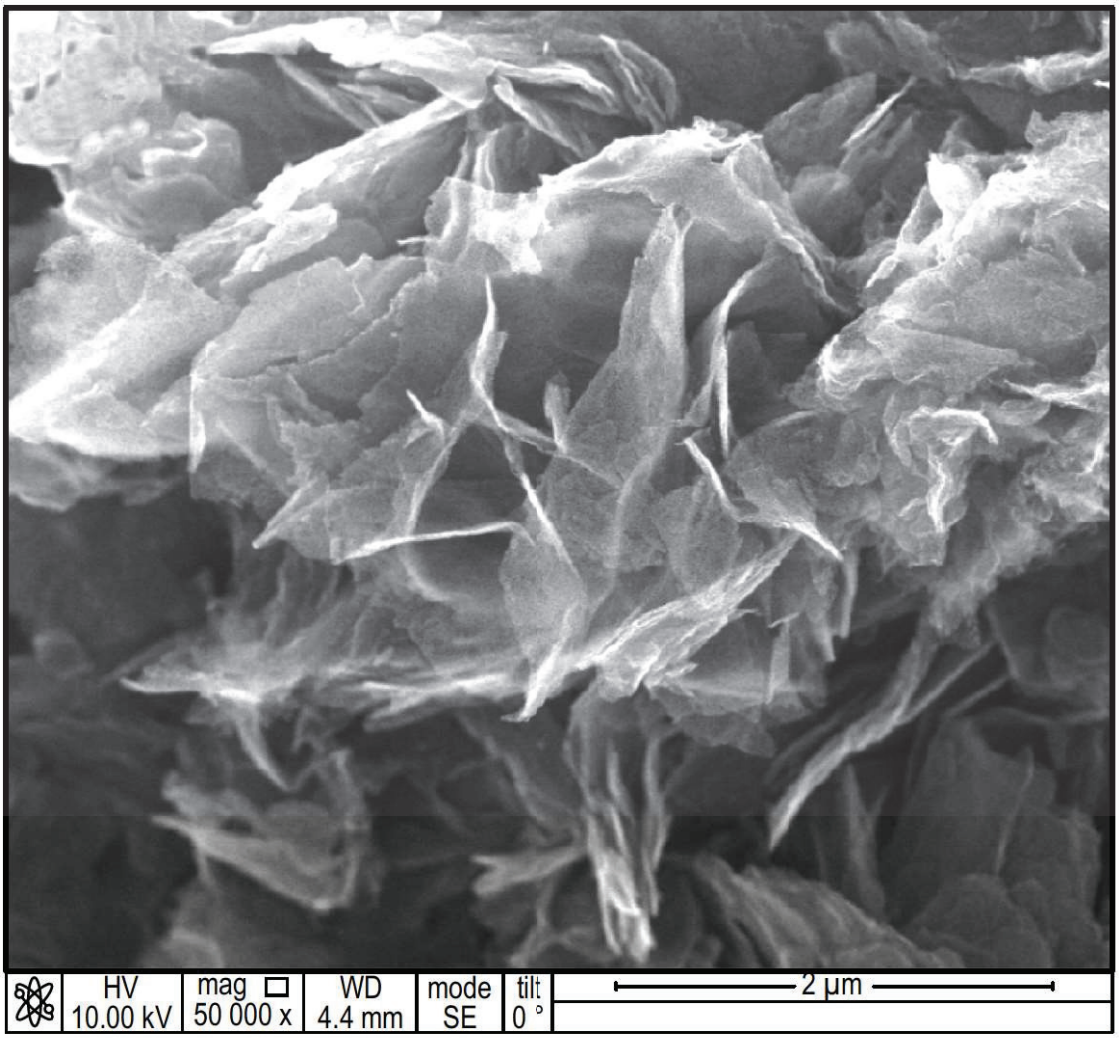

FIG. 49E

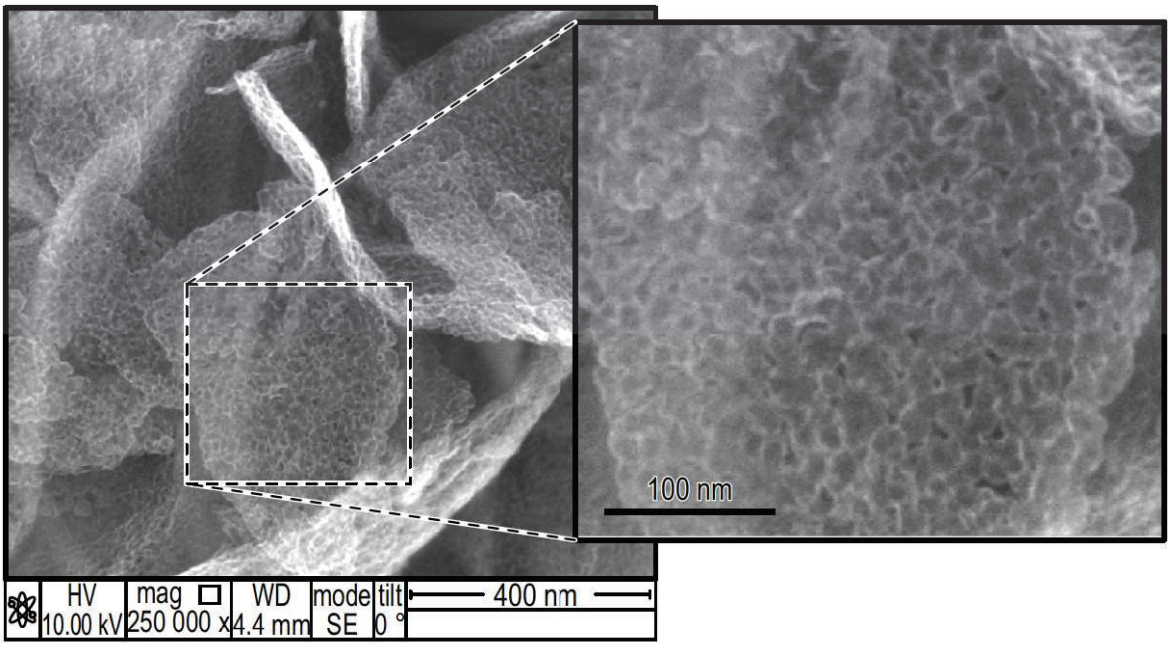

FIG. 49F

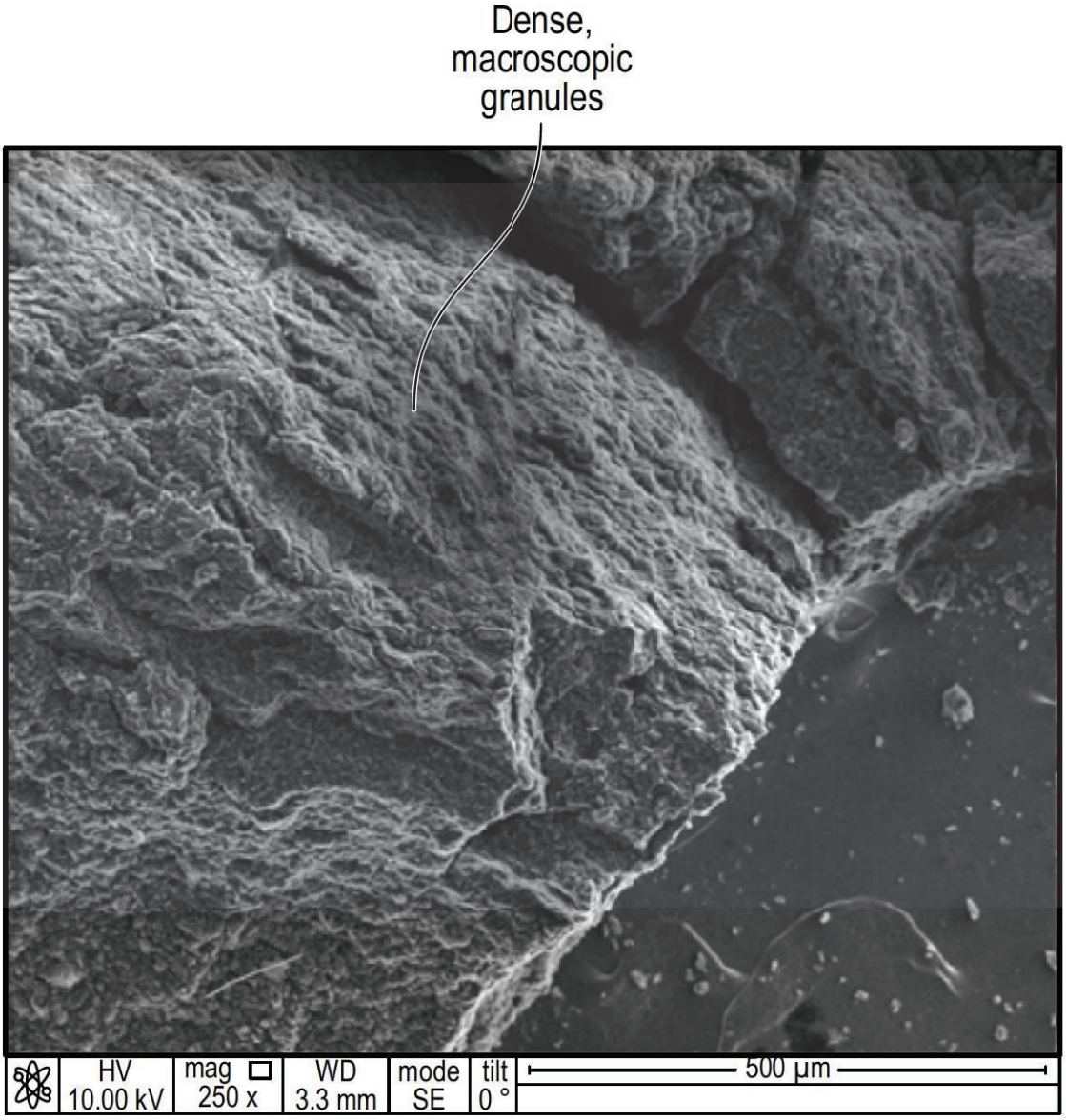
Dense,
macroscopic
granules
HV
10.00 kV
mag
250 x
WD
3.3 mm
mode
SE
tilt
0 °
500 µm

FIG. 50A

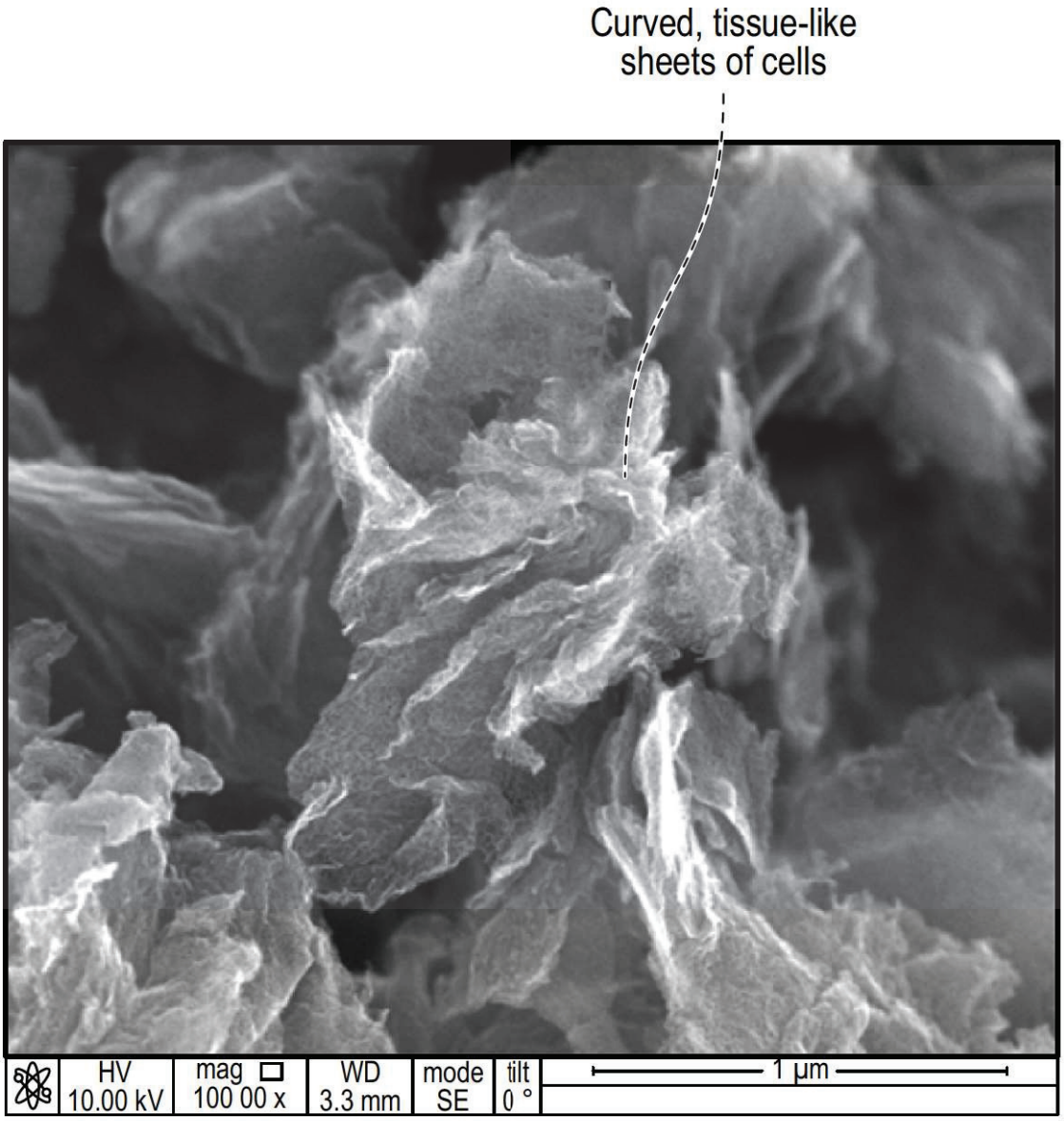
Curved, tissue-like
sheets of cells
HV
10.00 kV
mag
100 00 x
WD
3.3 mm
mode
SE
tilt
0 °
1 µm

FIG. 50B

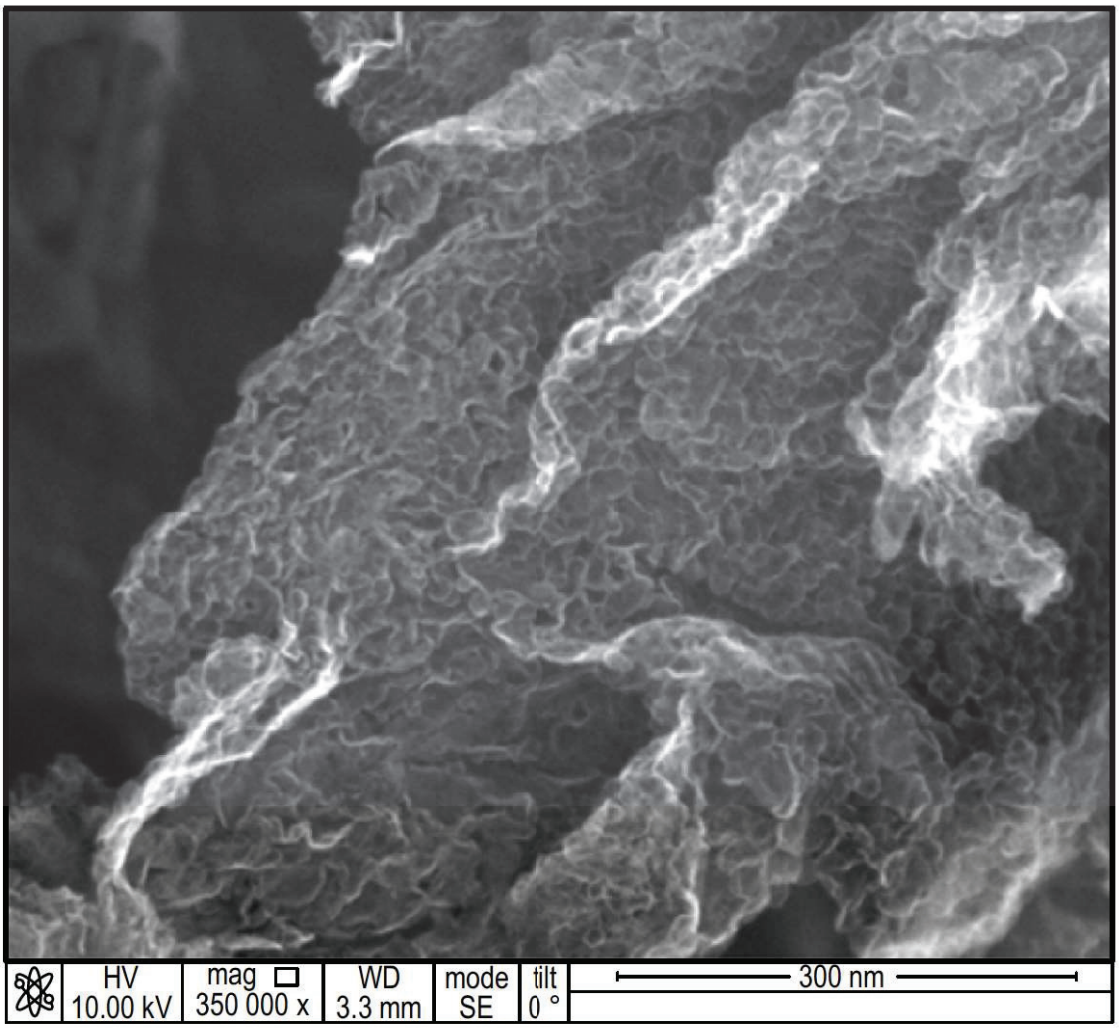

FIG. 50C

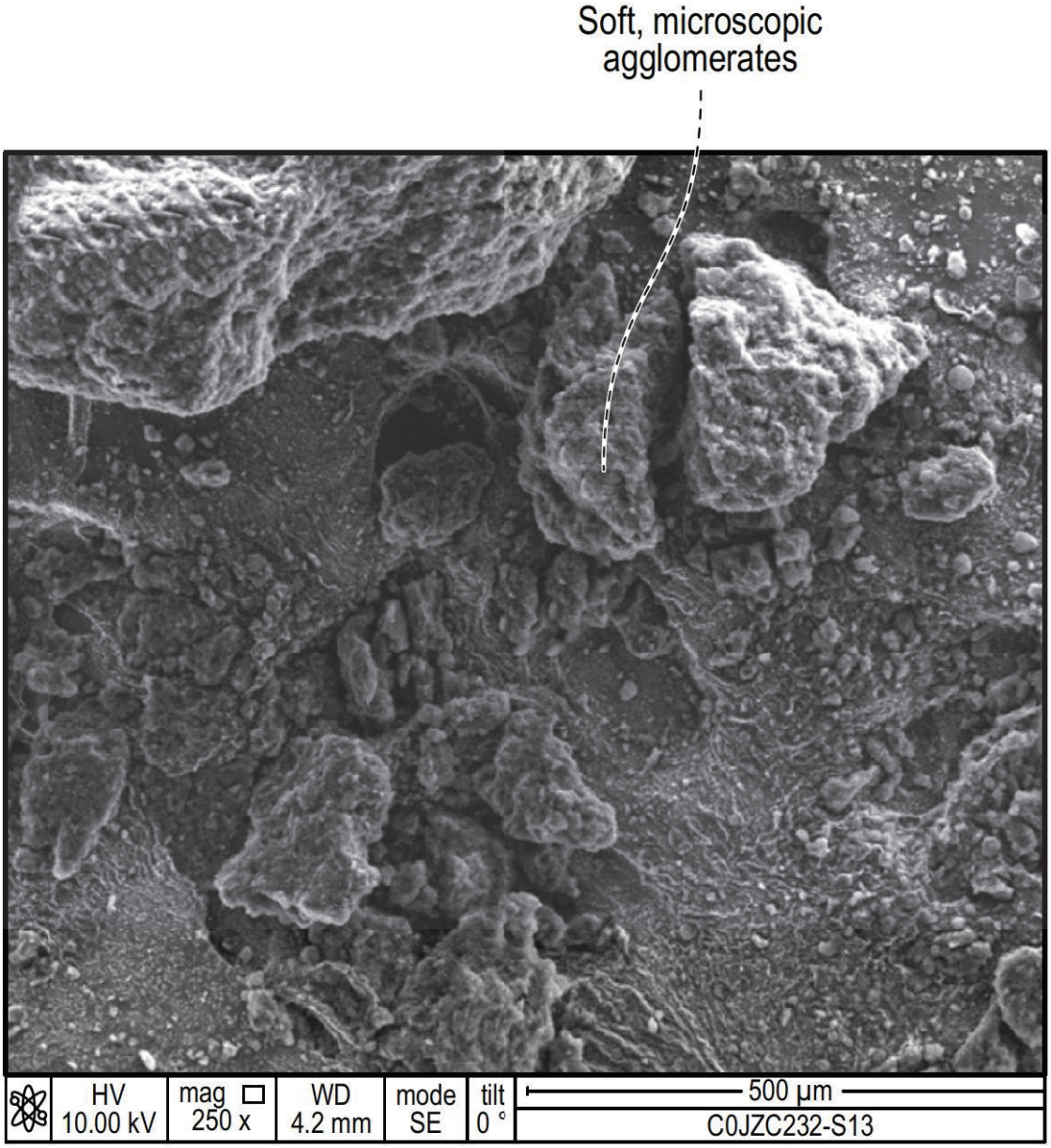
Soft, microscopic agglomerates
HV
10.00 kV
mag
250 x
WD
4.2 mm
mode
SE
tilt
0 °
500 µm
C0JZC232-S13

FIG. 50D

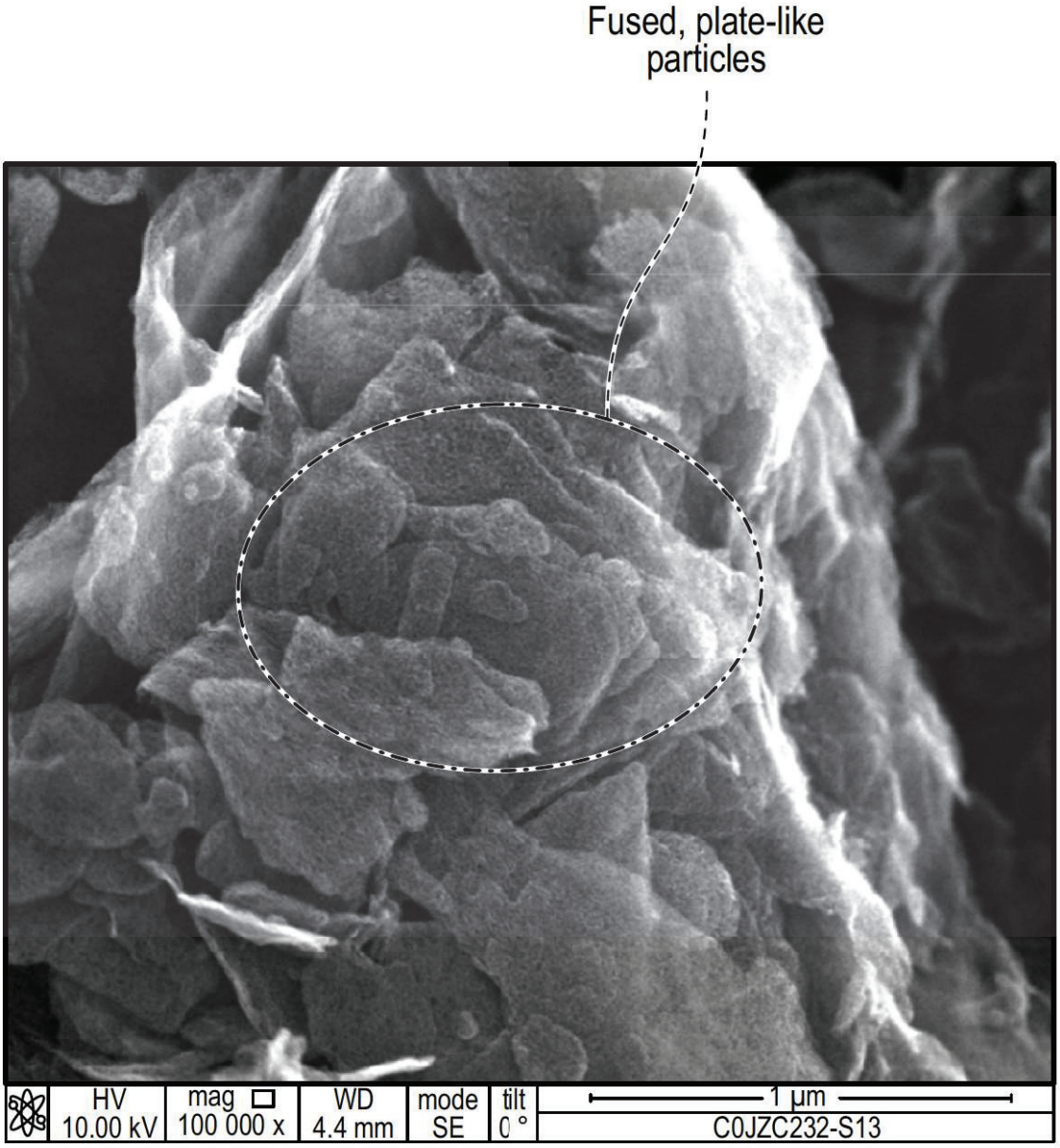
Fused, plate-like particles
HV
10.00 kV
mag
100 000 x
WD
4.4 mm
mode
SE
tilt
0 °
1 µm
C0JZC232-S13

FIG. 50E

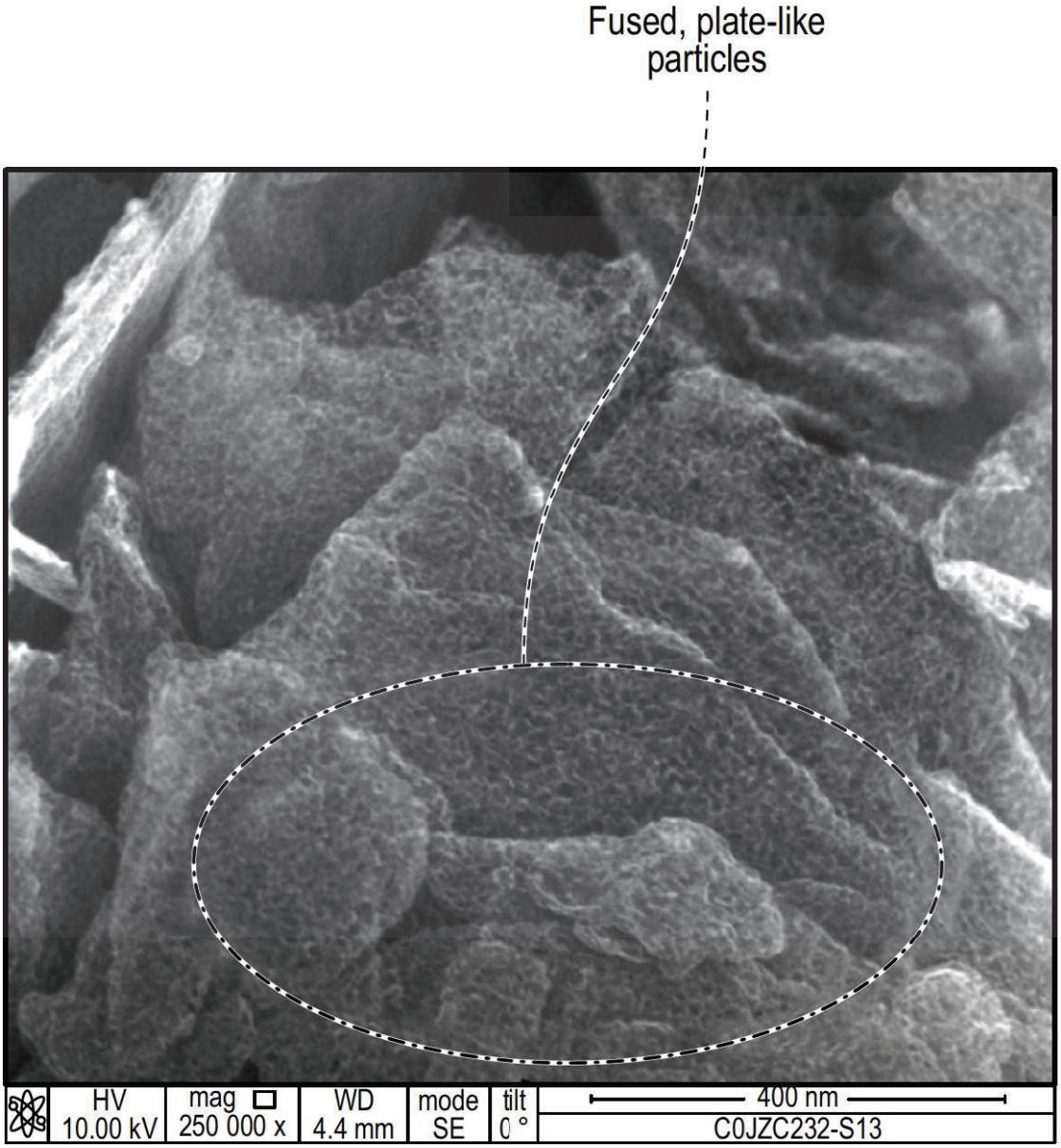
Fused, plate-like particles
HV
10.00 kV
mag
250 000 x
WD
4.4 mm
mode
SE
tilt
0 °
400 nm
C0JZC232-S13

FIG. 50F

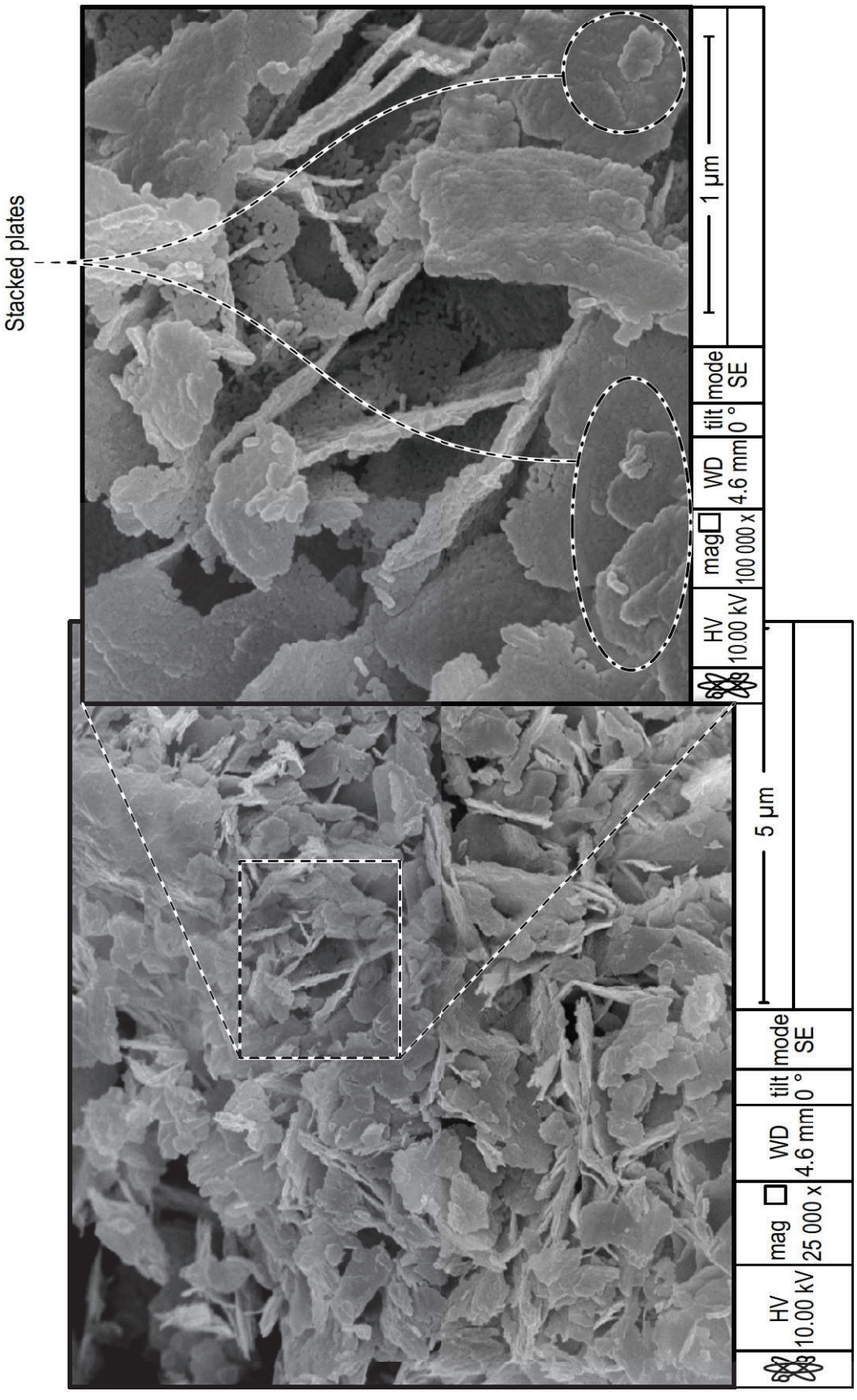
Stacked plates
HV 10.00 kV
mag 25 000 x
WD 4.6 mm
tilt 0 °
mode SE
5 µm
HV 10.00 kV
mag 100 000 x
WD 4.6 mm
tilt 0 °
mode SE
1 µm

FIG. 51

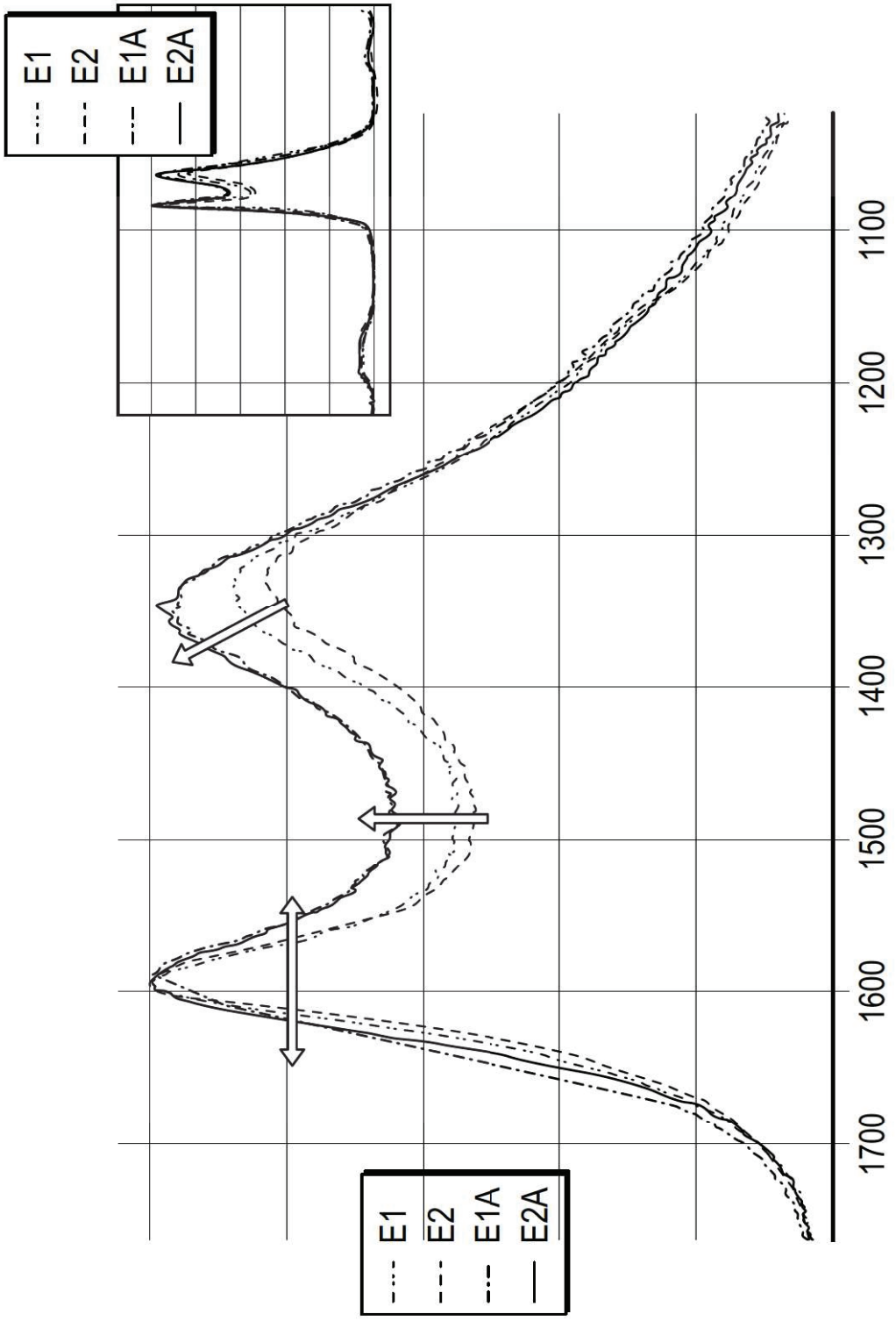

FIG. 52

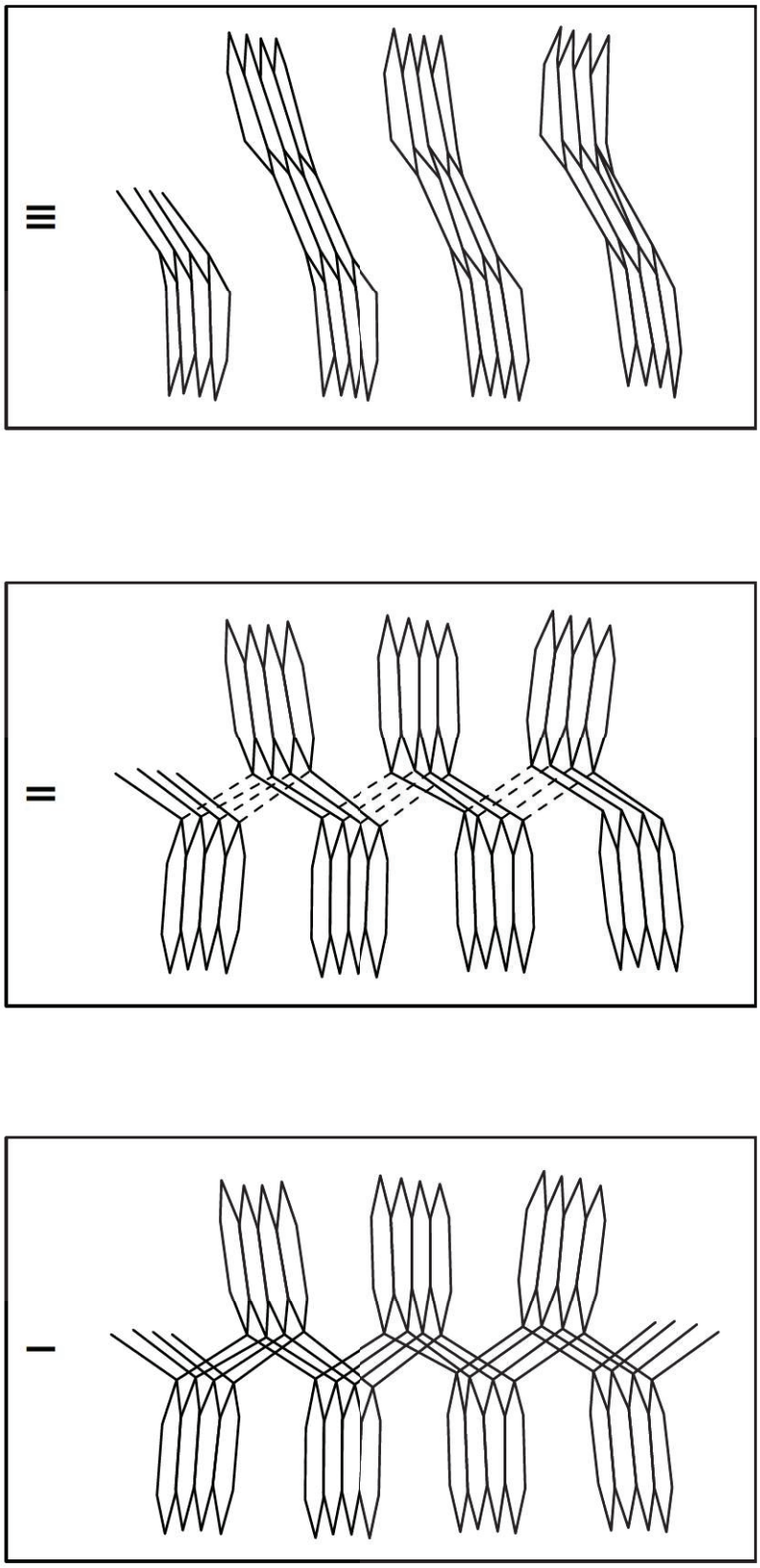

FIG. 53

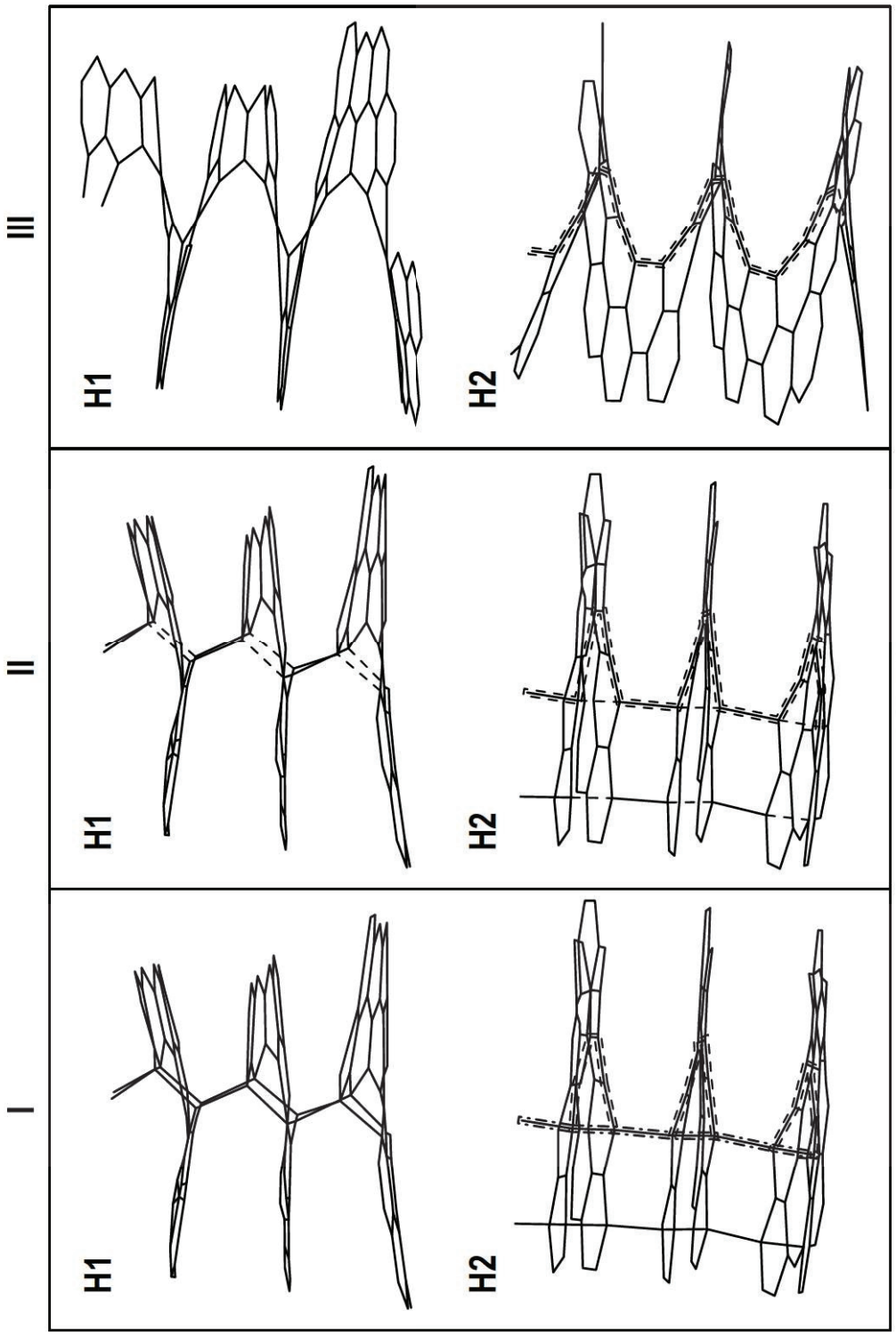

FIG. 54

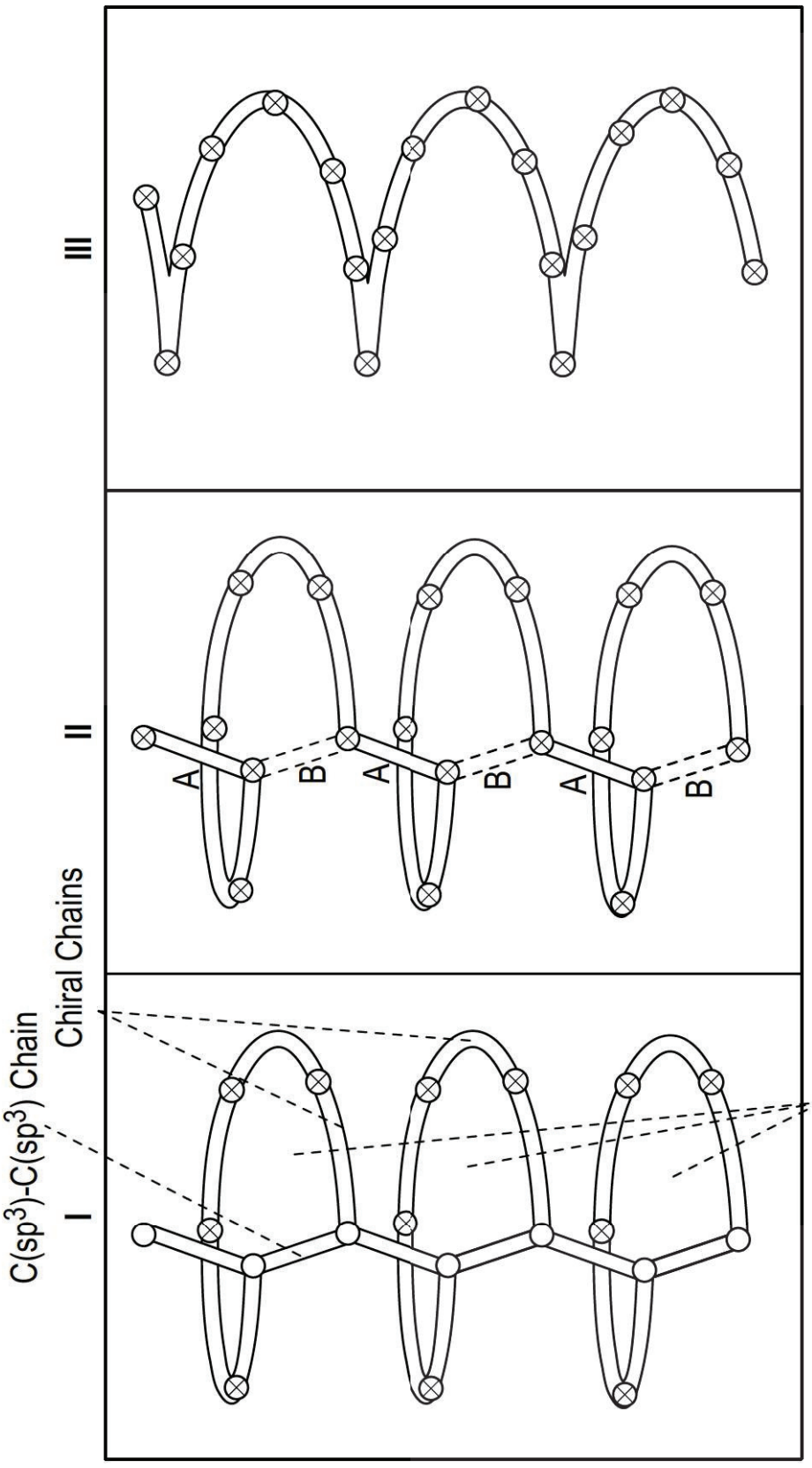

FIG. 55

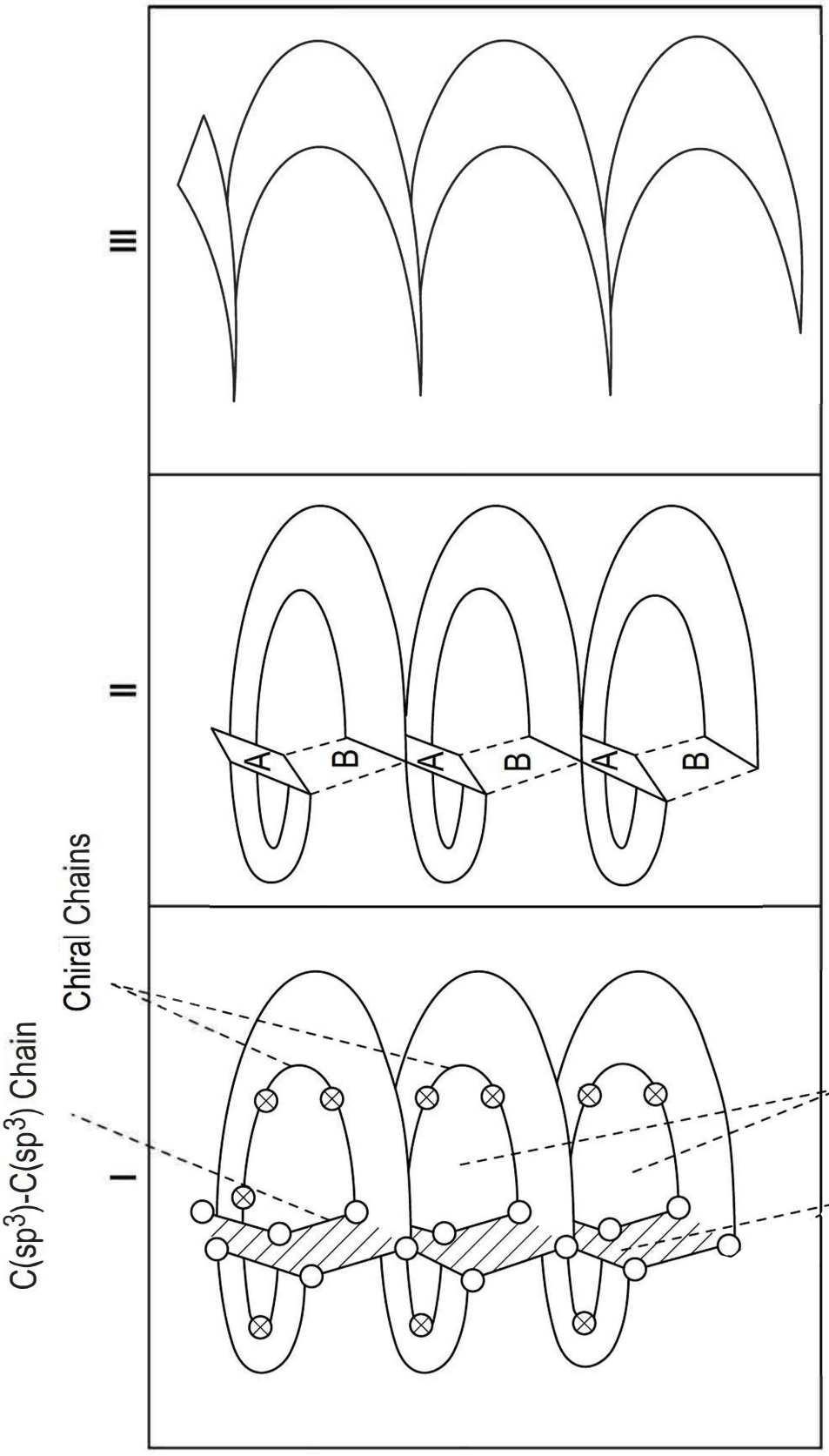
III
II
I
A
B
A
B
A
B
Chiral Chains
C(sp3)-C(sp3) Chain
Seam
Chiral Rings

FIG. 56

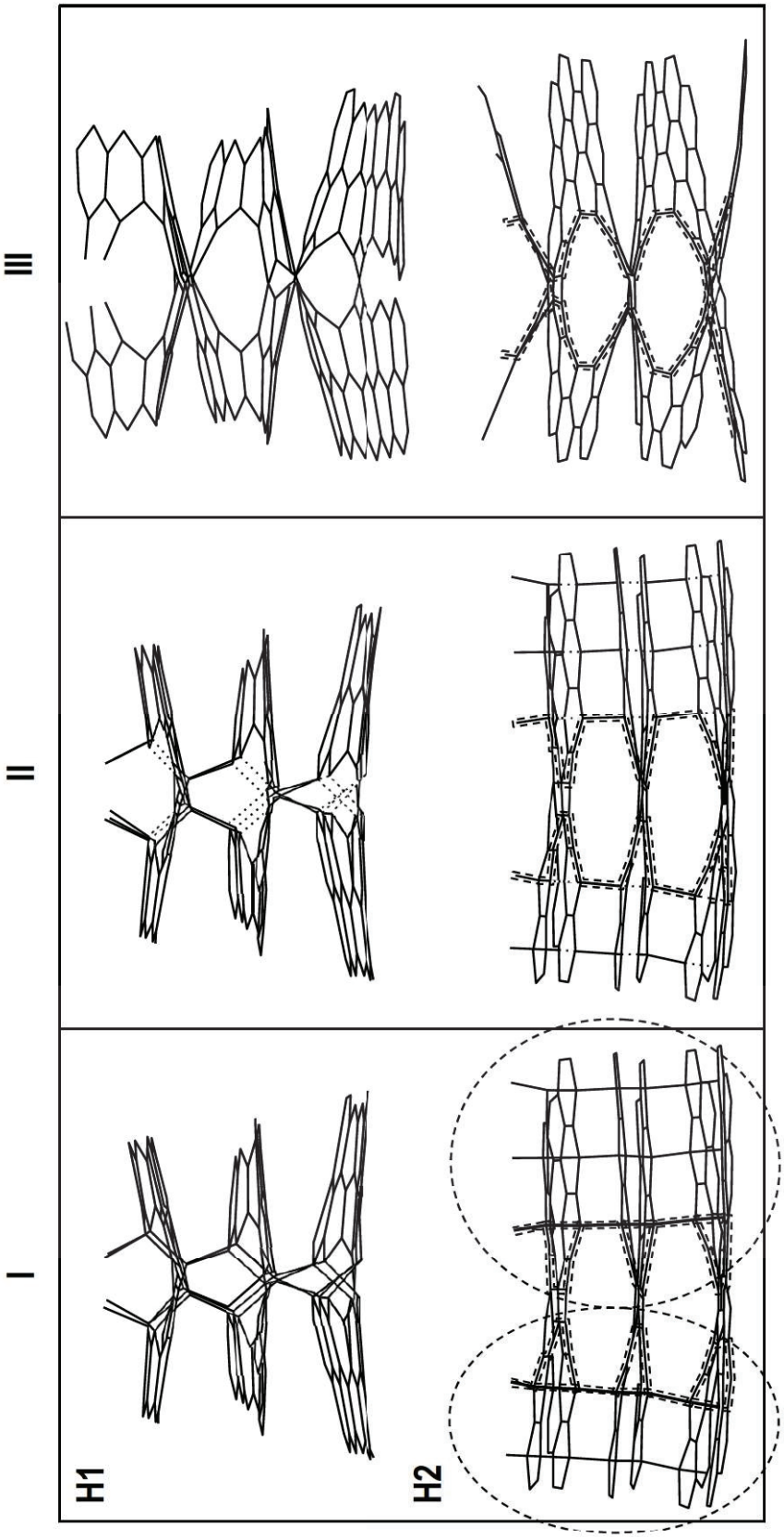

FIG. 57

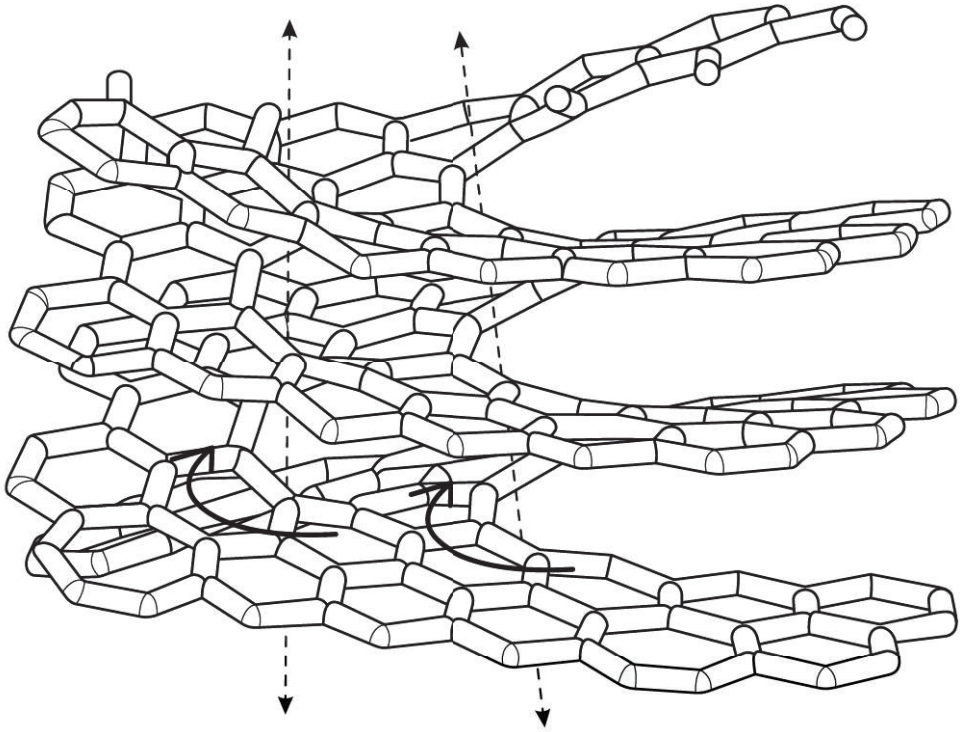

FIG. 58

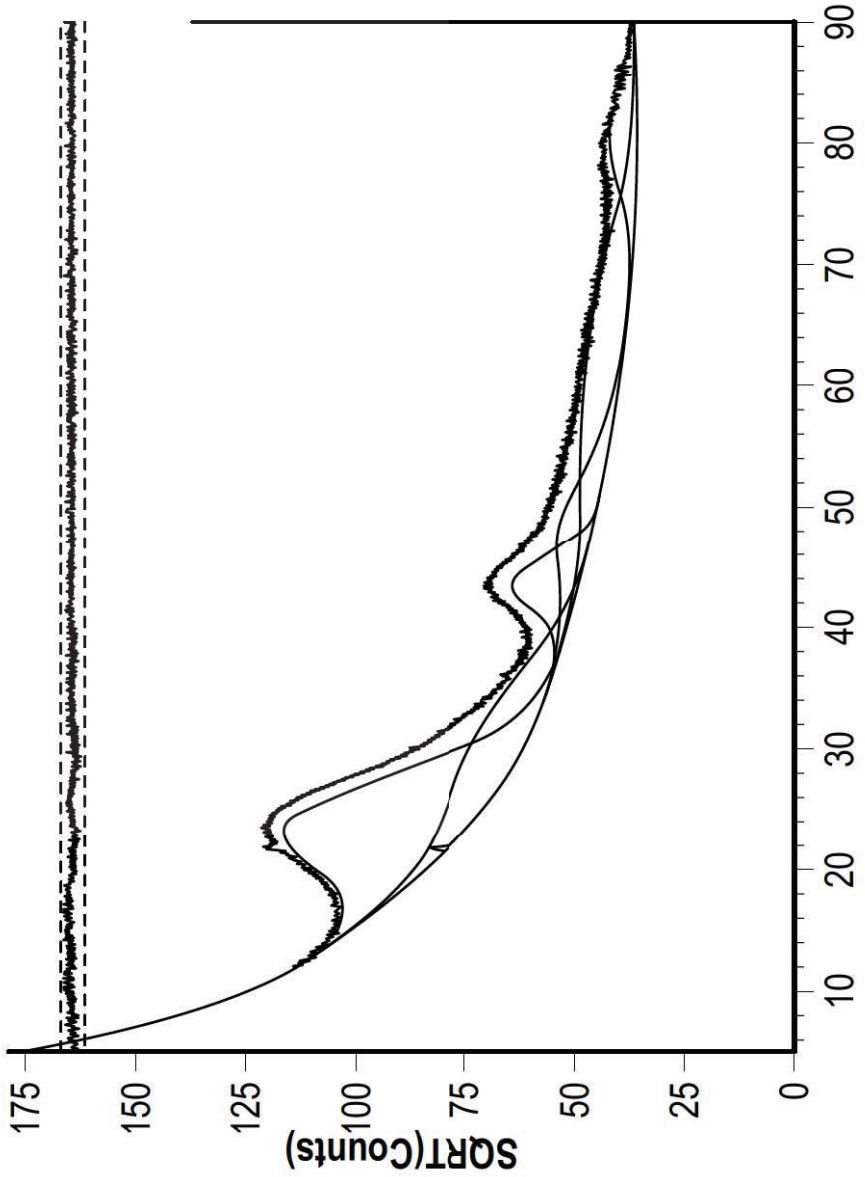
SQRT(Counts)
0
25
50
75
100
125
150
175
10
20
30
40
50
60
70
80
90
Two-Theta (deg)

FIG. 59

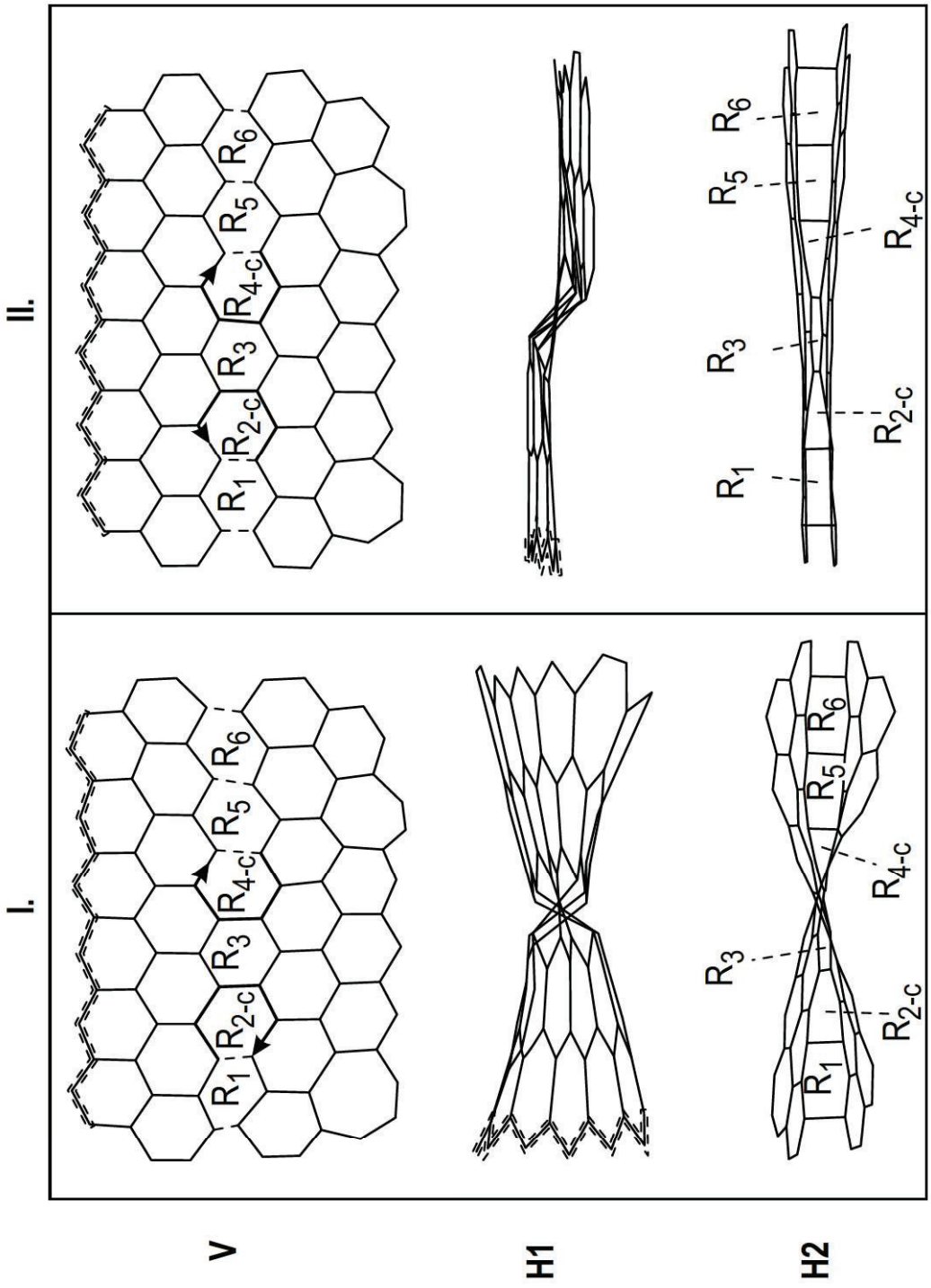

FIG. 60

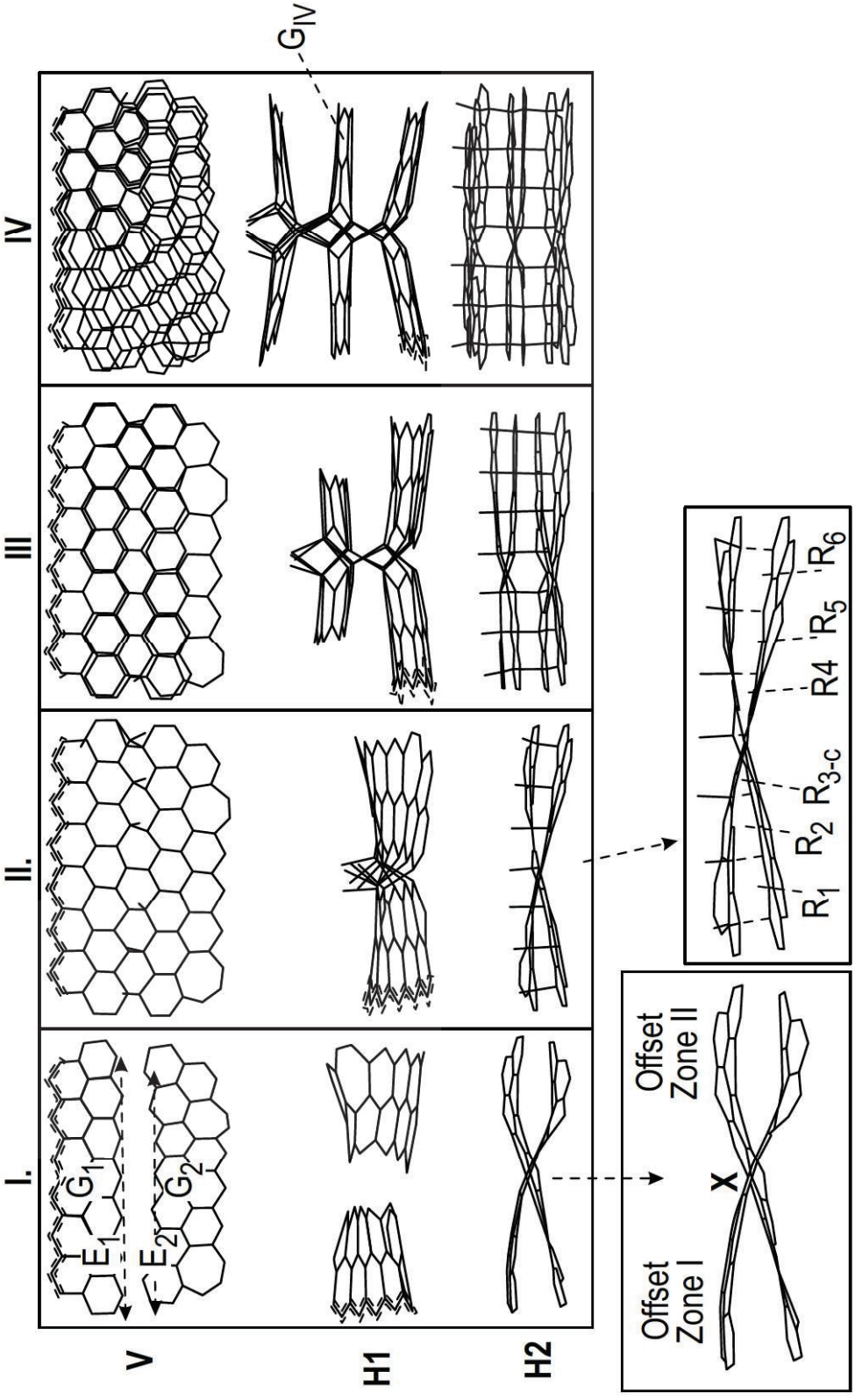
I.
II.
III
IV
V
H1
H2
G_1
E_1
E_2
G_2
G_{IV}
Offset Zone I
Offset Zone II
X
R_1' R_2 R_{3-c} R4 R_5' R_6'

FIG. 61

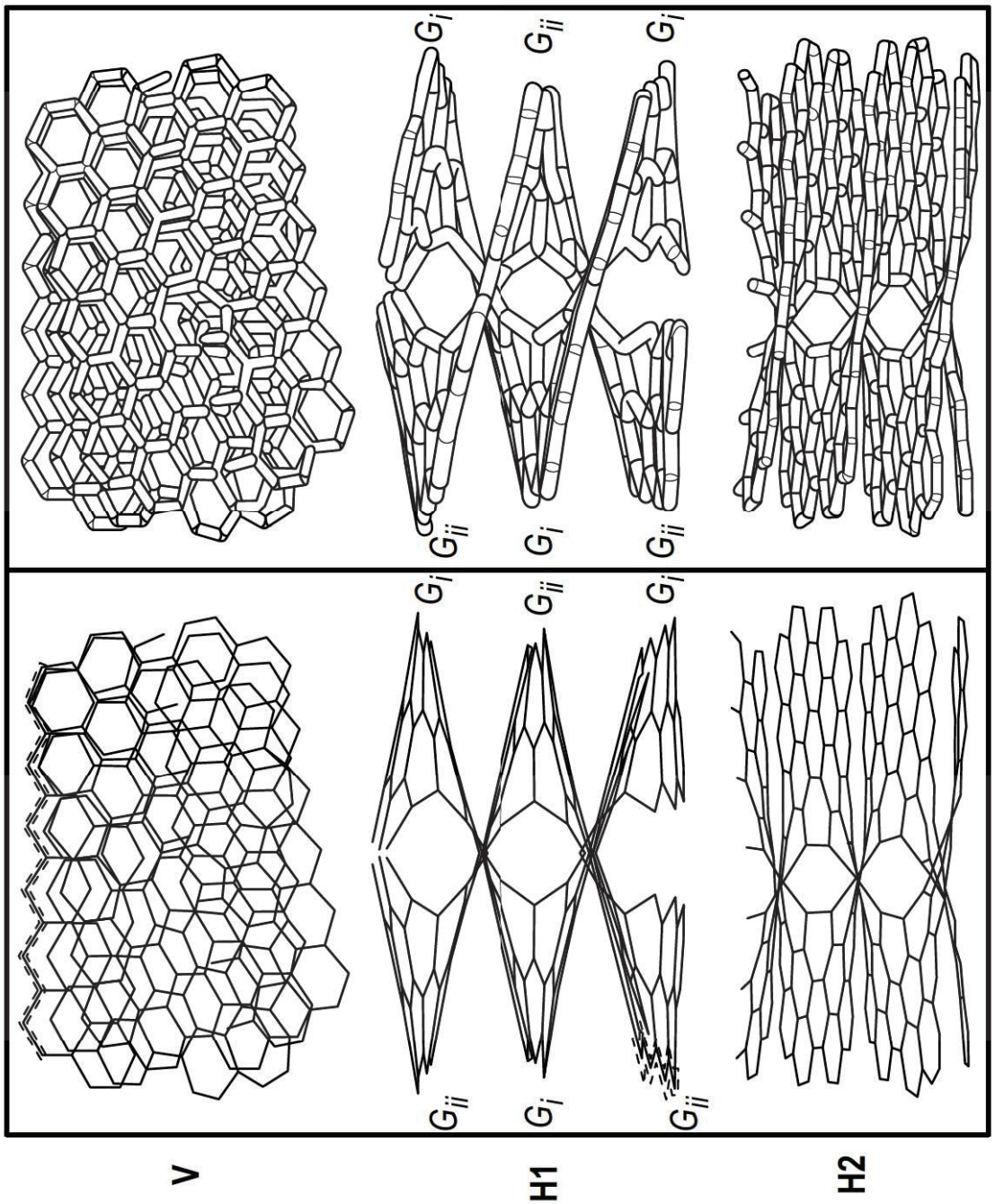

FIG. 62

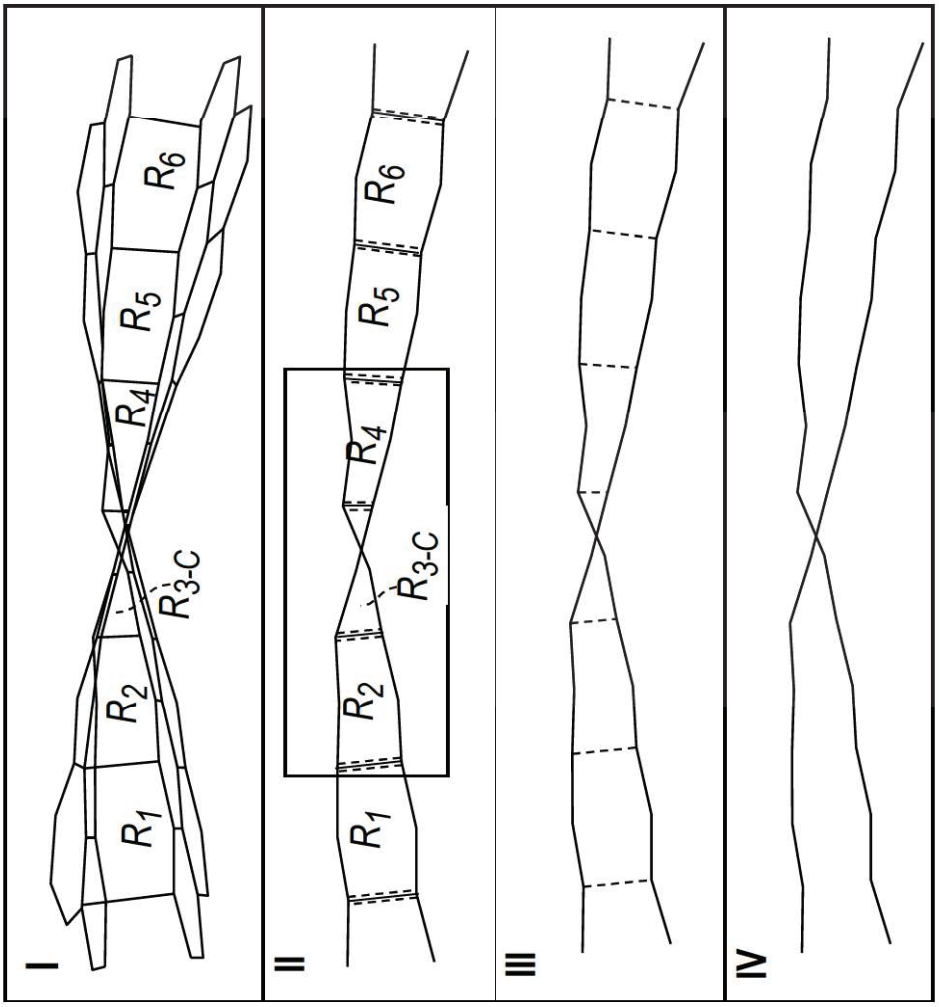

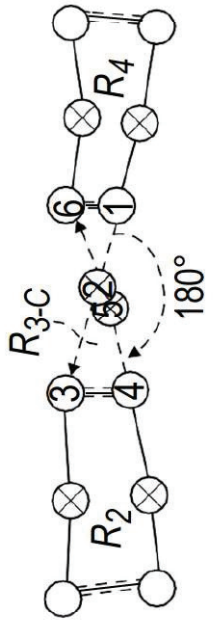

FIG. 63

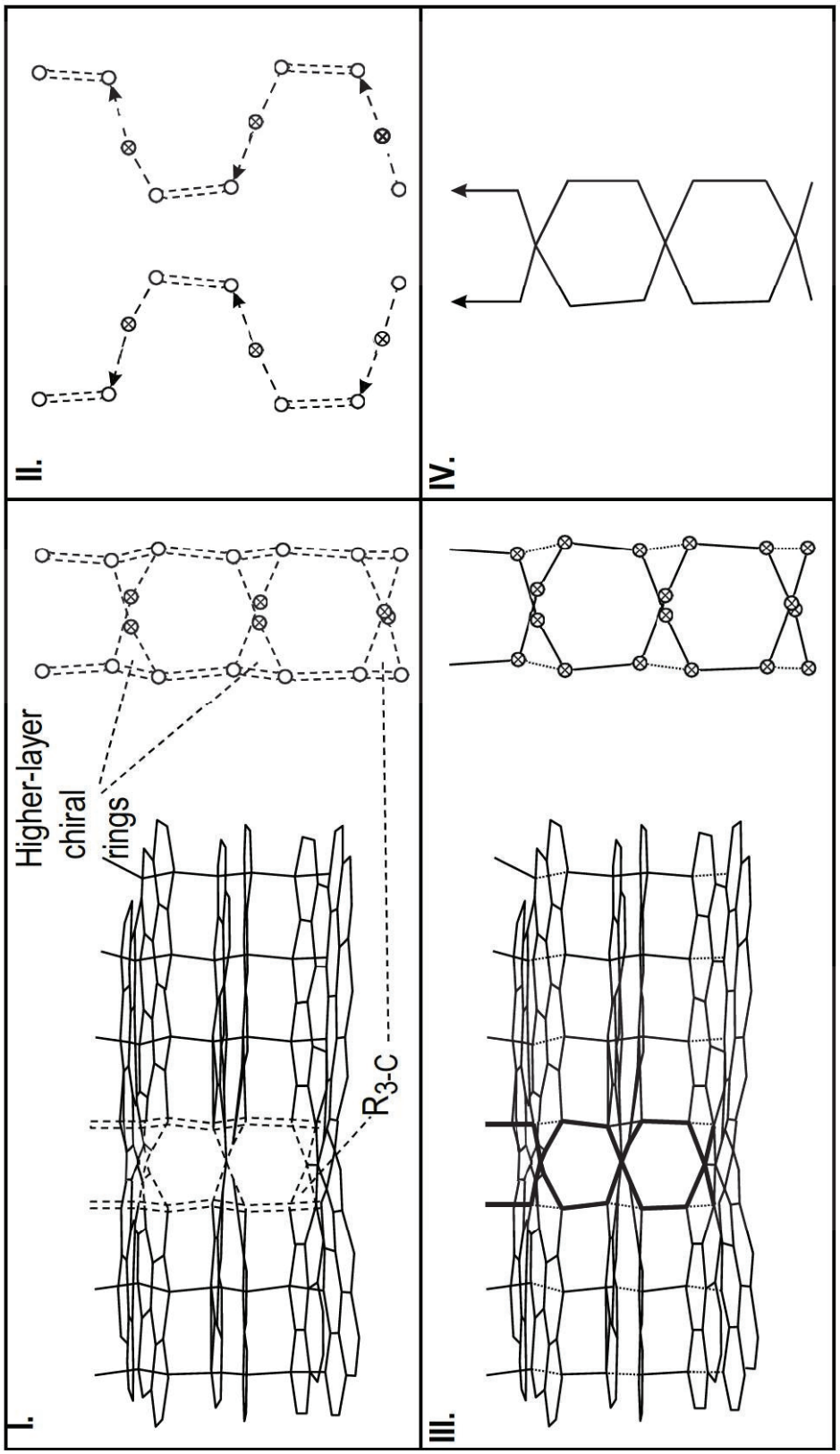

FIG. 64

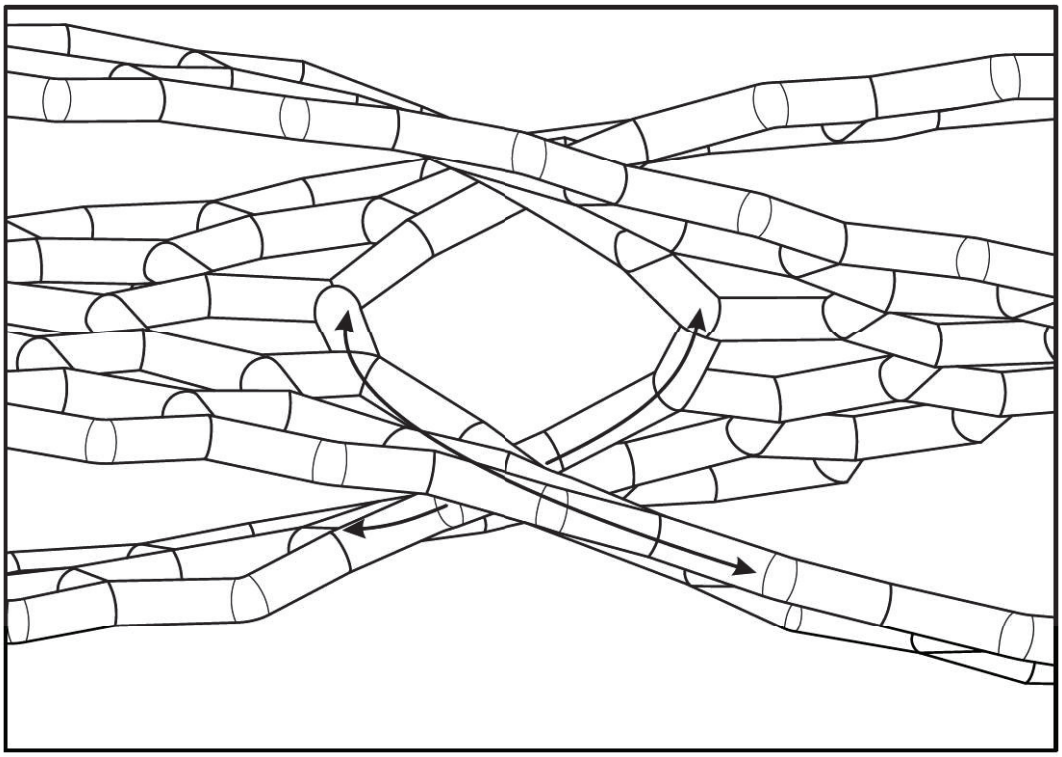

FIG. 65A

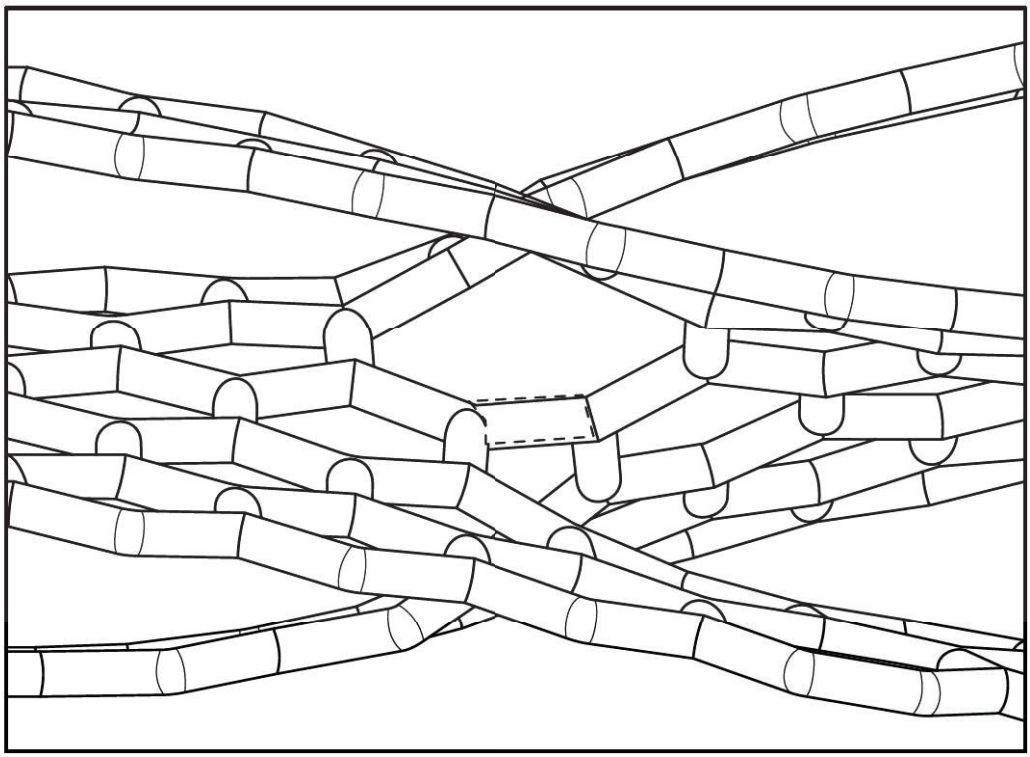

FIG. 65B

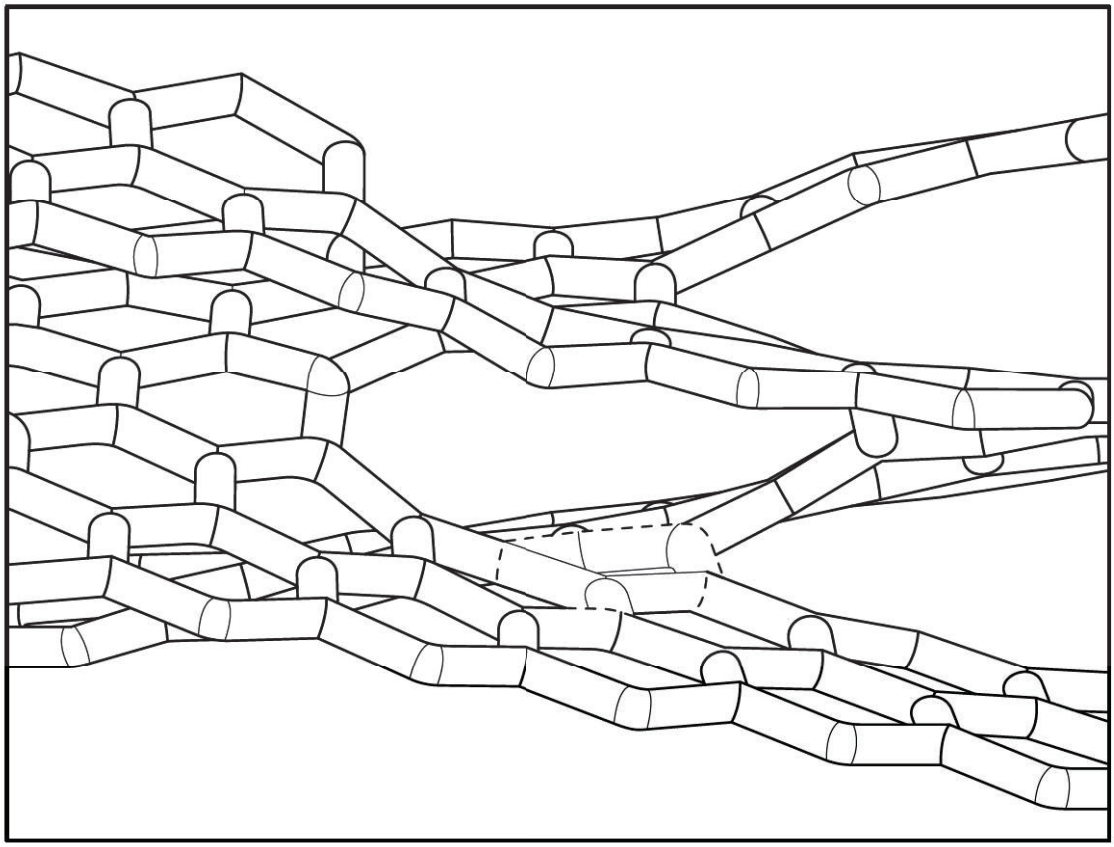

FIG. 65C

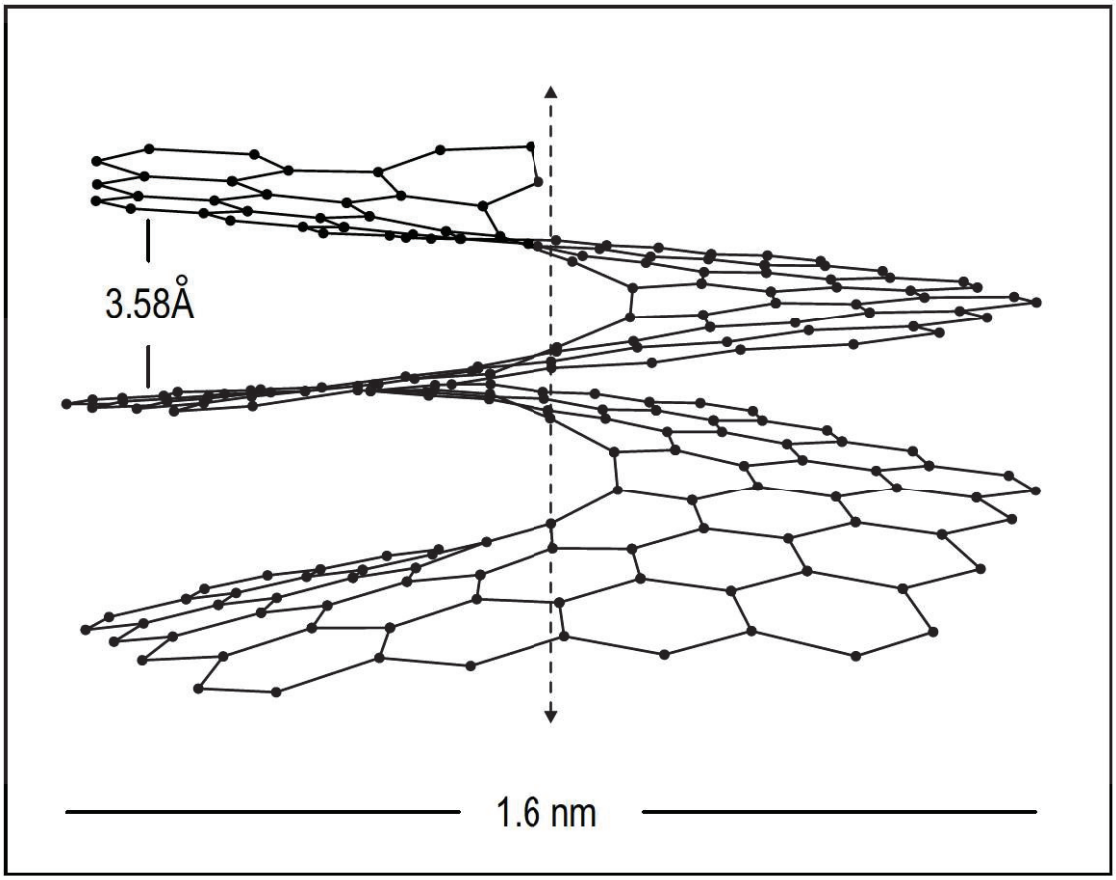

FIG. 66A

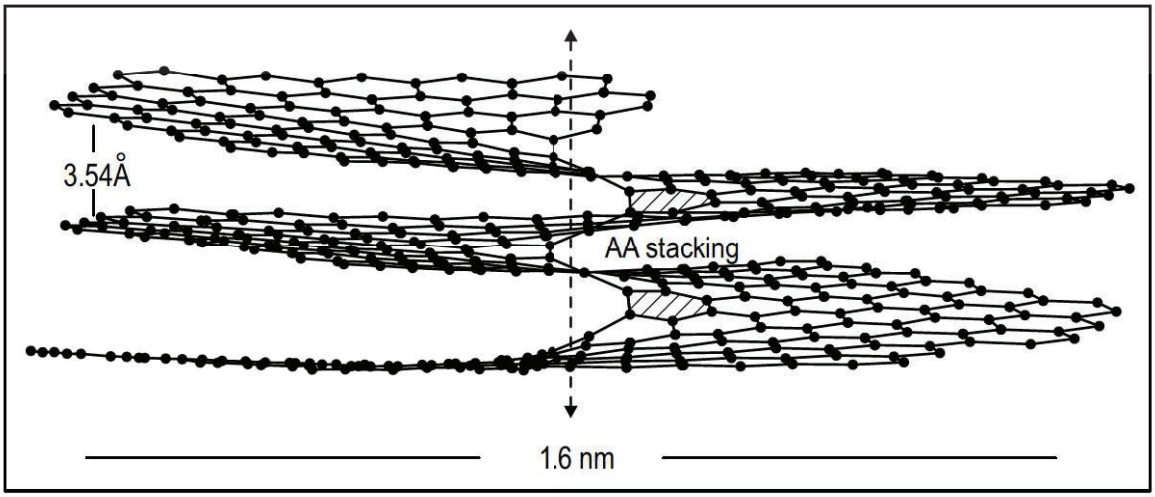

FIG. 66B

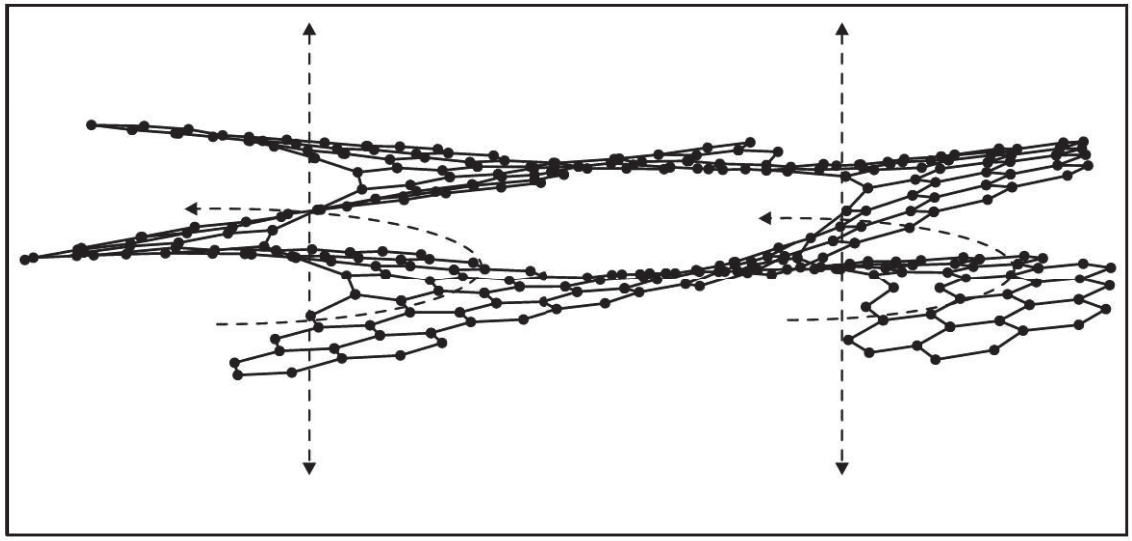

FIG. 66C

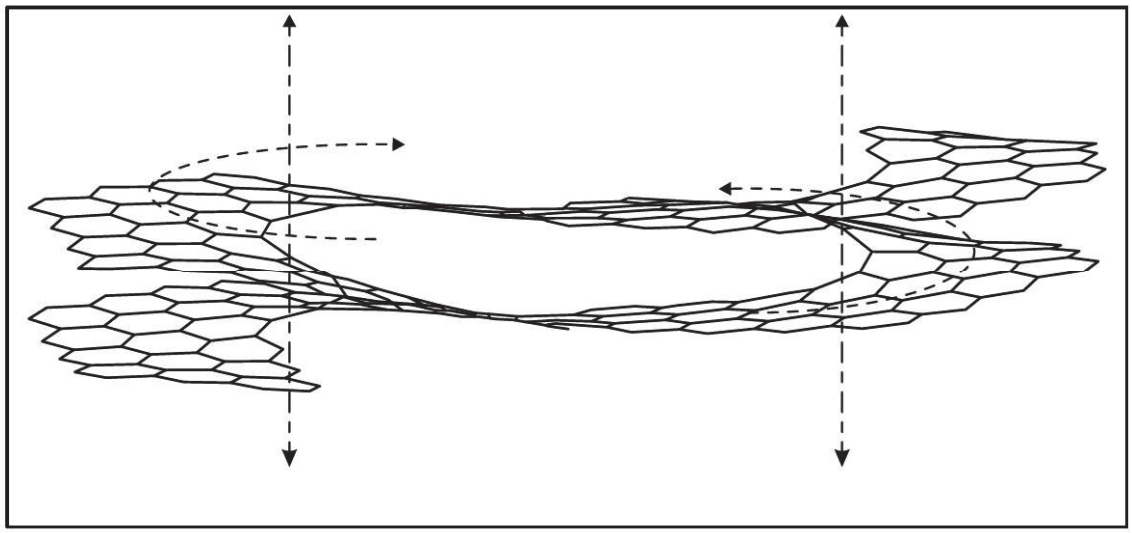

FIG. 66D

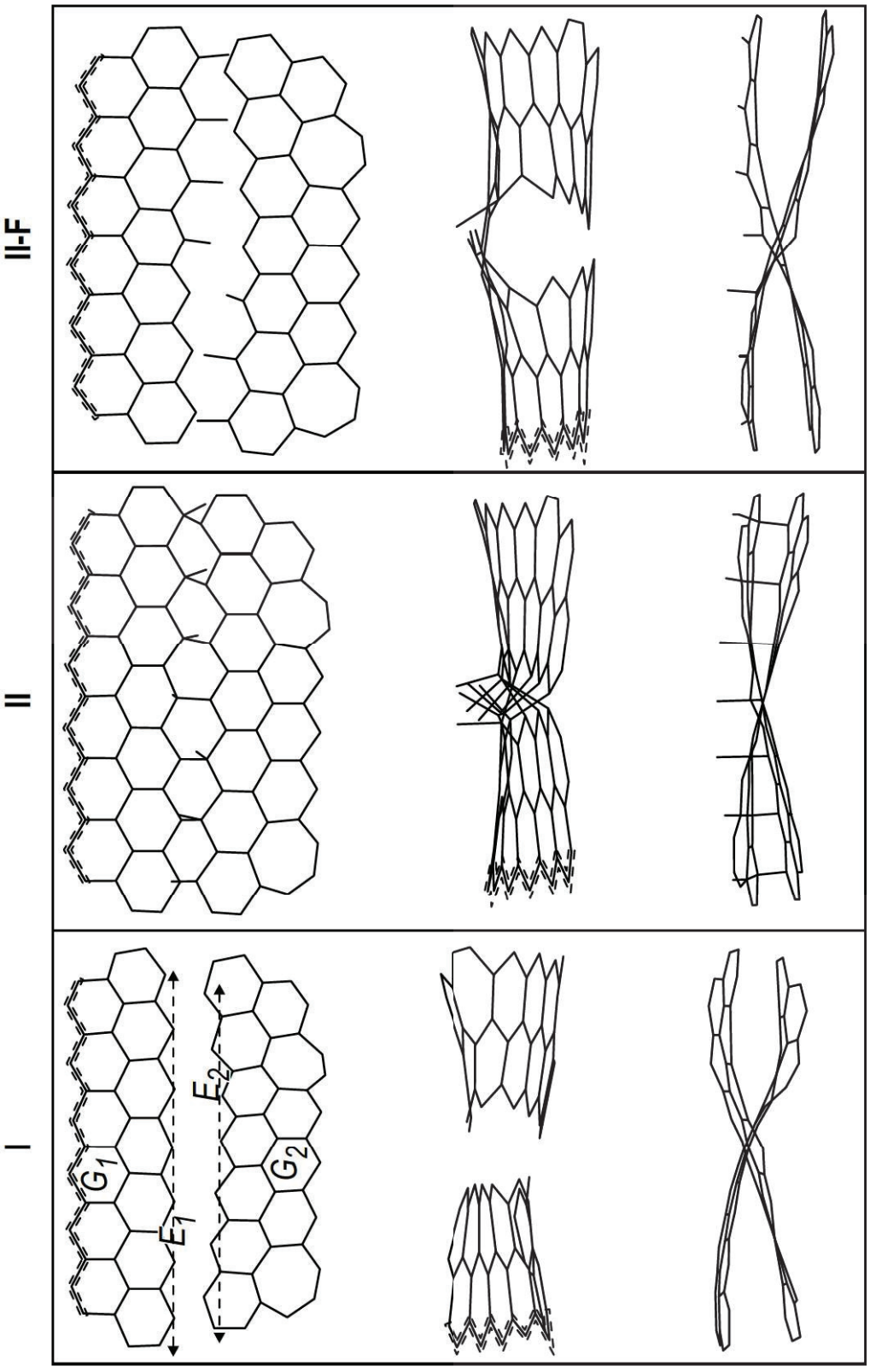

FIG. 67

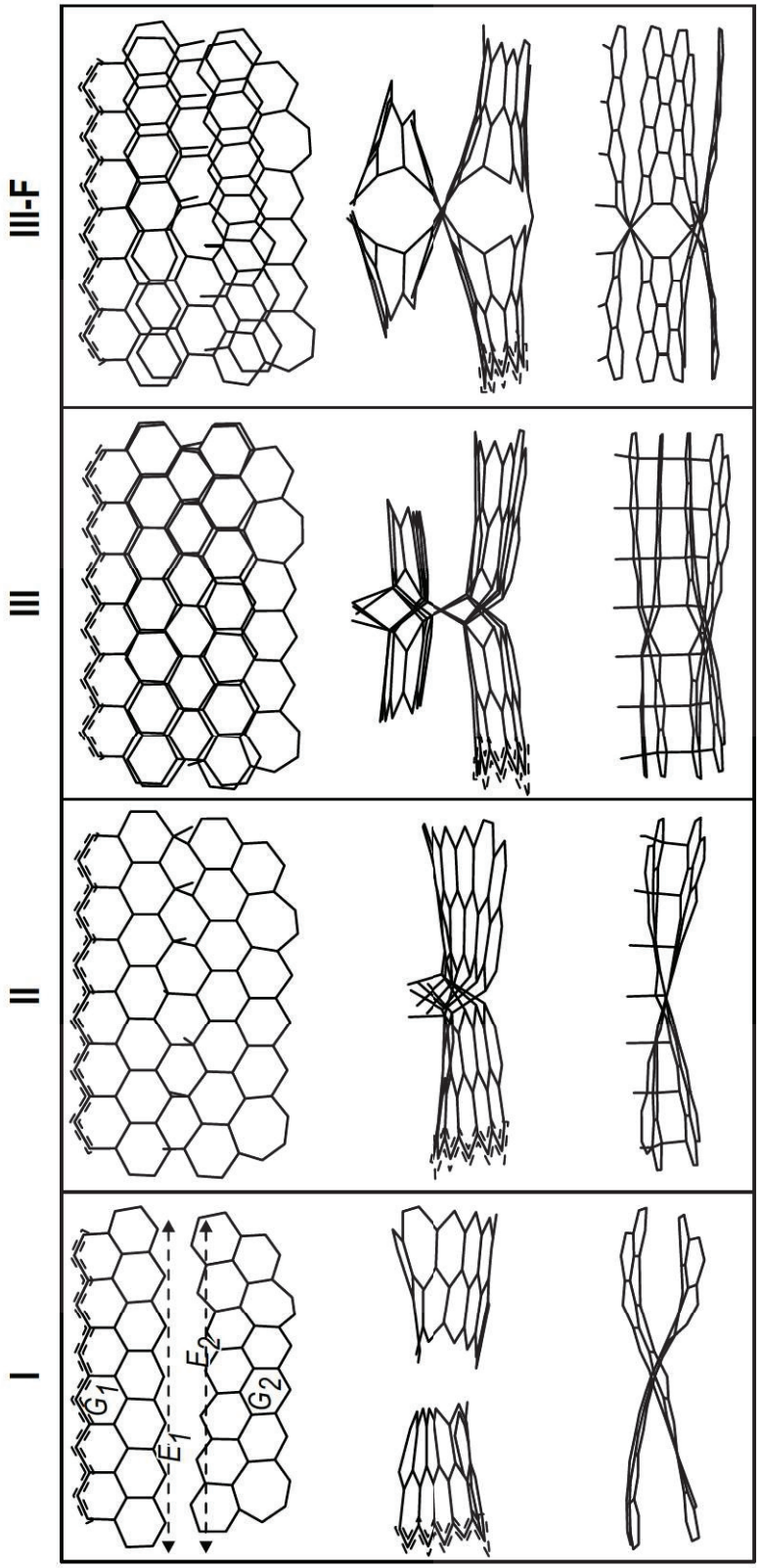

FIG. 68

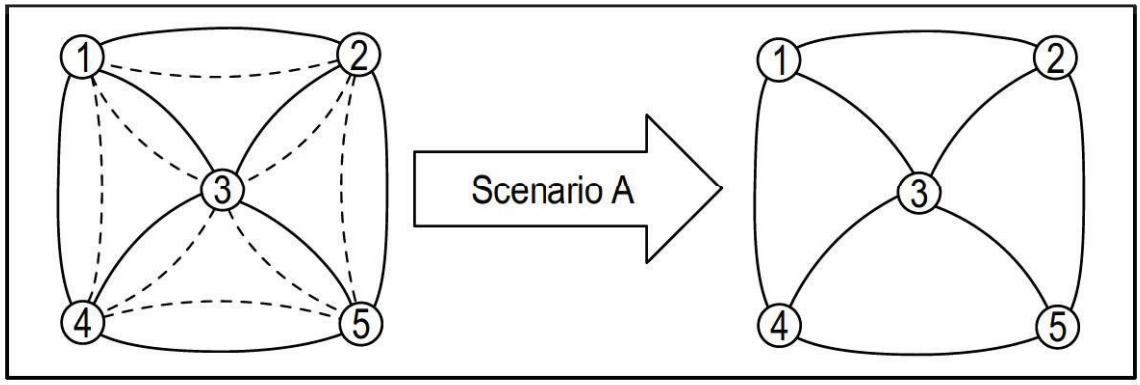

FIG. 69A

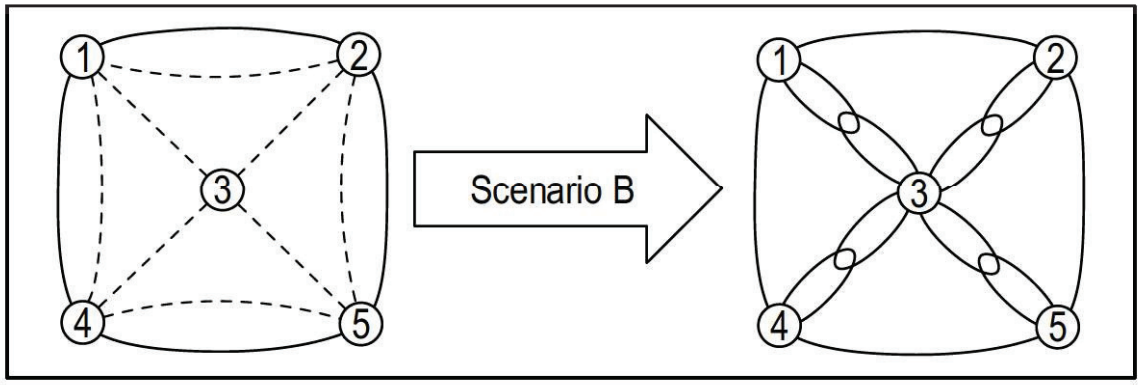

FIG. 69B

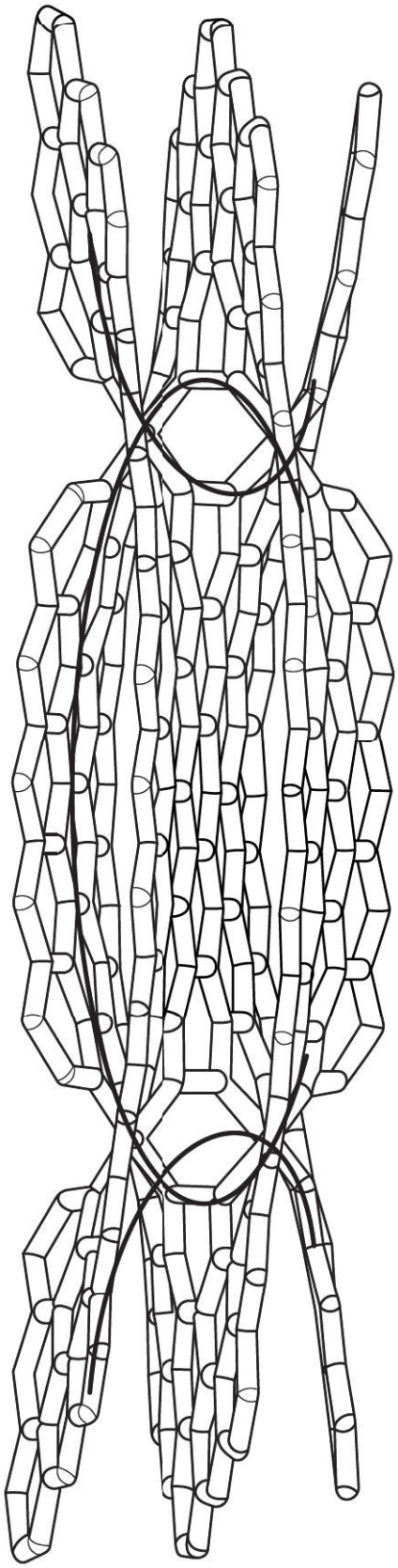

FIG. 70



FIG. 71A

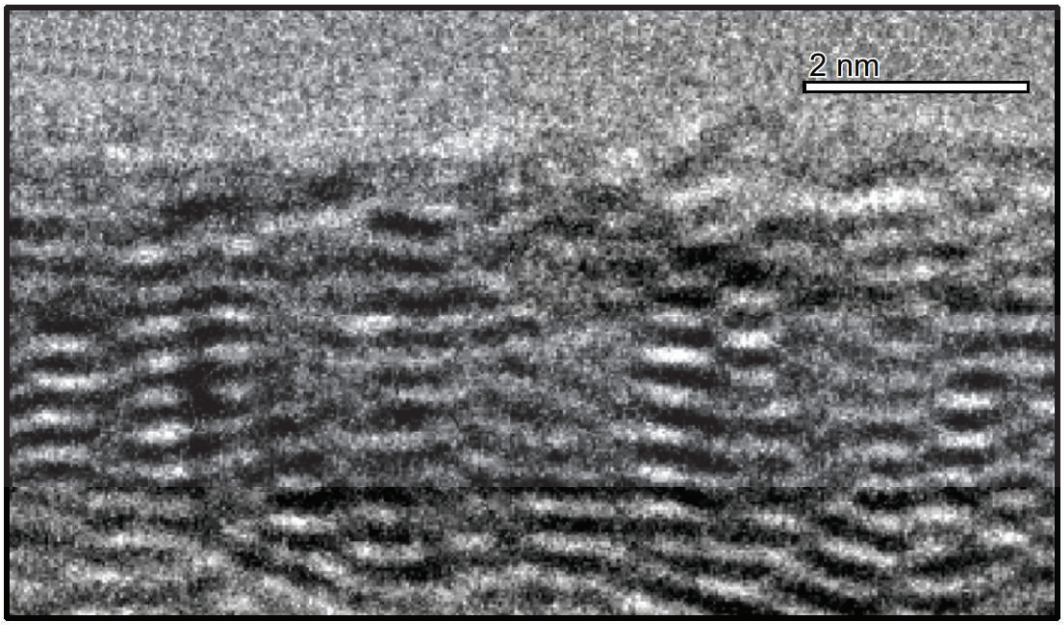

FIG. 71B

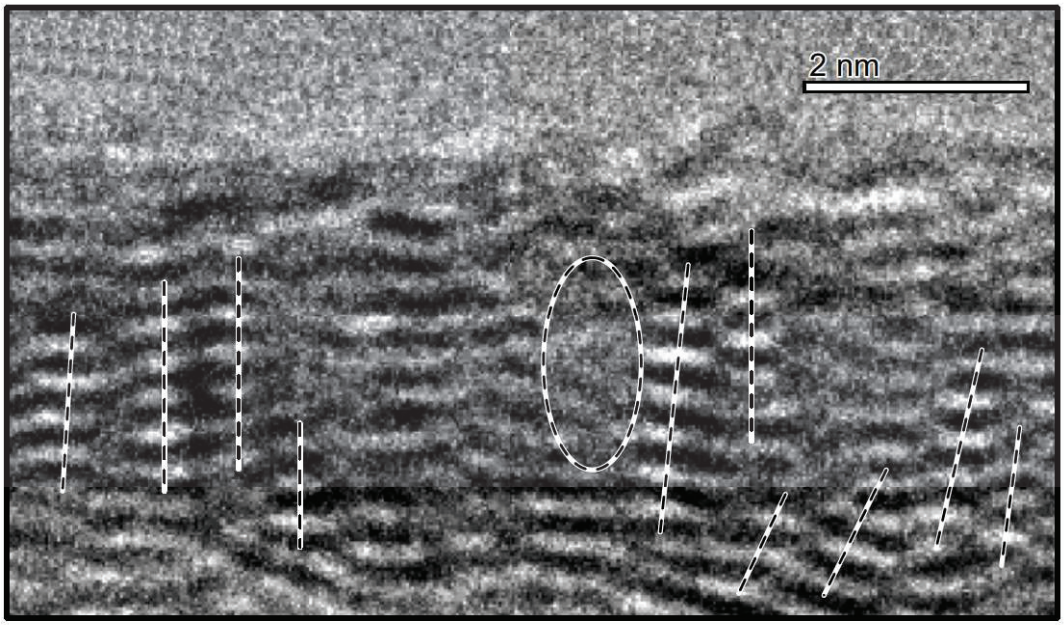

FIG. 71C

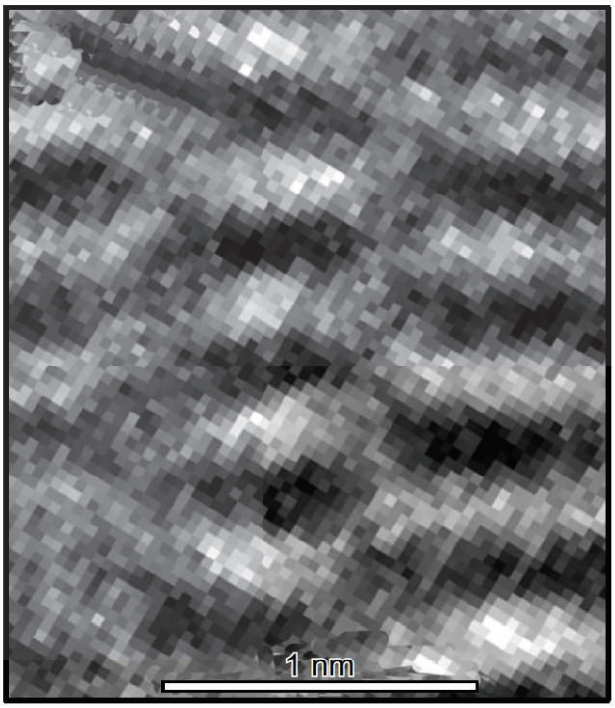

FIG. 71D

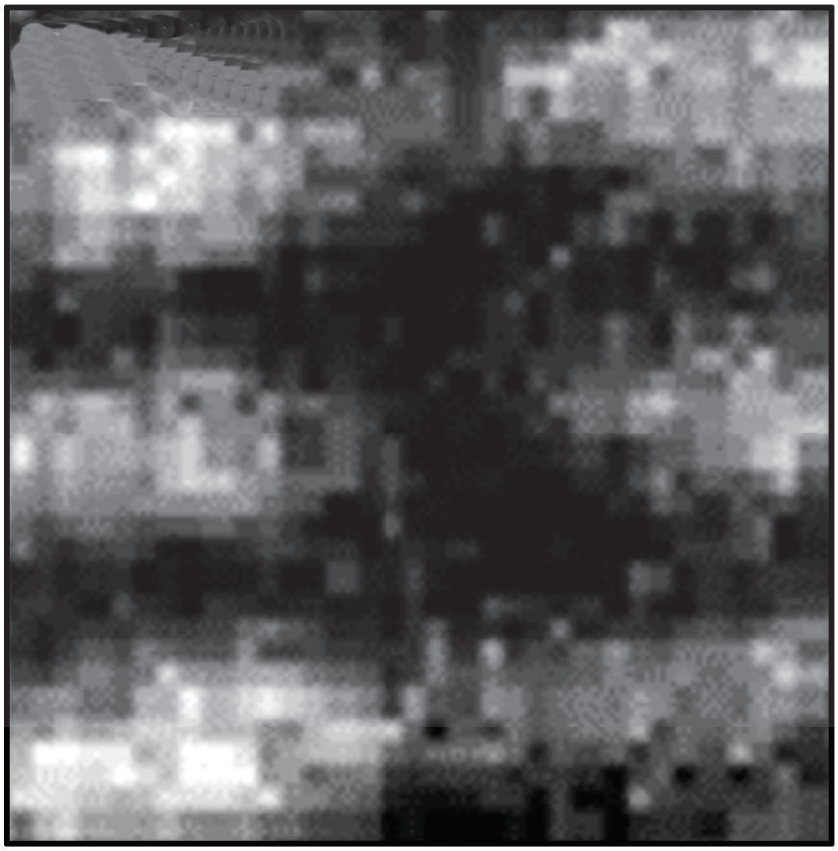

FIG. 71E

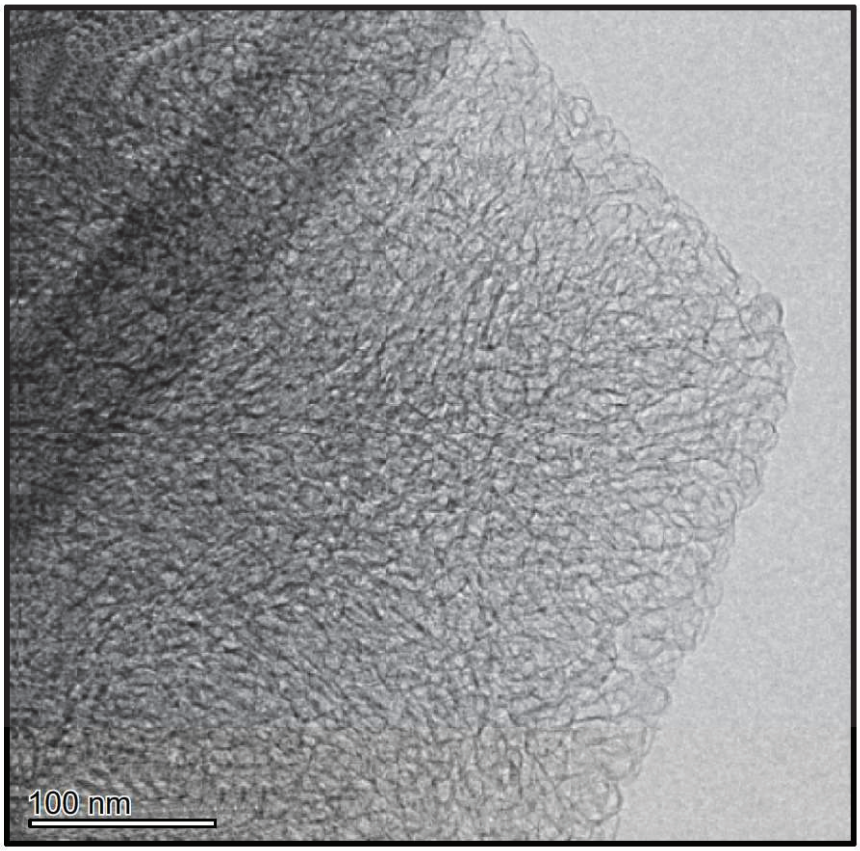

FIG. 72A

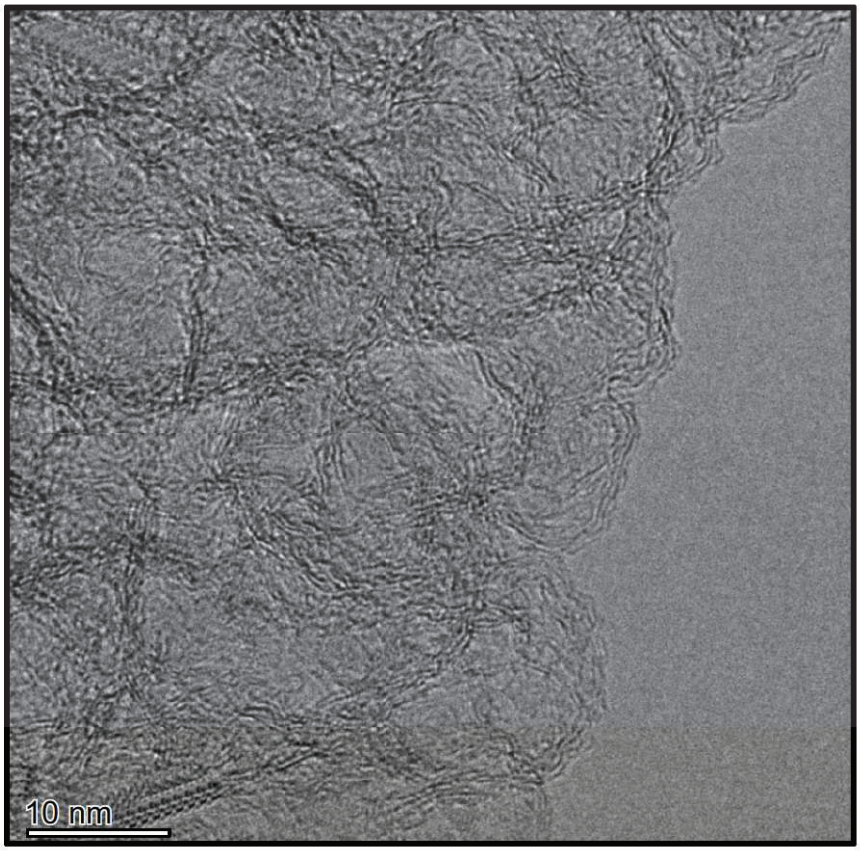

FIG. 72B

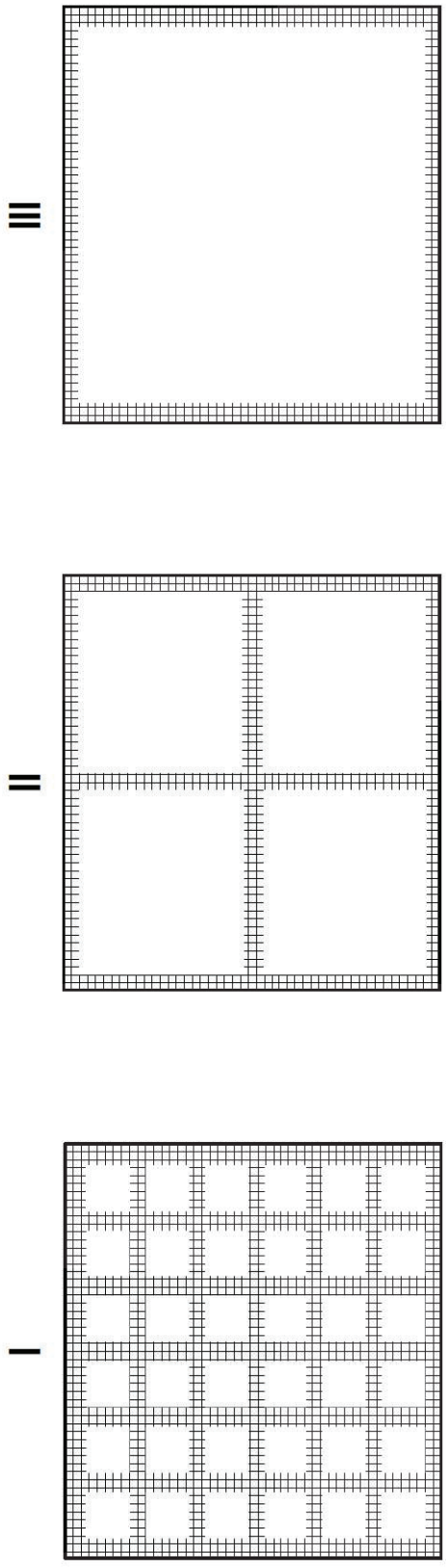

FIG. 73

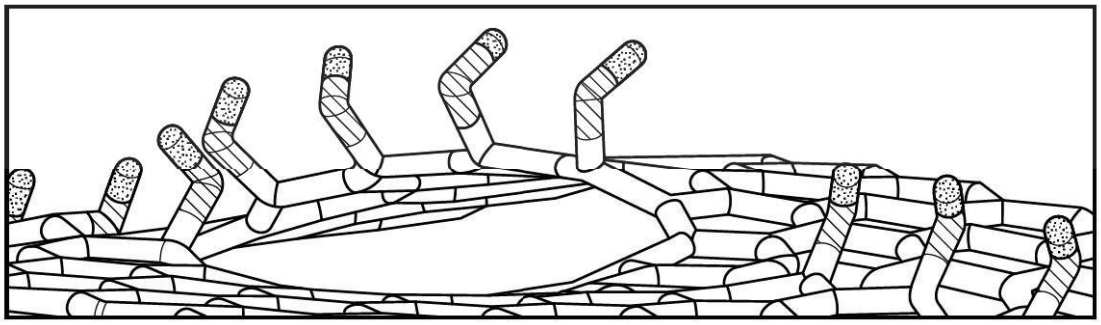

FIG. 74A

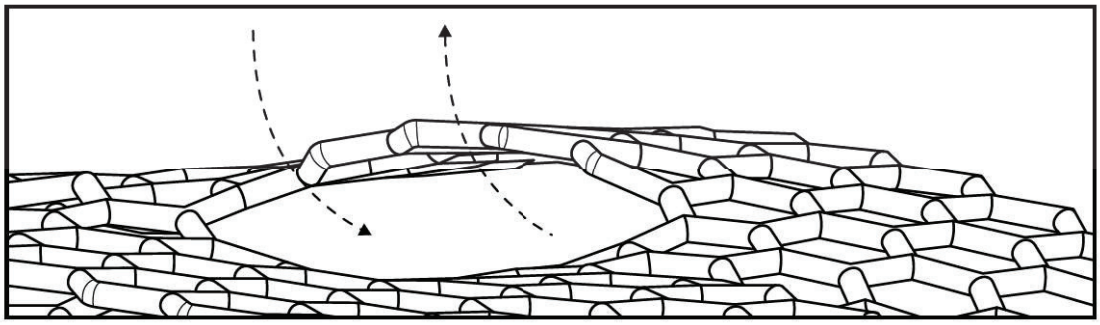

FIG. 74B

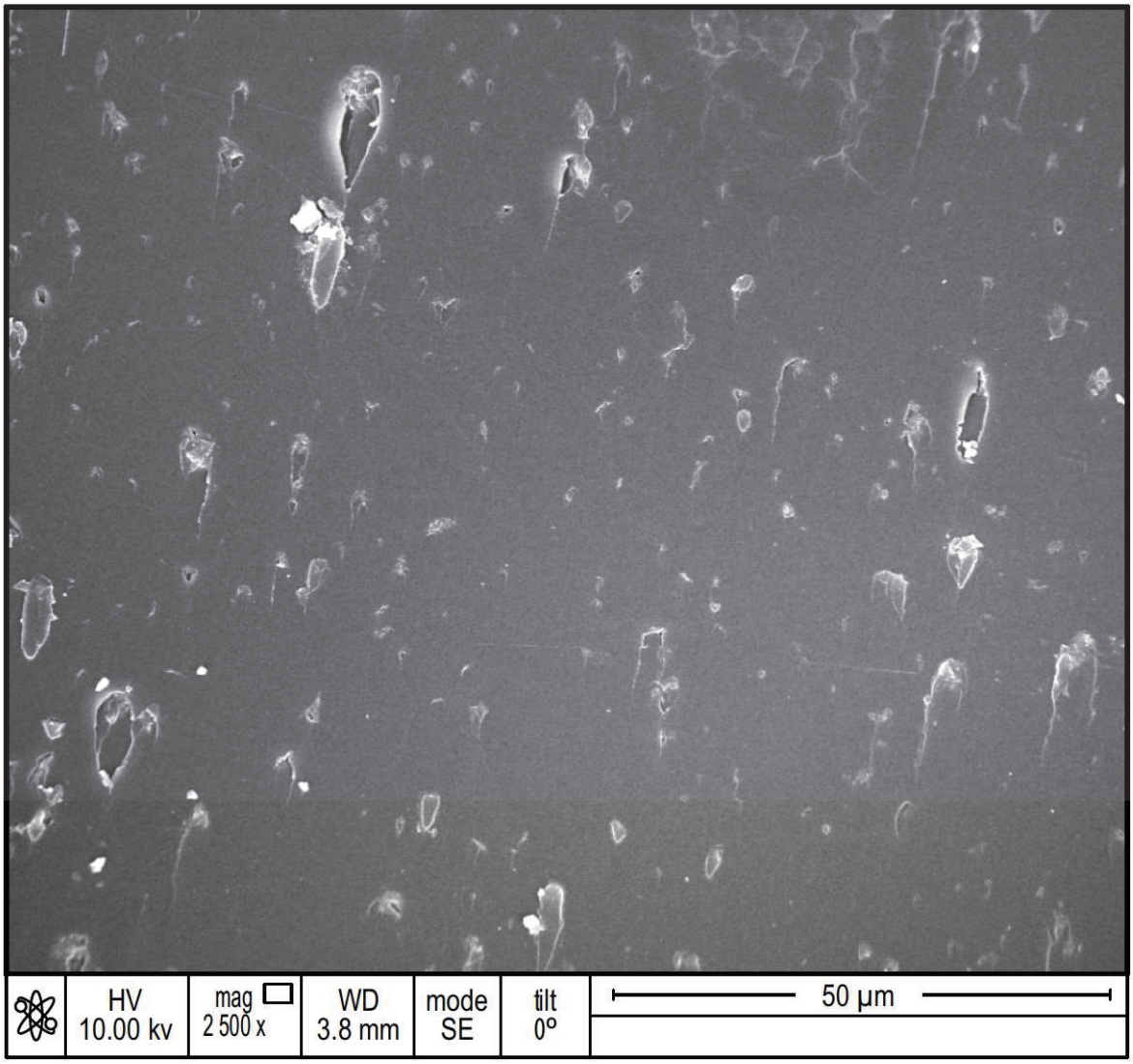

FIG. 75A

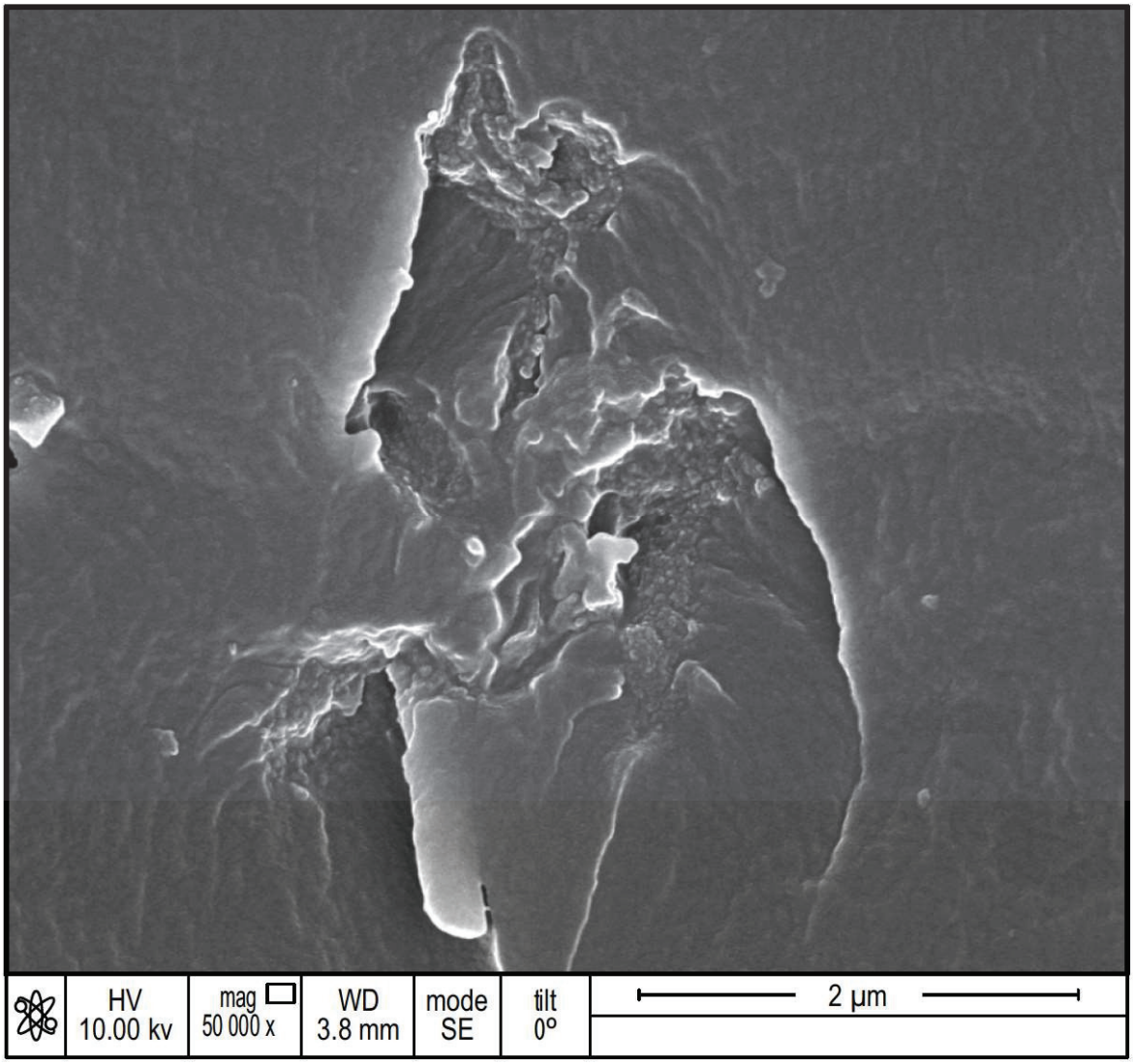

FIG. 75B

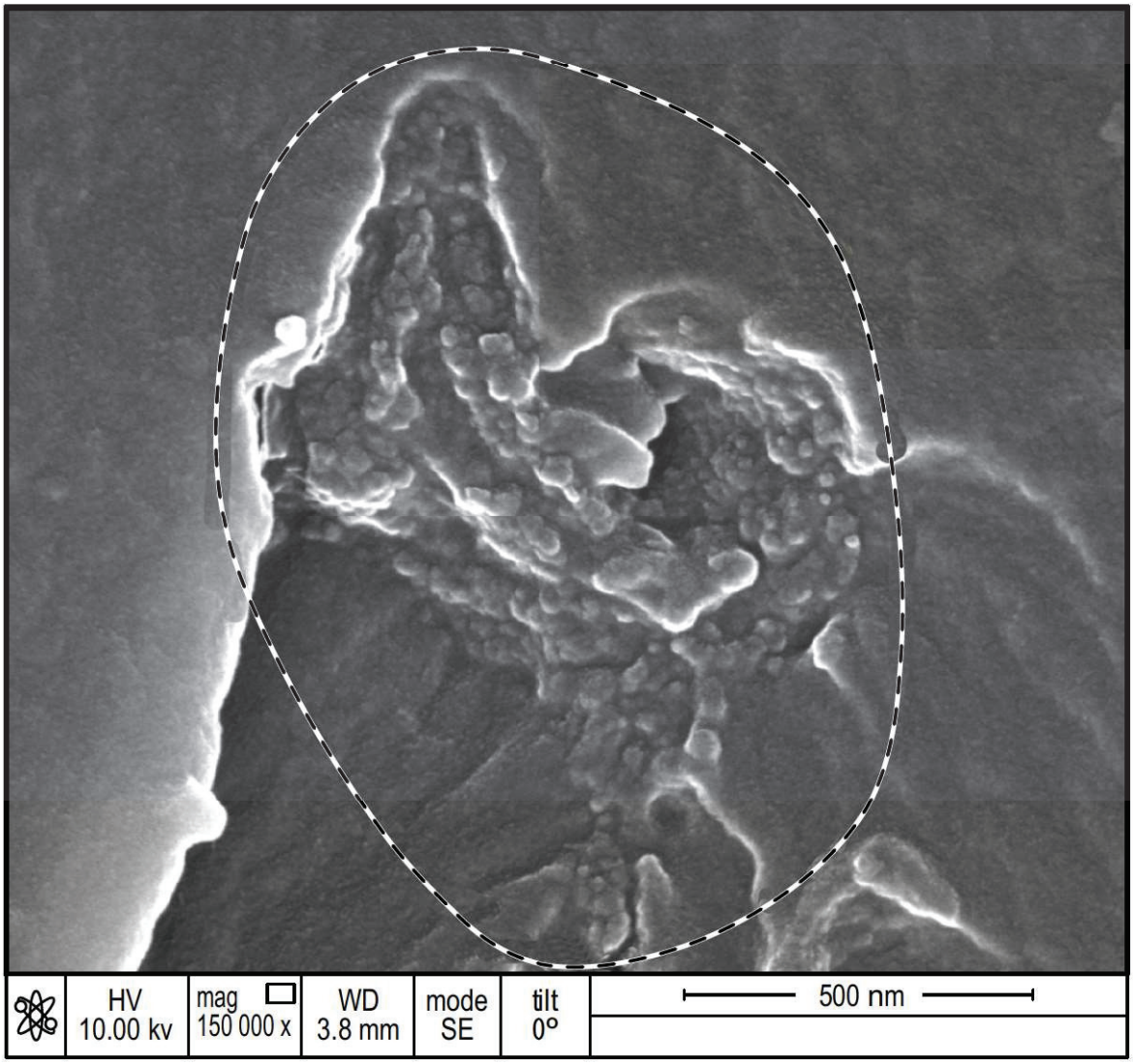

FIG. 75C

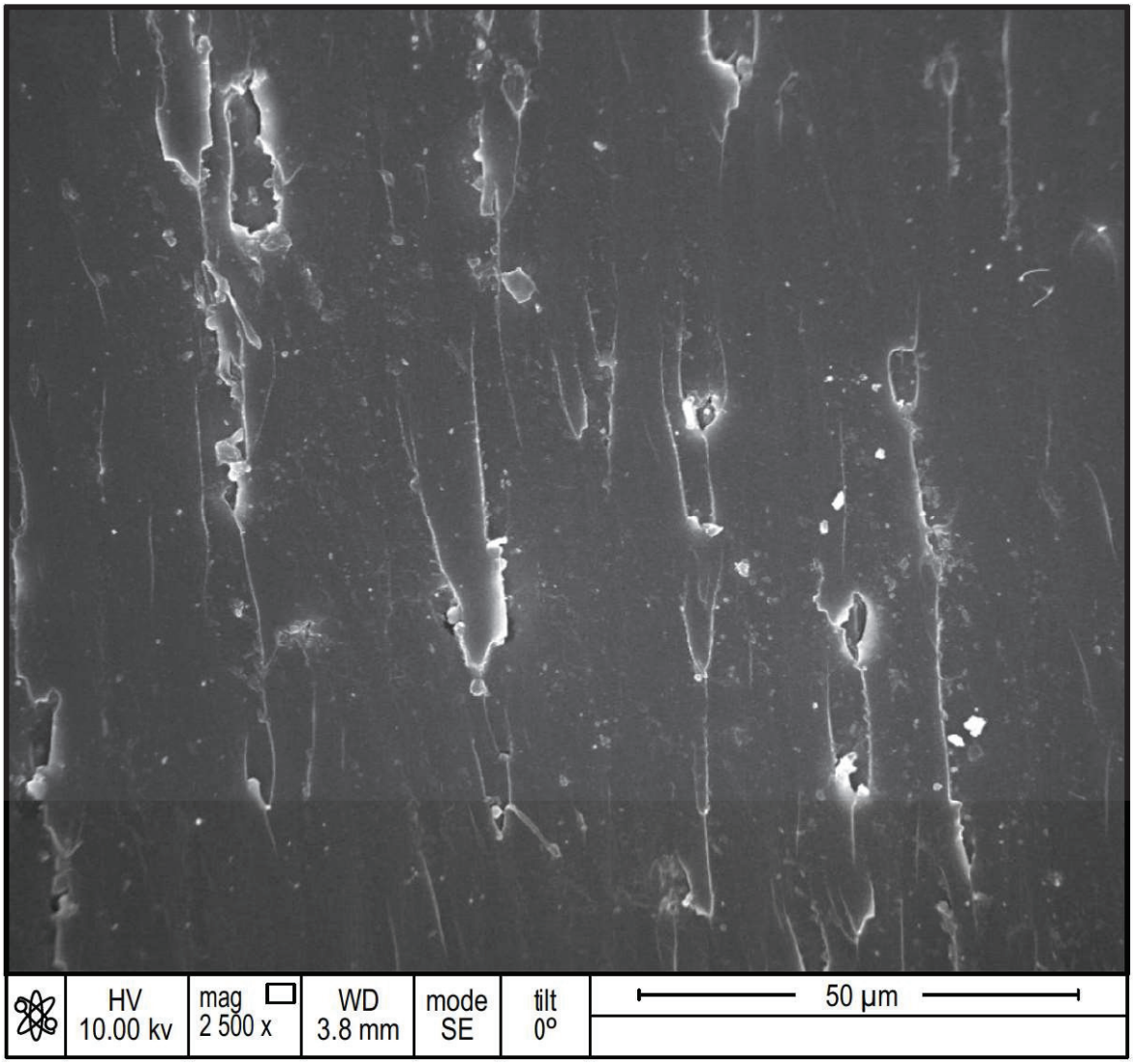

FIG. 76A

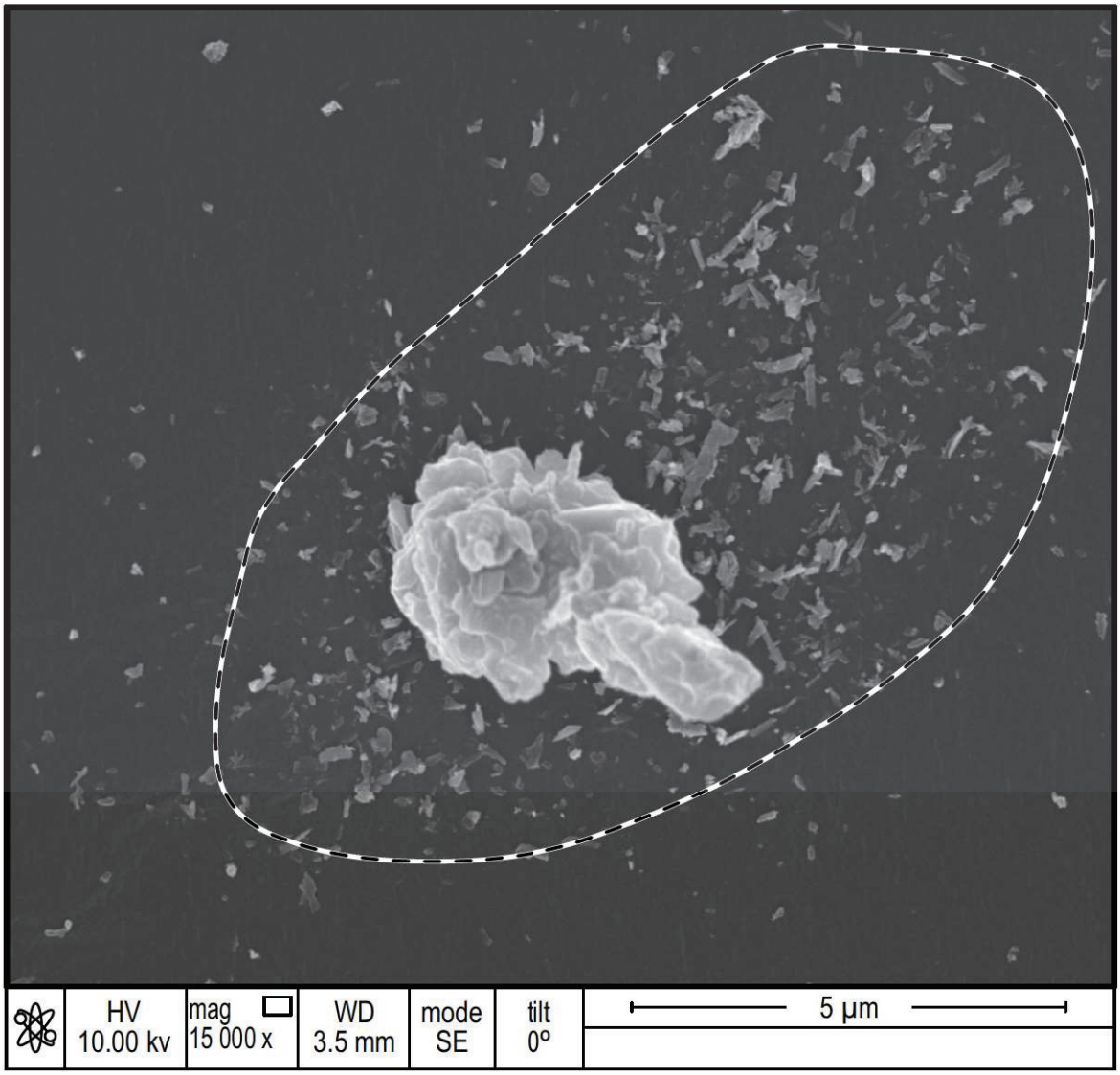

FIG. 76B

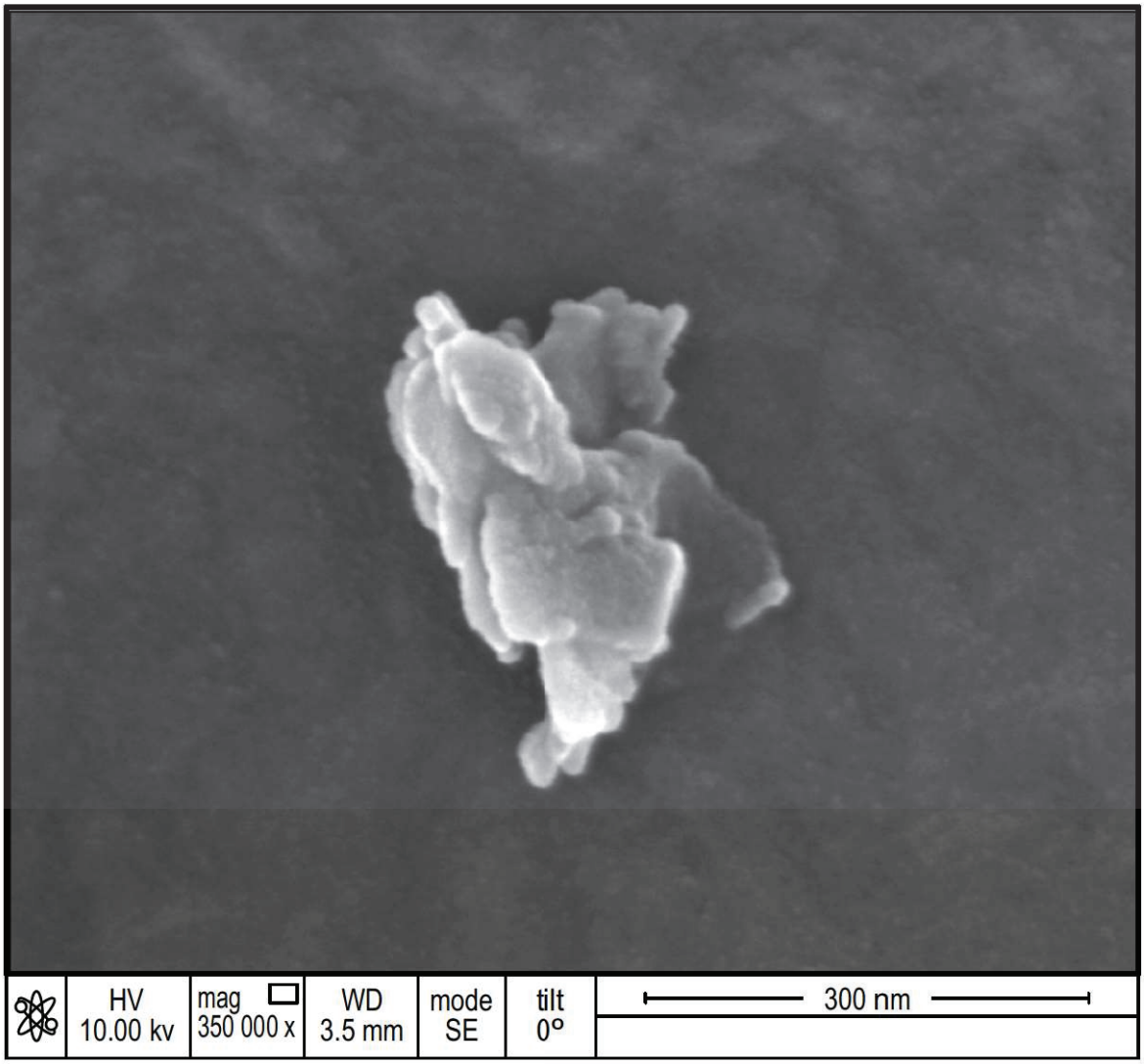

FIG. 76C

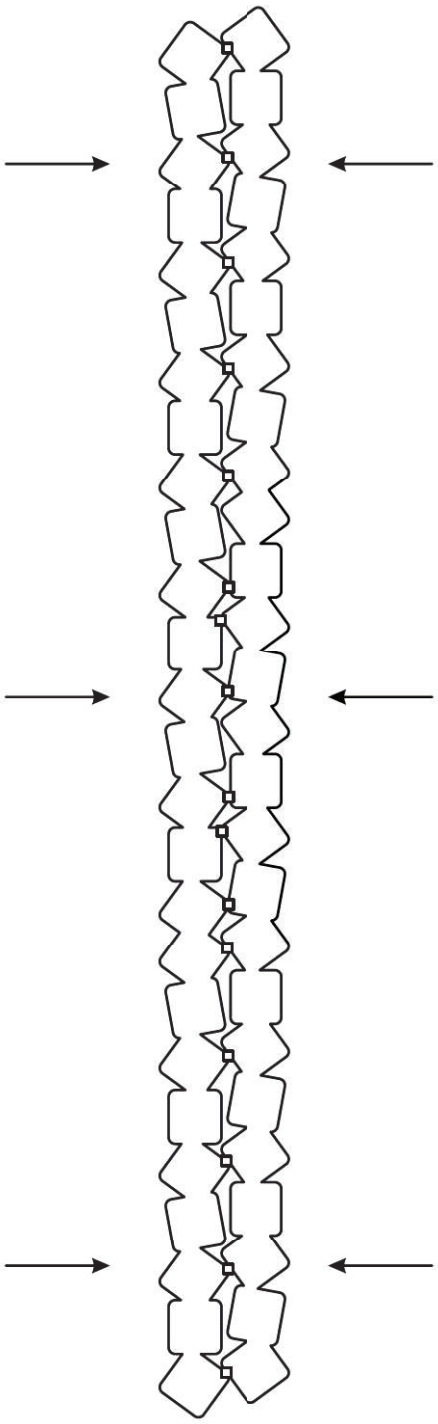

FIG. 77

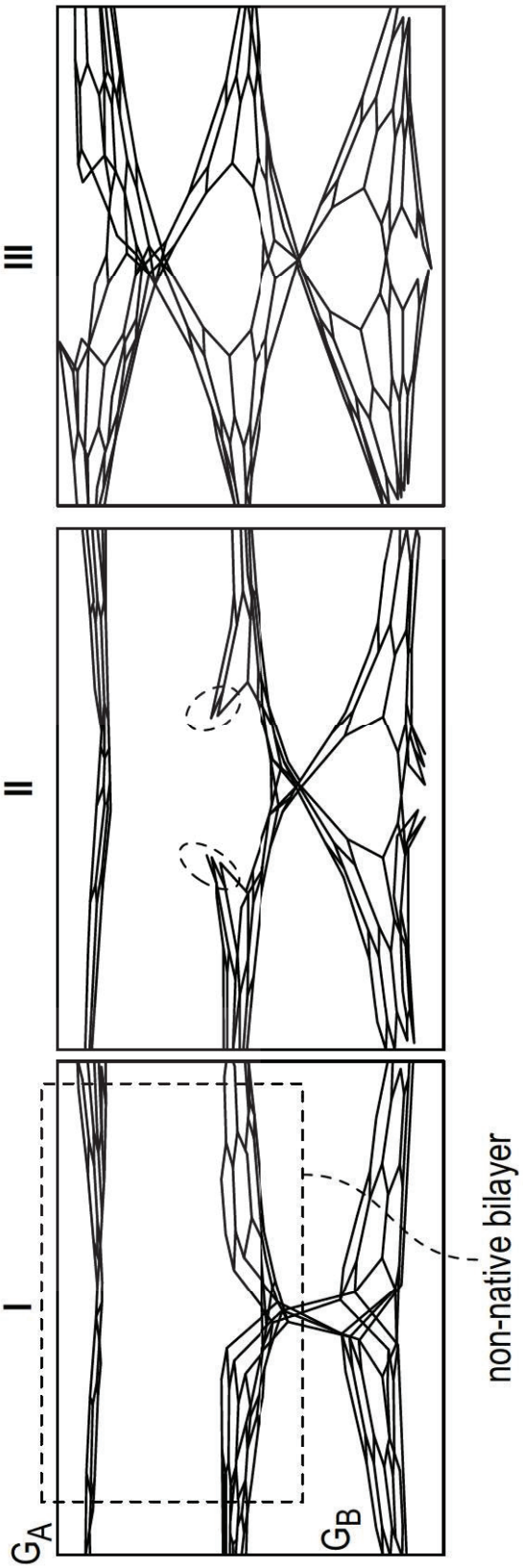

FIG. 78

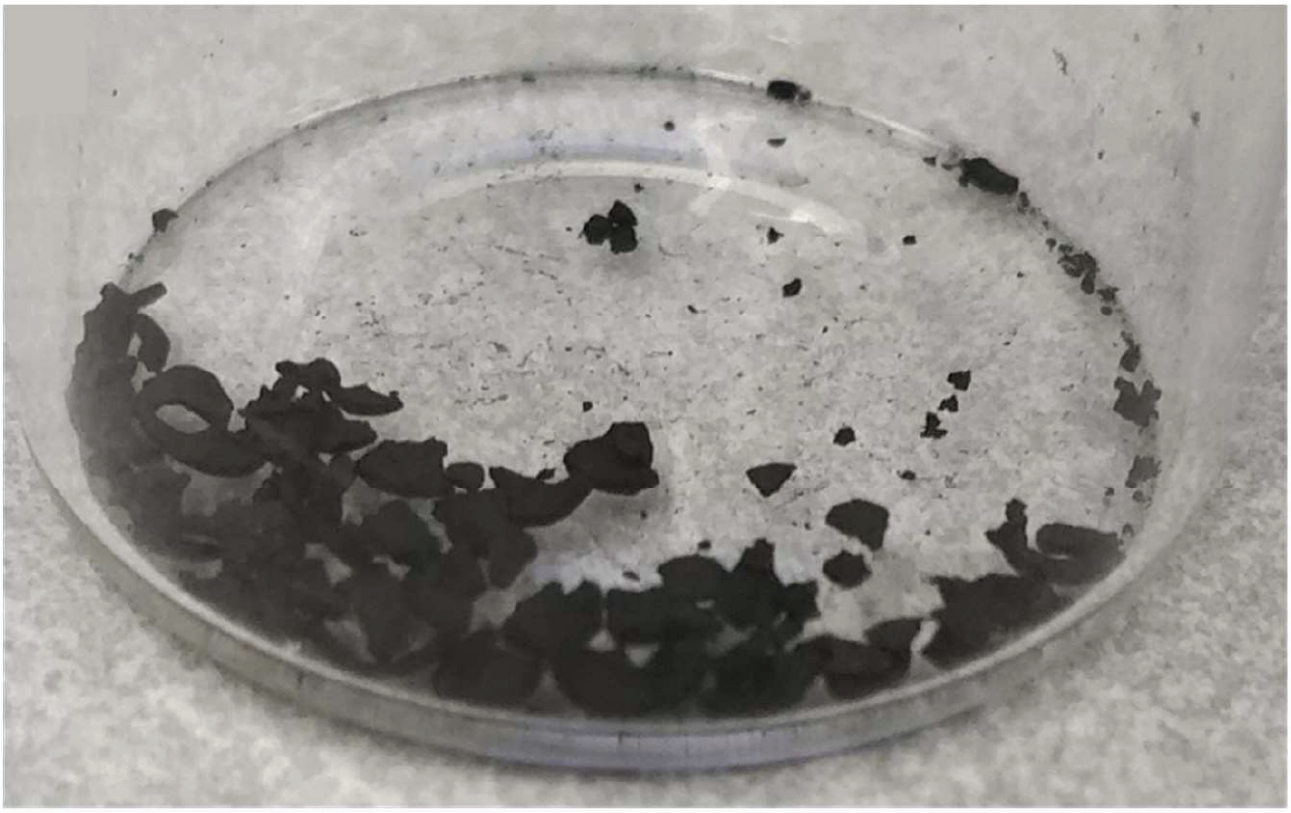

Fig. 79A

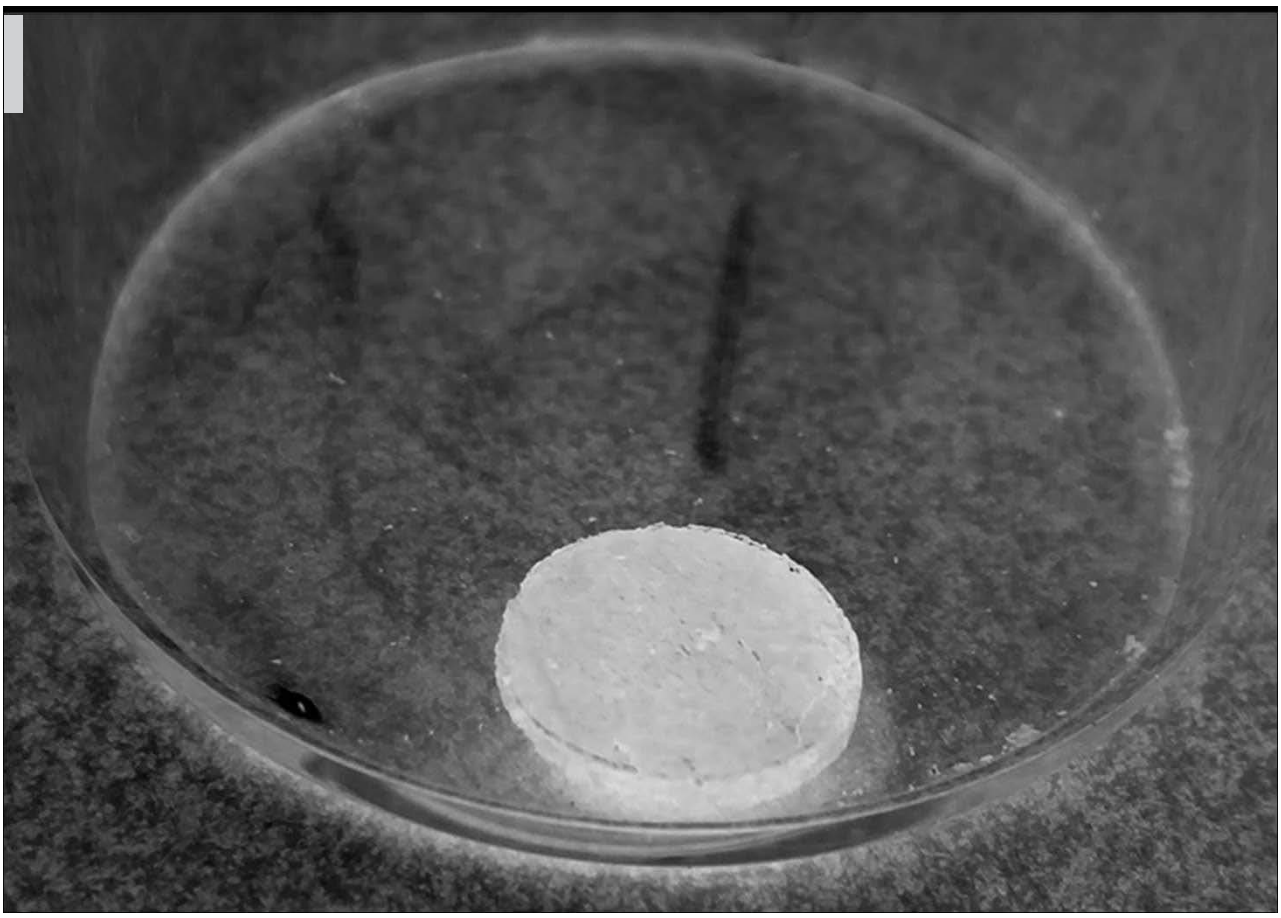

Fig. 79B

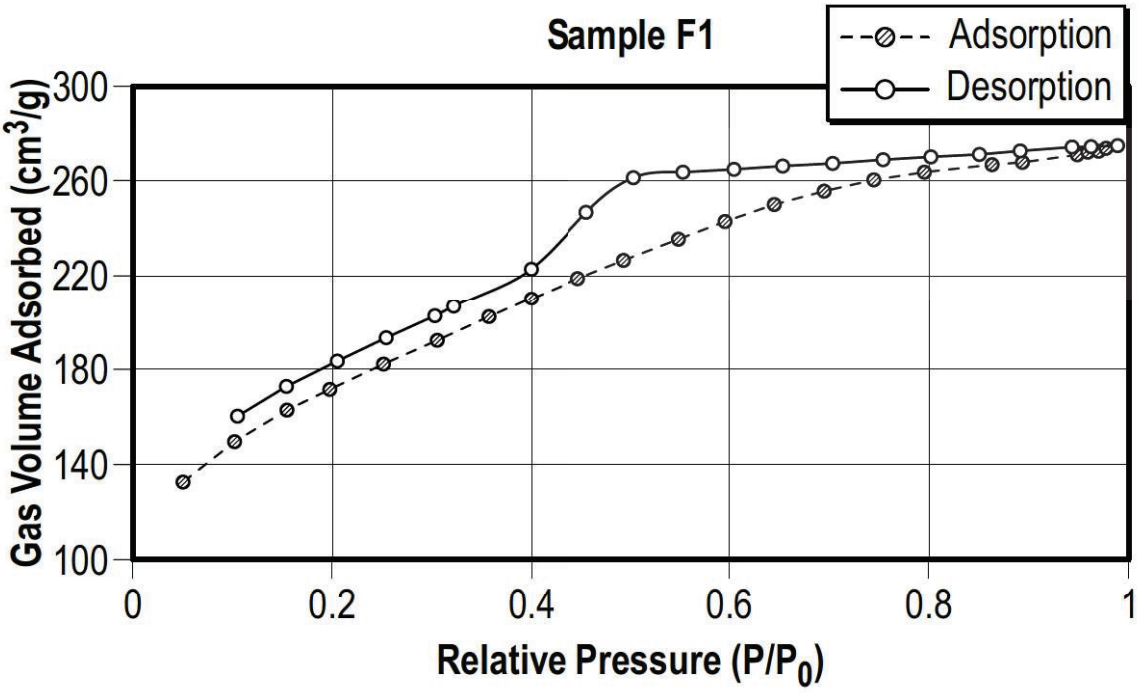
Sample F1
Adsorption
Desorption
Gas Volume Adsorbed (cm3/g)
300
260
220
180
140
100
0
0.2
0.4
0.6
0.8
1
Relative Pressure (P/P0)

FIG. 80A

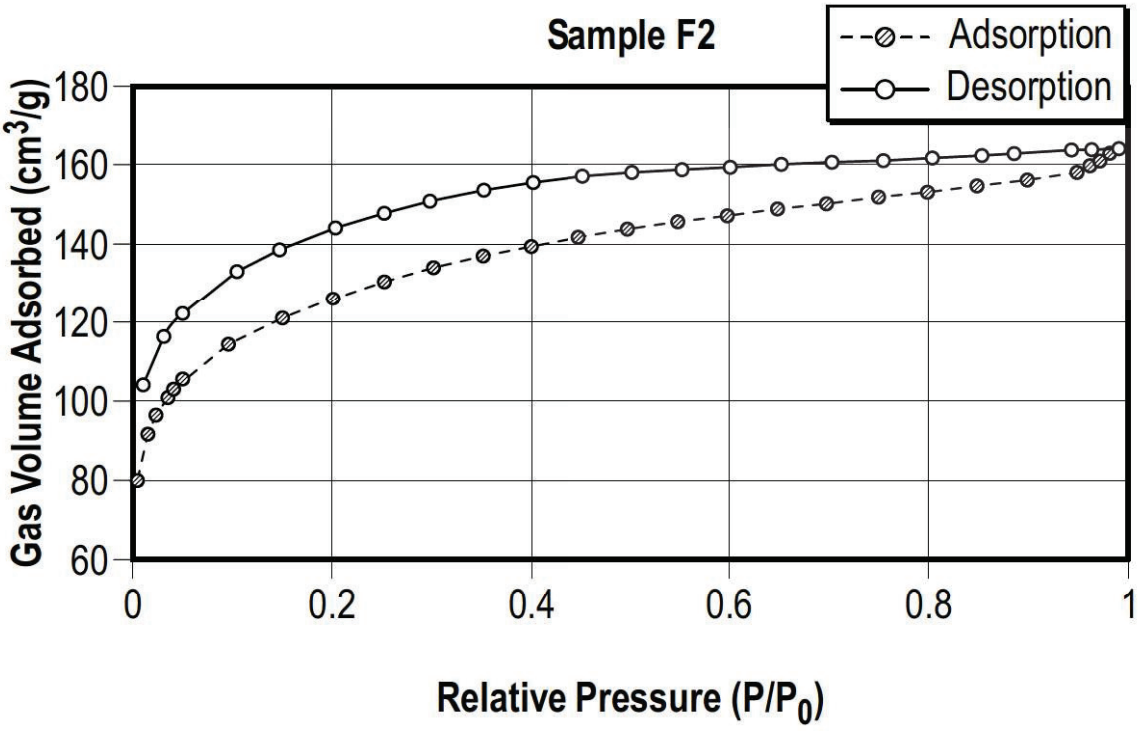
Sample F2
Adsorption
Desorption
Gas Volume Adsorbed (cm3/g)
180
160
140
120
100
80
60
0
0.2
0.4
0.6
0.8
1
Relative Pressure (P/P0)

FIG. 80B

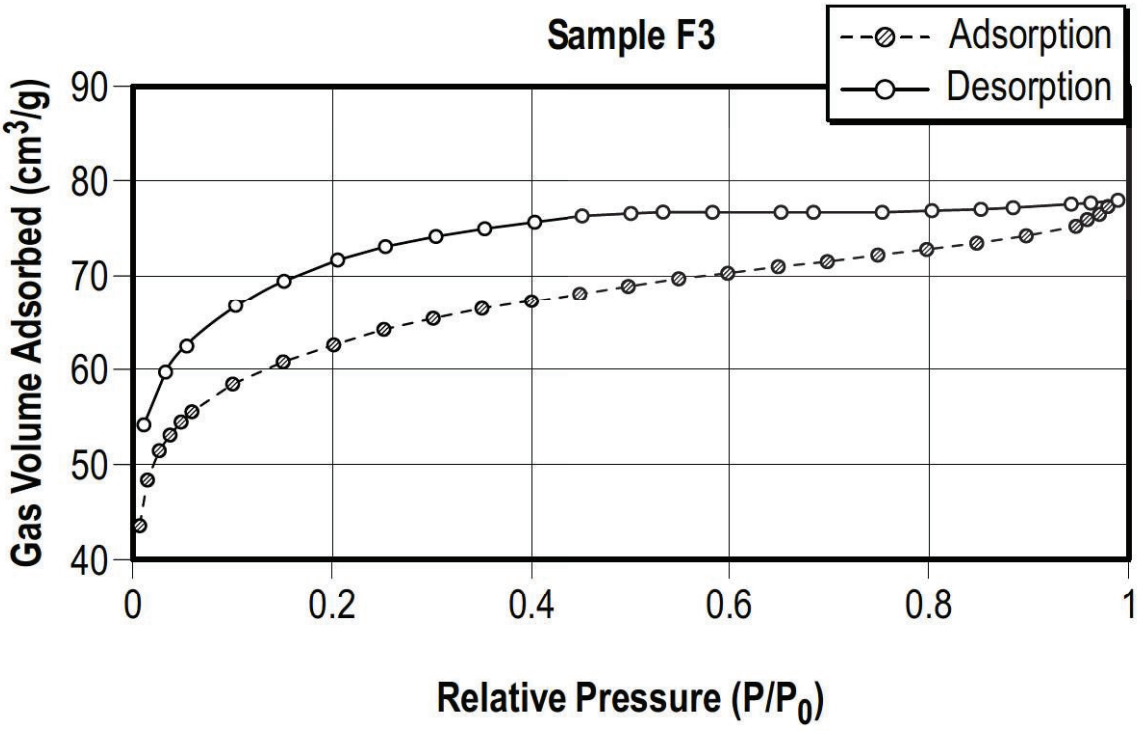
Sample F3
Adsorption
Desorption
Gas Volume Adsorbed (cm3/g)
90
80
70
60
50
40
0
0.2
0.4
0.6
0.8
1
Relative Pressure (P/P0)

FIG. 80C

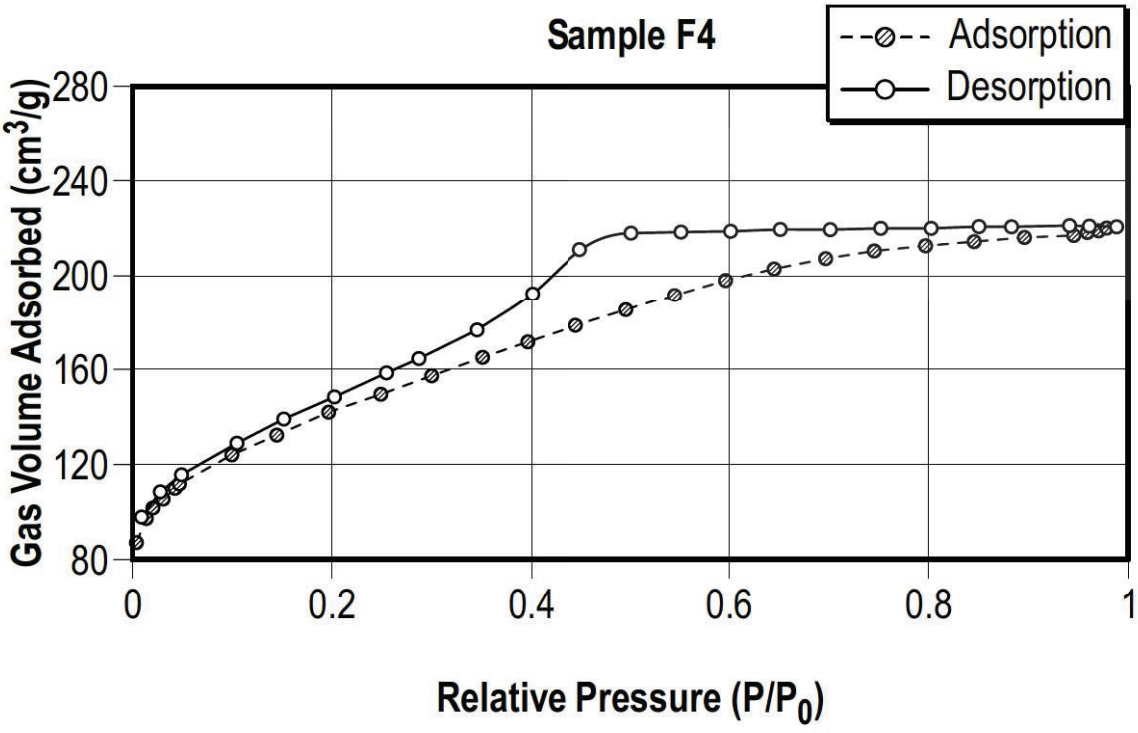
Sample F4
Adsorption
Desorption
Gas Volume Adsorbed (cm3/g)
280
240
200
160
120
80
0
0.2
0.4
0.6
0.8
1
Relative Pressure (P/P0)

FIG. 80D

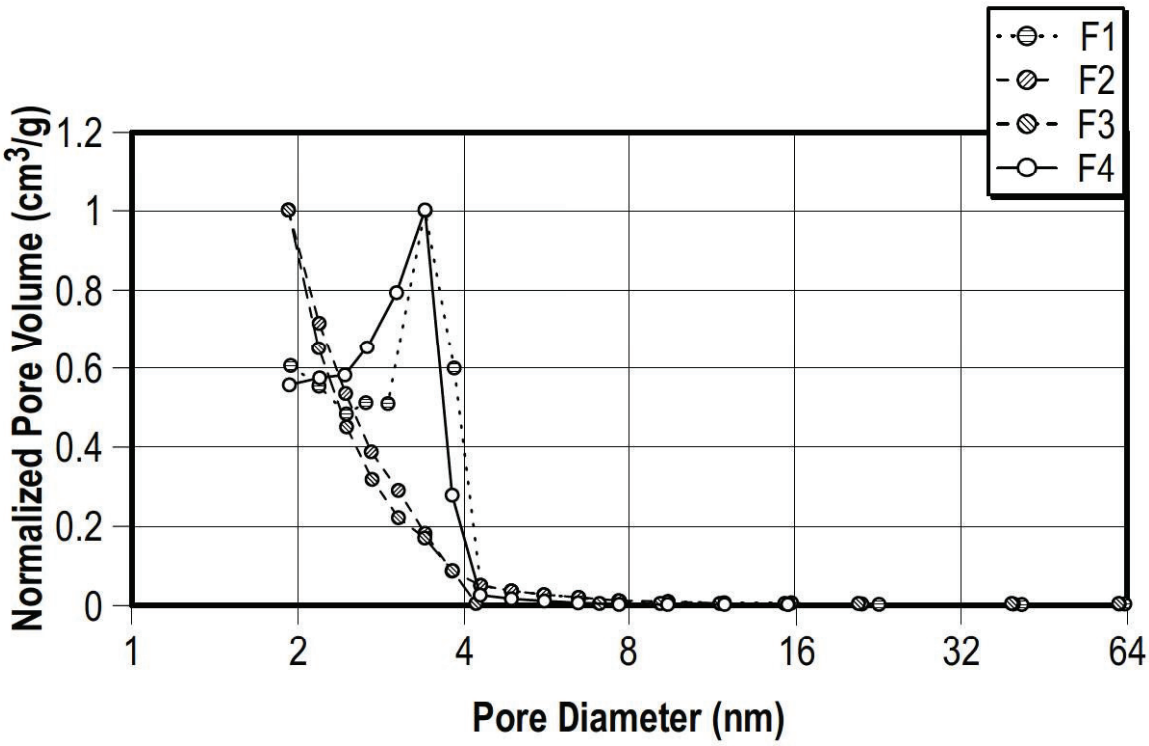
F1
F2
F3
F4
Normalized Pore Volume (cm3/g)
1.2
1
0.8
0.6
0.4
0.2
0
1
2
4
8
16
32
64
Pore Diameter (nm)

FIG. 81

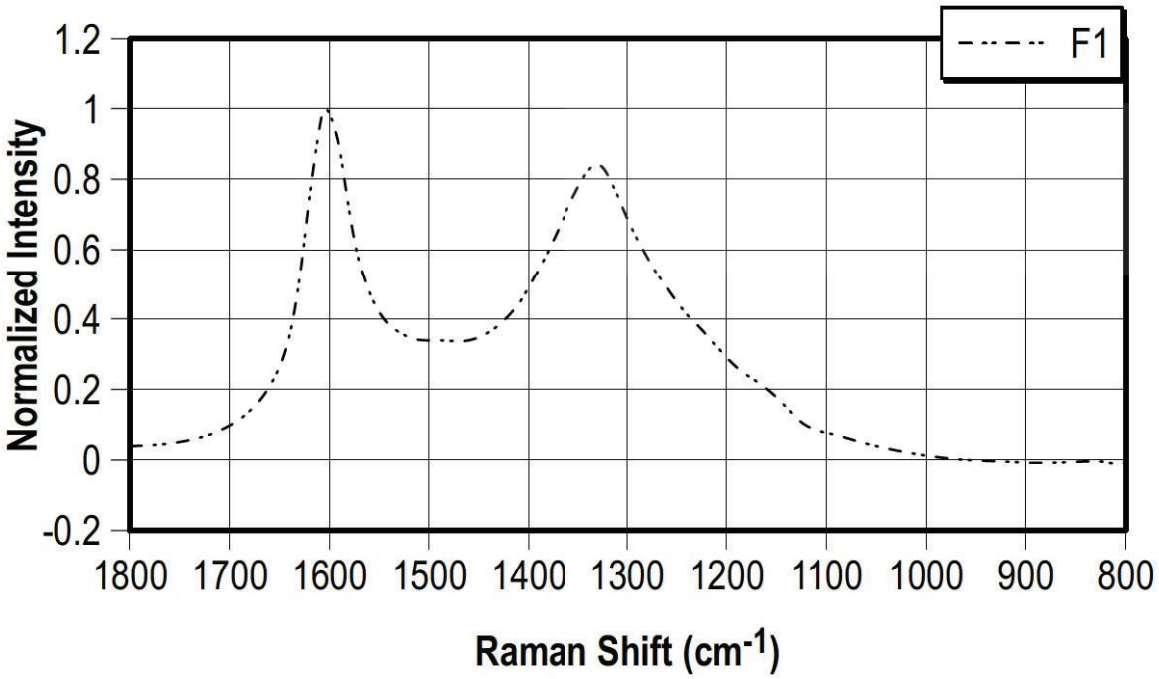
F1
1.2
1
0.8
0.6
0.4
0.2
0
-0.2
Normalized Intensity
1800 1700 1600 1500 1400 1300 1200 1100 1000 900 800
Raman Shift (cm-1)

FIG. 82A

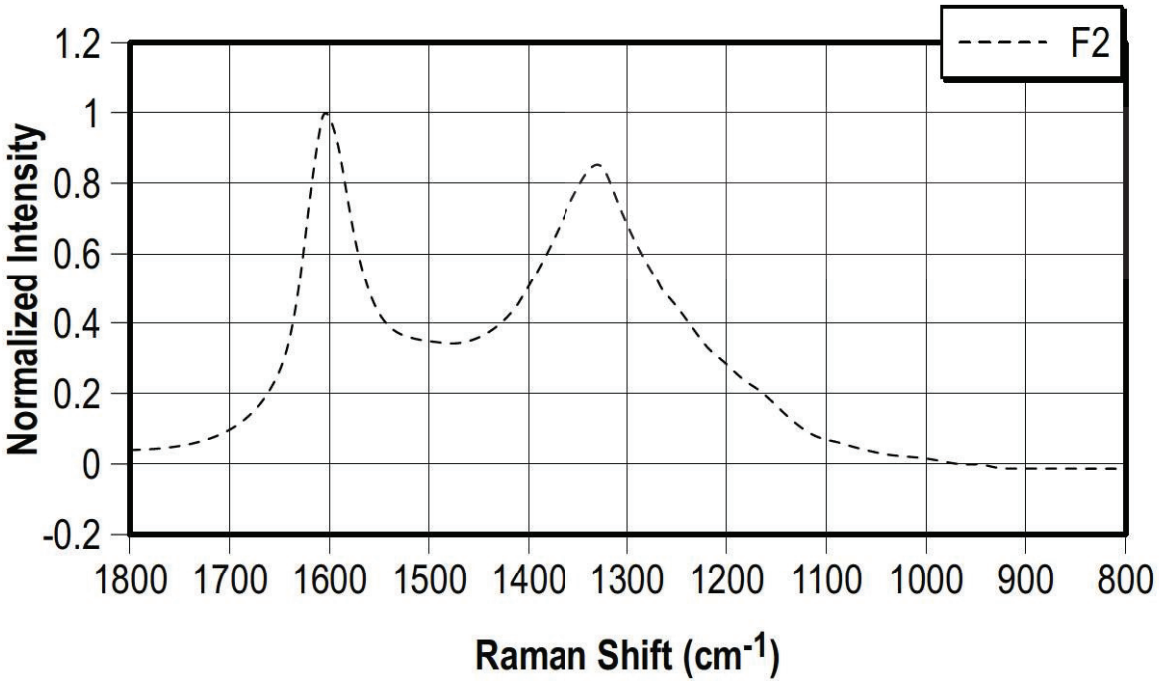
F2
1.2
1
0.8
0.6
0.4
0.2
0
-0.2
Normalized Intensity
1800 1700 1600 1500 1400 1300 1200 1100 1000 900 800
Raman Shift (cm-1)

FIG. 82B

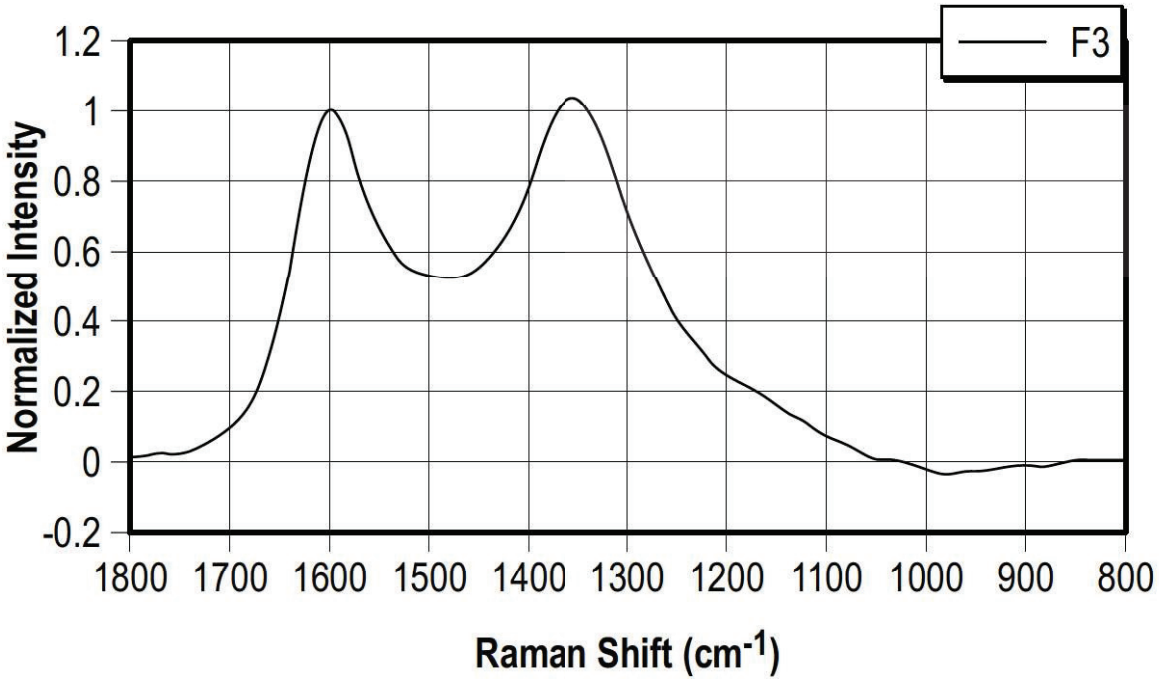
F3
1.2
1
0.8
0.6
0.4
0.2
0
-0.2
Normalized Intensity
1800 1700 1600 1500 1400 1300 1200 1100 1000 900 800
Raman Shift (cm-1)

FIG. 82C

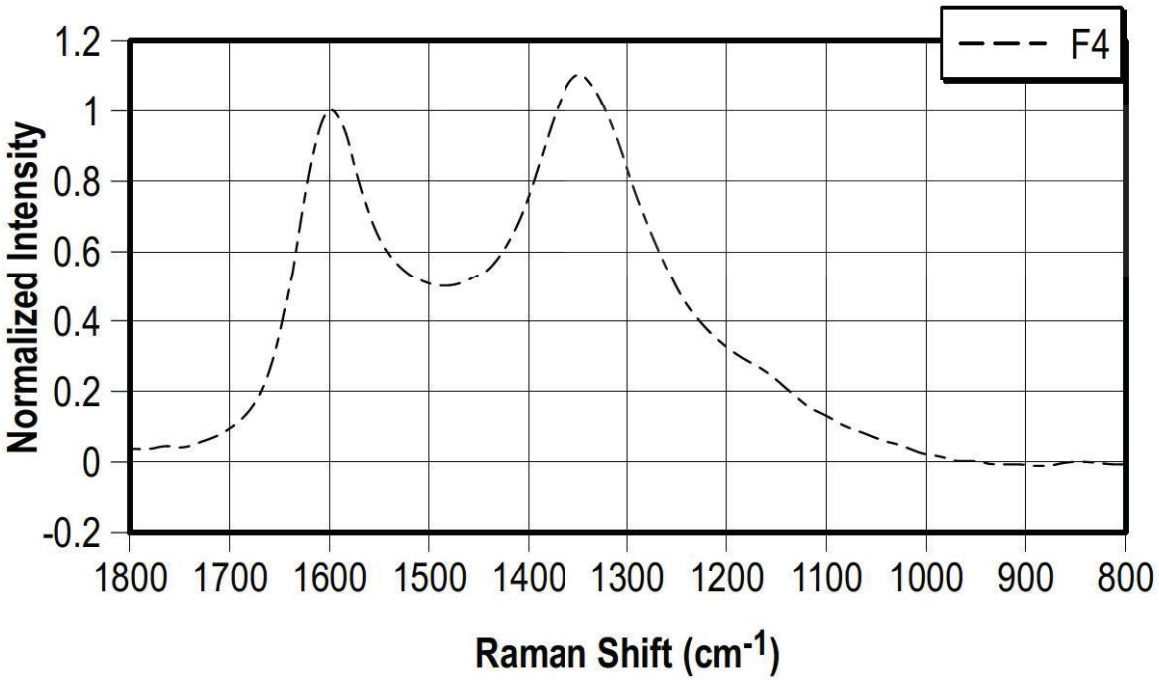
F4
1.2
1
0.8
0.6
0.4
0.2
0
-0.2
Normalized Intensity
1800 1700 1600 1500 1400 1300 1200 1100 1000 900 800
Raman Shift (cm-1)

FIG. 82D

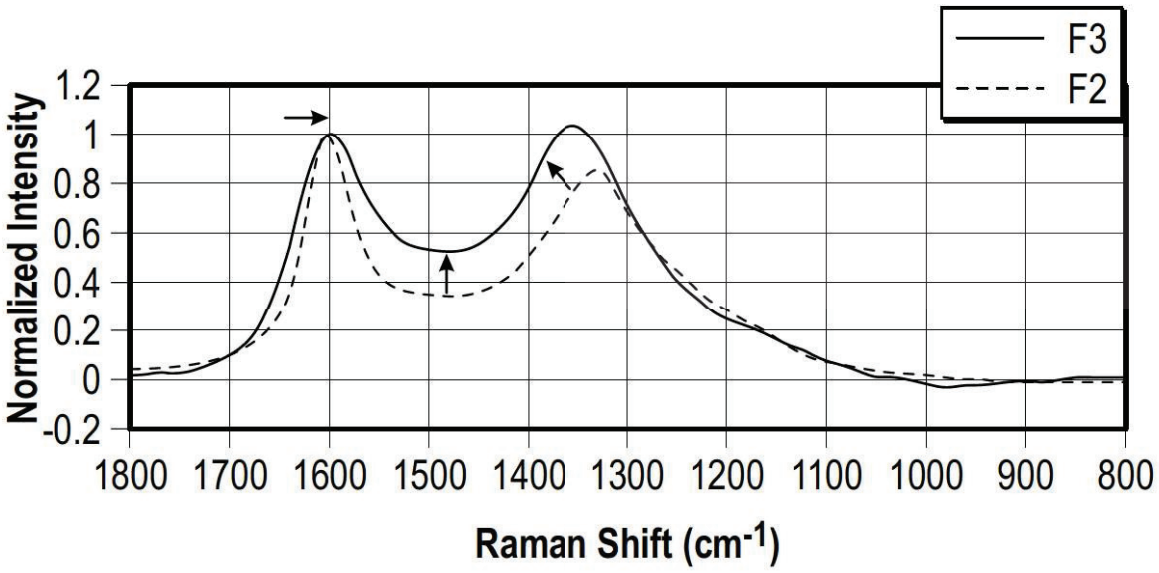
F3
F2
Normalized Intensity
1.2
1
0.8
0.6
0.4
0.2
0
-0.2
1800 1700 1600 1500 1400 1300 1200 1100 1000 900 800
Raman Shift (cm-1)

FIG. 83

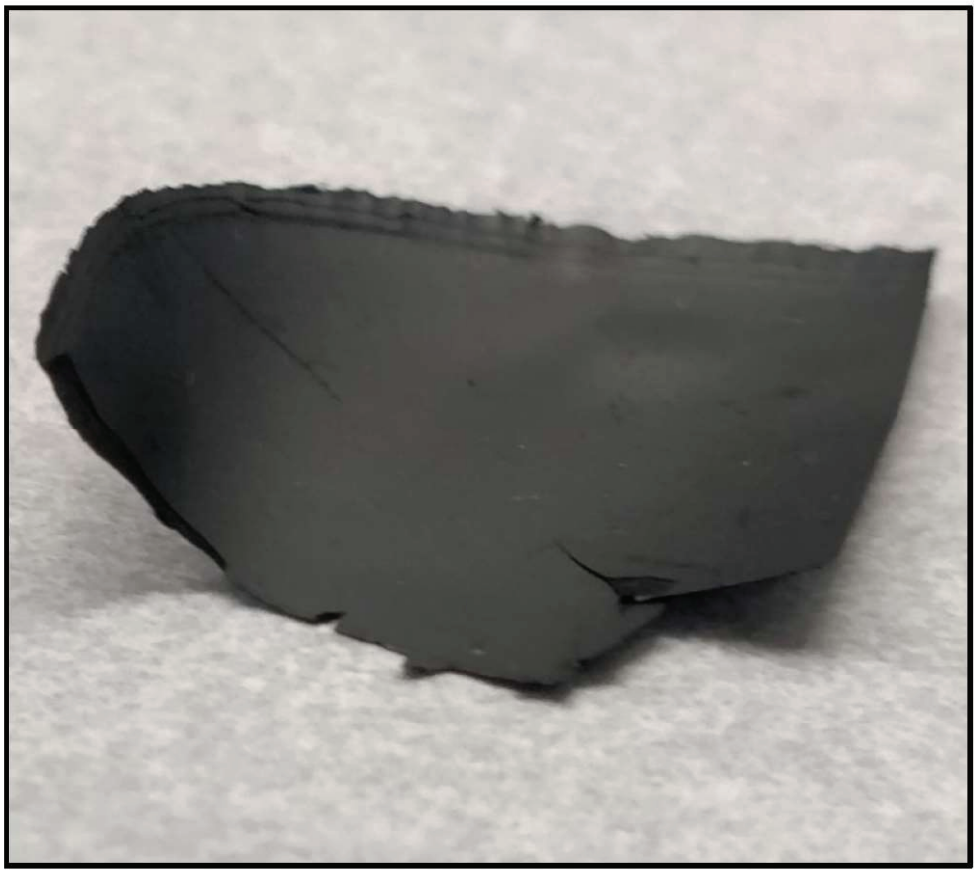

FIG. 84A

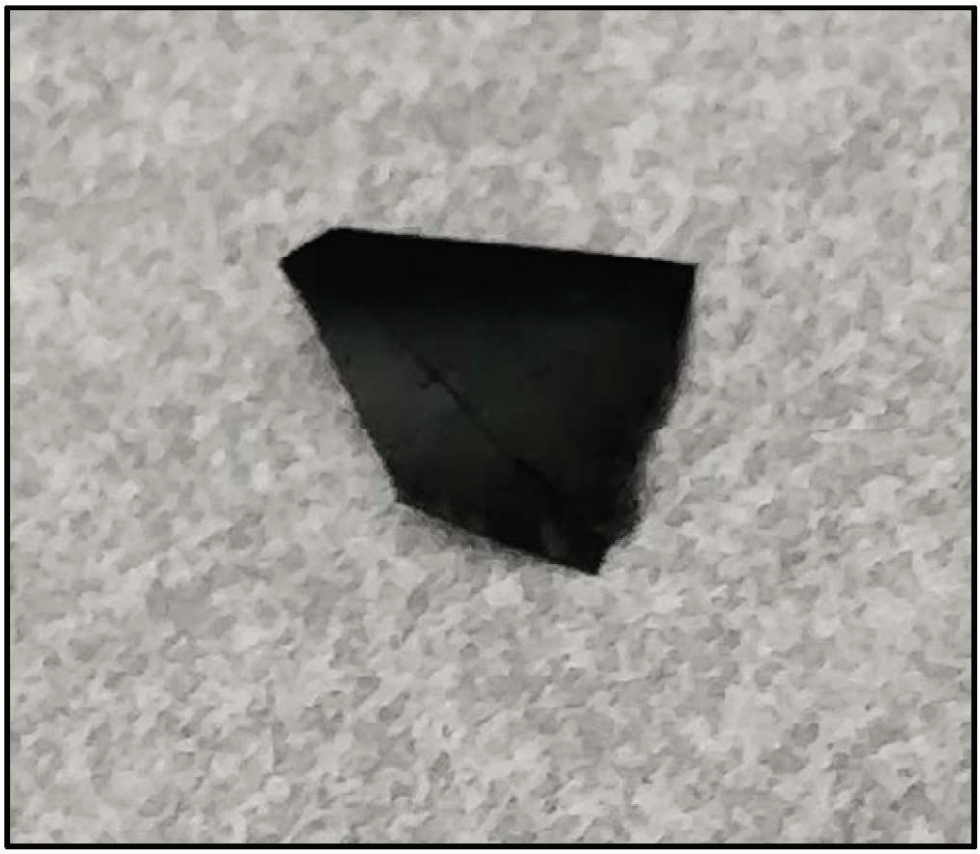

FIG. 84B

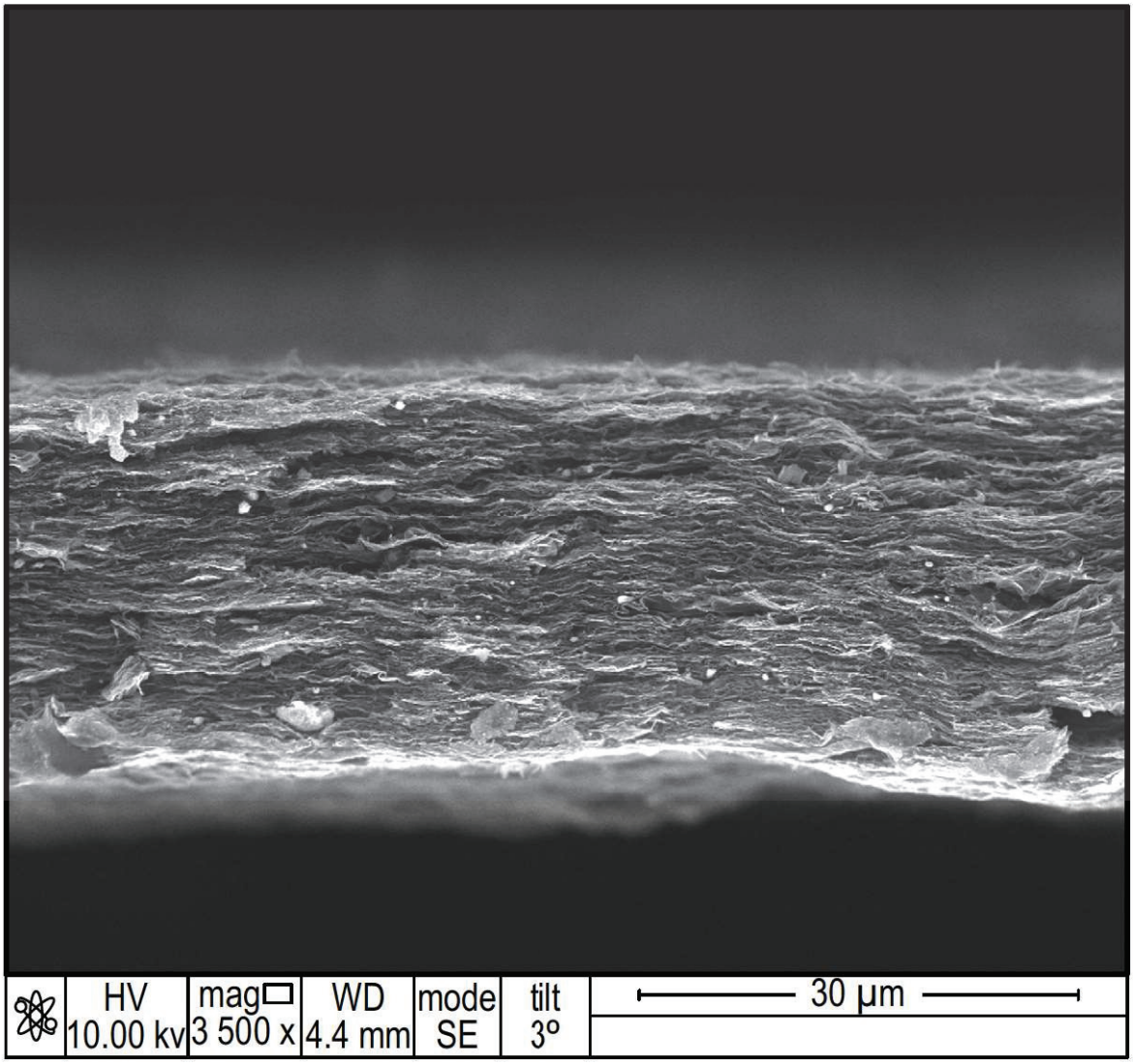

FIG. 85A

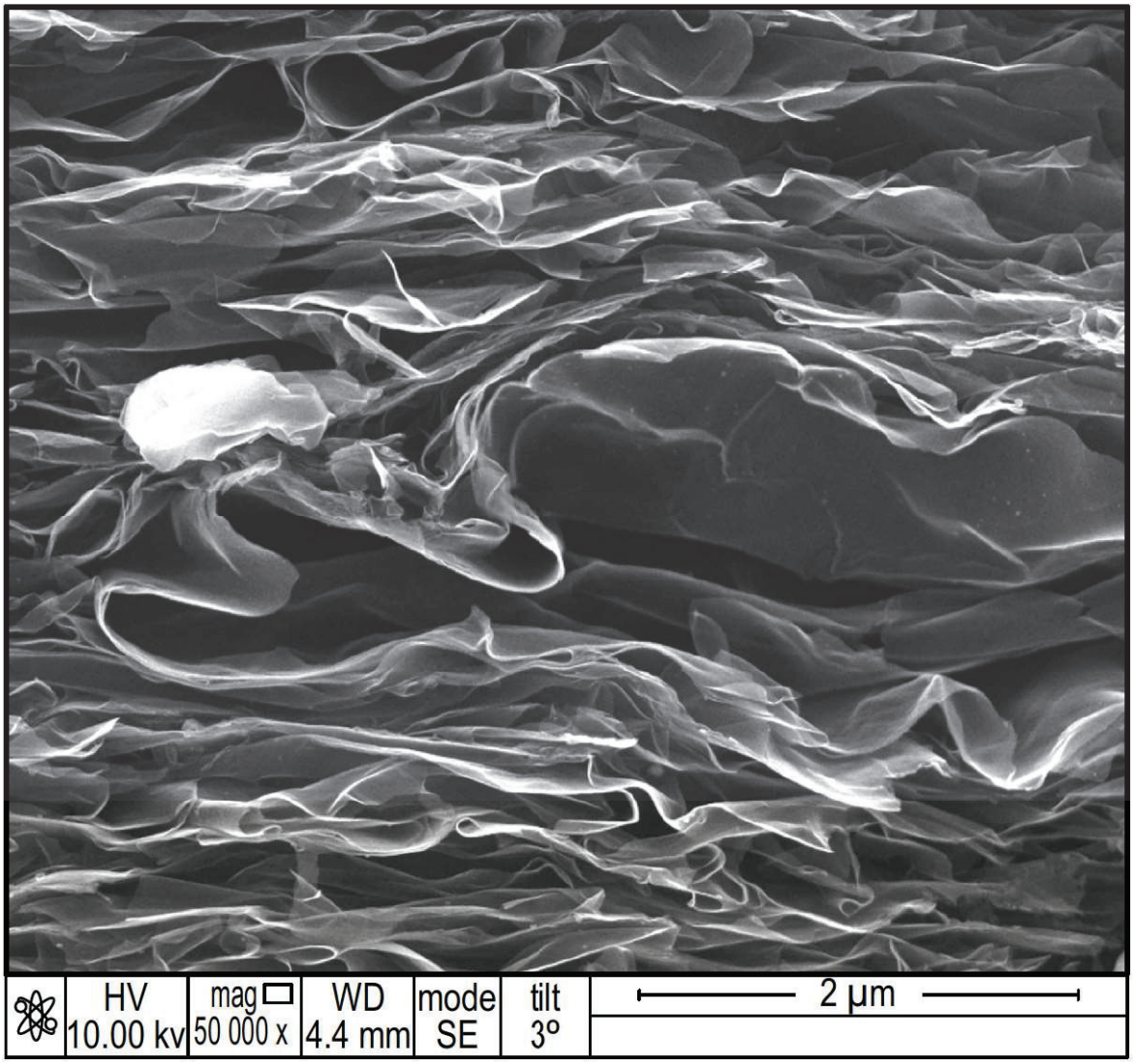

FIG. 85B

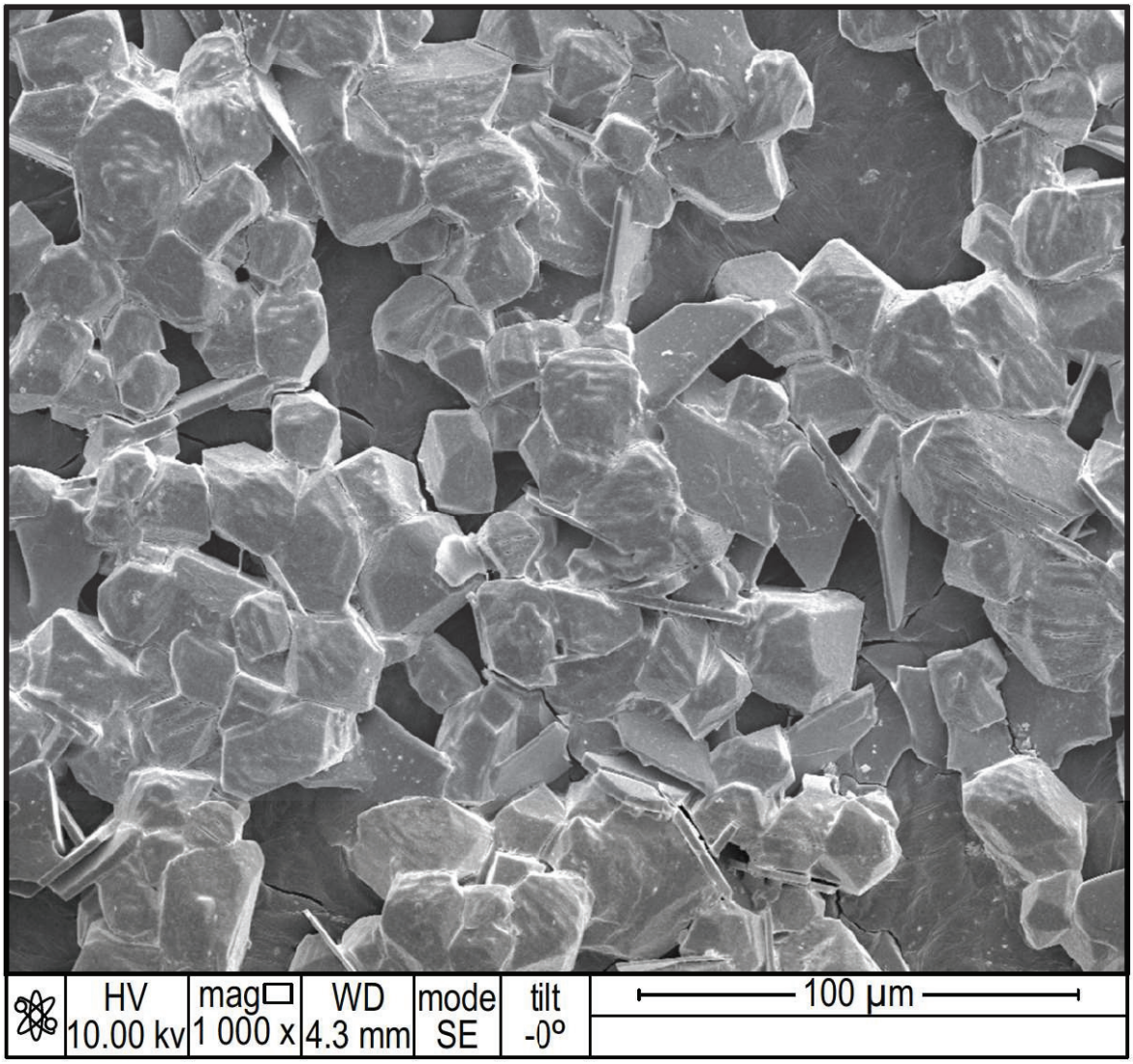

FIG. 85C

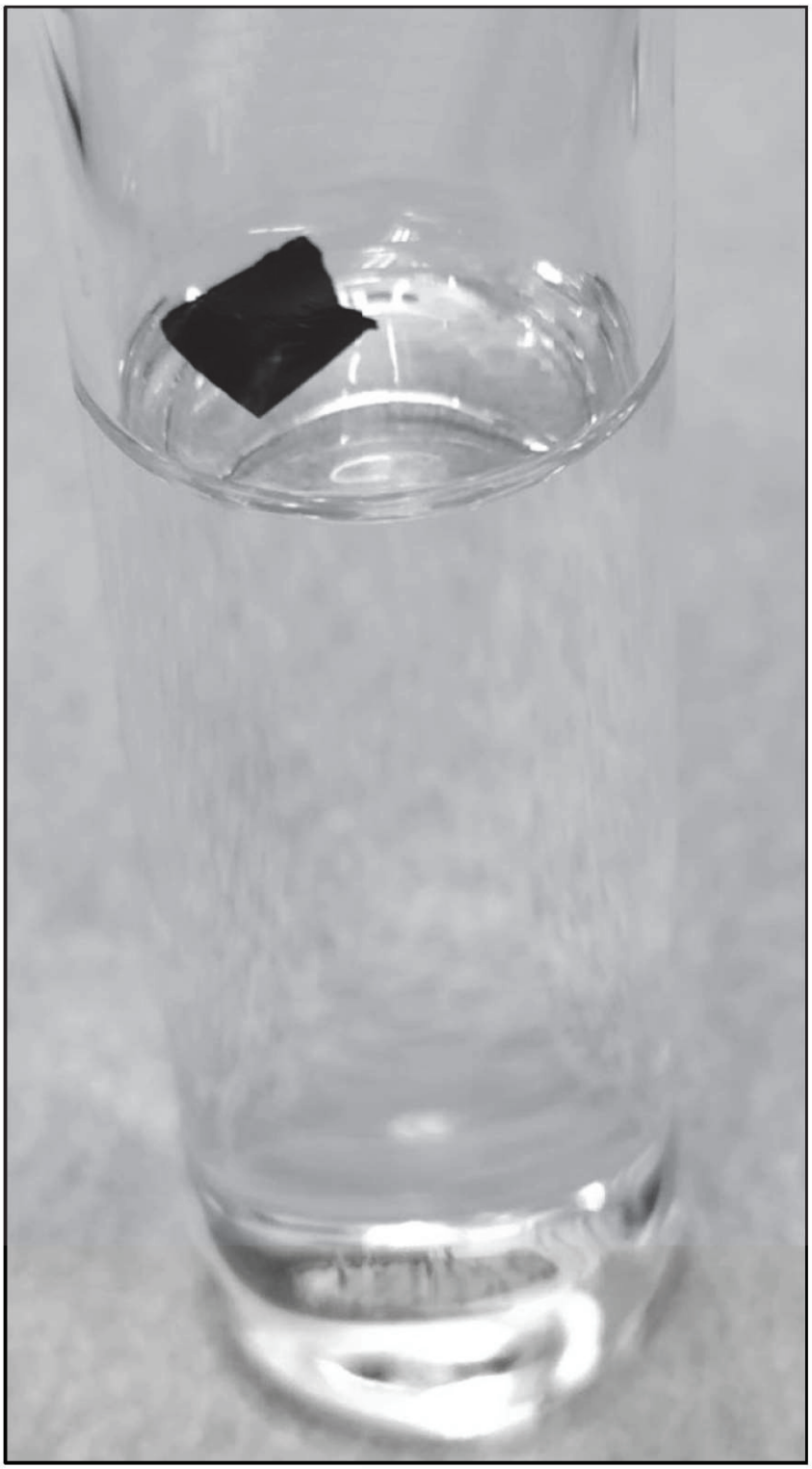

FIG. 86A

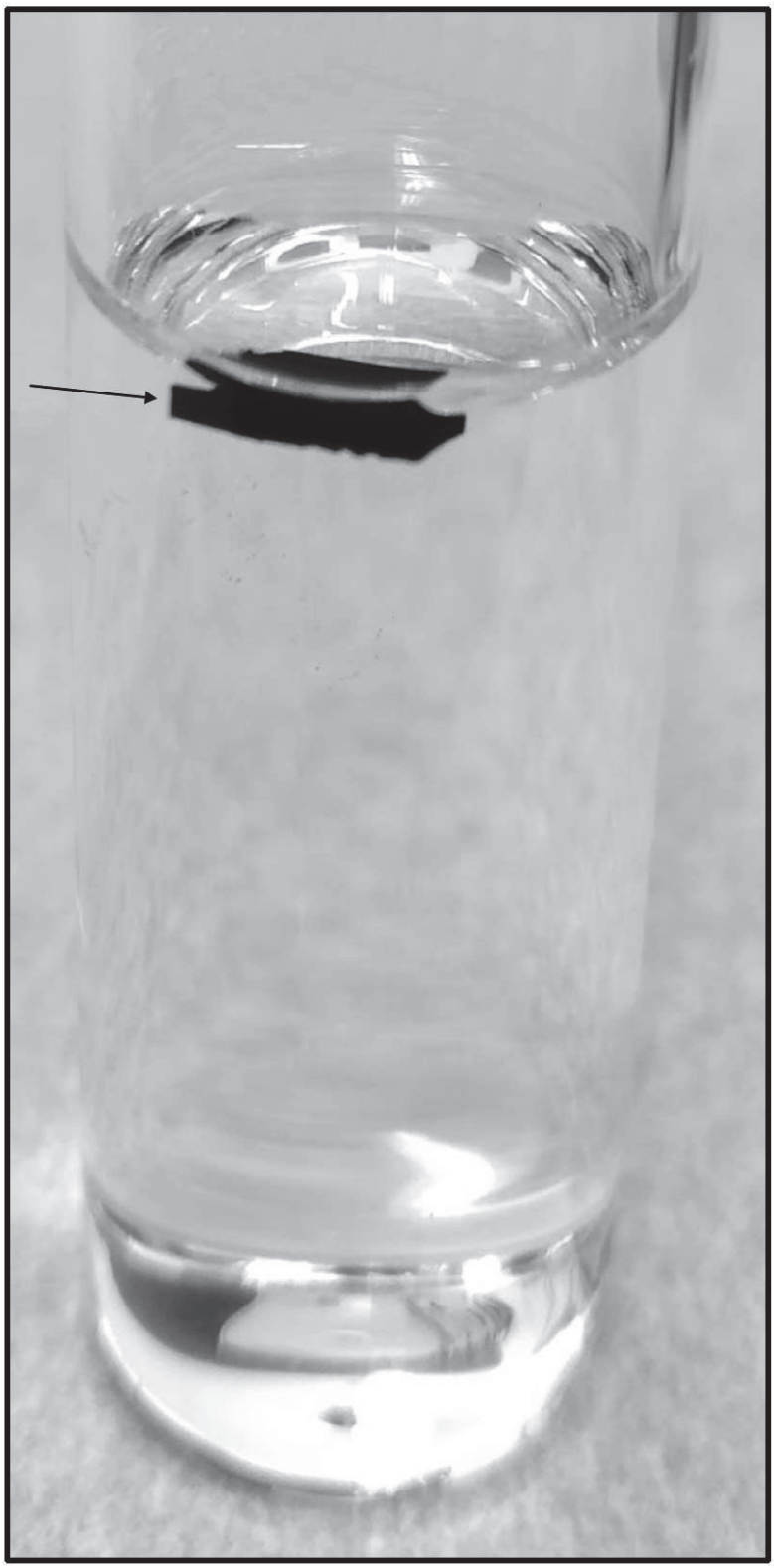

FIG. 86B

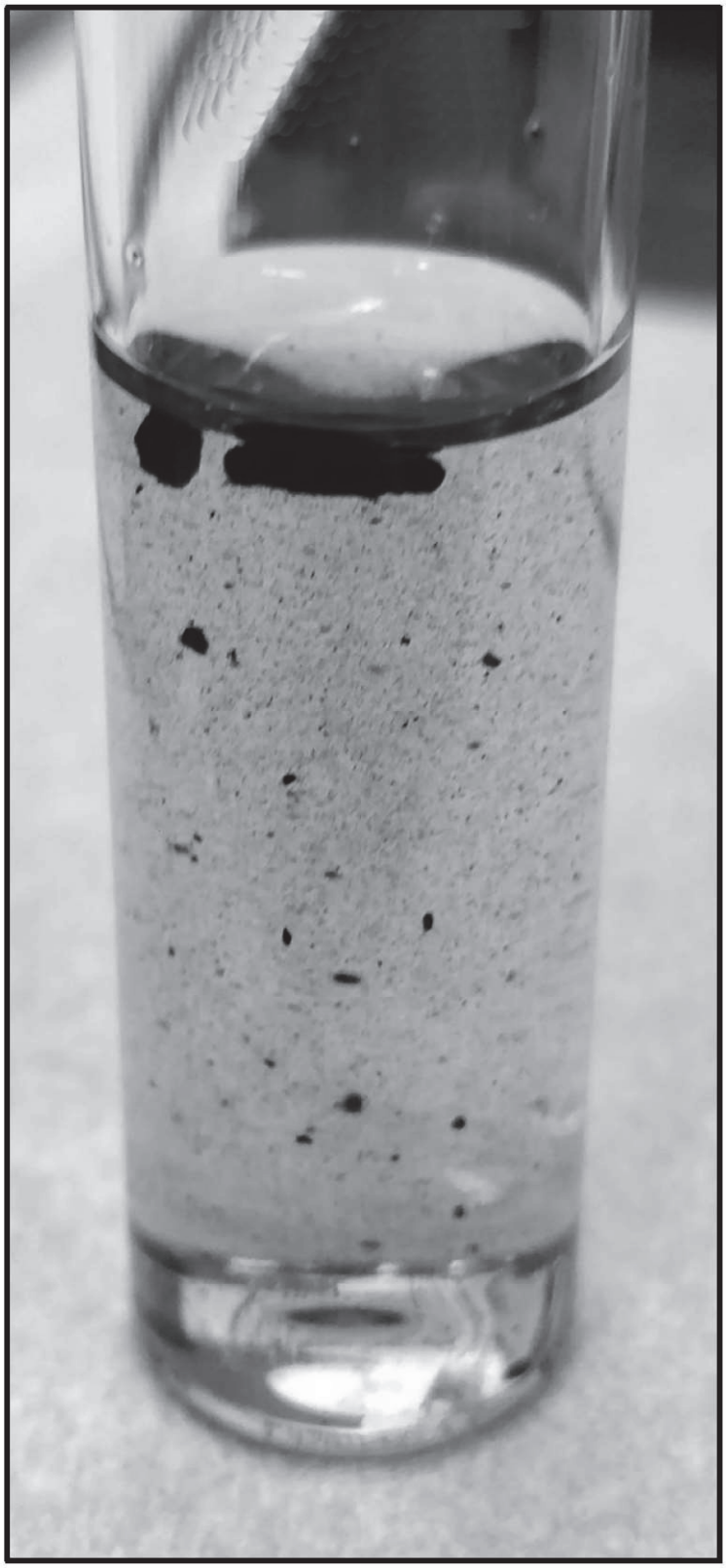

FIG. 86C

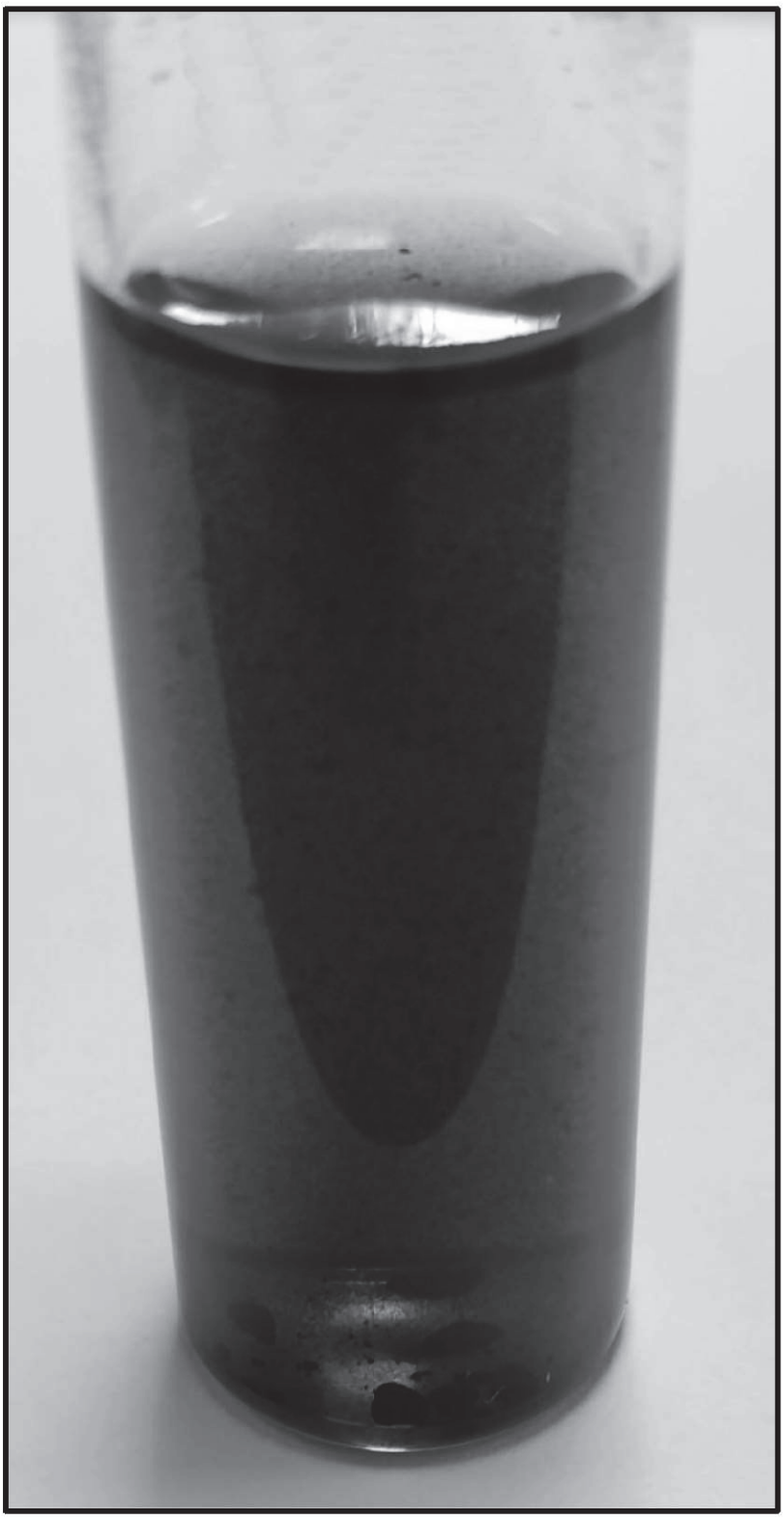

FIG. 86D



FIG. 87A



FIG. 87B



FIG. 87C

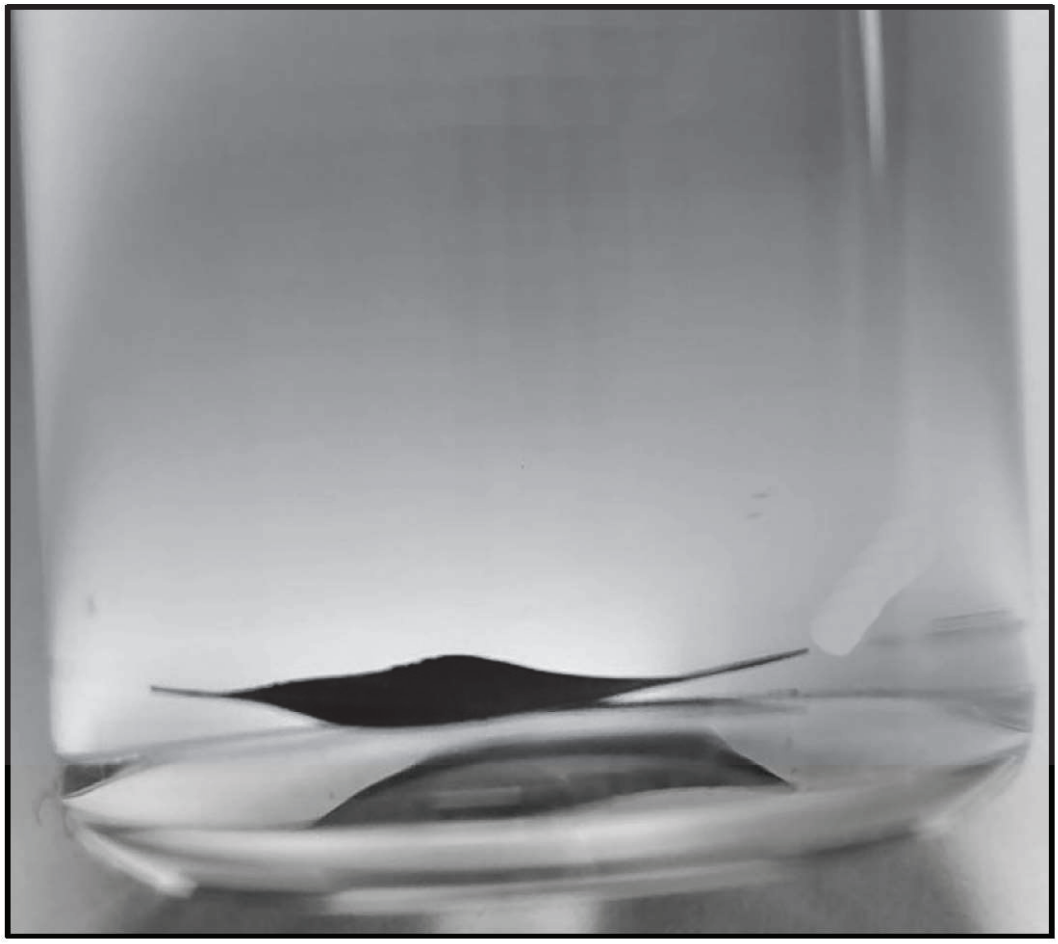

FIG. 87D

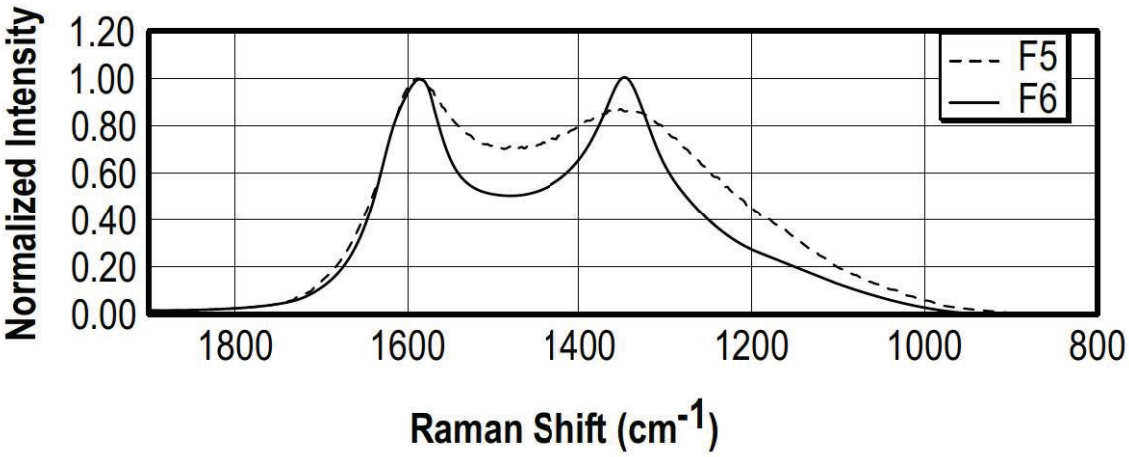
Normalized Intensity
1.20
1.00
0.80
0.60
0.40
0.20
0.00
1800
1600
1400
1200
1000
800
Raman Shift (cm-1)
F5
F6

FIG. 88A

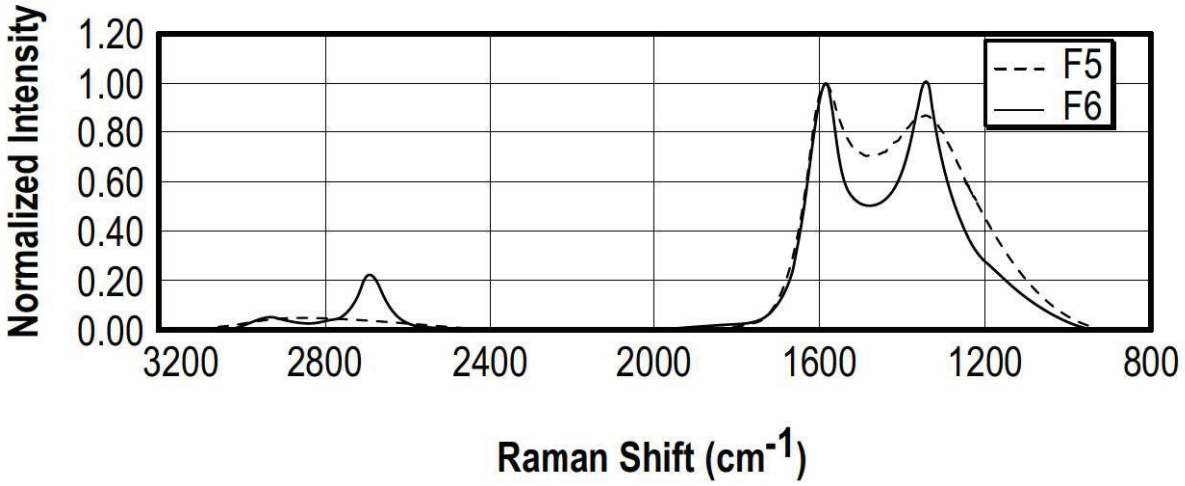
Normalized Intensity
1.20
1.00
0.80
0.60
0.40
0.20
0.00
3200
2800
2400
2000
1600
1200
800
F5
F6
Raman Shift (cm-1)

FIG. 88B

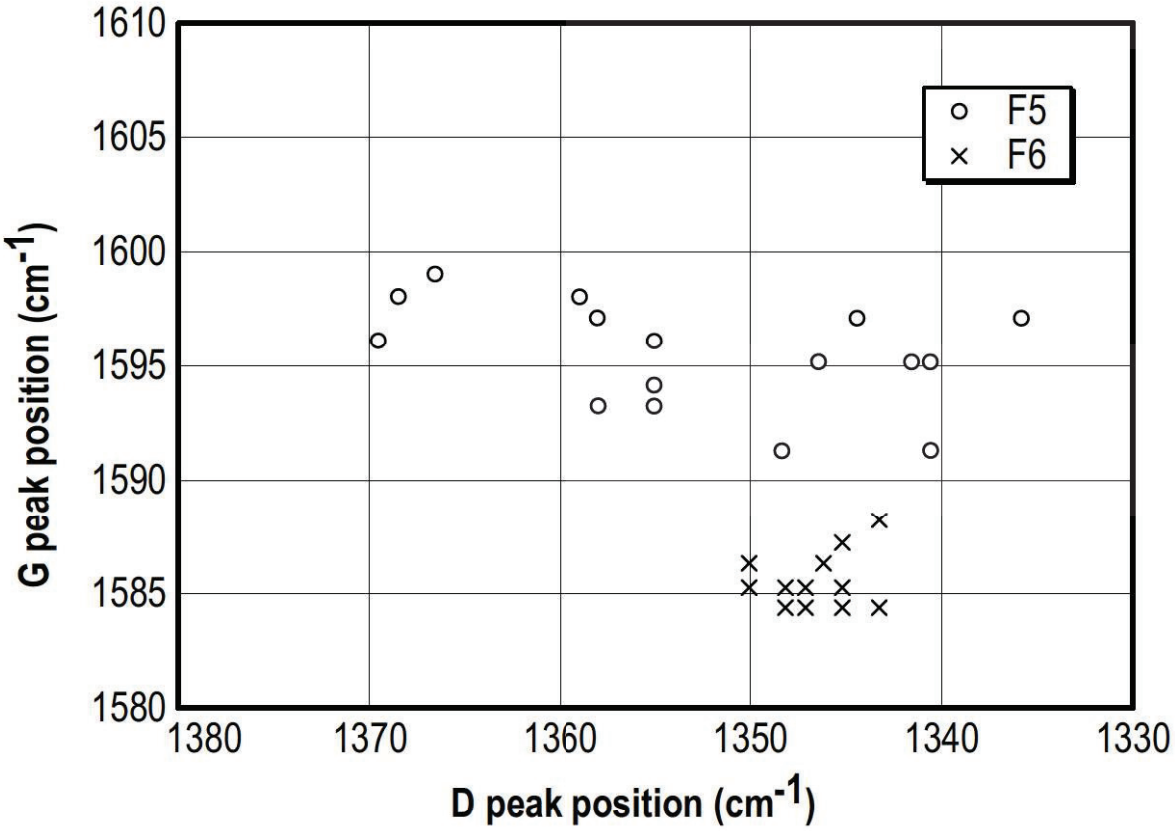
1610
1605
1600
1595
1590
1585
1580
1380
1370
1360
1350
1340
1330
G peak position (cm-1)
D peak position (cm-1)
F5
F6

FIG. 88C

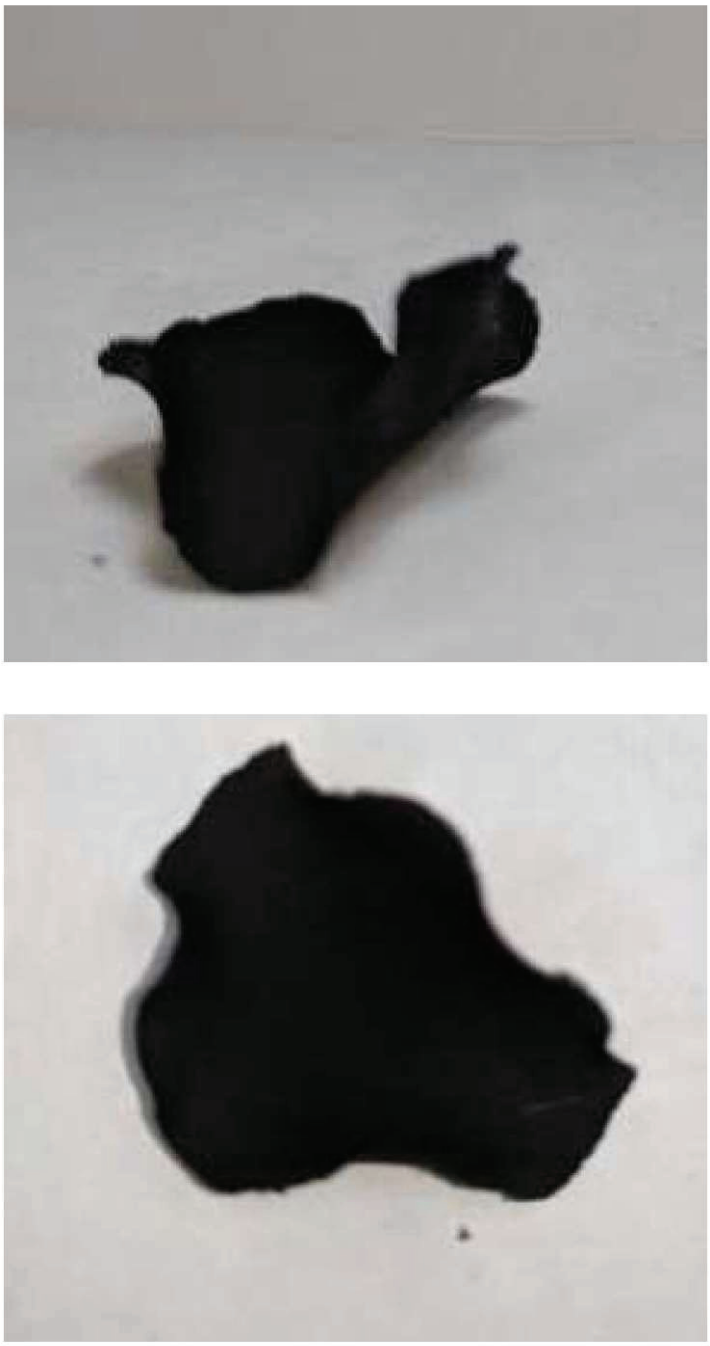

Fig. 89

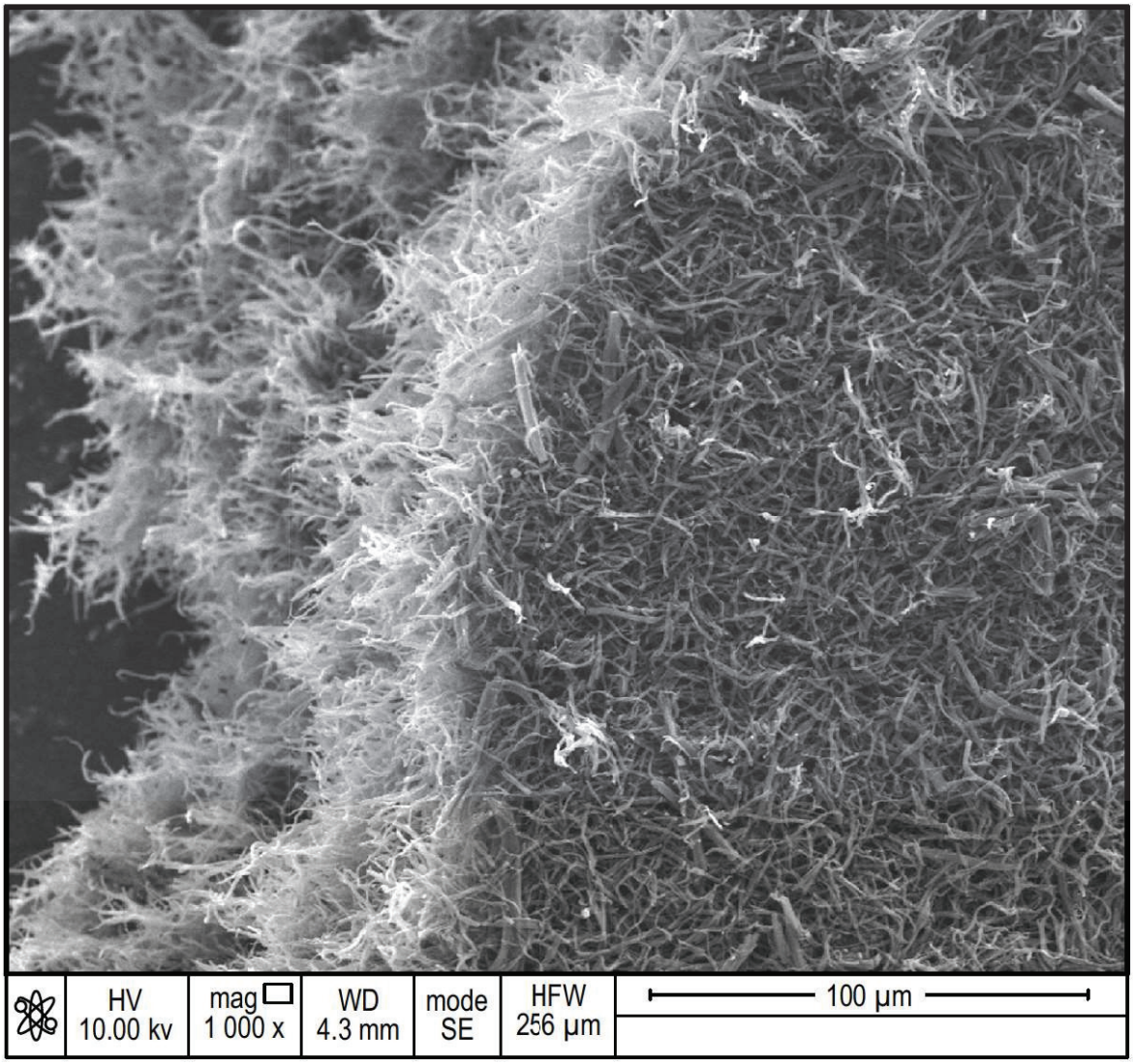

FIG. 90A

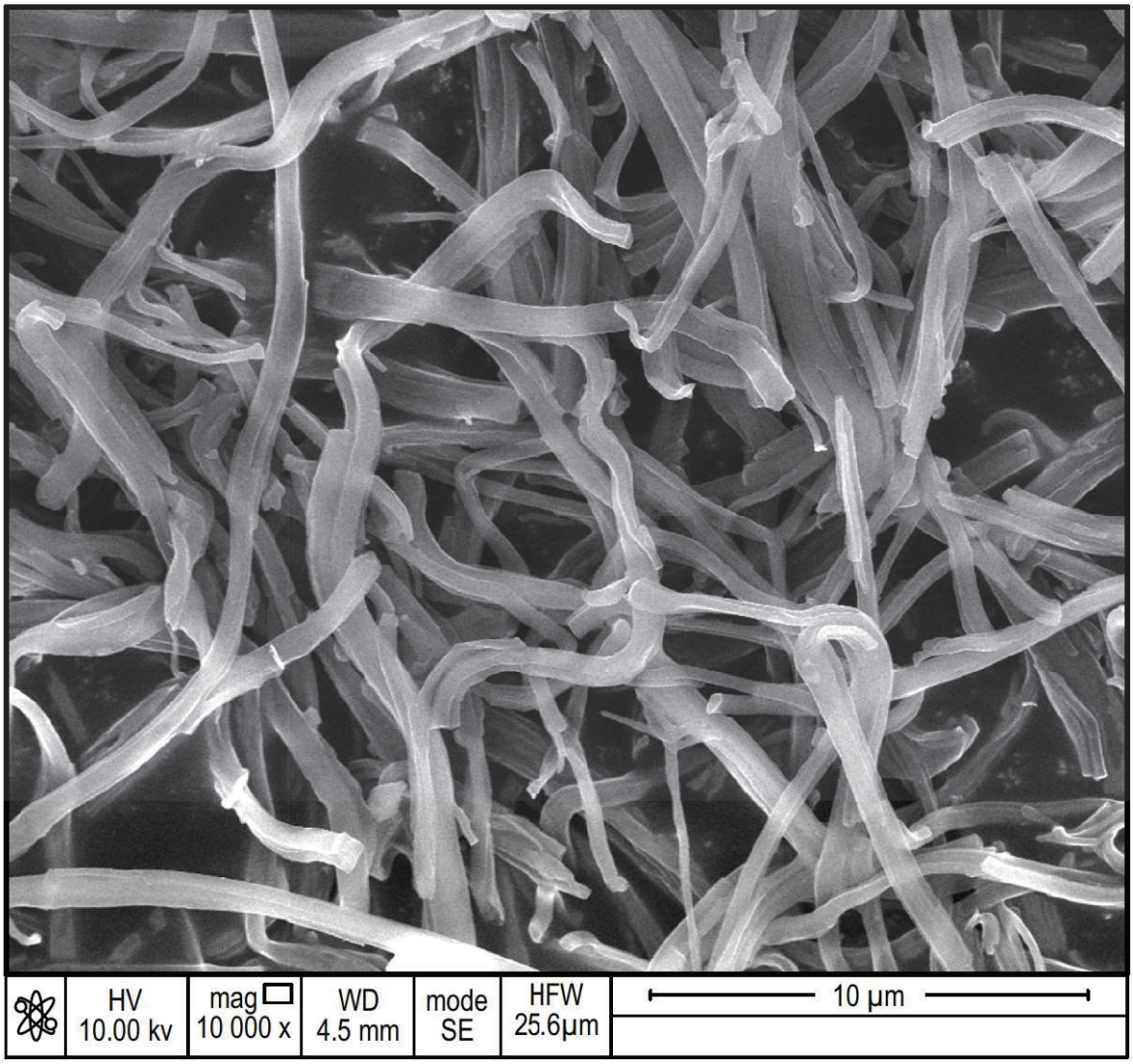

FIG. 90B

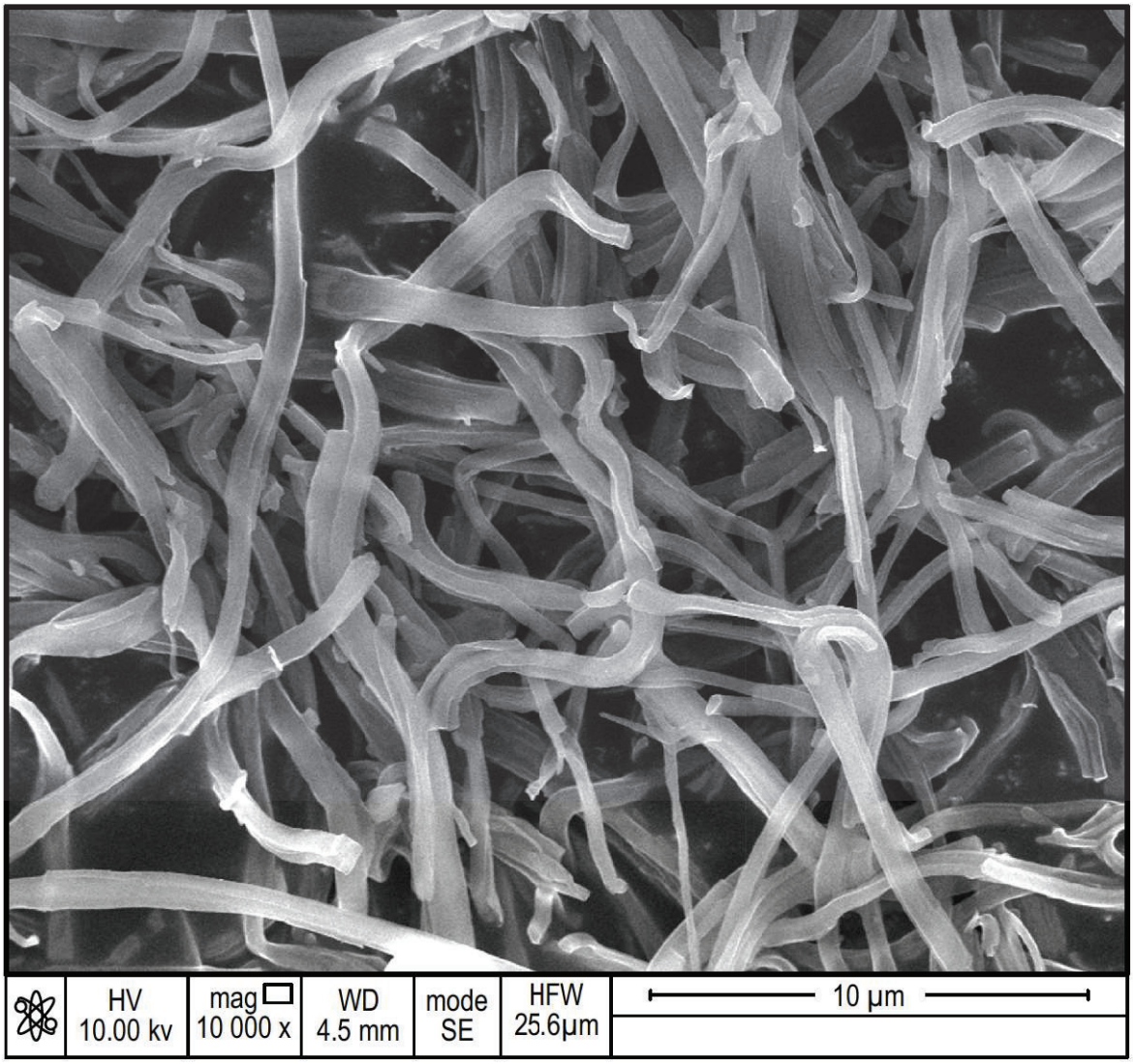

FIG. 91A

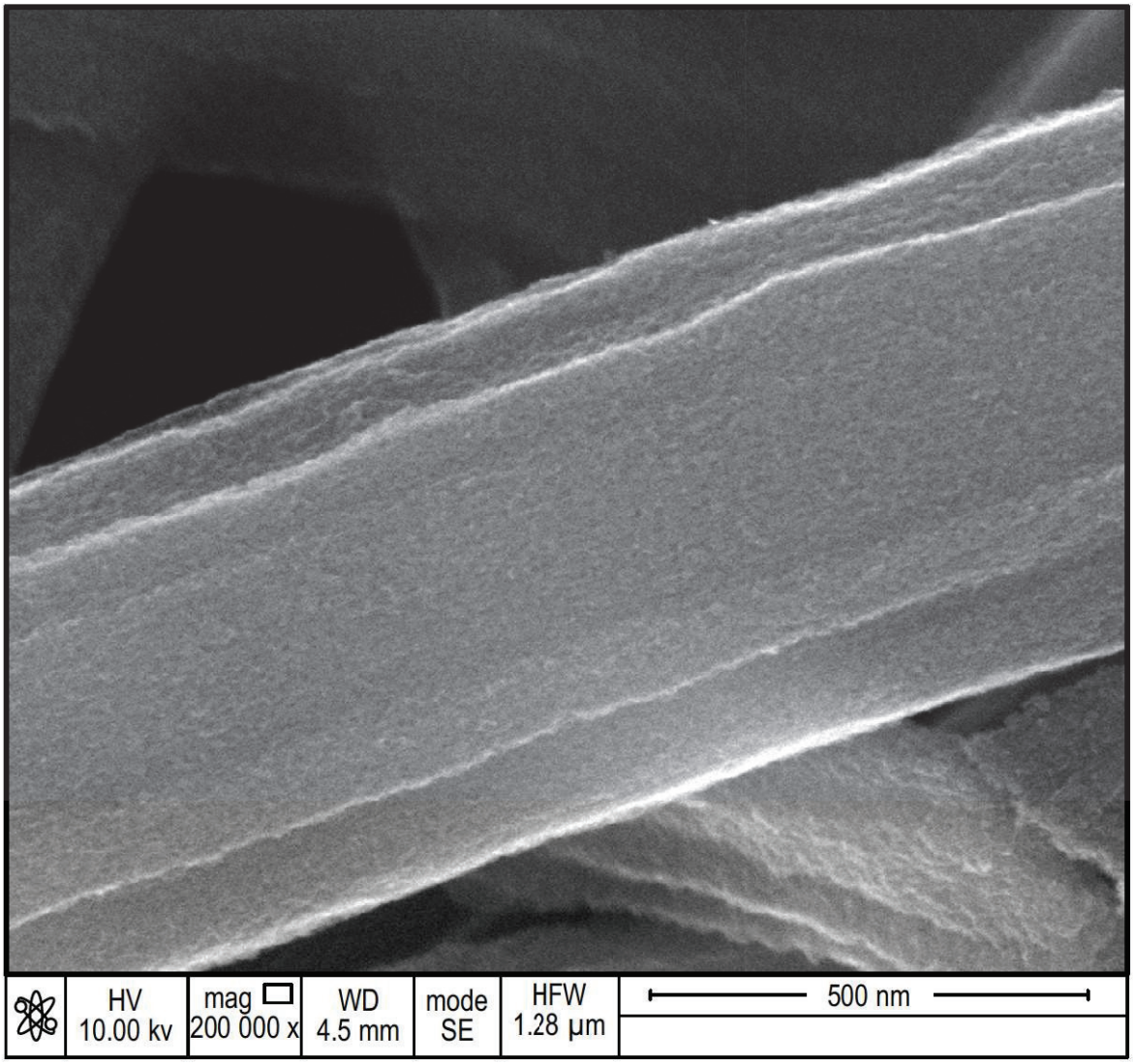

FIG. 91B

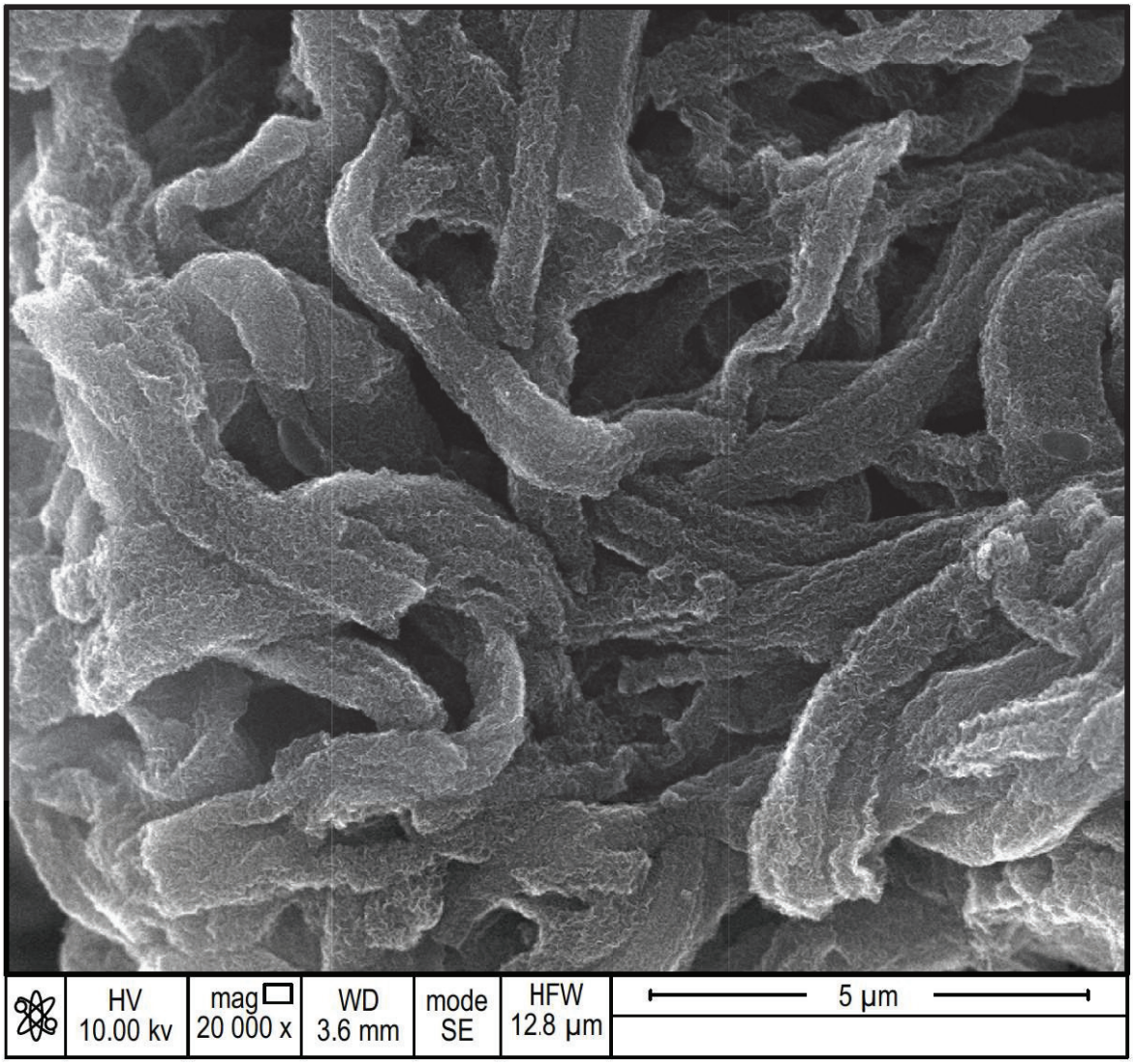

FIG. 92A

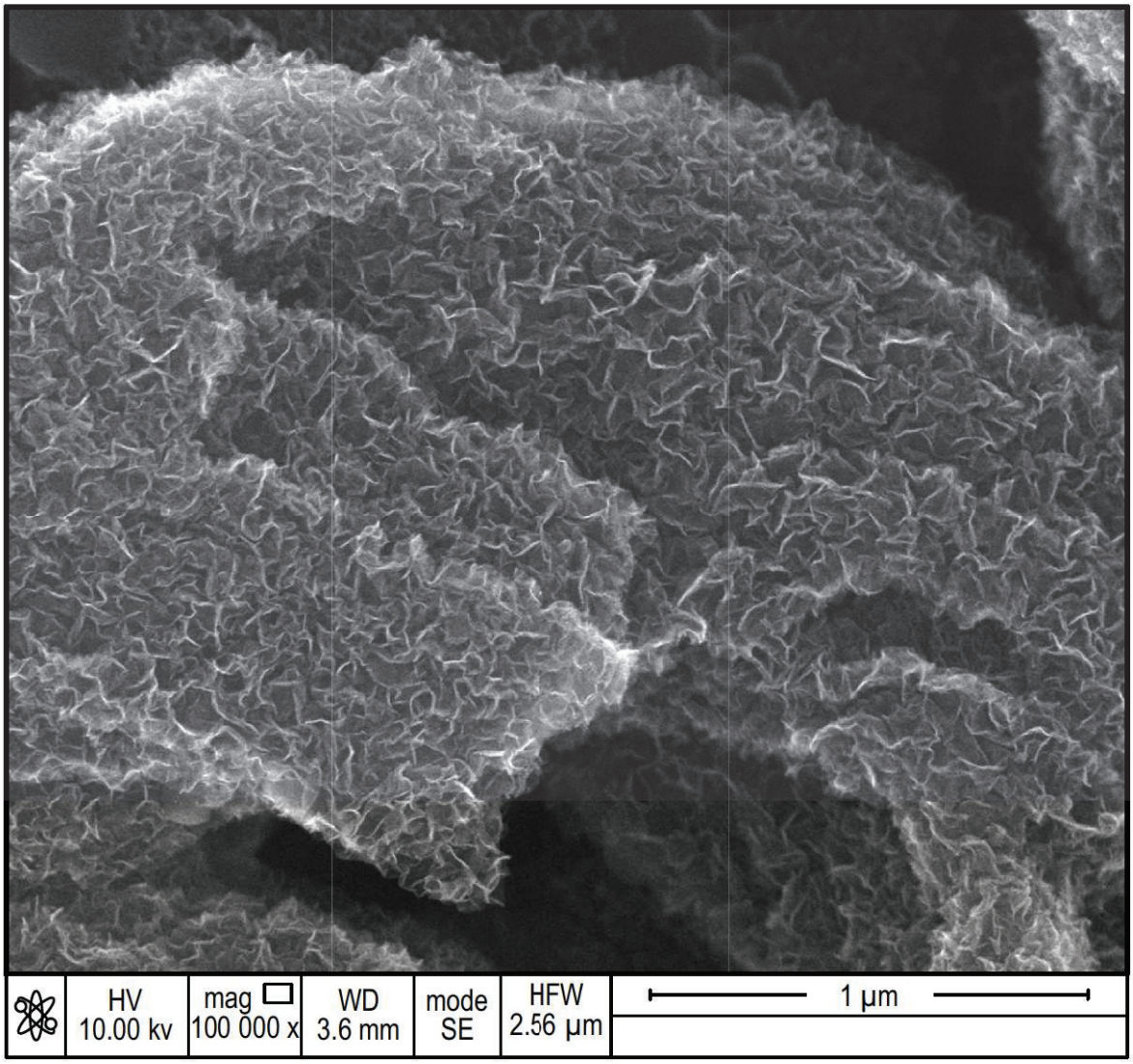

FIG. 92B

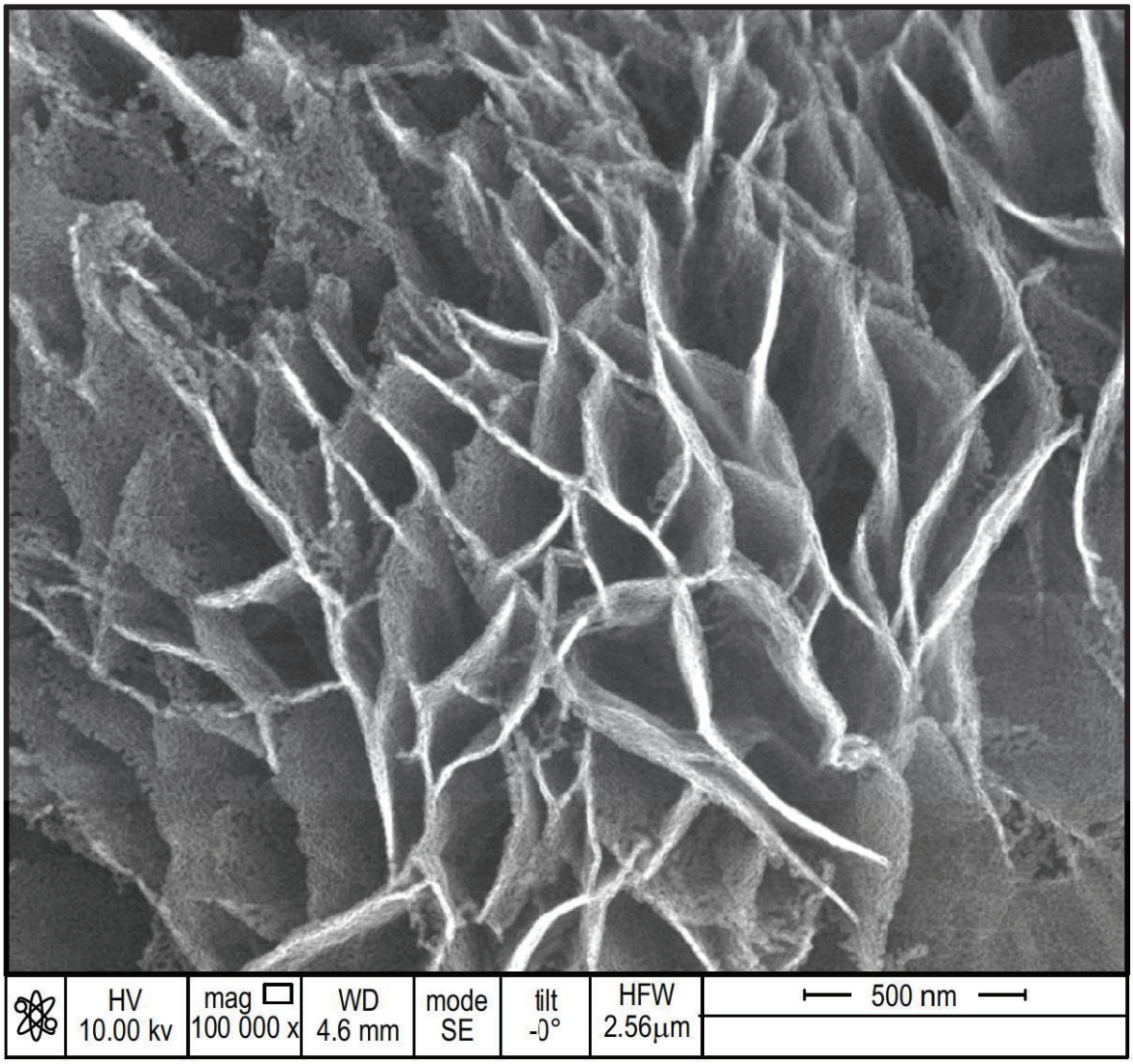

FIG. 93

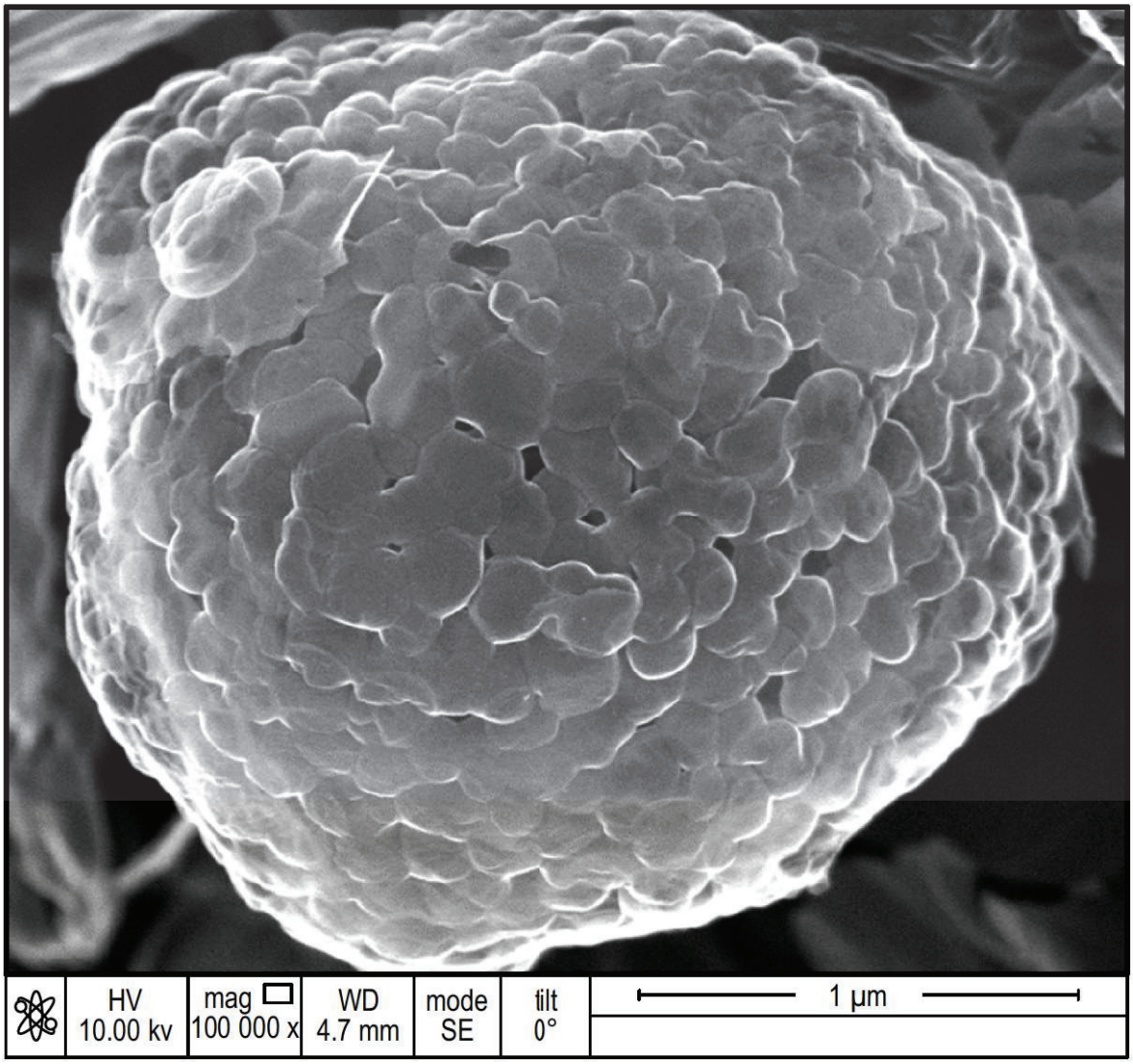

FIG. 94A

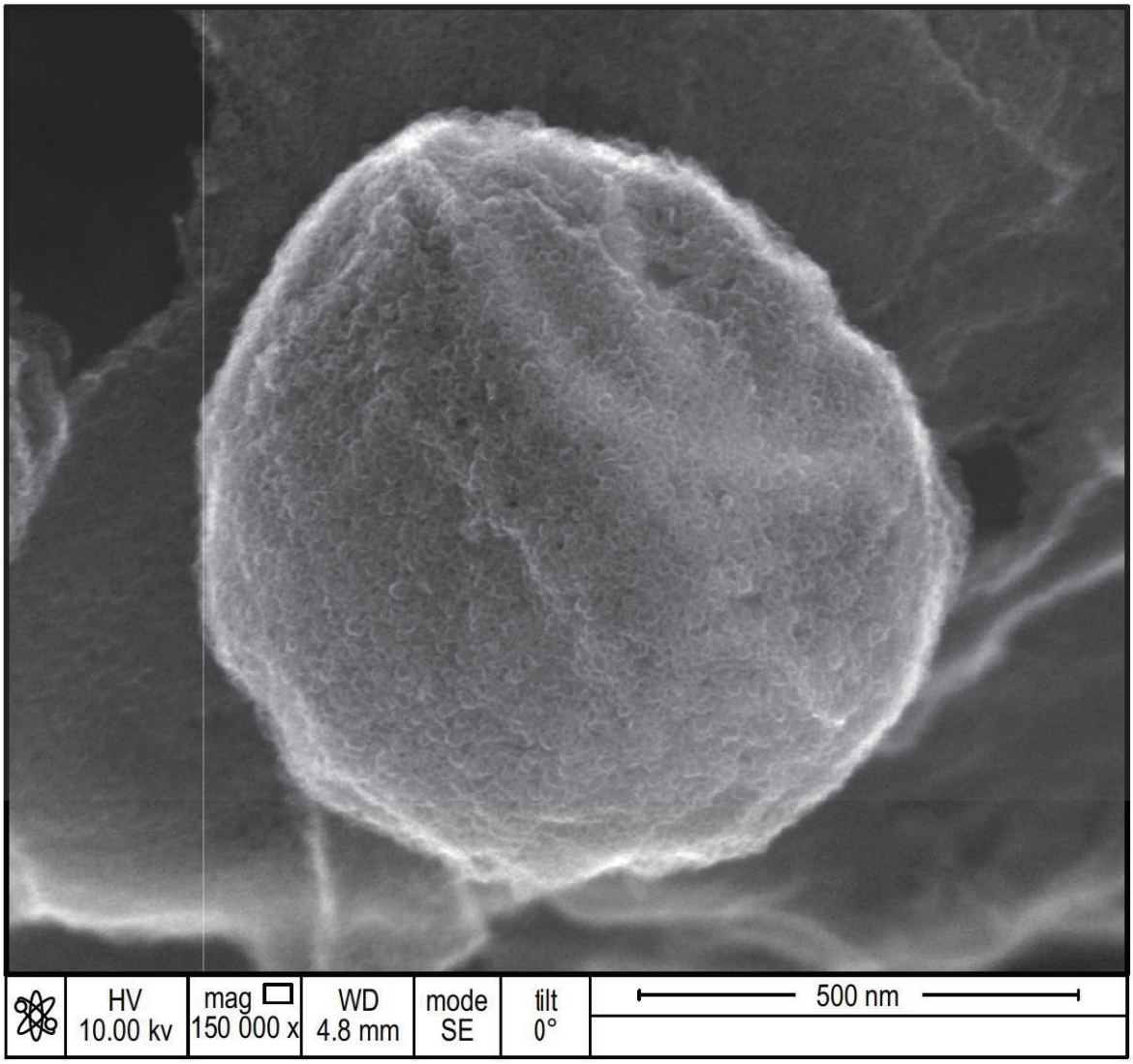

FIG. 94B

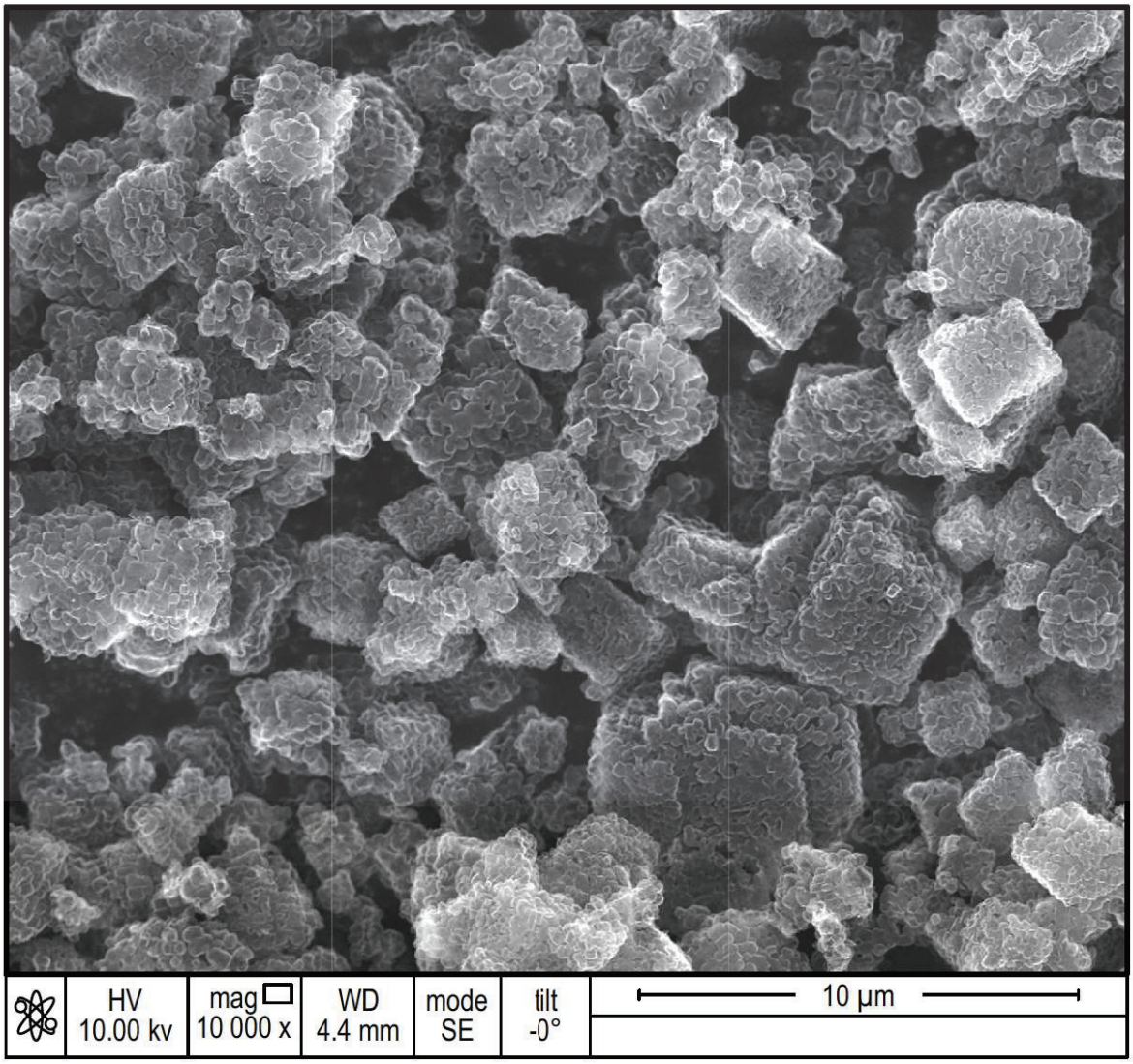

FIG. 95A

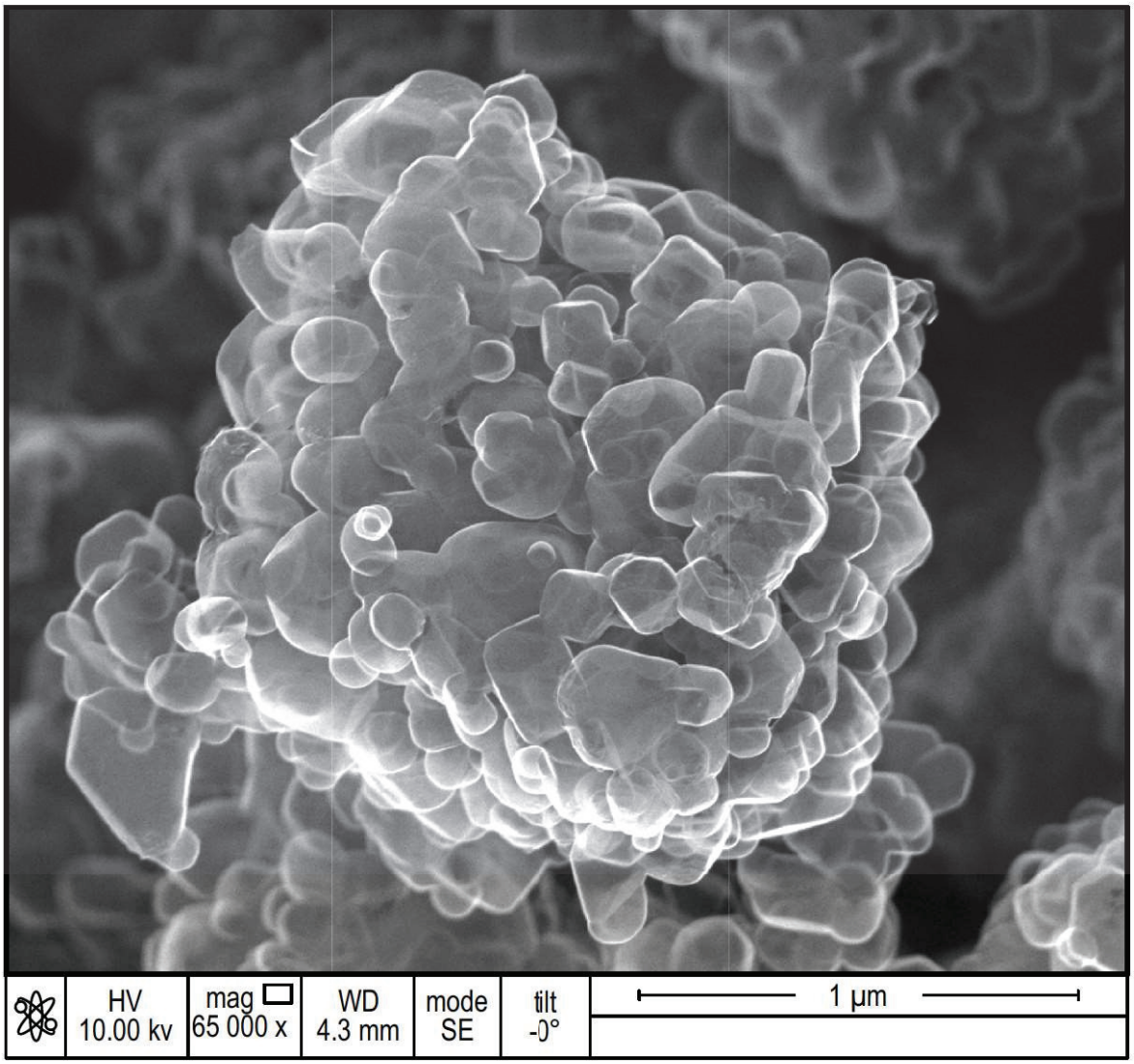

FIG. 95B

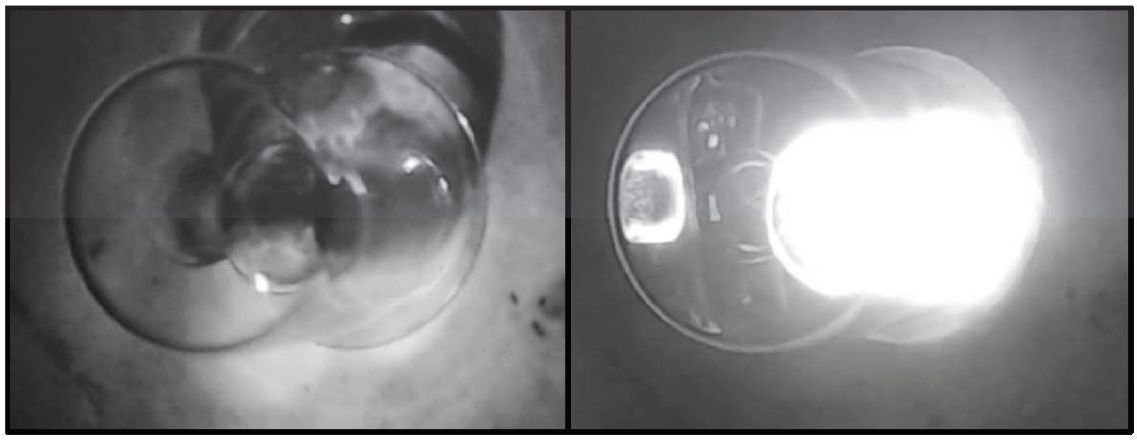

Before microwave irradiation During microwave irradiation

FIG. 96

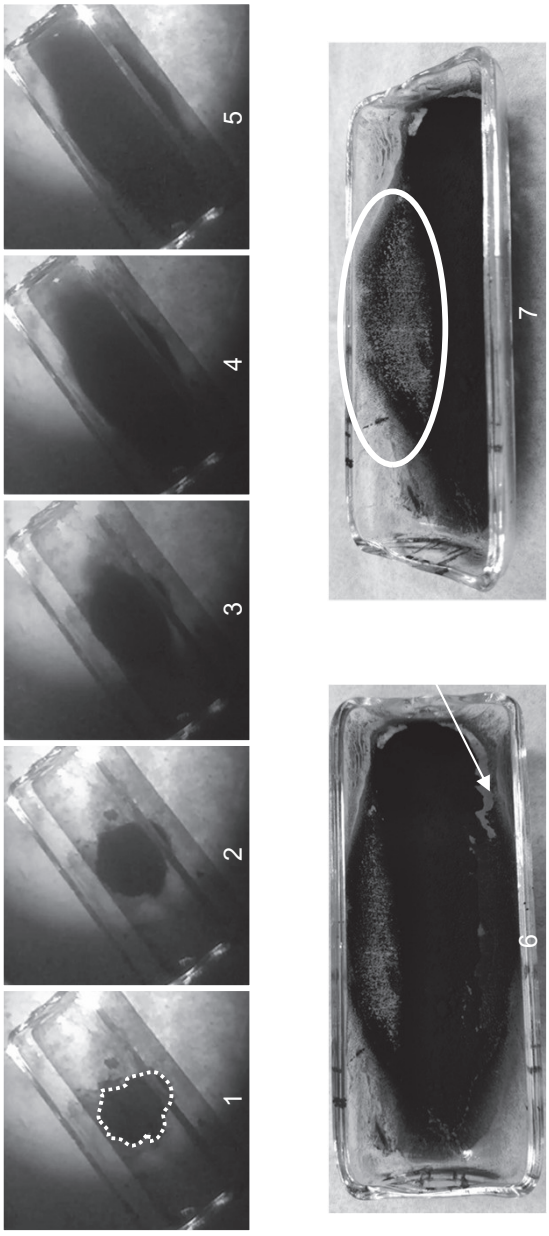

FIG. 97

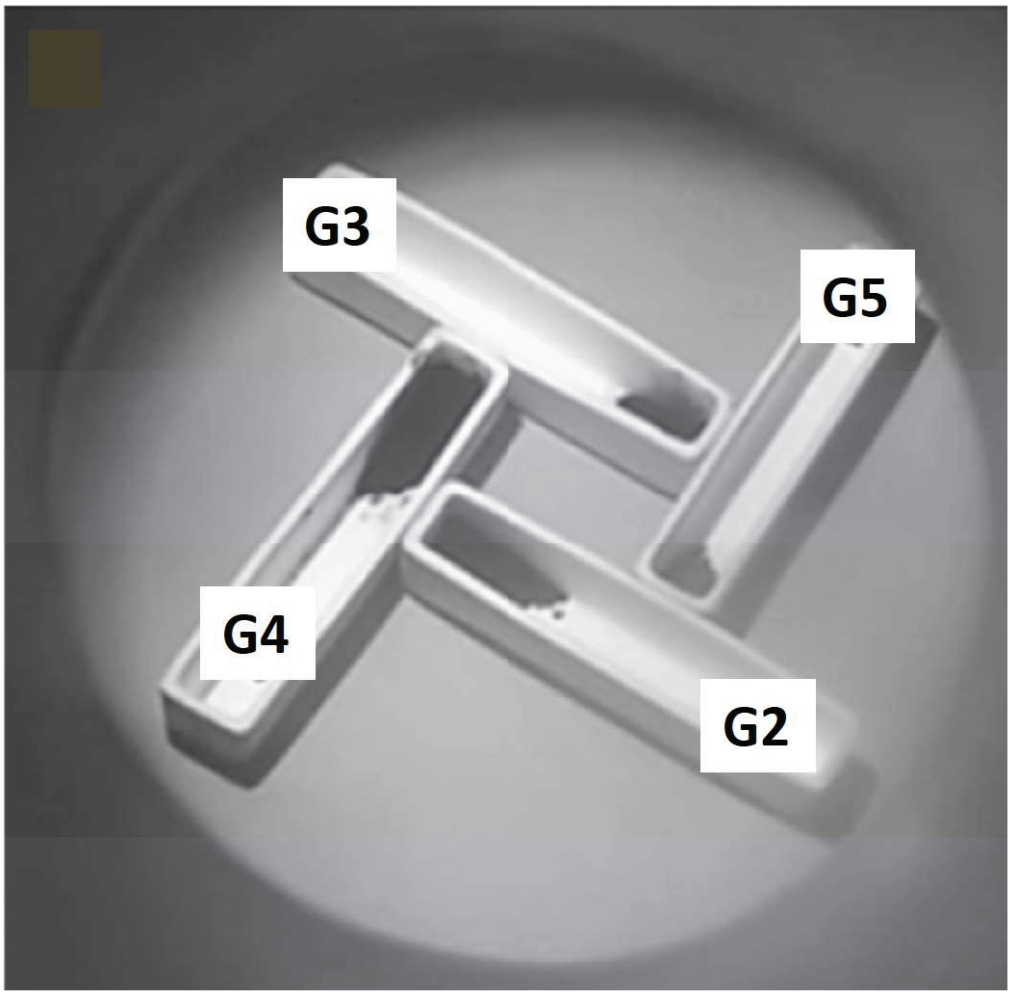

Fig. 98A

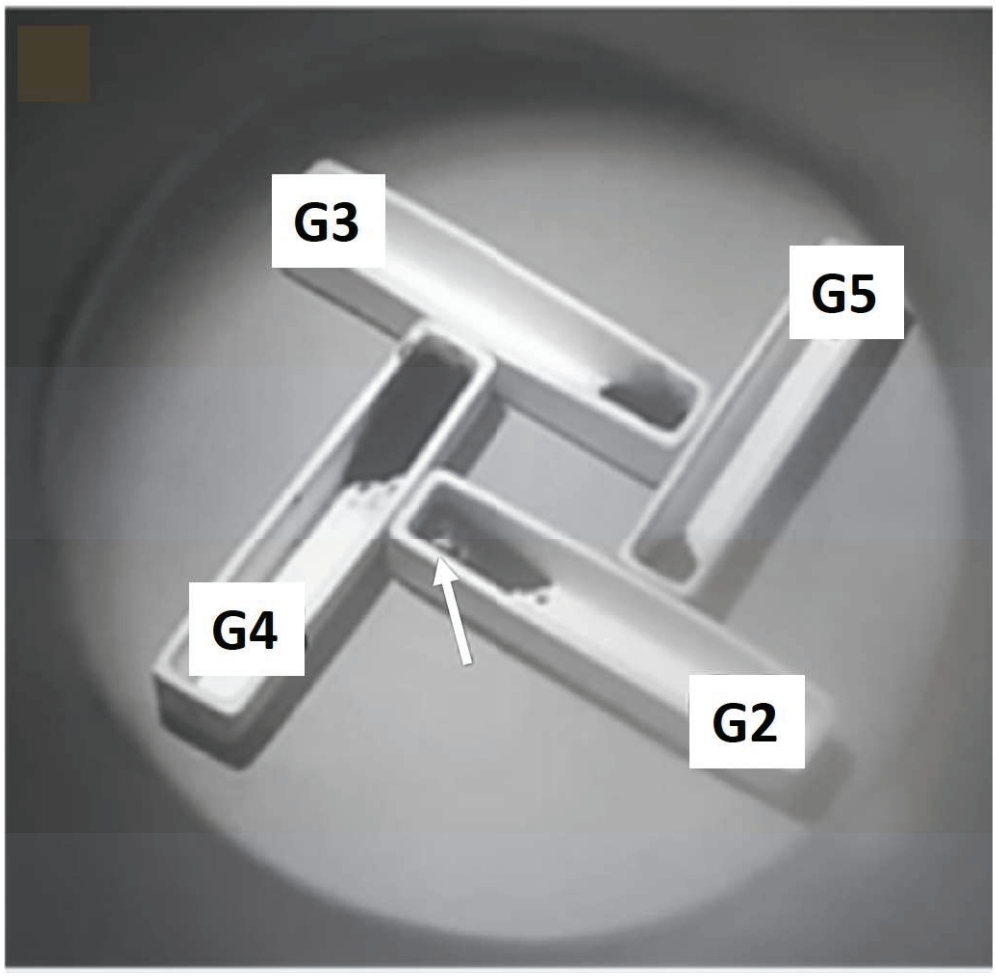

Fig. 98B

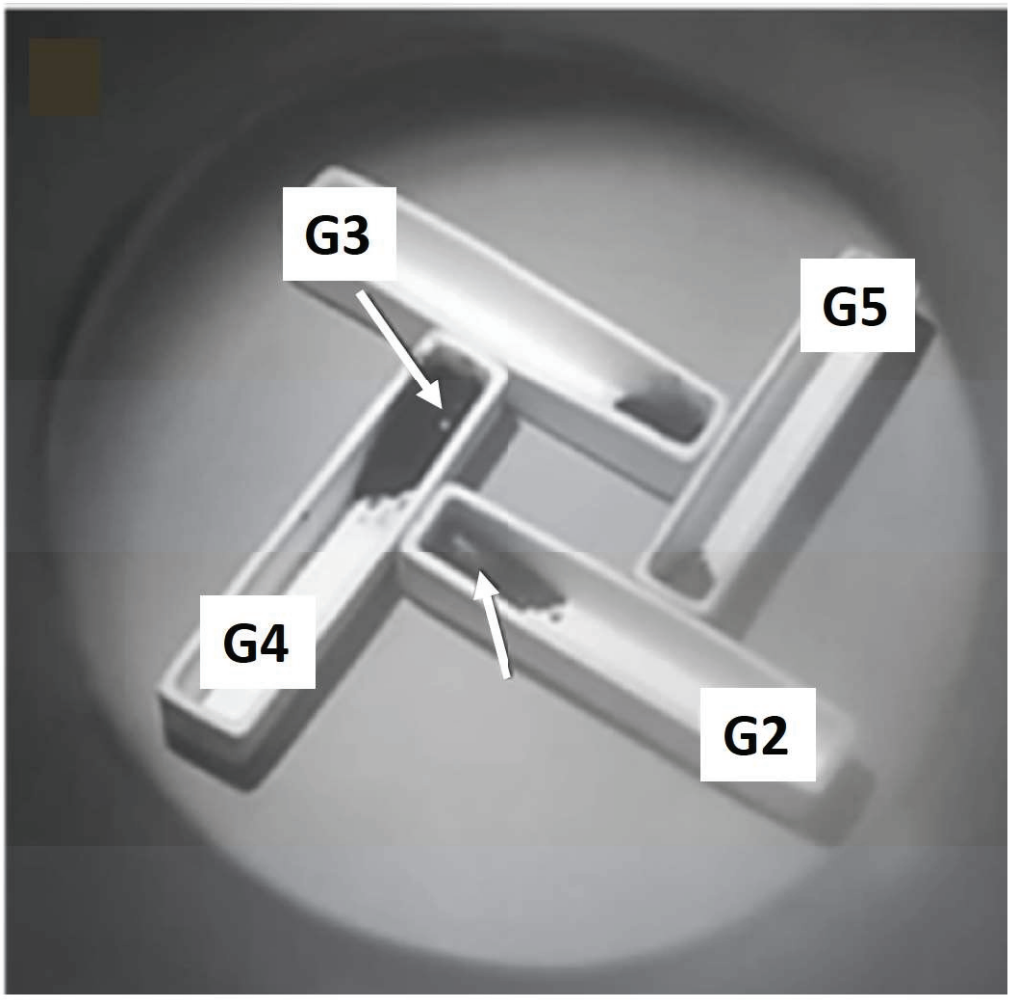

Fig. 98C

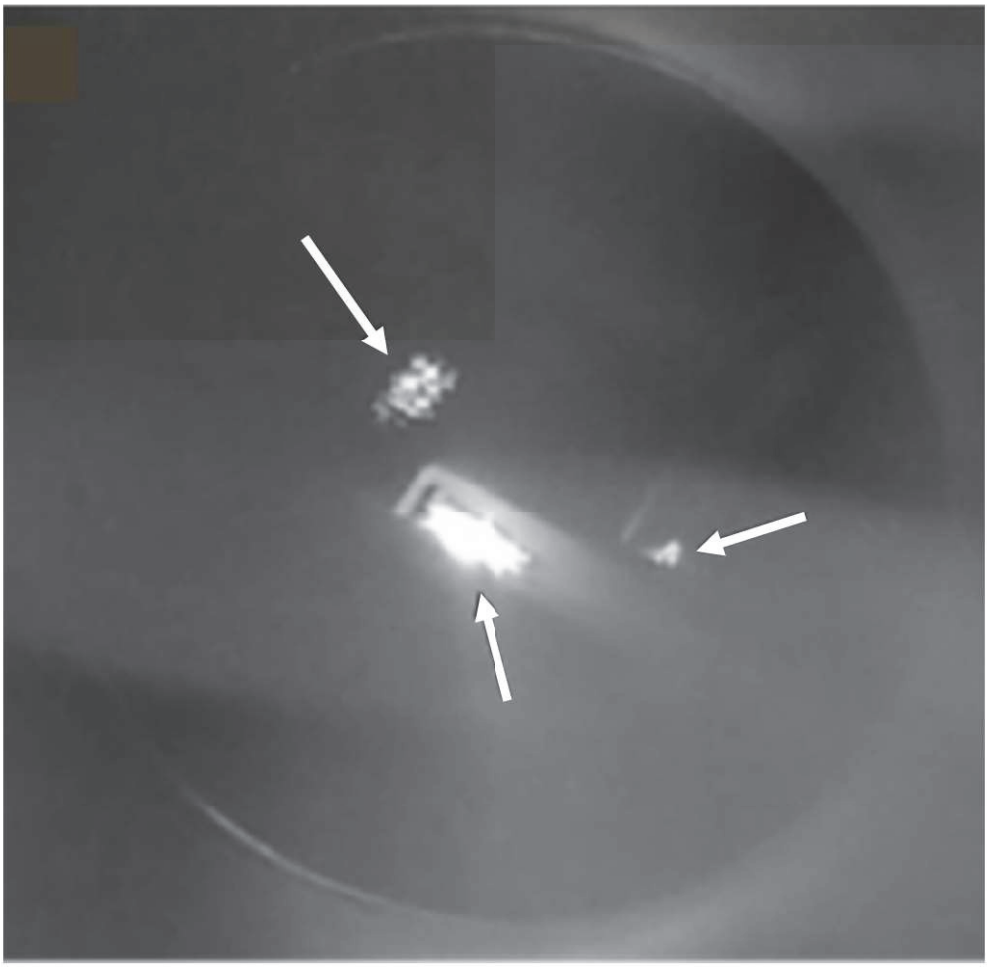

Fig. 98D

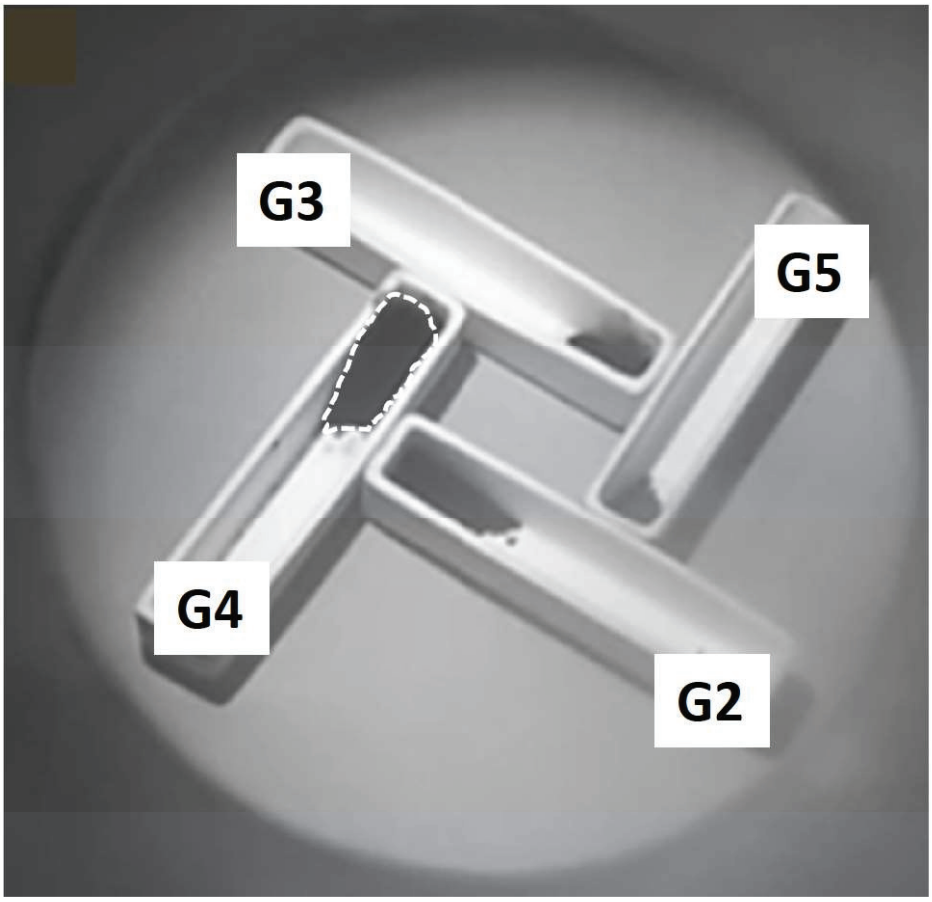

Fig. 99A

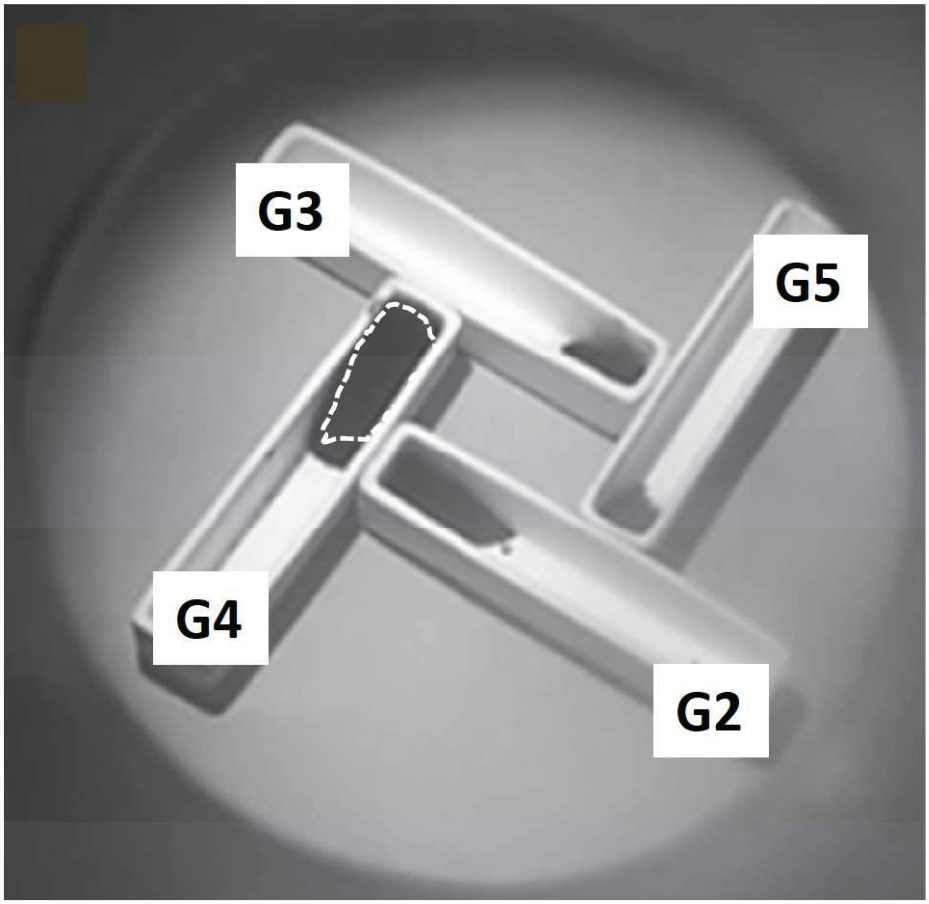

Fig. 99B

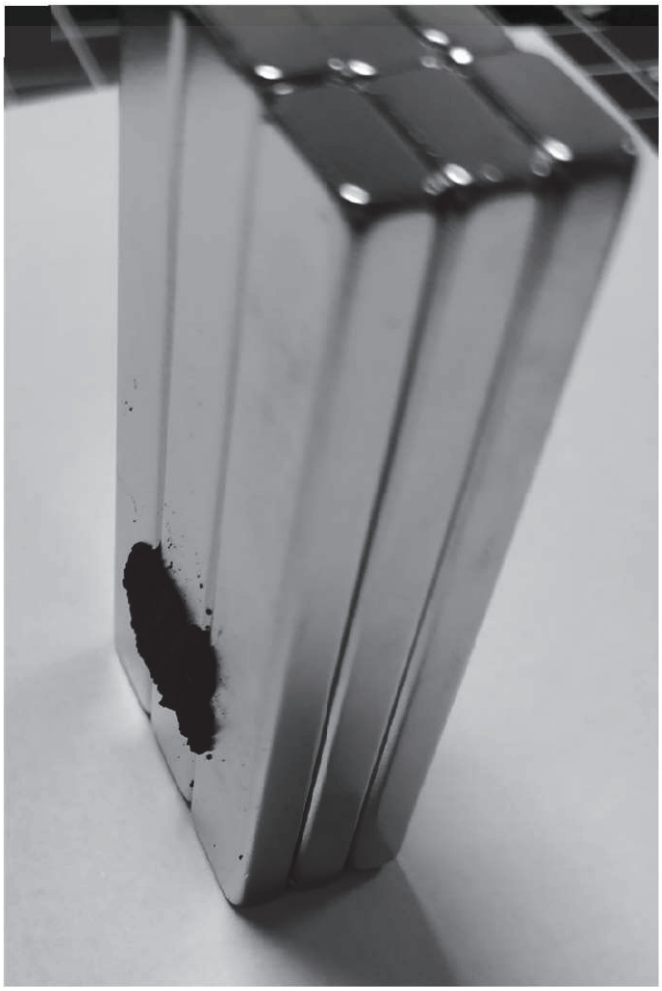

Fig. 100A

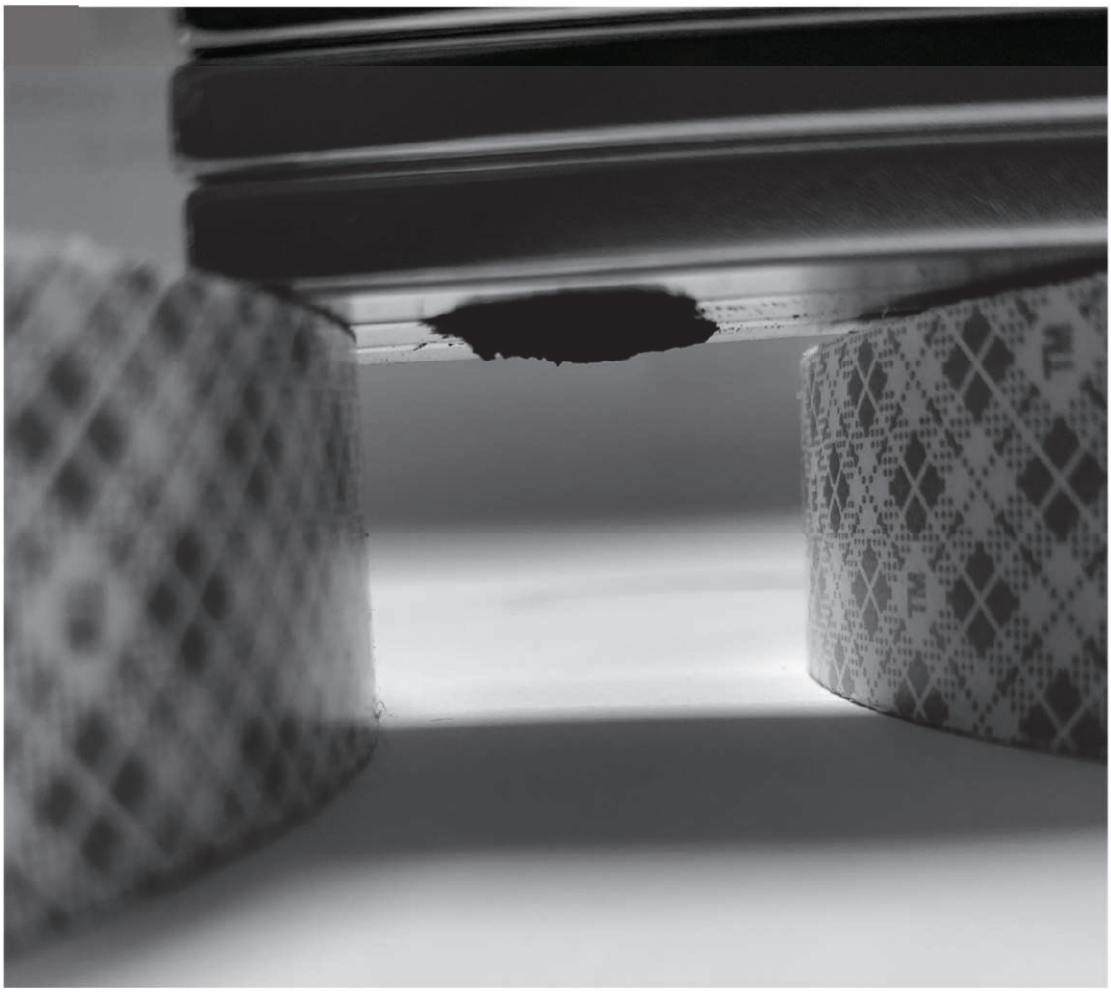

Fig. 100B

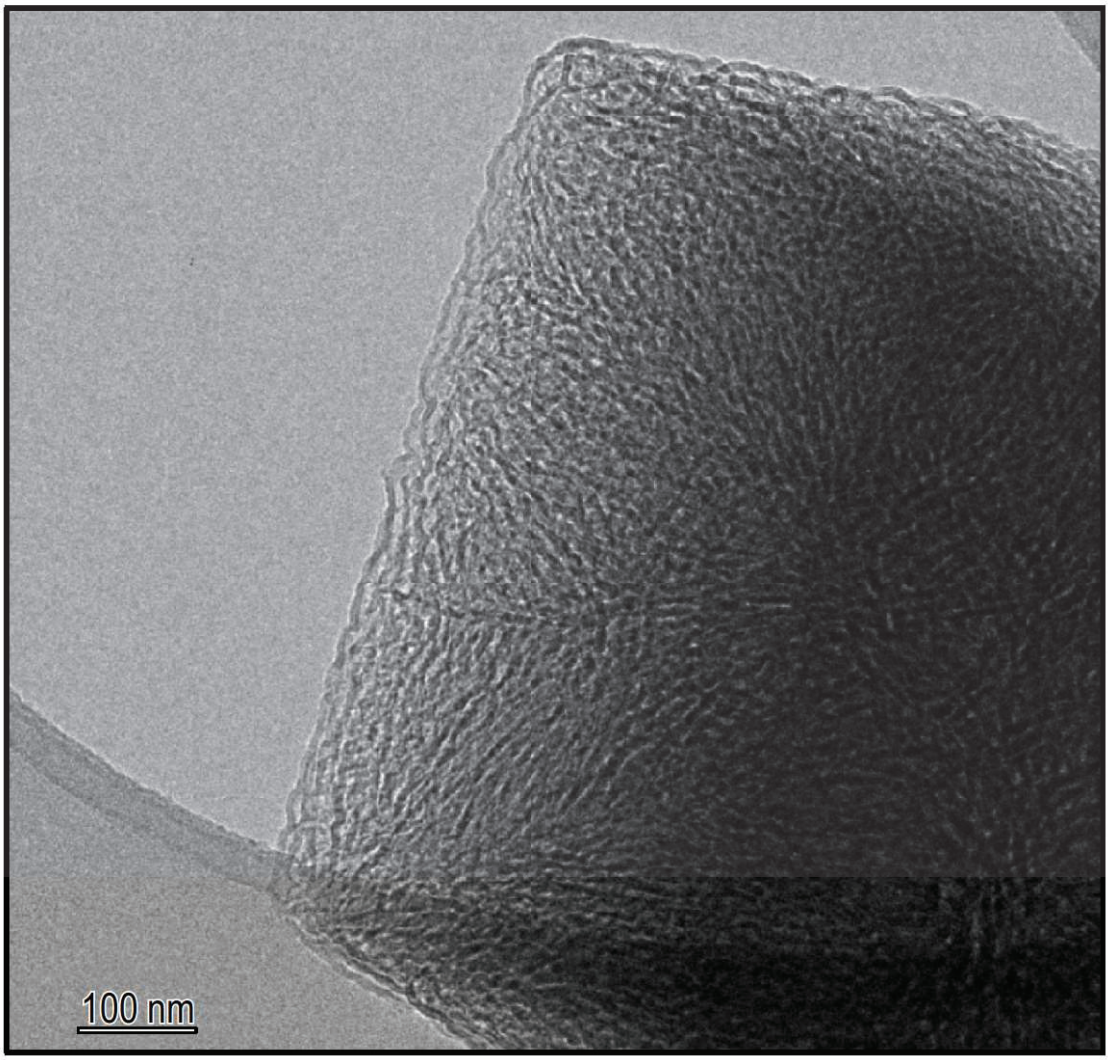

FIG. 101A

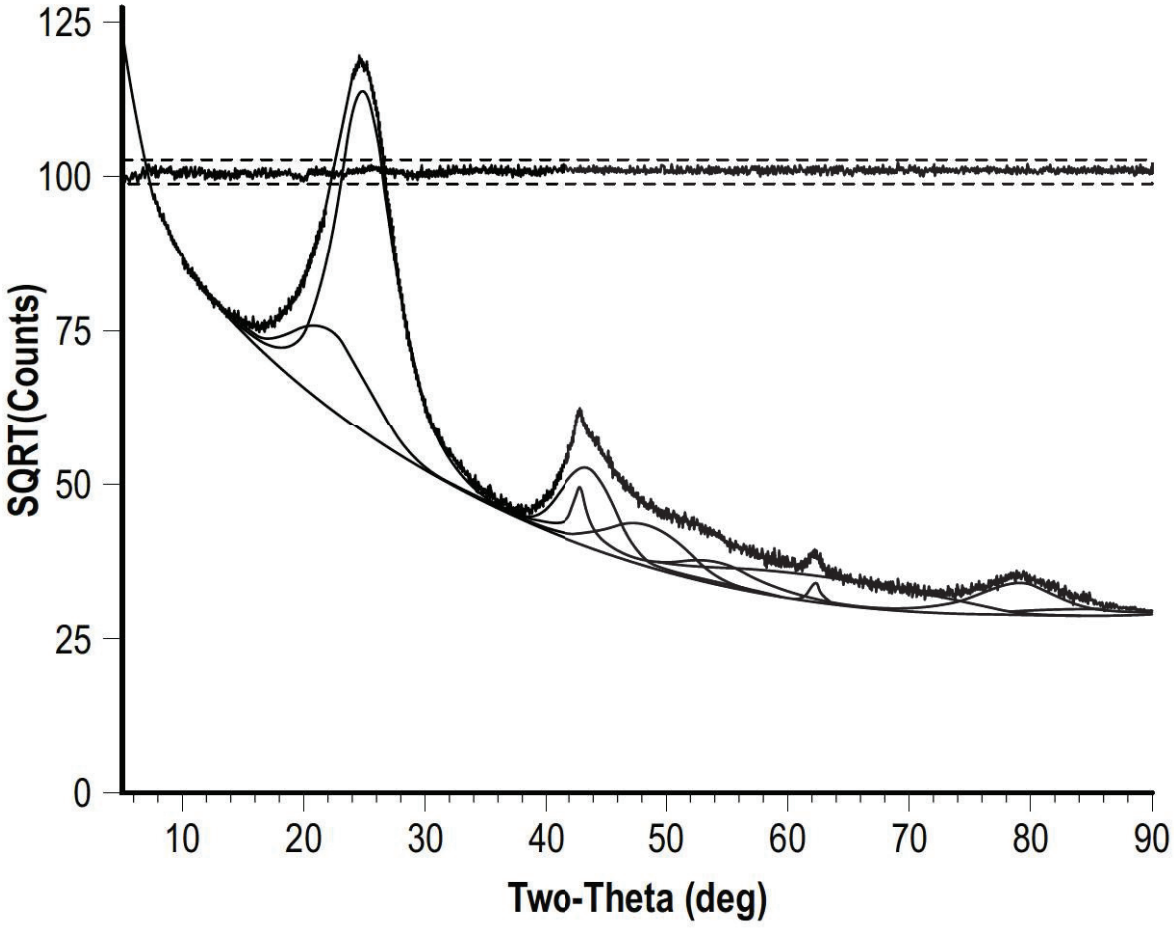
125
100
75
50
25
0
SQRT(Counts)
10
20
30
40
50
60
70
80
90
Two-Theta (deg)

FIG. 101B

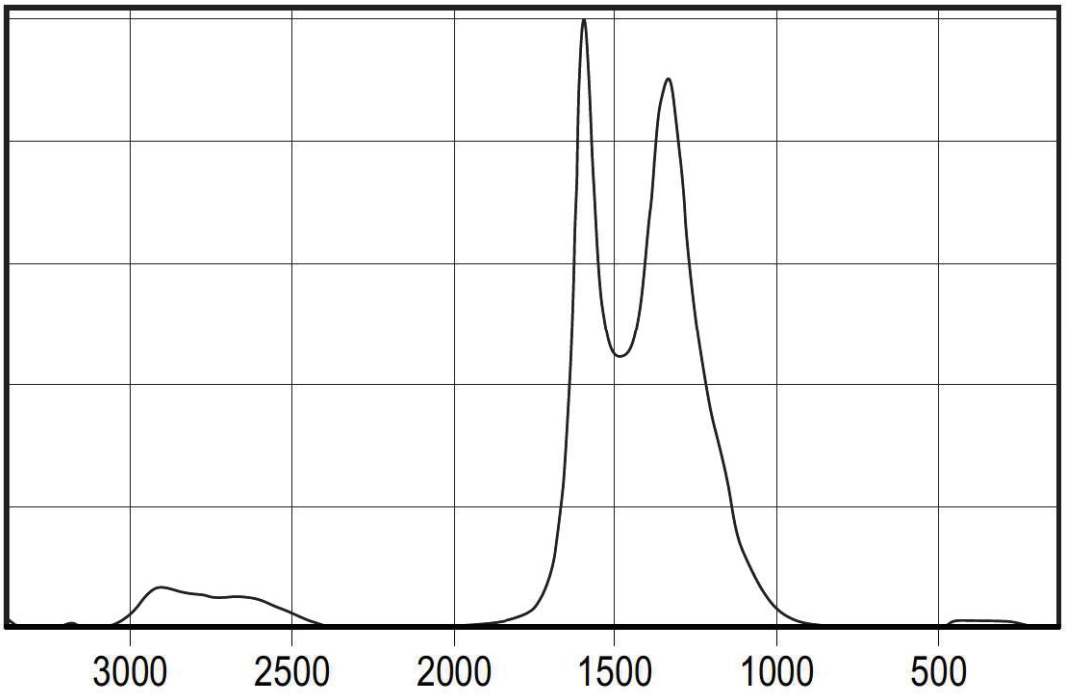

FIG. 101C

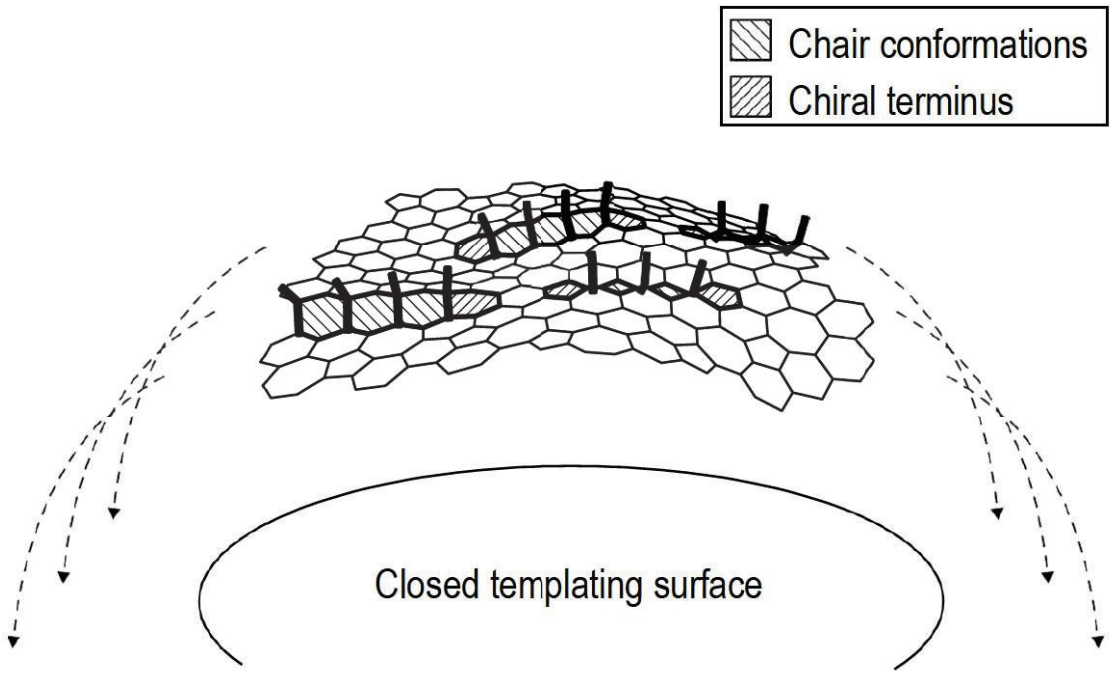
Chair conformations
Chiral terminus
Closed templating surface

FIG. 102



FIG. 103A



FIG. 103B

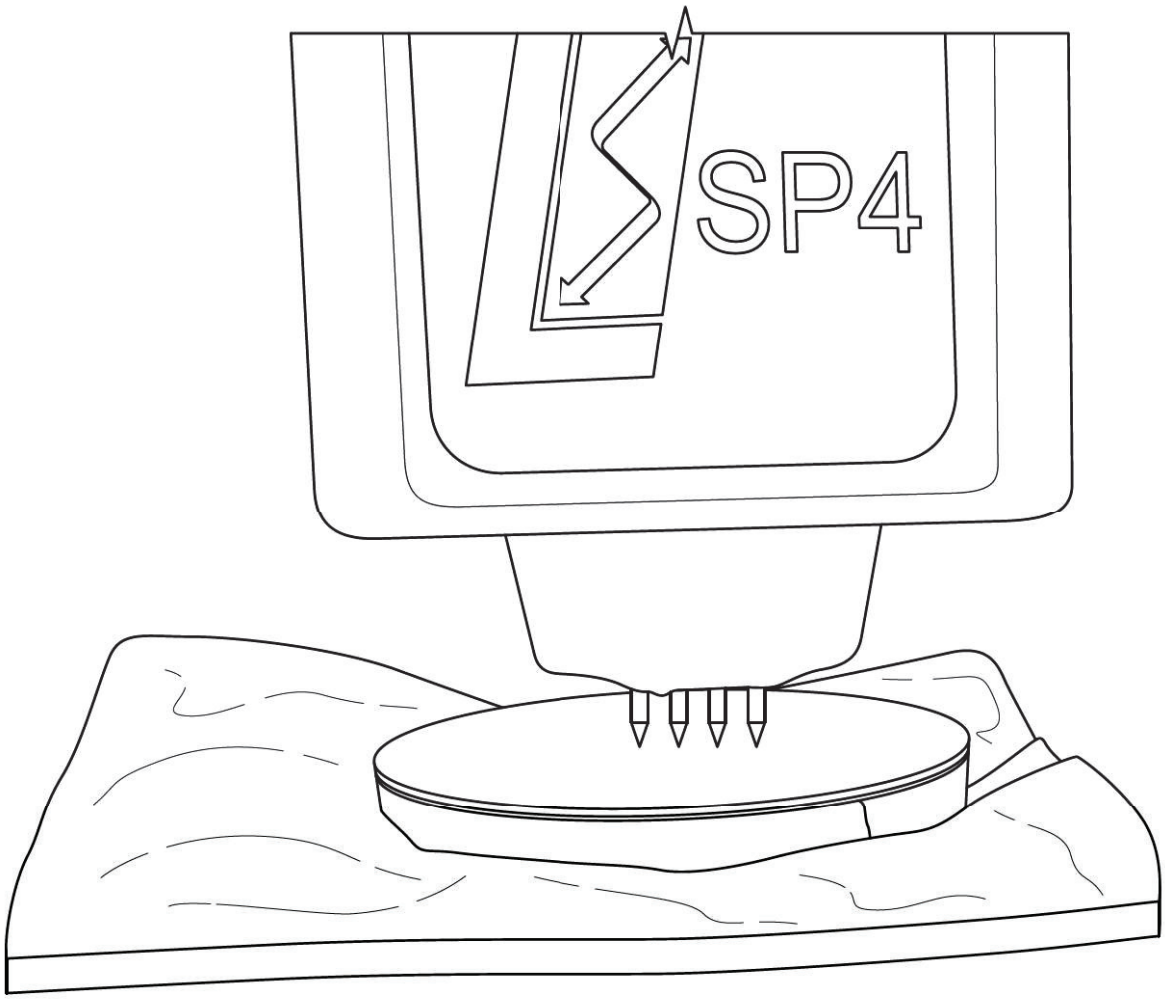

FIG. 104

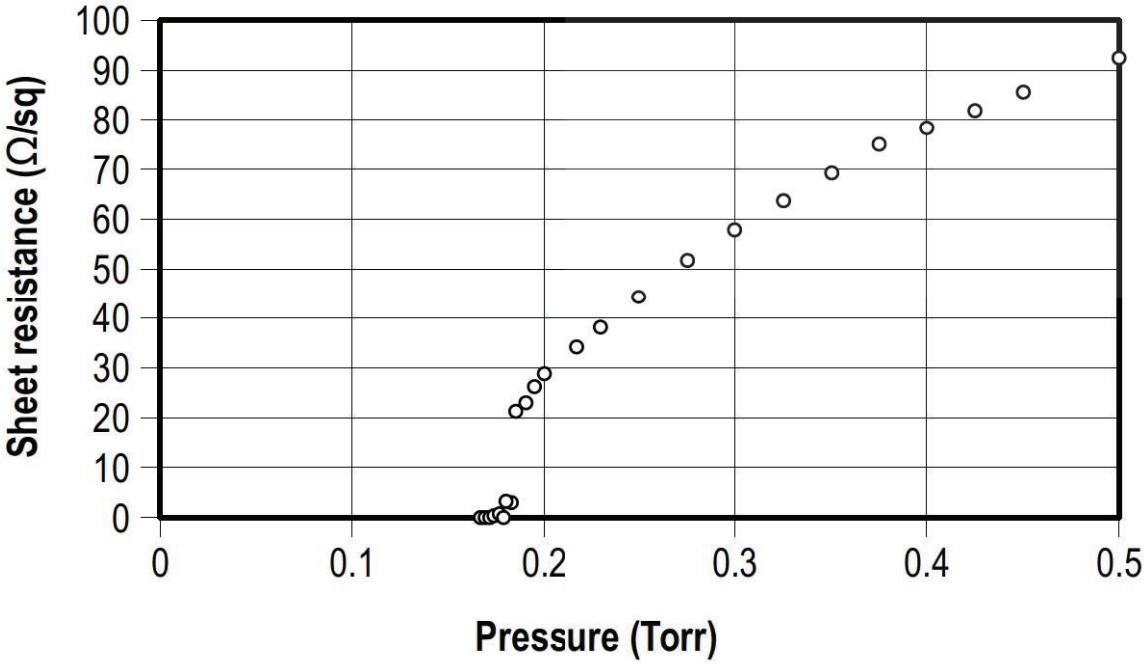
Sheet resistance (Ω/sq)
100
90
80
70
60
50
40
30
20
10
0
0
0.1
0.2
0.3
0.4
0.5
Pressure (Torr)

FIG. 105

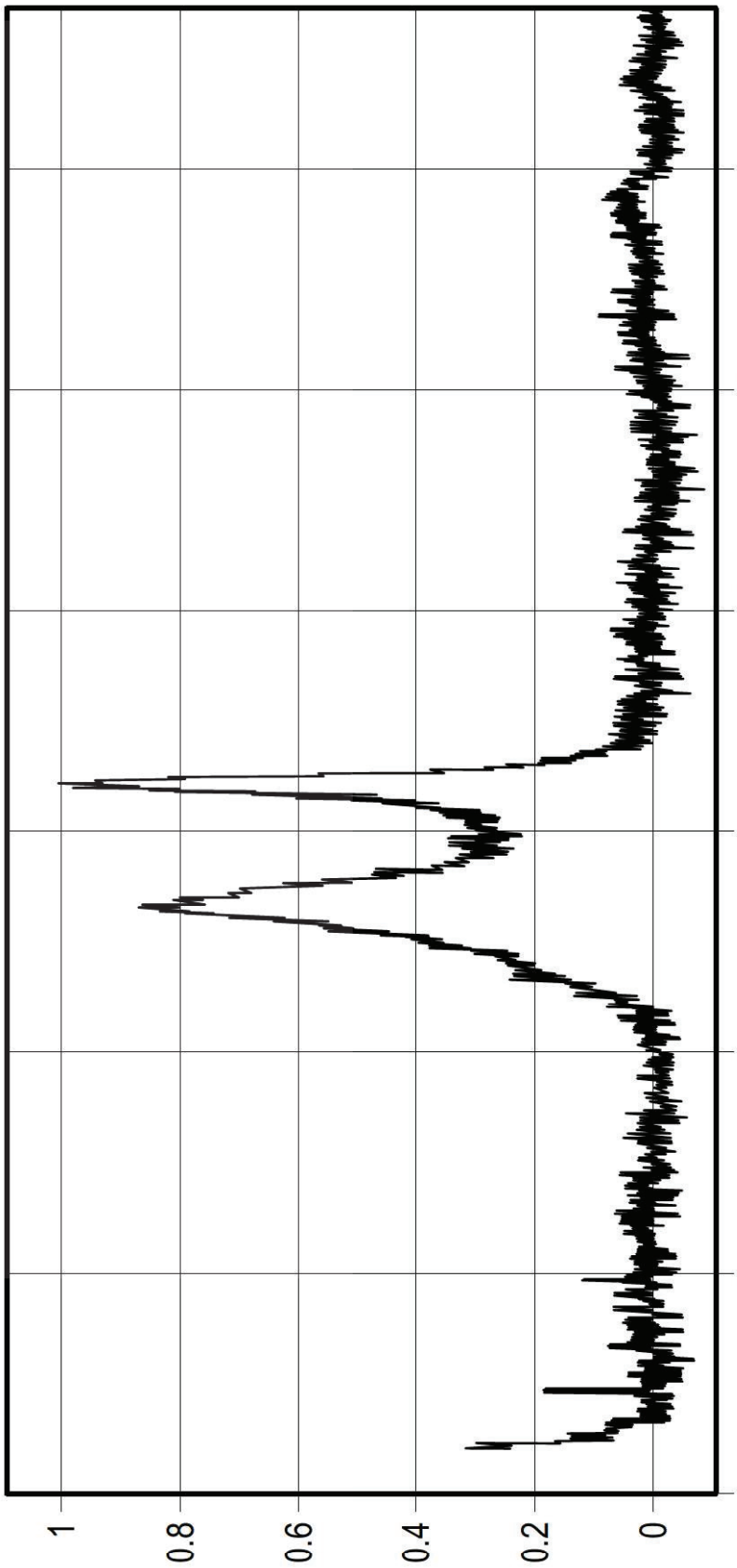

FIG. 106

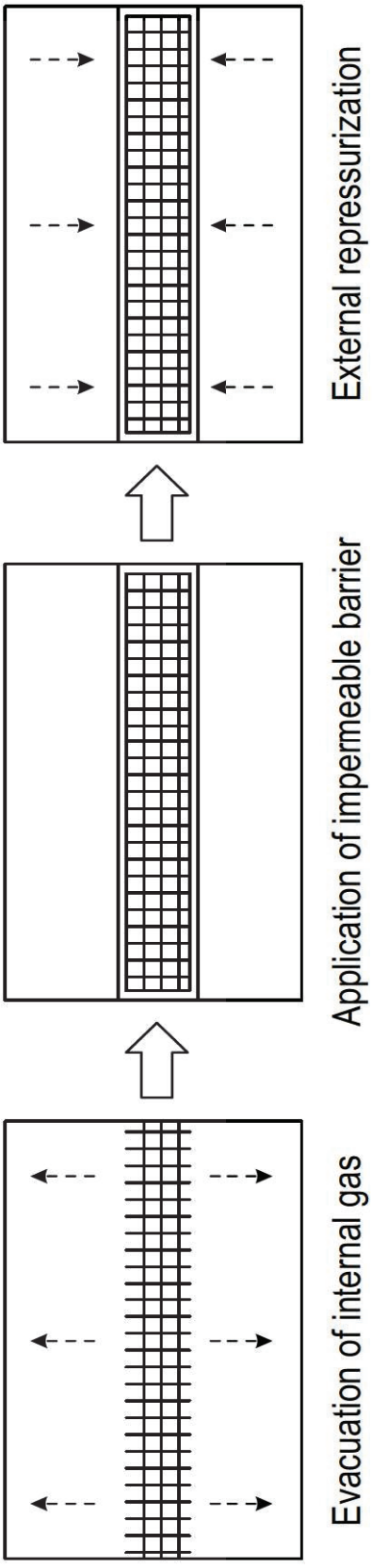
Evacuation of internal gas
Application of impermeable barrier
External repressurization

FIG. 107

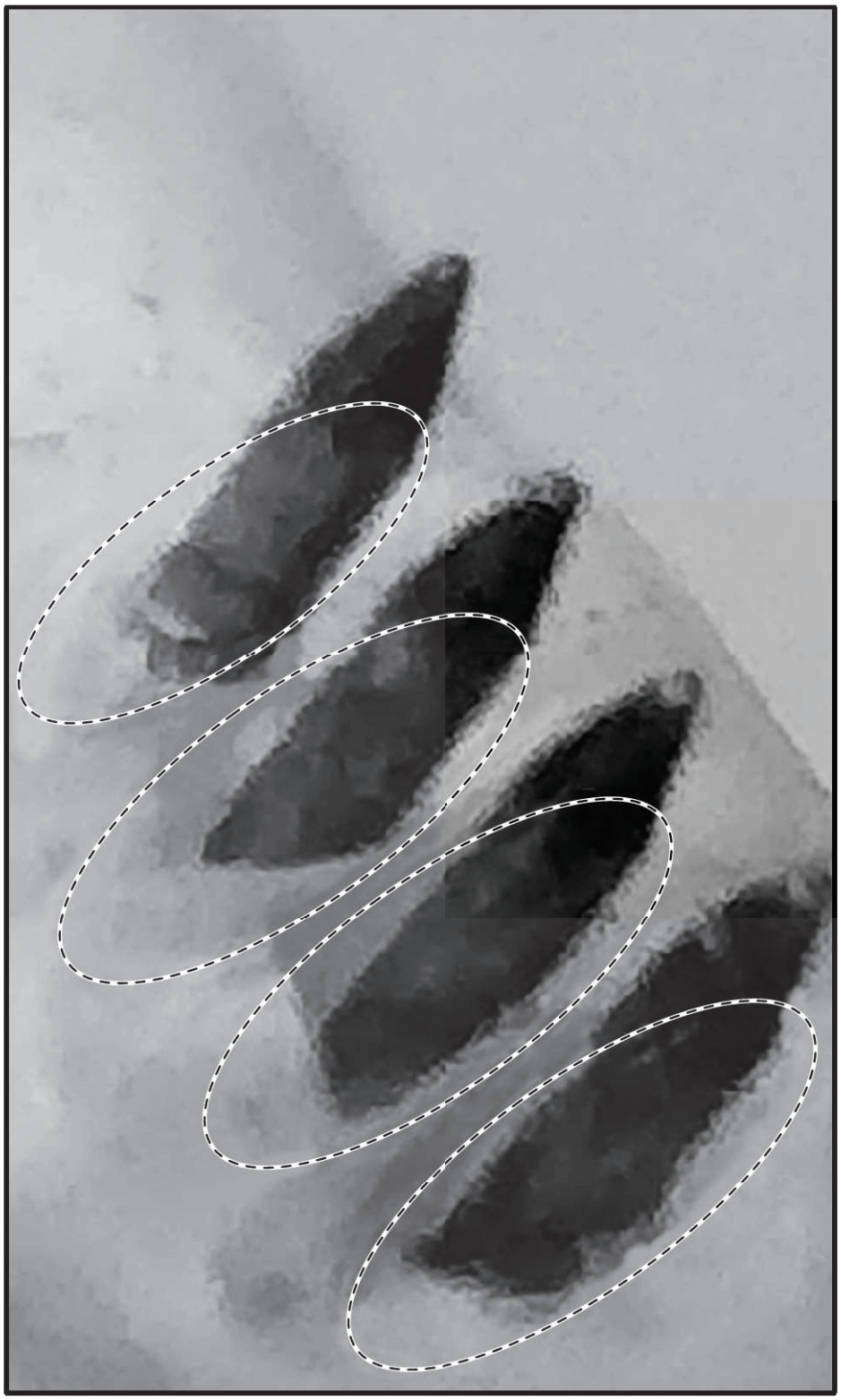

FIG. 108

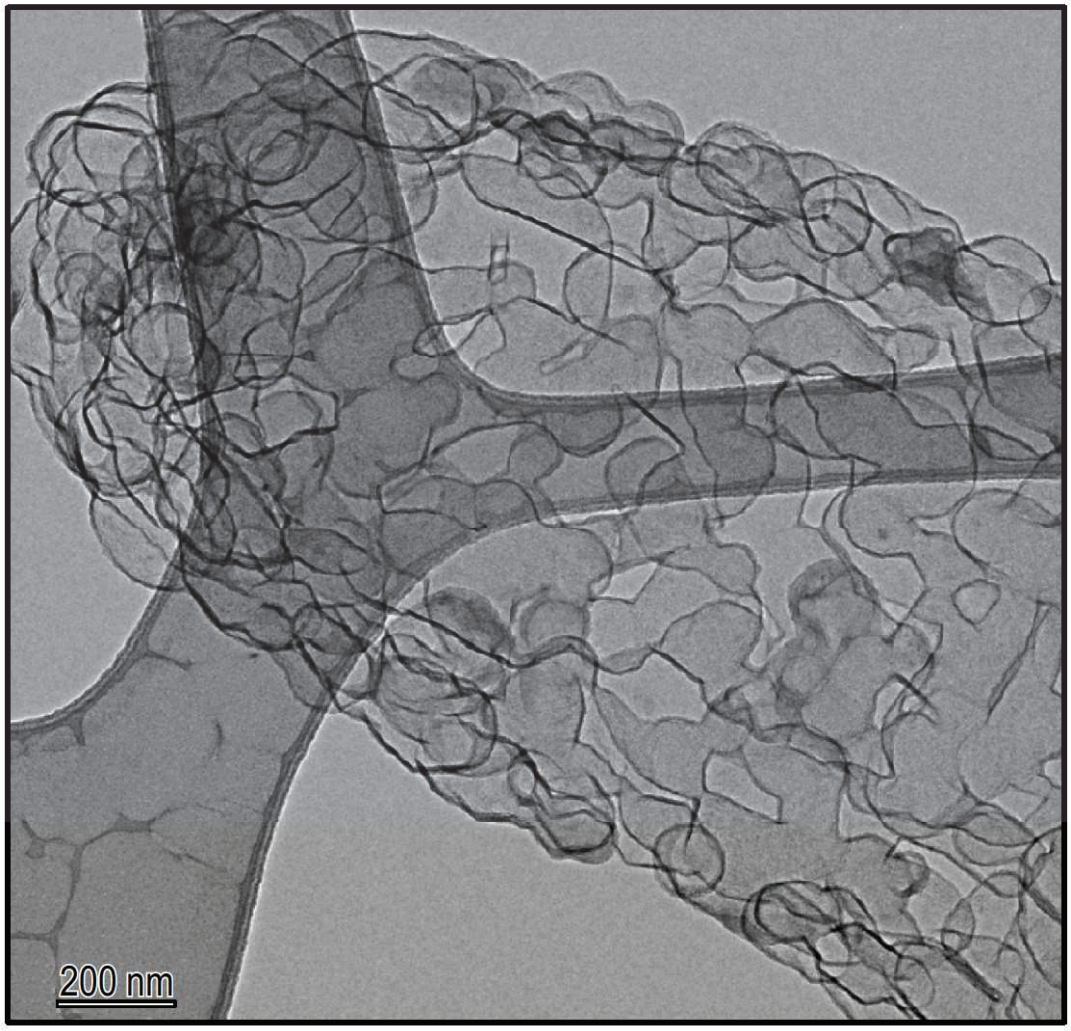

FIG. 109A

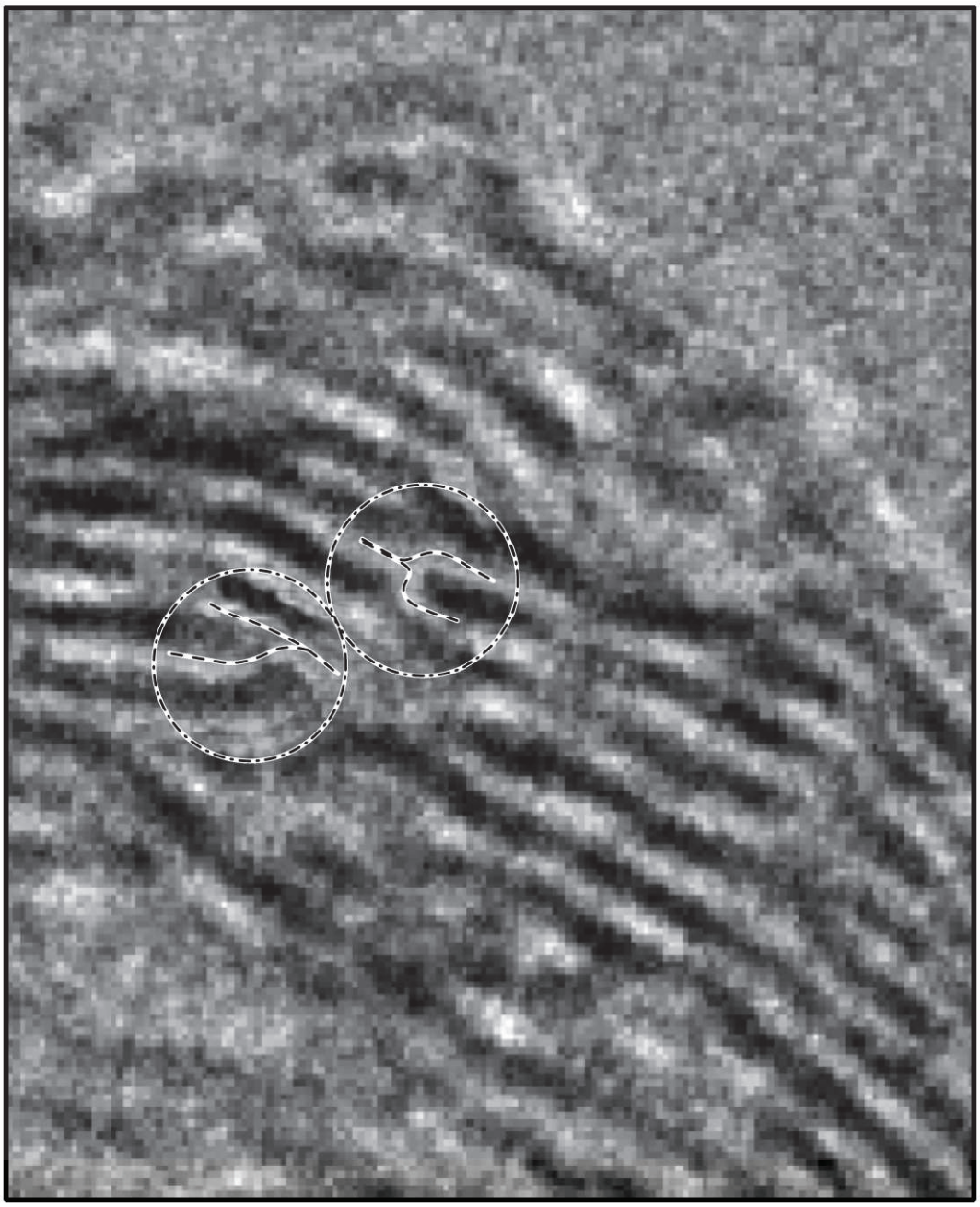

FIG. 109B

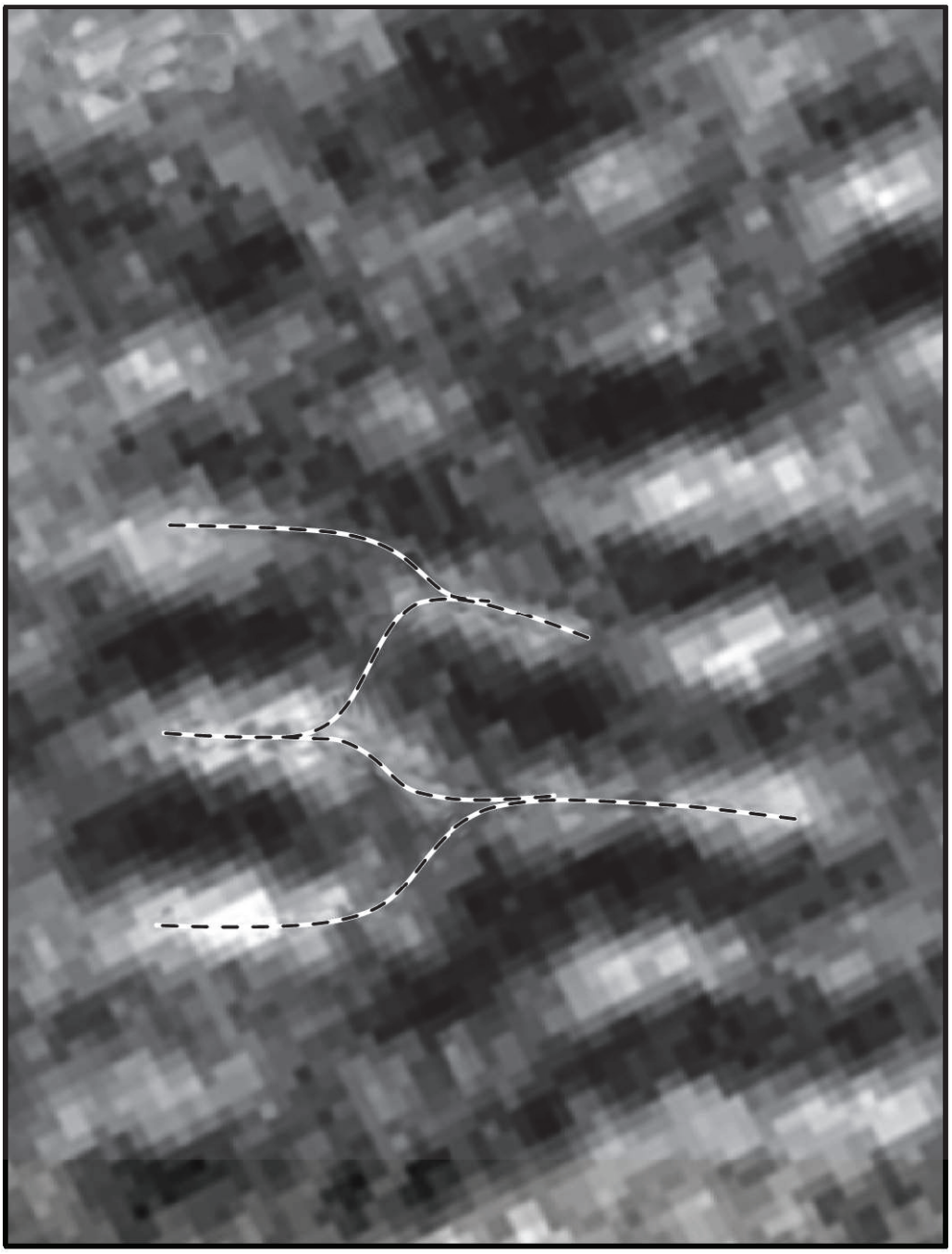

FIG. 109C